

**SYNTHESIS AND BIOLOGICAL EVALUATION OF THE
DERIVATIVES OF 1,3,5-TRIAZIN-2,4-DIONES AND THEIR
FUSED ANALOGUES**

HRIDAY BERA

NATIONAL UNIVERSITY OF SINGAPORE

2012

**SYNTHESIS AND BIOLOGICAL EVALUATION OF THE
DERIVATIVES OF 1,3,5-TRIAZIN-2,4-DIONES AND THEIR
FUSED ANALOGUES**

HRIDAY BERA

(M. PHARM. (FIRST CLASS), JADAVPUR UNIVERSITY, INDIA)

**A THESIS SUBMITTED FOR THE DEGREE OF
DOCTOR OF PHILOSOPHY**

**DEPARTMENT OF PHARMACY
NATIONAL UNIVERSITY OF SINGAPORE**

2012

DECLARATION

I hereby declare that this thesis is my original work and it has been written by me in its entirety. I have duly acknowledged all the sources of information which have been used in the thesis.

This thesis has also not been submitted for any degree in any university previously.

Hriday Bera.

Hriday Bera
29 May, 2012

ACKNOWLEDGEMENTS

I convey my most sincere regards, respect and deepest gratitude to **Assoc. Prof. Chui Wai Keung**, for his inspiration, encouragement and valuable guidance throughout the period of this research. His unremitting advice, affection and help are responsible for successful completion of this thesis.

I am thankful to **Assoc. Prof. Chan Sui Yung**, Head, Department of Pharmacy, for providing the required facilities for this project, and the National University of Singapore for offering the research scholarship.

I also express my sincere thanks to **Dr. Anton Dolzhenko** for his valuable help and support during the hard time of my PhD study. My gratitude is also extended to **Dr. Gigi Chui** and **Miss Tan Bee Jen** for providing me the necessary facilities and guidance for the cell culture work and biological studies. I am also grateful to **Dr. Yap Chun Wei** for his help and advice on the QSAR study.

Special thanks go to **Dr. Giorgia Pastorin** and **Dr. Koh Hwee Ling** for their valuable comments on my research work. I would also like to express my gratitude to Miss Ng Sek Eng, Miss Ley Pey Pey and Madam Han for their technical support thought out my research work. I am equally grateful to my lab mates particularly Yang Hong, Pauline Ong, Nikhil Sachdeva, Sun Lingyi and Ng Hui Li for their co-operation and support in daily laboratory work.

I am very much indebted to my close friends Asim, Srimanta, Sonali, Anumita, Subhajit, Surojit, Sandeep, Sewata, Vamsi, Sadananda, Tanay, Animesh, Rajkumar, Krishna, Sandip, Pradipta, Nimai, Bijay, Tarapada, Sabhya, Jayandra da and many others for their constant help and assistant at various stages of this entire research work.

Finally, I would like to express my deepest gratitude to my parents and other family members for their immense support, inspirations and encouragement during the entire course.

TABLE OF CONTENTS

	Page
ACKNOWLEDGEMENTS	i
TABLE OF CONTENTS.....	ii
SUMMARY	viii
LIST OF TABLES	x
LIST OF SCHEMES.....	xiv
ABBREVIATIONS	xvi
Chapter 1-Introduction - Review of 1,3,5-triazin-2,4-diones, Thymidine Phosphorylase and 3D-QSAR study	1
Introduction.....	2
1.1 Synthesis of 1,3,5-triazin-2,4-dione and its fused derivatives	2
1.1.1 Synthesis of 1,3,5-triazin-2,4-dione.....	3
1.1.2 Synthesis of fused 1,3,5-triazin-2,4-dione and its thioxo analogues	5
1.1.2.1 Synthesis of 1,2,4-triazole fused 1,3,5-triazin-2,4-dione analogues.....	6
1.1.2.2 Synthesis of pyrazolo fused 1,3,5-triazine-2,4-dione analogues	11
1.1.3 Applications of 1,3,5-triazine and its fused analogues in medicine and agriculture	17
1.2 Thymidine phosphorylase (TP) as a target of drug design.....	21
1.2.1 Structure of thymidine phosphorylase	23
1.2.2 Biological functions of thymidine phosphorylase	24
1.2.3 Role of thymidine phosphorylase in tumour development and progression	27

1.2.4 Thymidine phosphorylase inhibitors	31
1.2.5 Thymidine phosphorylase mediated activation of anticancer prodrug.....	36
1.2.6 Structural aspect and crystal structure of human thymidine phosphorylase	38
1.3 CoMFA, a 3D-QSAR method, as a means of lead optimization	40
1.4 Summary	42
Chapter 2-The Study Proposal - Hypotheses and Objectives.....	43
2.1 Importance of the development of thymidine phosphorylase inhibitors as a novel antiangiogenic agents.....	44
2.2 Hypotheses and objectives	47
2.3 Significance of the study.....	49
Chapter 3-The Preliminary Studies - Establishing Lead Compounds through Synthesis and Bioassay	51
3.1 Synthesis of 1,3,5-triazin-2,4-dione and their fused analogues to explore lead inhibitor compounds of thymidine phosphorylase	52
3.2 Chemistry	55
3.2.1 Synthesis of 1,3,5-triazin-2,4-diones derivatives	55
3.2.2 Synthesis of fused 1,2,4-triazolo[1,5- <i>a</i>][1,3,5]triazin-5,7(<i>4H,6H</i>)-dione and their thioxo-bioisosteres	58
3.2. 3 Synthesis of pyrazolo[1,5- <i>a</i>][1,3,5]triazin-2,4(<i>1H,3H</i>)-dione and its thioxo bioisostere.....	65
3.3 Evaluation of anti-thymididine phosphorylase (Anti-TP) activity.....	70
3.4 Summary	76

Chapter 4-Lead Optimization for more Active Inhibitors of Thymidine

Phosphorylase	78
4.1 Craig plot directed structural optimization of the lead compounds and the evaluation of their anti-thymidine phosphorylase activity	79
4.1.1 Chemistry.....	81
4.1.1.1 Synthesis of 5-thioxo-5,6-dihydro-4 <i>H</i> -[1,2,4]triazolo[1,5- <i>a</i>][1,3,5]triazin-7-one analogues	81
4.1.1.2 Synthesis of 2-thioxo-2,3-dihydro-1 <i>H</i> -pyrazolo[1,5- <i>a</i>][1,3,5]triazin-4-one analogues.....	87
4.1.2 Evaluation of anti-thymidine phosphorylase (Anti-TP) activity	90
4.2 Further miscellaneous structural modification.....	97
4.2.1 Chemistry.....	98
4.2.2 Evaluation of anti-thymididine phosphorylase (Anti-TP) activity	100
4.3 Summary	103
Chapter 5-Structural Investigation – Regiochemistry of Synthetic Intermediates...	106
5.1 Synthesis and tautomerism study of the key intermediates, 3(5)-amino/ carbethoxythiourea-5(3)-aryl-1,2,4-triazoles	107
5.1.1 Synthesis of 3(5)-amino-5(3)-(het)aryl-1,2,4-triazoles	108
5.1.2 Tautomerism study of 3(5)-amino-5(3)-(het)aryl-1,2,4-triazoles.....	111
5.1.3 Synthesis of <i>N</i> -(3(5)-aryl-1,2,4-triazol-5(3)-yl)- <i>N</i> '-carbethoxythioureas	115
5.1.4 Tautomerism study of <i>N</i> -(3(5)-aryl-1,2,4-triazol-5(3)-yl)- <i>N</i> '-carbethoxythioureas.....	118

5.2 Synthesis of 4-carbethoxy-1-[4-(<i>N,N</i> -dimethylamino)benzoyl]thiosemicarbazide	123
5.3 Summary	124
Chapter 6-A Quantitative Structure Activity Relationship (QSAR) Study.....	125
6.1 CoMFA based 3D-QSAR study of synthesized TP inhibitors.....	126
6.2 3D-QSAR study design	128
6.2.1 Dataset	128
6.2.2 Preparation of dataset	129
6.2.3 Alignment	129
6.2.4 CoMFA analysis	130
6.3 Results and discussion.....	131
6.4 Summary	137
Chapter 7-Biological Characterization of the Active Thymidine Phosphorylase	
Inhibitors	138
7.1 Investigation of enzyme inhibition kinetics and TP associated antiangiogenic activity of synthesized compounds	139
7.2 Results	141
7.2.1 Enzyme inhibition kinetics characterization.....	141
7.2.1 Antiangiogenic activity determination	149
7.2.2 Antimetastasis activity determination	158
7.2.3 Antiproliferative activity determination	160
7.3 Discussion	161

7.4 Summary	167
Chapter 8-Conclusion and Future work	169
8.1 Conclusion.....	170
8.2 Future work	176
Chapter 9-Materials and Methods	179
9.1 Chemistry	180
9.1.1 Reagents and general methods	180
9.1.2 General procedure for the synthesis of 1,3,5-triazin-2,4-dione (H1a-H1f)	181
9.1.2 General procedure for the synthesis of 1,2,4-triazolo[1,5- <i>a</i>][1,3,5]triazine (H2-H6)	185
9.1.4 General procedure for the synthesis 2-benzyl-5-thioxo-5,6- dihydro[1,2,4]triazolo[1,5- <i>a</i>][1,3,5]triazin-7(4 <i>H</i>)-one and its derivatives (H7, H8 and H9).....	215
9.1.5 General procedure for the synthesis pyrazolo[1,5- <i>a</i>][1,3,5]triazin (H10, H11, H12 and H14).....	225
9.1.6 General procedure of synthesis of (8-benzyl-4-oxo-2-thioxo-1,2,3,4- tetrahydro pyrazolo[1,5- <i>a</i>][1,3,5]triazin-7-yl)-thiourea and their derivatives (13- 13n).....	236
9.2 Molecular modeling study.....	252
9.3 Biological characterisation.....	253
9.3.1 <i>In vitro</i> thymidine phosphorylase enzyme assay	253
9.3.2 Enzyme Inhibition kinetics Study.....	254

9.3.3 MTT assay	254
9.3.4 Gelatine zymography.....	255
9.3.5 Cell invasion assay	256
9.3.6 VEGF assay.....	256
9.3.7 IL-8 assay	257
Chapter 10-References	259

SUMMARY

Inhibition of the enzyme, thymidine phosphorylase (TP) may lead to development of chemotherapeutic agents for overcoming the pathological effect of TP such as tumour progression *via* angiogenesis. The main purpose of this study was to investigate the hypothesis that derivatives of 1,3,5-triazin-2,4-diones and their fused analogues would exhibit TP inhibitory activity. To test this hypothesis, several objectives for this study were identified, namely to synthesize a series of 1,3,5-triazin-2,4-diones and their fused analogues *viz.* 1,2,4-triazolo[1,5-*a*][1,3,5]triazin-5,7-dione, pyrazolo[1,5-*a*][1,3,5]triazin-2,4-dione and their thioxo analogues and to evaluate their TP inhibitory potential. Moreover, to generate pharmacophoric requirements of these new classes of TP inhibitors, 3D-QSAR studies were conducted. In addition, evaluation of the effects of the test compounds on the expression of downstream markers of angiogenesis and cell viability of breast cancer cell line were performed to investigate their potential antiangiogenic and antiproliferative property respectively.

The synthetic schemes involved ring transformation reactions and annulation of 1,3,5-triazine ring onto suitably substituted 1,2,4-triazoles and/or pyrazole ring through intramolecular heterocyclization reactions. A continuous UV spectrophotometric enzyme assay was performed on recombinant human TP (EC 2.4.2.4), using thymidine as substrate. Information on the enzyme inhibition kinetic was also derived from the enzyme assay. In addition, pharmacophore elucidation of the synthesized TP inhibitors was carried out *via* comparative molecular field analysis (CoMFA). Moreover, gelatinase zymography and enzyme-linked immunosorbent assay were performed to evaluate MMP-9 and VEGF expression level respectively in breast cancer cell line. A total of 82 compounds was successfully synthesized and

characterized. Among all the synthesized compounds evaluated, compounds having keto group (C=O) and thioketo group (C=S) at particular orientation *viz.* 5-thioxo-5,6-dihydro-4*H*-[1,2,4]triazolo[1,5-*a*][1,3,5]triazin-7-one and 2-thioxo-2,3-dihydropyrazolo[1,5-*a*][1,3,5]triazin-4(1*H*)-one their thiomethyl derivatives showed varying degrees of TP inhibitory activity comparable to positive control, 7-Deazaxanthine (IC₅₀ value = 42.63 μM). In addition, compounds **H5bxvii**, **H5bxix**, **H8i**, **H11g** and **H13a** were found to exhibit significant TP inhibitory potential with low micro molar IC₅₀ values (IC₅₀ = 10.84, 13.09, 2.95, 13.07, and 3.82 μM respectively). The enzyme assay provided evidence that these inhibitors might inhibit TP in mixed fashion in the presence of variable Thymidine (dThd) and phosphate (KPi) concentrations. The 3D-QSAR studies based on CoMFA method was satisfactory according to statistical validation results and contour map analysis. Moreover, it is evident from biological experiments that selected compounds can inhibit expression of angiogenic markers including MMP-9 and VEGF expression without exhibiting significant cytotoxicity.

The use of ring transformation and intra-molecular annulation reactions to generate the target compounds were practical synthetic approaches. The compounds were found to exhibit TP enzyme inhibition as well as its associated antiangiogenic potential.

(Words – 415)

LIST OF TABLES

Table		Page
1	Representative examples of different types of TP inhibitors	34
2	Synthesis of 6 substituted 1,3,5-triazin-2,4-diones	57
3	Synthesis of 1,2,4-triazolo[1,5- <i>a</i>][1,3,5]triazin-5,7(4 <i>H</i> ,6 <i>H</i>)-dione and its derivatives	63
4	Synthesis of pyrazolo[1,5- <i>a</i>][1,3,5]triazin-2,4(1 <i>H</i> ,3 <i>H</i>)-dione and its derivatives	69
5	Thymidine phosphorylase inhibitory activity of the synthesized compounds (H1-H13)	74
6	Synthesis of 5-thioxo-5,6-dihydro-4 <i>H</i> -[1,2,4]triazolo[1,5- <i>a</i>][1,3,5]triazin-7-one analogues	85
7	Synthesis of 2-thioxo-2,3-dihydro-1 <i>H</i> -pyrazolo[1,5- <i>a</i>][1,3,5]triazin-4-one analogues	89
8	Thymidine phosphorylase inhibitory activity of H5bi-H5bxix	91
9	Thymidine phosphorylase inhibitory activity of H8a-H8i and H11a-H11g	94
10	Thymidine phosphorylase inhibitory activity of H13a-H13k	96
11	Synthesis of target compounds (derivatives of H5 , H11 , H13 and compound H14)	99
12	Thymidine phosphorylase inhibitory activity of the synthesized compounds (derivatives of H5 , H11 , H13 and compound H14).	102
13	Tautomerism in 3(5)-amino-1,2,4-triazoles in DMSO- <i>d</i> 6 solution	112
14	Optimization of reaction condition of N-(3(5)-3-pyridyl-1,2,4-triazol-5(3)-yl)-N'-carbethoxythioureas	116
15	Tautomerism of N-(3(5)-aryl-1,2,4-triazol-5(3)-yl)-N'-carbethoxythioureas in DMSO- <i>d</i> 6 solution	119
16	Training set compounds with observed and predicted pIC ₅₀ values	131

17	Statistical results from CoMFA analysis	132
18	Test set compounds with observed and predicted pIC ₅₀ values	133
19	A summary of the kinetic parameters	148
20	A summary of biological activities of reference compounds (TPI and 7-DX) and synthesized TP inhibitors	173
21	Synthesis of N-(3(5)-aryl-1,2,4-triazol-5(3)-yl)-N'-carbethoxythioureas and their ¹ H NMR spectral data	193
22	Synthesis of N-(3(5)-substituted-benzyl-1,2,4-triazole-5(3)-yl)-N'-carbethoxythioureas/carbethoxyurea and their ¹ H NMR spectral data	218
23	Synthesis of N-carbethoxy-N'-(3-aryl-pyrazolyl)thiourea/urea derivatives and their ¹ H NMR spectral data	229
24	Synthesis of corresponding thiourea derivatives of pyrazole-3,5-diamine and their ¹ H NMR spectral data	243

LIST OF FIGURES

Figure		Page
1	Structures of the three isomeric forms of triazine	2
2	Structures of purine, 1,2,4-triazolo[1,5- <i>a</i>][1,3,5]triazine and pyrazolo[1,5- <i>a</i>][1,3,5]triazine	5
3	Structures of representative biologically active compounds of 1,3,5-triazine and its fused analogues	20
4	Structure of human thymidine phosphorylase	24
5	The function of thymidine phosphorylase and 2-deoxy-D-ribose in tumour development – a schematic representation	28
6	Metabolic conversion and mode of action of 5FU, an anticancer drug, and its prodrugs	37
7	Schematic representation of the human TP active site and important interactions with TPI	39
8	Structures of known TP inhibitor (TPI and 7-DX) and target compounds (a , b and c)	47
9	Structures of target compounds to be synthesized in the preliminary study	54
10	Structures of lead compounds and their IC ₅₀ values	79
11	Planned Craig plot guided structural modification of lead compounds H5b , H8 , H11 and H13	81
12	A schematic diagram describing the structure-TP inhibitory activity relationship of the 1,2,4-triazolo and pyrazolo fused triazines	105
13	Structures of 1,2,4-triazole derivatives	108
14	Correlation of ΔG for the tautomeric equilibrium of 3(5)-amino-1,2,4-triazoles with the Hammett constant (σ) of the R group	114
15	Correlation of ΔG for the tautomeric equilibrium of N-(3(5)-aryl-1,2,4-triazol-5(3)-yl)-N'-carbethoxythioureas with the Hammett constant (σ) of the R group	122

16	X-ray structure of 4-carbethoxy-1-[4-(N,N-dimethylamino)benzoyl]thiosemicarbazide	124
17	Structures of synthesized TP inhibitors used in CoMFA study	128
18	CoMFA analysis	136
19	Structures of synthesized TP inhibitors with low micromolar IC ₅₀ value	141
20	Lineweaver-Burk plots of TP inhibition by H5bxix	144
21	Lineweaver-Burk plots of TP inhibition by H5bxvii	145
22	Lineweaver-Burk plots of TP inhibition by H8i	146
23	Lineweaver-Burk plots of TP inhibition by H11g	147
24	Lineweaver-Burk plots of TP inhibition by H13a	148
25	Screening of compounds (IC _{50TP} < 30 μM) (series H5 and reference compounds) based on their inhibitory effect of MMP expression on breast cancer cell line, MDA-MB-231	152
26	Antiangiogenic effect (MMP-9 expression) of compounds (series H5 and reference compounds) on breast cancer cell line	153
27	Antiangiogenic potential (MMP expression) of selected synthesized compounds (series H11 , H8 and H13) on breast cancer cell line	154
28	Densitometry analysis of MMP expression of selected synthesized compounds (series H11 , H8 and H13) on breast cancer cell line	155
29	Antiangiogenic potential (VEGF expression) of selected synthesized compounds on breast cancer cell line	157
30	Antimetastasis potential of selected synthesized compounds on breast cancer cell line	159
31	Antiproliferative effect of compounds on breast cancer cell line	160
32	Structures of proposed compounds	177

LIST OF SCHEMES

Scheme		Page
1	Synthesis of 1,3,5-triazin-2,4-dione from 2,4-dimethoxy-1,3,5-triazine	3
2	Synthesis of 1,3,5-triazin-2,4-dione from condensation of urea with orthoester	3
3	Synthesis of 1,3,5-triazin-2,4-dione from thiourea derivatives	4
4	Synthesis of 1,3,5-triazin-2,4-dione from aromatic and aliphatic isocyanates	4
5	Synthesis of 1,2,4-triazolo[1,5- <i>a</i>][1,3,5]triazine <i>via</i> two-bond formation through (3+3) atoms heterocyclization	7
6	Synthesis of 1,2,4-triazolo[1,5- <i>a</i>][1,3,5]triazine <i>via</i> two-bond formation and (5+1) atoms heterocyclization	8
7	Synthesis of 5,7-dioxo or dithioxo analogues of 1,2,4-triazolo[1,5- <i>a</i>][1,3,5]triazine <i>via</i> two-bond formation and (5+1) atoms heterocyclization	9
8	Synthesis of 1,2,4-triazolo[1,5- <i>a</i>][1,3,5]triazine <i>via</i> one-bond formation and (6+0) atoms heterocyclization	10
9	Synthesis of 5,7-dioxo or dithioxo analogues of 1,2,4-triazolo[1,5- <i>a</i>][1,3,5]triazine <i>via</i> one-bond formation and (6+0) atoms heterocyclization	11
10	Synthesis of 2,4-dioxo-pyrazolo[1,5- <i>a</i>][1,3,5]triazine <i>via</i> two bond formation through (3+3) atoms heterocyclization	13
11	Synthesis of 2,4-dithioxo-pyrazolo[1,5- <i>a</i>][1,3,5]triazine <i>via</i> two bond formation through (4+2) atoms heterocyclization	14
12	Synthesis of 2,4-dioxo-pyrazolo[1,5- <i>a</i>][1,3,5]triazine <i>via</i> two-bond formation through (5+1) atoms heterocyclization	15
13	Synthesis of pyrazolo[1,5- <i>a</i>][1,3,5]triazine <i>via</i> one bond formation through intramolecular heterocyclization	16
14	Enzymatic reaction of thymidine phosphorylase	22
15	Synthesis of monocyclic 1,3,5-triazin-2,4-dione derivatives (H1a–H1f)	55

16	Synthesis of 2-substituted-1,2,4-triazolo[1,5- <i>a</i>][1,3,5]triazin-5,7(4 <i>H</i> ,6 <i>H</i>)-dione and its derivatives (H2, H3, H4, H5 and H6)	61
17	Synthesis of 2-benzyl-[1,2,4]triazolo[1,5- <i>a</i>][1,3,5]triazin-5,7(4 <i>H</i> ,6 <i>H</i>)-dione and its derivatives (H7, H8 and H9)	63
18	Synthesis of 7-phenyl-pyrazolo[1,5- <i>a</i>][1,3,5]triazin-2,4(1 <i>H</i> ,3 <i>H</i>)-dione and its derivatives (H10, H11 and H12)	67
19	Synthesis of (8-benzyl-4-oxo-2-thioxo-1,2,3,4-tetrahydro pyrazolo[1,5- <i>a</i>][1,3,5]triazin-7-yl)-thiourea (H13)	68
20	Synthesis of 5-thioxo-5,6-dihydro-4 <i>H</i> -[1,2,4]triazolo[1,5- <i>a</i>][1,3,5]triazin-7-one (H5bi-H5bix and H8a-H8i)	85
21	Tautomerism of 1,2,4-triazoles	86
22	Synthesis of 2-thioxo-2,3-dihydro-1 <i>H</i> -pyrazolo[1,5- <i>a</i>][1,3,5]triazin-4-one analogues (H11a-H11g)	88
23	Synthesis of (8-benzyl-4-oxo-2-thioxo-1,2,3,4-tetrahydro pyrazolo[1,5- <i>a</i>][1,3,5]triazin-7-yl)-thiourea analogues (H13a-H13k)	88
24	Synthesis of 3(5)-amino-5(3)-(het)aryl-1,2,4-triazoles (87, 91)	110
25	Tautomers of 3(5)-amino-1,2,4-triazoles	112
26	Synthesis of <i>N</i> -(3(5)-aryl-1,2,4-triazol-5(3)-yl)- <i>N'</i> -carbethoxythioureas (88, 93)	115
27	Nucleophilicity of 3(5)-amino-5(3)-2-pyridyl-1,2,4-triazoles	118
28	Synthesis of 4-carbethoxy-1-[4-(<i>N,N</i> -dimethylamino)benzoyl]thiosemicarbazide (109)	123
29	Mixed type inhibition model	142

ABBREVIATIONS

2DDR	2-deoxy-D-ribose
2DDR-1P	2-deoxy-alpha-D-ribose-1-phosphate
2DLR	2-deoxy-L-ribose
3-D	three-dimensional
5'DFUR	5-fluoro-5'-deoxyuridine
5C6-2'AIMU	5-chloro-6-(2'-aminoimidazol-1'-yl)methyluracil
5FU	5-fluorouracil
5FU	5-fluorouracil
5-HT	5-hydroxytryptophan
6A5BU	6-amino-5-bromouracil
6A5CU	6-amino-5-chlorouracil
6AT	6-aminothymine
7-DX	7-deazaxanthine
ADP	adenosine diphosphate
AEAC	6-(2-aminoethylamino)-5-chlorouracil
BVDU	5-(E)-(2-bromovinyl)-2'-deoxyuridine
CAM	chorioallantoic membrane
CB	cannabinoid
CDK2	cyclin-dependent kinase type 2
CNS	central nervous system
CoMSIA	molecular similarity indices analysis
Cpd	compound
CRF receptor	corticotrophin releasing hormone receptor

DBU	diazabicycloundecene
DFCR	5'-deoxy-5-fluorocytidine
DFUR	5'-deoxy-5-fluorouridine
DMF	dimethylformamide
DMSO	dimethyl sulfoxide
DNA	deoxyribonucleic acid
DPD	dihydropyrimidine dehydrogenase
dThd	thymidine
EC	enzyme commission
ECM	extracellular matrix
EI	enzyme-Inhibitor complex
ELISA	enzyme-linked immunosorbent assay
EPC	endothelial progenitor cells
ESI	enzyme-Substrate-Inhibitor complex
ESI	electrospray ionization
FAK	focal adhesion kinase
FDHU	5-fluorodihydrouracil
FdUMP	5-fluorodeoxyuridine monophosphate
FdUrd	5-fluorodeoxyuridine
FUDP	5-fluorouridine diphosphate
FUMP	5-fluorouridine monophosphate
FUrd	5-fluorouridine
FUTP	5-fluorouridine triphosphate
HO-1	heme oxygenase-1
HPLC	high-performance liquid chromatography

HUVECs	human umbilical vein endothelial cells
IC₅₀	concentration of inhibitor that causes 50% of Inhibition
IFN	interferons
IL	interleukin
ISRE	interferon-sensitive response element
KIN59	5'-O-trityl-inosine
Kpi	phosphate
LOO	leave-one-out
MMPs	matrix metalloproteinase
MNGIE	mitochondrial neurogastrointestinal encephalomyopathy
mRNA	messenger RNA
MS	mass spectrometry
MTT	3-(4,5-dimethylthiazol-2-yl)-2,5-diphenyl tetrazolium bromide
MW	microwave
NF_κB	nuclear factor-kappaB
NMR	nuclear magnetic resonance
OPRT	orotate phosphoribosyl transferase
PDE	phosphodiesterase
PD-ECGF	platelet-derived endothelial cell growth factor
PMA	phorbol myristate acetate
QSAR	quantitative structure–activity relationship
RNA	ribonucleic acid
SD	standard deviation
SDS-PAGE	sodium dodecyl sulphate –poly acrylamide gel electrophoresis
siRNA	small interfering RNA

TAM	tumour-associated macrophages
TFT	5-trifluorothymidine
TFT	trifluorothymidine
TIMP	tissue inhibitor of metalloproteinases
TK	thymidine kinase
TLC	thin layer chromatography
TNF	tumour necrosis factor
TNF-α	tumour necrotic factor-alpha
TP	thymidine phosphorylase
TPI	5-chloro-6-[1-(2-iminopyrrolidinyl)methyl]uracil hydrochloride
TS	thymidylate synthase
UK	uridine kinase
UP	uridine phosphorylase
UV	ultra violet
VEGF	vascular endothelial growth factor
XO	xanthine oxidase

Chapter 1

Introduction - Review of 1,3,5-triazin-2,4-diones, Thymidine Phosphorylase and 3D-QSAR study

Introduction

The triazine is among the oldest known heterocyclic organic compound. Three isomeric forms of triazine are distinguishable and they are referred to as 1,2,3-triazine (**1**), 1,2,4-triazine (**2**) and 1,3,5-triazine (**3**) (Figure 1). Among these three possible triazine isomers, the 1,3,5-triazine, also known as symmetric or *s*-triazine, is found in the chemical structures of a wide range of therapeutic agents that exhibit antifolate¹, antibacterial², antiherpetic³ and antihypertensive activities⁴. Therefore, there is an interest in developing new methods for incorporating the 1,3,5-triazine scaffold into new generation of bioactive compounds in drug discovery projects. In this first introductory section, a mini review on the reported synthetic procedures and biological activities of 1,3,5-triazin-2,4-dione and its fused derivatives will be described.

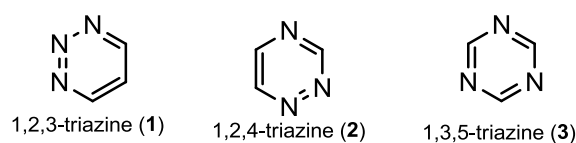


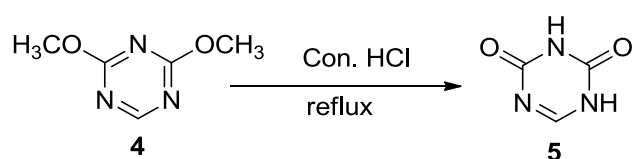
Figure 1. Structures of the three isomeric forms of triazine

1.1 Synthesis of 1,3,5-triazin-2,4-dione and its fused derivatives

The synthesis of 1,3,5-triazin-2,4-dione and its fused analogues *viz.* 1,2,4-triazolo[1,5-*a*][1,3,5]triazine and pyrazolo[1,5-*a*][1,3,5]triazine can be achieved *via* various different synthetic strategies using different starting materials. A complete listing of all possible synthetic routes is beyond the scope of this mini review. Therefore, a review of selected reported synthetic procedures related to 1,3,5-triazin-2,4-dione and its fused derivatives will be presented in the following sub-sections.

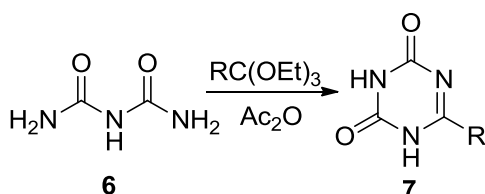
1.1.1 Synthesis of 1,3,5-triazin-2,4-dione

Several synthetic strategies have been employed to prepare 1,3,5-triazin-2,4-diones. In 1959, Flament et al,⁵ developed a method to synthesize 1,3,5-triazin-2,4-dione (**5**) *via* the dealkylation of 2,4-dimethoxy-1,3,5-triazine (**4**) in refluxing aqueous medium in the presence of concentrated hydrochloric acid (Scheme 1). Compound **5** was exclusively isolated from the reaction mixture with 95 % yield.



Scheme 1. Synthesis of 1,3,5-triazin-2,4-dione from 2,4-dimethoxy-1,3,5-triazine

Alternatively, derivatives of 1,3,5-triazin-2,4-dione (**7**) could also be successfully synthesized by the condensation of urea (**6**) with orthoester (Scheme 2).

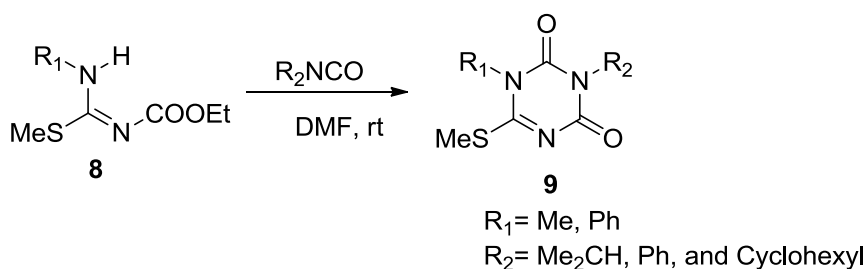


Scheme 2. Synthesis of 1,3,5-triazin-2,4-dione from the condensation of urea with orthoester

In 1963, Piskala et al⁶ synthesized 1,3,5-triazin-2,4-dione derivatives by the treatment of urea with ethyl orthoformate in the presence of acetic anhydride with excellent yield (90 %). Using different substituted orthoesters, this reaction condition allowed the introduction of different functional groups at position C6 of 1,3,5-triazine.

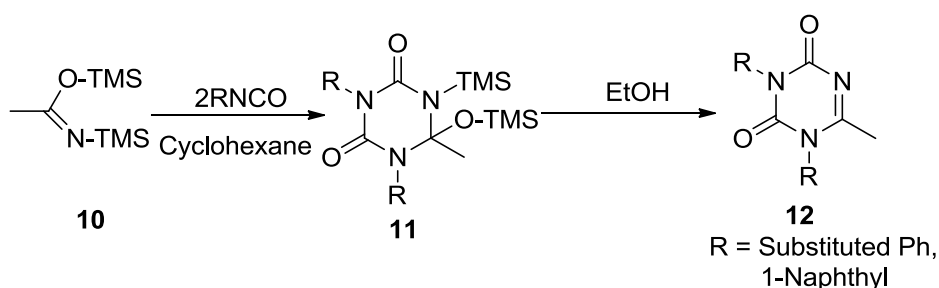
The reaction of thiourea derivatives with an isocyanate could be an alternative route to the synthesis of 1,3,5-triazin-2,4-dione too. In 1984, Sanemitsu et al⁷ reported that

the reaction between N-ethoxycarbonyl-s-methylisothioureas (**8**) and isocyanates in DMF at room temperature could afford 1,3,5-triazin-2,4-dione (**9**) with reasonable good yield (Scheme 3). Using this synthetic methodology, incorporation of various substituents at positions N3 and N5 of 1,3,5-triazin-2,4-dione could be possible by using different starting materials substituted with aromatic and aliphatic groups.



Scheme 3. Synthesis of 1,3,5-triazin-2,4-dione from thiourea derivatives

In addition, Kantlehner et al.⁸ established a method using a range of substituted aromatic isocyanates with N,O-bis(trimethylsilyl)acetamide to produce an intermediate, silylated azauracil (**11**) which after desilylation with alcohol would afford 1,3,5-triazin-2,4-dione (**12**) (Scheme 4).



Scheme 4. Synthesis of 1,3,5-triazin-2,4-dione from aromatic and aliphatic isocyanates

1.1.2 Synthesis of fused 1,3,5-triazin-2,4-dione and its thioxo analogues

Section 1.1.1 described the methods for synthesizing monocyclic 1,3,5-triazin-2,4-dione. Herein, the synthetic procedure of 1,2,4-triazolo and pyrazolo fused 1,3,5-triazin-2,4-dione and their thioxo derivatives will be discussed. 1,2,4-triazolo[1,5-*a*][1,3,5]triazine (**14**) and pyrazolo[1,5-*a*][1,3,5]triazine (**15**), also known as 5-azapurine and 5-aza-9-deazapurine respectively, are the isosteres of purine (Figure 2). As a matter of fact, it is reported that derivatives of these scaffold would target the purinergic signalling receptors and enzymes involved in the metabolism of biogenic purines. Therefore, development of 1,2,4-triazolo[1,5-*a*][1,3,5]triazine and pyrazolo[1,5-*a*][1,3,5]triazine derivatives as biological active agents has drawn considerable interest in recent years. Several methods were developed and reported for the synthesis of 1,2,4-triazolo[1,5-*a*][1,3,5]triazine⁹ and pyrazolo[1,5-*a*][1,3,5]triazine¹⁰. These methods are broadly classified as A) annulation of the triazine ring onto a triazole or pyrazole scaffold; B) annulation of the triazole or pyrazole ring onto a triazine scaffold; C) concurrent formation of both rings; D) synthesis *via* ring transformation reactions. In the following sections, the methods that generate triazolo and pyrazolo fused 1,3,5-triazin-2,4-dione and their thioxo analogues will be elaborated and representative examples will be included.

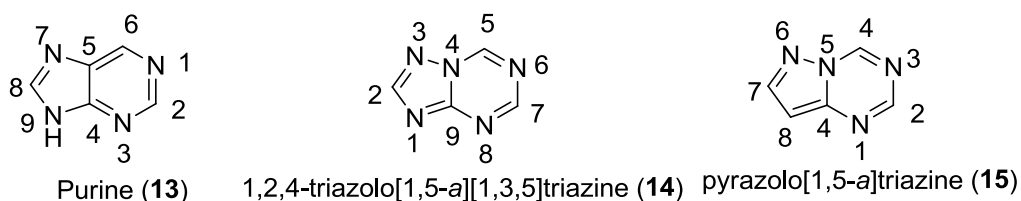


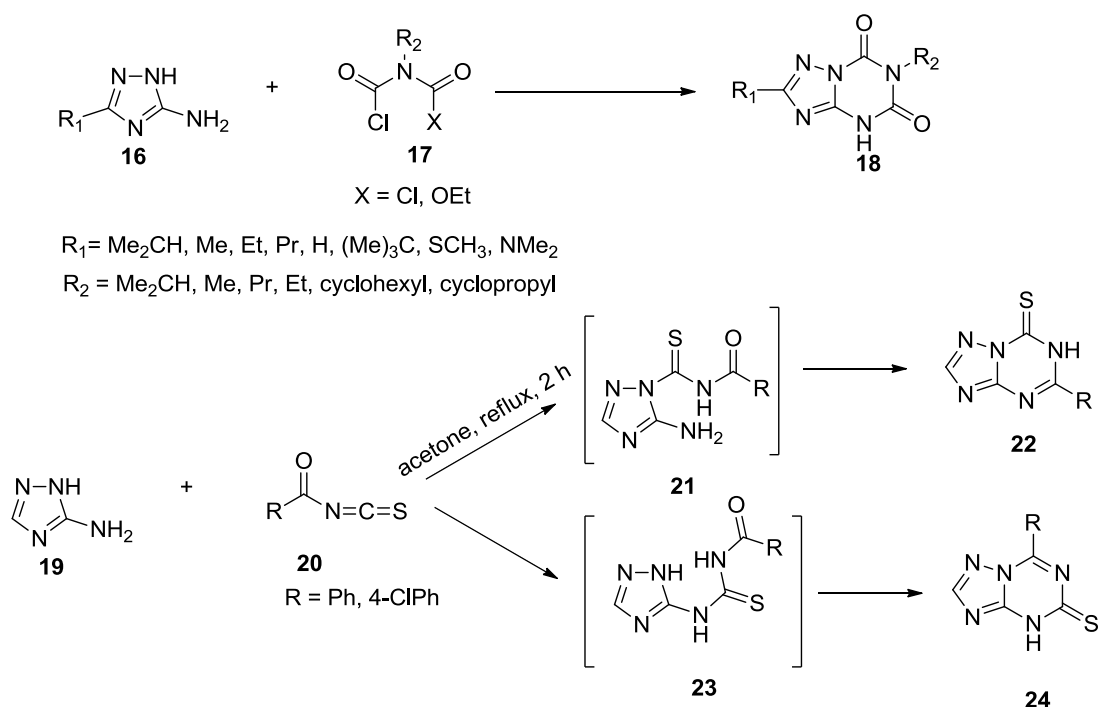
Figure 2. Structures of purine, 1,2,4-triazolo[1,5-*a*][1,3,5]triazine and pyrazolo[1,5-*a*][1,3,5]triazine

1.1.2.1 Synthesis of 1,2,4-triazole fused 1,3,5-triazin-2,4-dione analogues

The 1,2,4-triazolo[1,5-*a*][1,3,5]triazine scaffold was first described by Pellizzari and Roncaglilo in 1901¹¹. However, the original structure was only established recently by X-ray crystallography¹². Although many different ways have been reported on the construction of 1,2,4-triazolo[1,5-*a*][1,3,5]triazine, our target scaffolds *viz.* 1,2,4-triazolo fused 1,3,5-triazin-2,4-dione and thioxo analogues were synthesized extensively *via* annulation of the 1,3,5-triazine ring onto a 1,2,4-triazole scaffold. In addition, special attention was given to the ways for introducing different substituents at various positions around the target scaffold.

Two-bond formation through (3+3) atoms heterocyclization

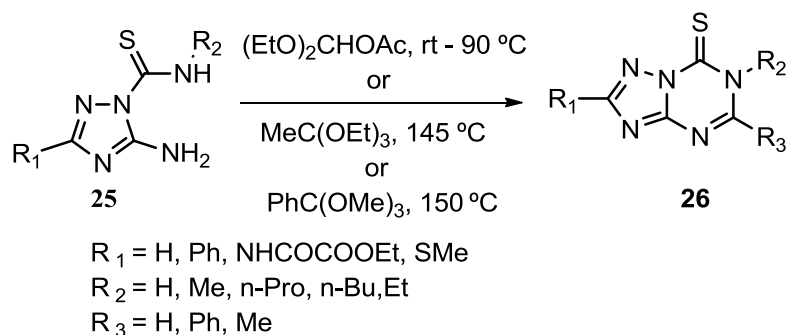
Several reports have described that a number of electrophilic reagents may be employed as triatomic synthons which will provide the C-N-C fraction for annulation of the 1,3,5-triazine ring onto a 3(5)-amino-1,2,4-triazoles. For example, the synthesis of 5,7-dioxo-1,2,4-triazolo[1,5-*a*][1,3,5]triazines (**18**) could be achieved *via* the condensation of 3(5)-amino-1,2,4-triazoles (**16**) with **17**¹³. In addition, it is reported that reaction of **19** with N-royl isothiocyanates (**20**) in refluxing acetone led to the formation of 7-thioxo substituted-1,2,4-triazolo[1,5-*a*][1,3,5]triazines¹⁴ (**22**). In this reaction, it has been postulated that after initial attack of endocyclic nitrogen N1 by isothiocyanate, it formed an intermediate (**21**) affording target compound (**22**) after further rearrangement. However, isothiocyanate has been reported to react with the exocyclic nitrogen upon heating and thus gave rise to different intermediates (**23**) which underwent spontaneous rearrangement resulting in the formation of the isomeric product (**24**)⁹ (Scheme 5).



Scheme 5. Synthesis of 1,2,4-triazolo[1,5-*a*][1,3,5]triazine *via* two-bond formation through (3+3) atoms heterocyclization

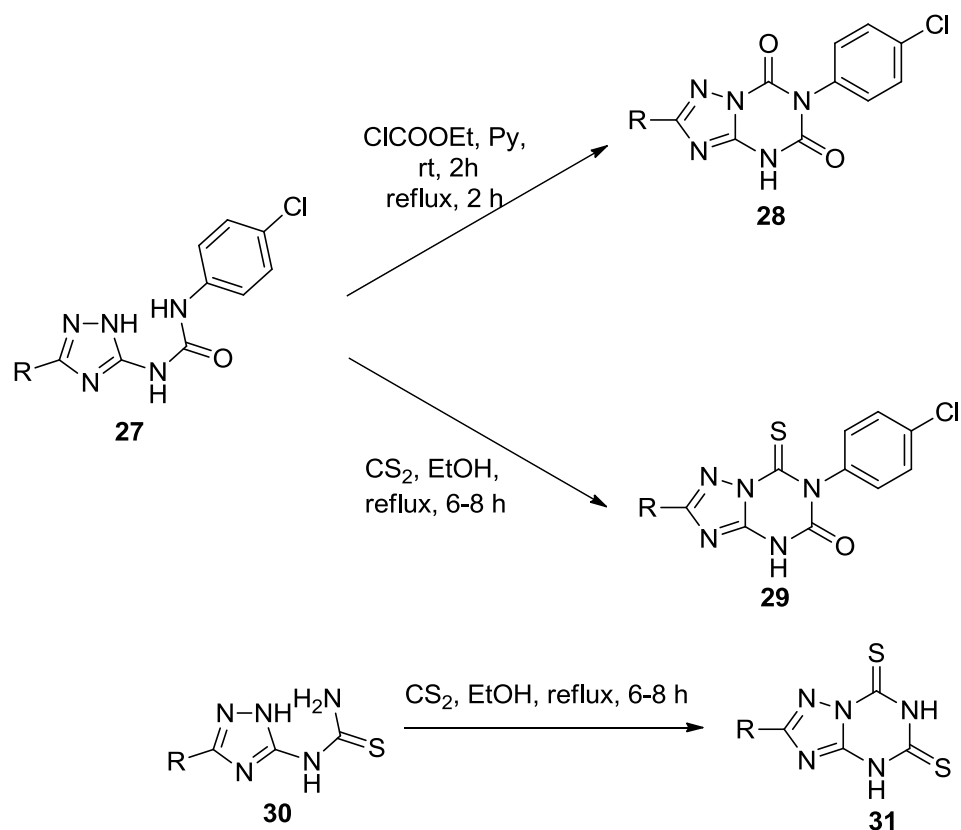
Two-bond formation through (5+1) atoms heterocyclization

The synthesis of 7-oxo or thioxo analogues of 1,2,4-triazolo[1,5-*a*][1,3,5]triazines has been achieved *via* two-bond formation through (5+1) atoms heterocyclization using 5-amino-1,2,4-triazoles having carboxamidic or carbothioamidic moiety at N1. In this category of reaction, one carbon inserting reagents like triethyl orthoesters, diethoxy methyl acetate, formic acid, ethyl chloroformate have been employed depending on the reaction conditions used^{9,15-17}. The reaction of 5-amino-1,2,4-triazolo-1-carbothiamides (**25**) with triethyl orthoester or diethoxymethyl acetate under different conditions which produced 7-thio-oxo[1,2,4]triazolo[1,5-*a*][1,3,5]triazines (**26**) (Scheme 6)¹⁵ represents this category of synthesis. These kind of reactions help to incorporate a wide range of functional groups including aromatic and aliphatic moieties at positions C2, C5 and N7 of the triazolo fused triazine scaffold depending on the starting materials used.



Scheme 6. Synthesis of 1,2,4-triazolo[1,5-*a*][1,3,5]triazine *via* two-bond formation and (5+1) atoms heterocyclization

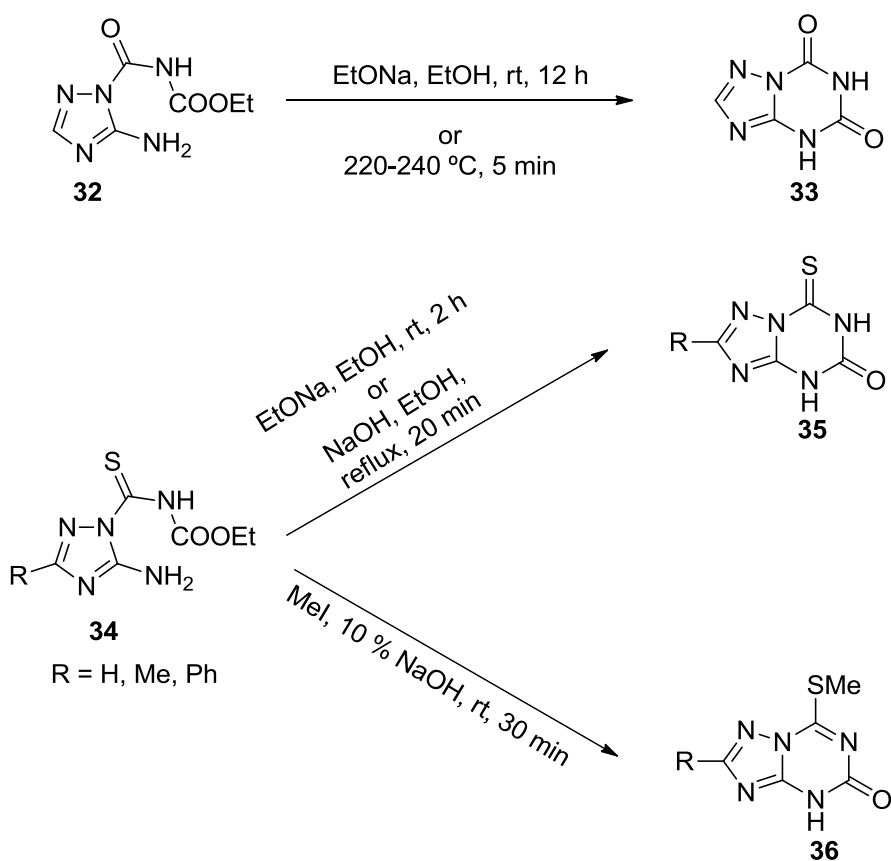
Alternatively, 5,7-dioxo or dithioxo analogues of triazolo fused triazine can also be synthesized *via* the use of 1,2,4-triazoles having -N-C-N appendage (ureas and thioureas) at C3(5). In this case, one carbon atom inserting synthons like triethyl orthoformate¹⁸, trichloroacetonitrile¹⁹, phosgene²⁰, carbon disulfide²¹, ethylchloroformate²² and diethyl carbonate²³ have been reported to be successful in producing the fused triazine ring. Previously, it has been described that the heterocyclization of N-(1,2,4-triazol-3(5)-yl)-N'-(4-chlorophenyl)ureas (**27**) using ethyl chloroformate or carbon disulfide would result in the formation of 5,7-dioxo or 5-oxo-7-thioxo substituted 1,2,4triazolo[1,5-*a*][1,3,5]triazines (**28** and **29**) respectively^{22, 24}. Similarly, treatment of N-(1,2,4-triazol-3(5)-yl)thioureas (**30**) with carbon disulfide afforded 2-aryl-5,7-dithioxo[1,2,4]triazolo[1,5-*a*][1,3,5]triazines (**31**)²¹ (Scheme 7).



Scheme 7. Synthesis of 5,7-dioxo or dithioxo analogues of 1,2,4-triazolo[1,5-*a*][1,3,5]triazine *via* two-bond formation and (5+1) atoms heterocyclization

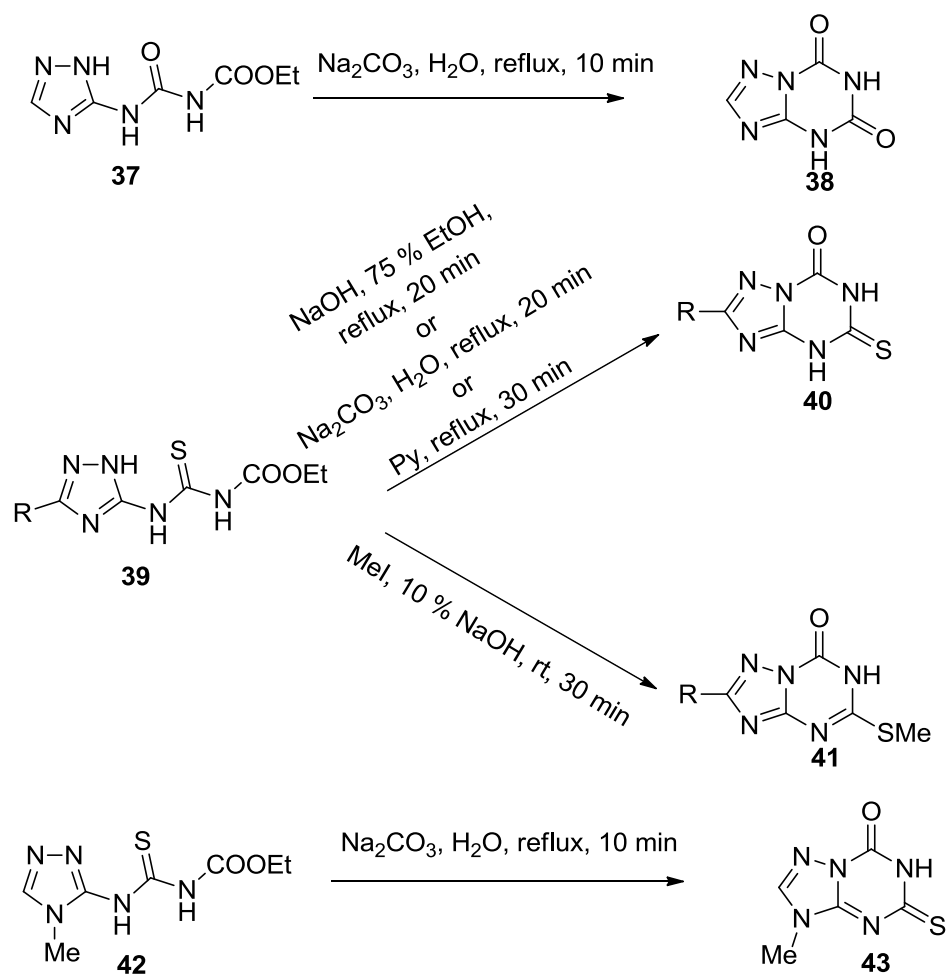
One-bond formation through (6+0) atoms intramolecular heterocyclization

In alkaline medium, 5-amino-1,2,4-triazoles having -N-C-N appendage (carbethoxycarbamoyl (**32**) and carbethoxythiocarbamoyl (**34**)) at N1 underwent intramolecular heterocyclization and afforded 5,7-dioxo[1,2,4]-triazolo[1,5-*a*][1,3,5]triazines (**33**) and 5-oxo-7-thioxo[1,2,4]-triazolo[1,5-*a*][1,3,5]triazines (**35**) respectively^{25,26, 27} (Scheme 8). In this reaction condition, 3(5)-amino-1,2,4-triazole was commonly used as 1,2,4-triazole scaffold. However, 3(5) amino triazole substituted with aromatic (phenyl) or aliphatic (methyl) moiety could also be employed to achieve corresponding target compounds.



Scheme 8. Synthesis of 1,2,4-triazolo[1,5-*a*][1,3,5]triazine *via* one-bond formation and (6+0) atoms heterocyclization

Intramolecular cyclization of N-(1,2,4-triazol-3(5)-yl)-N'-carbethoxyurea (**37**) in aqueous solution of sodium carbonate produced 5,7-dioxo-[1,2,4]triazolo[1,5-*a*][1,3,5]triazines (**38**)²⁷ (Scheme 9). This reaction is an example of the formation of 5,7-dioxo substituted 1,2,4-triazolo[1,5-*a*][1,3,5]triazines through intramolecular heterocyclization of 1,2,4-triazoles that have a -N-C-N-C appendage attached at position N5. Similarly, N-(1,2,4-triazol-3(5)-yl)-N'-carbethoxyurea (**39**) and 4 methyl substituted carbethoxyurea (**42**) could be cyclised to 7-oxo-5-thioxo-[1,2,4]triazolo[1,5-*a*][1,3,5]triazine derivatives (**40** and **43**) respectively in alkaline medium²⁶⁻²⁸. The corresponding 5-methylthio substituted compounds (**41**) were prepared using iodomethane in aqueous alkali²⁶.



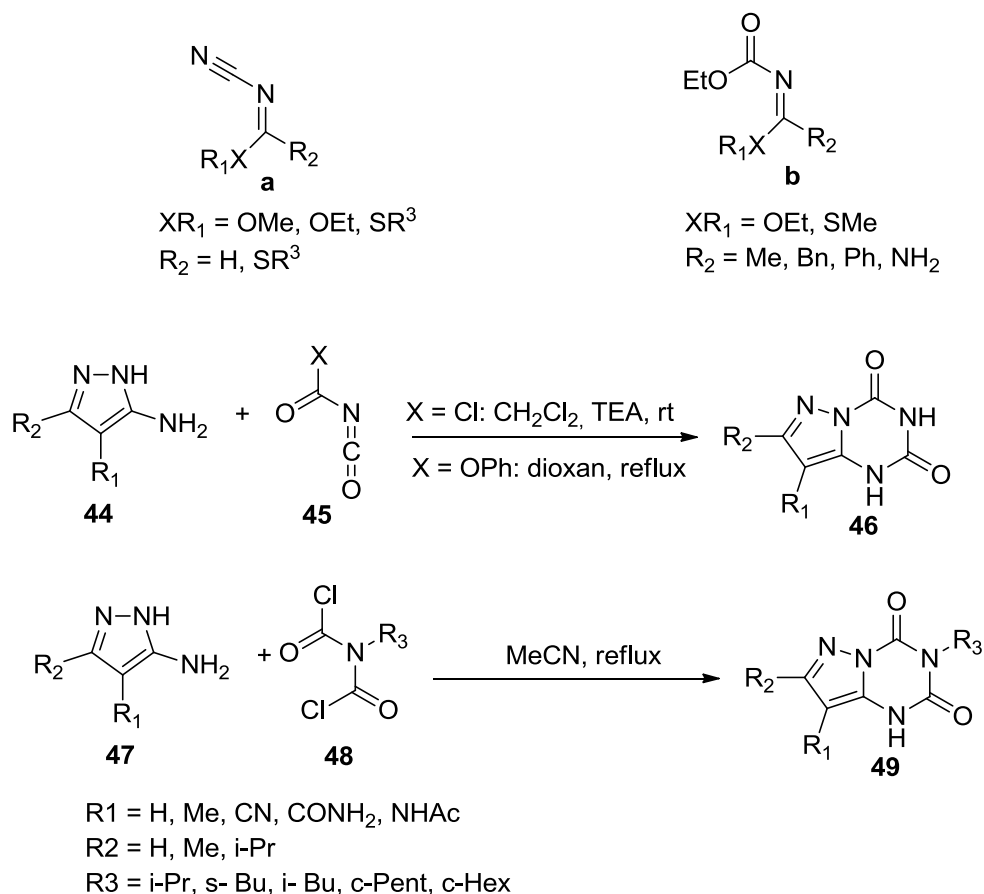
Scheme 9. Synthesis of 5,7-dioxo or dithiooxo analogues of 1,2,4-triazolo[1,5-*a*][1,3,5]triazine *via* one-bond formation and (6+0) atoms heterocyclization

1.1.2.2 Synthesis of pyrazolo fused 1,3,5-triazin-2,4-dione analogues

The pyrazolo[1,5-*a*][1,3,5]triazine scaffold was first synthesized by Checchi and Ridi in 1957²⁹. As described, although several methods are adopted to prepare pyrazolo[1,5-*a*][1,3,5]triazine scaffold, the synthesis of pyrazolo fused 1,3,5-triazin-2,4-dione and its thio-oxo analogues was achieved *via* the annulation of the triazine ring onto a pyrazole scaffold. These methods are described as the following sections.

Two bond formation through (3+3) atoms heterocyclization

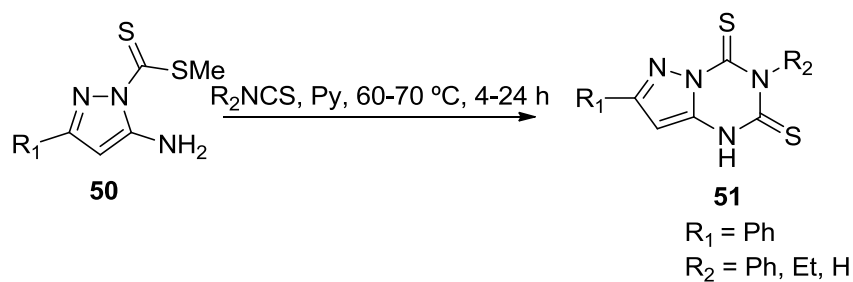
The reaction between triatomic C-N-C synthons *viz.* the substituted imidates (N-cyano-(**a**), and N-carbethoxyimidates (**b**))¹⁰ with 3(5)-aminopyrazoles has been shown to afford 2,4-dioxo analogues of pyrazolo[1,5-*a*][1,3,5]triazine with a wide range of functionalizations. It is reported that the reaction of substituted 3(5)-aminopyrazoles (**44**) with chlorocarbonyl isocyanates or phenoxy carbonyl isocyanates (**45**) gave 2,4-dioxo-pyrazolo[1,5-*a*][1,3,5]triazine (**46**)³⁰. This synthetic scheme has been employed to introduce substituents at C7 and C8 of the fused ring system. Furthermore, 3-alkyl-2,4-dioxopyrazolo[1,5-*a*][1,3,5]triazine (**49**) was reported to be synthesized *via* the condensation of 3(5)-aminopyrazoles (**47**) and N-alkyl bis(chloroformyl)amines (**48**)³¹ (Scheme 10). Depending on the substituents present in 3(5)-aminopyrazoles, various substituents could be introduced at positions C7 and C8 of pyrazolo[1,5-*a*][1,3,5]triazine scaffold. In addition, using different substituted bis(chloroformyl)amines, incorporation of different moieties including cycloalkyl, and branched alkyl chain at the position N3 of the fused ring could be achieved through this reaction.



Scheme 10. Synthesis of 2,4-dioxo-pyrazolo[1,5-*a*][1,3,5]triazine via two bond formation through (3+3) atoms heterocyclization

Two bond formation through (4+2) atoms heterocyclization

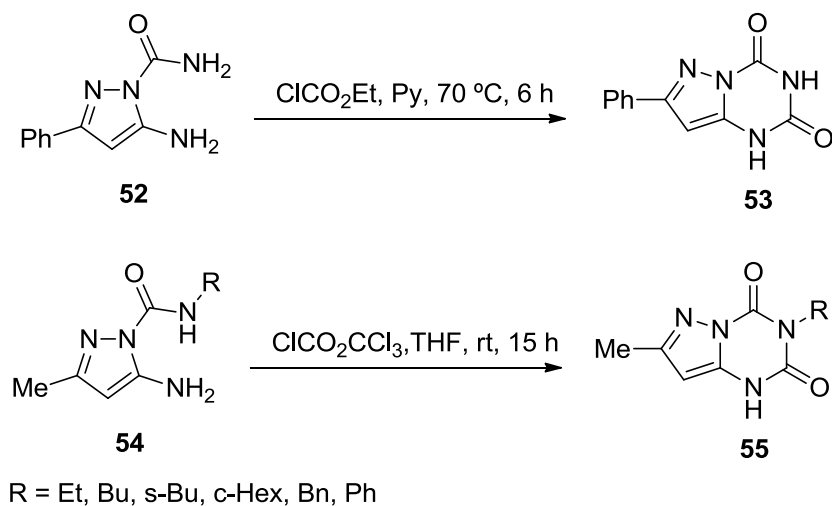
The thioxo analogues of the pyrazolo fused triazin-2,4-dione are prepared by two bond formation through (4+2) atoms heterocyclization. For example, the 2,4-dithioxo-pyrazolo[1,5-*a*][1,3,5]triazine (**51**) could be produced by heterocyclization of methyl 5-amino-3-arylpyrazole-1-carbodithioates (**50**) with cyanamide or isothiocyanates^{32, 33}(Scheme 11). Using different types of cyanamide or isothiocyanates, this reaction condition allows the introduction of aliphatic or aromatic functional group at position N3 of the fused ring.



Scheme 11. Synthesis of 2,4-dithioxo-pyrazolo[1,5-*a*][1,3,5]triazine *via* two bond formation through (4+2) atoms heterocyclization

Two bond formation through (5+1) atoms heterocyclization

The reaction of 5-aminopyrazoles having C-N appendage at N1 with one carbon inserting reagent can generate 2,4-dioxo substituted pyrazolo[1,5-*a*][1,3,5]triazine derivatives with diverse functionalities. One carbon inserting reagents that can be used for this reaction include orthoesters³⁴⁻³⁶, diethoxy methyl acetate³⁵, phenyl isocyanide dichloride³⁶ and diphosgene³⁷. It is reported that heating of 5-amino-1-carbonyl-3-phenylpyrazole (**52**) with ethylformate in pyridine resulted in the formation of 2,4-dioxo-7-phenylpyrazolo[1,5-*a*][1,3,5]triazine (**53**)³². Analogously, the synthesis of 3-substituted 2,4-dioxo-7-methylpyrazolo[1,5-*a*][1,3,5]triazine (**55**) could be achieved by reacting aminopyrazole (**54**) with diphosgene³⁷ (Scheme 12).

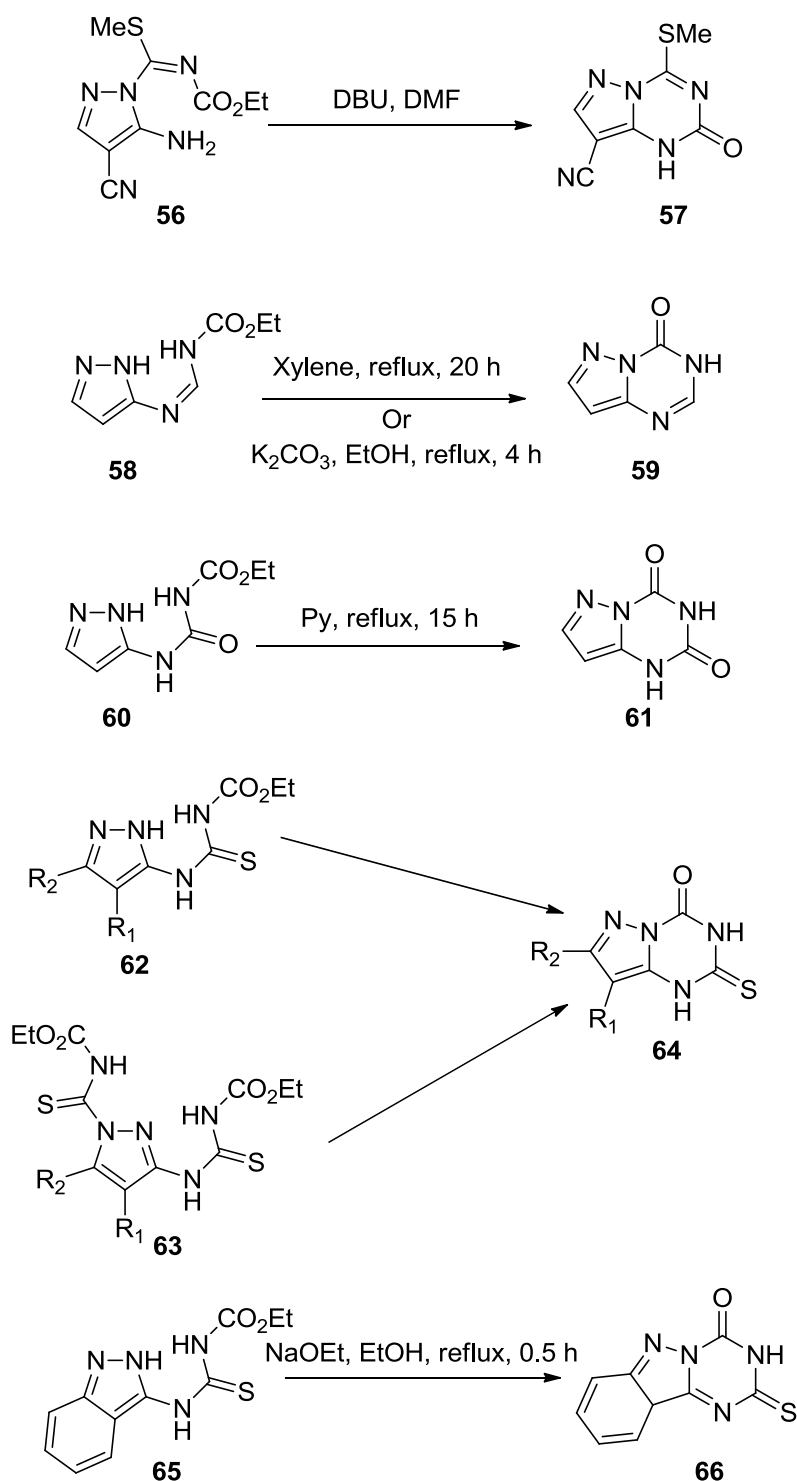


Scheme 12. Synthesis of 2,4-dioxo-pyrazolo[1,5-*a*][1,3,5]triazine *via* two-bond formation through (5+1) atoms heterocyclization

One bond formation through intramolecular heterocyclization

In alkaline medium, pyrazole having C-N-C appendage at N1 or a N-C-N-C appendage at C3(5) may undergo intramolecular heterocyclization to yield a wide range of 2,4-dioxo derivatives of pyrazolo[1,5-*a*][1,3,5]triazine. The heterocyclization of aminopyrazole (**56**) in the presence of DBU led to the formation of 8-cyano-4-methylthio-2-oxo pyrazolo[1,5-*a*][1,3,5]triazine (**57**)³⁸. On the other hand, 5-aza-9-deazahypoxanthine (**59**) was successfully synthesized by heating of N-carbethoxy-N⁷-(3(5)-pyrazolyl)formamidine (**58**) in the presence of a base or in xylene³⁹. In a similar way, Capuano and Schrepfer developed methods to synthesize 5-aza-9-deaxanthine (**61**) from N-carbethoxy-N⁷-(3(5)-pyrazolyl)urea (**60**)⁴⁰. Several reaction conditions were established, such as reflux at 180 °C⁴¹, heating in pyridine or triethylamine²⁸ and treatment with ammonium hydroxide³⁸, sodium hydroxide⁴¹, sodium methoxide⁴², sodium ethoxide⁴³ or potassium carbonate¹⁰ for heterocyclization of N-carbethoxythioureas (**62** and **63**) that resulted in the formation of compound **64**. A similar kind of reaction of intramolecular heterocyclization of N-carbethoxy-N⁷-

indazolylthiourea (**65**) was developed and reported⁴⁴, and this reaction scheme gave rise to a fused tricyclic compound instead (Scheme 13).



Scheme 13. Synthesis of pyrazolo[1,5-*a*][1,3,5]triazine *via* one bond formation through intramolecular heterocyclization

In the above section, a variety of effective methods for the preparation of 1,3,5-triazin-2,4-dione and its fused analogues have been reported. Several methods utilizing biurets, urea derivatives and substituted acetamides as starting materials were found to be practical for the construction of the 1,3,5-triazin-2,4-dione derivatives. In addition, the annulation of the 1,3,5-triazine ring onto a 1,2,4-triazole and/or pyrazole scaffold has been observed as convenient synthetic approaches to afford 1,2,4-triazolo and/or pyrazolo fused 1,3,5-triazin-2,4-dione and its thioxo analogues. Several reports have demonstrated that the 1,3,5-triazin-2,4-dione and its fused scaffolds have been utilized for the design of biologically active compounds exhibiting wide spectrum of activity ranging from pesticides to chemotherapeutic agents. In the following section, the reported biological effects of the 1,3,5-triazin-2,4-dione and its fused analogues will be described.

1.1.3 Applications of 1,3,5-triazine and its fused analogues in medicine and agriculture

It was mentioned earlier that derivatives of 1,3,5-triazin-2,4-diones have potential herbicidal activity. It is claimed that hexazinone (**67**)⁴⁵ is a potent herbicide, effective against annual and biennial weeds. In contrast, 1,2,4-triazolo[1,5-*a*][1,3,5]triazine, the fused structure of 1,3,5-triazine, is identified as an important scaffold in medicinal chemistry as its derivatives exhibited diverse biological activities (Figure 3). The derivatives of 5-amino-1,2,4-triazolo[1,5-*a*][1,3,5]triazine (**68**) has been found to be one of the most effective and selective class of adenosine receptor inhibitors⁴⁶⁻⁴⁹. As a result, these derivatives are claimed to be useful for the treatment of depression, anxiety, cerebrovascular disorder and parkinson's disease⁹. Due to structural similarity with purine, compounds having 1,2,4-triazolo[1,5-*a*][1,3,5]triazine scaffold

may interfere with the effect of biological purines (i.e. adenosine, guanine and xanthine). The metabolism of xanthine may be affected by some derivatives (**69**) through the inhibition of xanthine oxidase⁵⁰. As a matter of fact, some of compounds (**70**) are reported to be potent bronchodilator⁹. In addition, few derivatives show activity against the disease associated with inflammation and eosinophilia⁹. Furthermore, the 5,7-diaryl substituted derivatives (**71**) of 1,2,4-triazolo[1,5-*a*][1,3,5]triazine have promising antioxidant and antiproliferative potential⁵¹. Besides these activities, the derivatives of this scaffold are used as antibacterial, antifungal agents^{21, 52, 53} and herbicides in agriculture⁹.

On the other hand, due to structural similarity with purines, pyrazolo[1,5-*a*][1,3,5]triazine provides a rational design of medicinally useful compounds that may target the receptors and enzymes of biogenic purines producing diverse biological outcomes (Figure 3). Robins et al⁵⁴ reported 8-phenyl-5-aza-9-deazahypoxanthine (**72**) as XO inhibitor which is used in the treatment of hyperuricemia, particularly for gout attack. Substituted aminopyrazolo[1,5-*a*][1,3,5]triazine (**73**) has been reported to inhibit type 2 cyclin-dependent kinase (CDK2) which regulates cell cycle and thus shows antiproliferative activity¹⁰. Some compounds (**74**) bearing pyrazolo[1,5-*a*][1,3,5]triazine scaffold are identified as phosphodiesterase (PDE) inhibitors and are used for the treatment of autoimmune and inflammatory diseases⁵⁵. It is also reported that some pyrazolo[1,5-*a*][1,3,5]triazine derivatives (**75**) are able to inhibit bacterial DNA gyrase and therefore used as antibacterial agents⁴². In addition to these enzymes based activities, a number of pyrazolo[1,5-*a*][1,3,5]triazine derivatives targets several G-protein coupled receptors including adenosine, P2Y₁, corticotrophin-releasing factor, neuropeptide Y, 5-HT, cannabinoid and angiotensin receptors. Compound (**76**) is reported to exert A_{2A} adenosine receptor inhibitory activity⁵⁶ and compound

(77) has shown P2Y₁ associated ADP-induced platelet aggregation in *in vitro* and *in vivo* models⁵⁷. Some derivatives (78) of pyrazolo[1,5-*a*][1,3,5]triazine are believed to act as antagonist of CRF receptor and may be employed for the treatment of anxiety and mood disorders⁵⁸. Furthermore, 4-amino-8-aryl-2,7-dimethylpyrazolo[1,5-*a*][1,3,5]triazines are claimed to be the modulators of neuropeptide Y₁ receptor⁵⁹. In addition, some compounds are known to target cannabinoid (CB) receptor and they are used as therapeutic agent for CNS disorder⁶⁰.

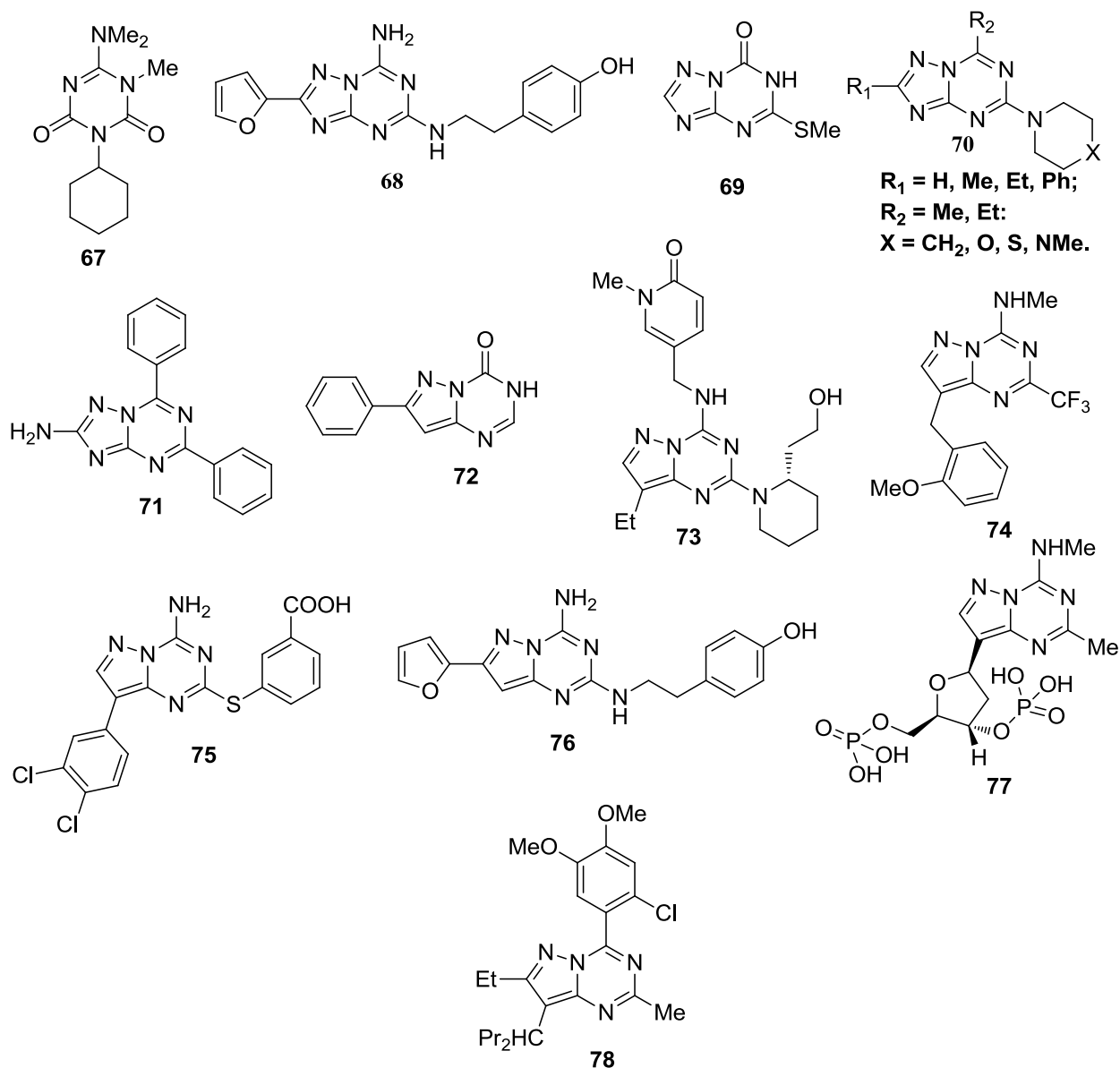


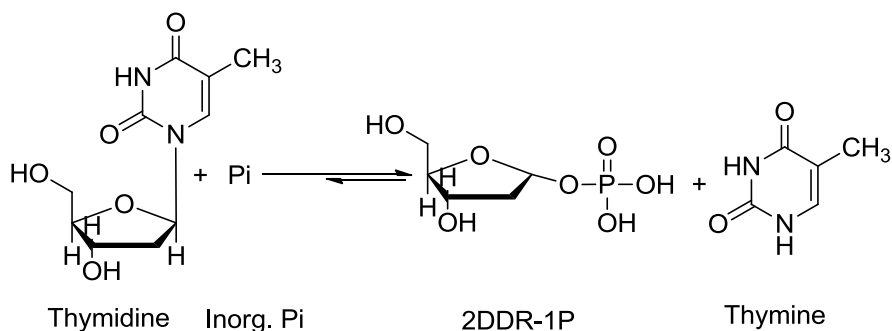
Figure 3. Structures of representative biologically active compounds of 1,3,5-triazine and its fused analogues

In this section, a short summary on the therapeutic effects of the derivatives of 1,3,5-triazine and its fused analogues is highlighted. It is revealed that although 1,3,5-triazine is found in many bioactive compounds either as monocyclic or triazolo and pyrazolo fused forms, a limited examples of biological effects of the 1,3,5-triazin-2,4-diones and its triazolo and/or pyrazolo fused analogues have been reported in the literature. As discussed, although significant efforts have been made to explore

exciting range of biological activities of 1,3,5-triazine and its fused analogues, the inhibitory activity of this scaffold against thymidine phosphorylase (TP) and its associated angiogenesis effects has not yet been established. Therefore, this field is open as a subject for further detail investigation. The following few sections will discuss the enzyme TP and its inhibitors known to date.

1.2 Thymidine phosphorylase (TP) as a target of drug design

During the last few decades, the target based drug design for anticancer therapy has met with increasing interest. In this approach, medicinal chemists identify and choose to interfere with a protein target molecule that plays a critical role in DNA replication or is involved in vital biochemical pathways. Initially, the natural ligand or substrate of this protein is modified structurally to generate lead compounds that can exhibit inhibition, antagonism or agonistic effect towards the identified target depending upon the intended therapeutic outcomes. This approach has produced rationally designed inhibitors of dihydrofolate reductase, thymidylate synthase, purine nucleoside phosphorylase, glycinamide ribonucleotide formyltransferase and matrix metalloproteases that can either inhibit DNA replication or block critical biochemical pathways resulting in the prevention of growth of the cancerous cells. Continuous efforts in this field, have discovered thymidine phosphorylase (TP, EC 2.4.2.4) as a potential therapeutic target in cancer therapy in 1954⁶¹. It catalyses the reversible phosphorolysis of thymidine-2'-deoxyuridine and their analogues to 2-deoxy-alpha-D-ribose-1-phosphate (2DDR-1P) and respective bases ⁶²(Scheme 14). It also acts in the salvage pathway of pyrimidine nucleotides by transferring the deoxyribosyl moiety between pyrimidine bases, resulting in the formation of a new pyrimidine nucleoside ⁶³.



Scheme 14. Enzymatic reaction of thymidine phosphorylase.

Although this reaction is reversible, the main enzymatic activity is catabolic in nature. The reason being the kinetic constants do not favour the synthetic reaction and the cells also lack sufficient concentration of 2DDR-1P^{64,65}. It has low substrate specificity. Besides its natural substrate, this enzyme can also recognize several pyrimidines or pyrimidine nucleosides that have potential antiviral and/or antitumoral activity *viz.* 5-(E)-(2-bromovinyl)-2'-deoxyuridine (BVDU)⁶⁶, 5-trifluorothymidine (TFT)⁶⁷, 5-fluorouracil (5FU)⁶⁸, and 5-fluoro-5'-deoxyuridine (5'DFUR), an intermediate metabolite of capecitabine⁶⁹. It was reported that anticancer agent *viz.* TFT is metabolized to the inactive base, and therefore, it exhibits poor pharmacokinetic profile in cancer patients.

Platelet-derived endothelial cell growth factor (PD-ECGF) was isolated from human blood platelets in 1987⁷⁰. It has been demonstrated to induce endothelial cell chemotaxis *in vitro* and angiogenesis *in vivo*⁷¹. It also involves in thymidine incorporation into the cells. Interestingly, amino acid sequence analysis and gel chromatography revealed that PD-ECGF and TP are identical with each other⁷². PD-ECGF/TP is also found to be identical to gliostatin, a glial growth inhibitory factor with survival promoting effects on neurons⁷³.

1.2.1 Structure of thymidine phosphorylase

TP was purified from both *Escherichia coli* and *Salmonella typhimurium* in mid-1970s^{74,75}. Several years later, human TP was extracted from the amniochorion⁷⁶(Figure 4). It was observed that the amino acid sequence of human TP was only 39% identical with *E. coli* TP⁷⁷. The human TP gene is located on chromosome 22q13⁷⁸ and is composed of 10 exons dispersed over a 4.3-kb region. Its promoter lacks a TATA box and a CCAAT box, which is prevalent in most eukaryotic promoters⁷⁹. Instead, six copies of potential Sp1-binding sites (GGGCGG or CCGCCC) are clustered just upstream from the transcription start sites⁸⁰. This SP1 sites are also involved in the transcription of VEGF and therefore, many studies suggested the tendency of co-expression of both VEGF and TP^{81,82}.

This enzyme functions as a homodimer, having two identical subunits, with a molecular mass ranging from 90 kDa in *E. coli* to 110 kDa in mammals^{83, 84}. The crystal structure of *E. coli* TP suggested that each subunit is composed of a large mixed α/β domain containing phosphate binding site and small α helical domain that contains the thymidine binding site. These two domains are separated by a cleft. The orientation of the active site seems to suggest that domain motion is critical to the generation of a closed catalytically active conformation of the enzyme. It was concluded that phosphate binding influences the formation of a hydrogen bond between His119 and Gly208 and helps to order the 115 to 120 loop. The formation of this hydrogen bond also induces the domain movement. The α domain moves as a rigid body, while the α/β domain shows some non-rigid body movement that is associated with the formation of the His119-Gly208 hydrogen bond^{85,86}. The closed active conformation resulting from the movement of two domains is also supported by

the crystal structure of the related pyrimidine nucleoside phosphorylase from *Bacillus stearothermophilus*⁸⁷.

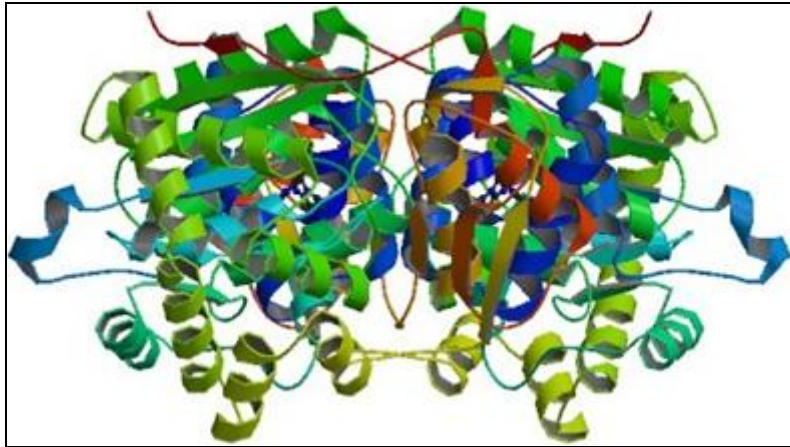


Figure 4. Structure of human thymidine phosphorylase

1.2.2 Biological functions of thymidine phosphorylase

- Physiological role

TP is distributed throughout various organs in the human body and is present in both cytoplasm and nucleus within the cell⁸⁸. This enzyme is highly expressed in blood platelets and it contributes towards wound healing⁸⁹. In addition, TP plays an important physiological role in the female reproductive cycle. A high level of TP is detected in endometrium, which undergoes extensive angiogenesis during each menstrual cycle. Its expression is inversely correlated to oestradiol concentration, whereas the combination of both progesterone and transforming growth factors- β 1^{90,91} are known to induce the expression of TP. It helps in the vascularisation of the endometrium and the placenta, and plays an important role in remodelling of the existing vasculature⁹².

- Pathological role

Various studies indicated that TP is involved in a wide variety of chronic inflammatory diseases like rheumatoid arthritis⁹³, atherosclerosis⁹⁴, psoriasis⁹⁵, inflammatory bowel disease⁹⁶ and chronic glomerulonephritis⁹⁷. Loss-of-function mutations of the TP gene has good contribution for mitochondrial neurogastrointestinal encephalomyopathy (MNGIE), an autosomal recessive human disorder associated with multiple deletions of skeletal muscle mitochondrial DNA⁹⁸. TP deficiency may lead to an increased level of plasma and tissue thymidine and deoxyuridine that may cause alteration of mitochondrial nucleoside and nucleotide pools leading to impaired mitochondrial DNA replication and repair. Therefore, therapies that can abrogate thymidine levels may provide beneficial effects for MNGIE patients. However, it was confirmed from different studies that loss-of-function mutation is not sufficient to produce MNGIE. Examination of chromosome 22q13.32 where the TP gene is located, revealed that the mutation of the SCO2 gene which overlaps with exon 10 of TP, contributes to MNGIE⁹⁹.

- The association of thymidine phosphorylase with cancer

Western blot and histological analysis showed that TP is overexpressed in many solid tumours¹⁰⁰ including oesophageal, gastric, pancreatic, ovarian, breast, renal, bladder and non-small cell lung cancers^{101,102}. In addition, TP expression is also up-regulated in lymph nodes of patients with classical Hodgkin lymphoma where the expression of TP is increased with disease progression¹⁰³. Moreover, it was reported that the TP expression is correlated well with higher microvessel density, higher tumour staging, and more metastasis. Besides tumour cells, it is also expressed in endothelial cells, fibroblasts, lymphocytes and particularly in tumour-associated macrophages (TAM).

TAM is believed to play a crucial role in stimulating tumour growth and metastasis through the production of various growth factors, proteinases, chemokines, and cytokines. An elevated level of TP has been demonstrated in TAM of melanoma, gastric, glioblastoma, breast, colon, astrocytic, uterine endometrial and prostate cancer. Furthermore, the overexpression of TP in macrophages of gastric adenocarcinoma, astrocytic tumours, breast, and uterine endometrial cancer has been demonstrated that it is associated with microvessel density and thus it is believed that this enzyme plays a key role in tumour invasion¹⁰⁴⁻¹⁰⁸.

Several studies suggested that TP expression is upregulated by various inflammatory cytokines. Tumour necrotic factor-alpha (TNF- α) upregulates the TP mRNA levels and TP activity in human colon carcinoma cells is increased *via* the activation of SP1 transcription factors. In the monocytic cell line THP-1, TNF- α influences the overexpression of TP mediated *via* TNF- α receptor 2 and NF κ B^{80, 109}. In addition, interferon (IFN)- α/β has been demonstrated a crucial role in upregulation of TP by stimulating IFN-stimulated response element (ISRE) in the TP promoter¹¹⁰. The IFN- γ stimulates the expression of TP in human monocyte U937 cells by increasing binding of signal transducer and activator of transcription (STAT)-1 to a gamma-activated sequence-like element in the TP promoter¹¹¹. Moreover, these interferons also increase the stability of TP-mRNA and upregulate its over expression¹¹⁰. Besides these factors, interleukins are also involved in stimulation of TP overexpression.

Cancer treatments protocol, such as X-ray irradiation and various chemotherapeutic agents including paclitaxel, docetaxel, doxorubicin, oxaliplatin, cyclophosphamide, and mitomycin C have been reported to increase the tumour TP levels *via* up regulation of cytokines such as TNF- α , IFN- γ , IL-1^{112, 113}. An increase level of TP and

its enzymatic activity have been detected in tumour microenvironment that are proximal to necrotic area and this fact suggested that the microenvironmental stress conditions such as low pH and hypoxia of tumour microenvironment may cause an elevated level of TP expression¹¹⁴.

Recently, it has been revealed that epigenetic modifications, such as methylation and histone deacetylation influence TP expression. In the breast carcinoma SKBR-3 cells, the high expression of TP is probably due to its complete demethylation of the CpG dinucleotides located in the TP promoter. The low TP expression is correlated with hypermethylation of the CpG islands as in DLD-1 colon carcinoma cells. However, the expression of TP in DLD-1 cells, could be achieved by demethylation with 5-aza-2'-deoxycytidine and to a lesser extent by histone deacetylation with trichostatin-A¹¹⁵.

1.2.3 Role of thymidine phosphorylase in tumour development and progression

- Angiogenesis

Angiogenesis, the formation of new blood vessels from pre-existing vascular network, serves many important roles in several physiological processes, such as embryonic development, wound healing, and reproduction. It involves a variety of coordinated events including degradation of the surrounding extracellular matrix (ECM), endothelial cell migration and proliferation, and differentiation into mature blood vessels. TP is considered as an important factor among others that are involved in this multistep processes. TP induces endothelial cell migration and tube formation *in vitro*^{71,116,117}. This enzyme also stimulates angiogenesis in the CAM⁷¹ and in several other *in vivo* models, such as the freeze-injured skin graft¹¹⁶, rat corneal¹¹⁸, and mouse dorsal air sac assays¹¹⁸ and in gelatine sponges subcutaneously implanted in rats or

mice¹¹⁹. Recently, it has been revealed that TP also regulates the angiogenic potential of endothelial progenitor cells (EPC), or bone marrow-derived cells, which can differentiate into endothelial cells and contribute to the repair of blood vessels after a myocardial attack¹²⁰.

The requirement for TP activity for angiogenesis was further confirmed by the fact that the mutants of TP that lack enzymatic activity cannot induce the formation of new blood vessels in the gelatine sponge assay. The angiogenic activity of TP can be abolished by using TP-directed neutralizing antibodies, by adding a specific TP inhibitor such as 5-amino-6-chlorouracil or by down-regulating TP by siRNA¹²⁰. It is further established that 2-deoxy-D-ribose (2DDR), which is a degradation product of the TP-metabolite 2DDR-1P, also induces the endothelial cell migration and angiogenesis¹²¹.

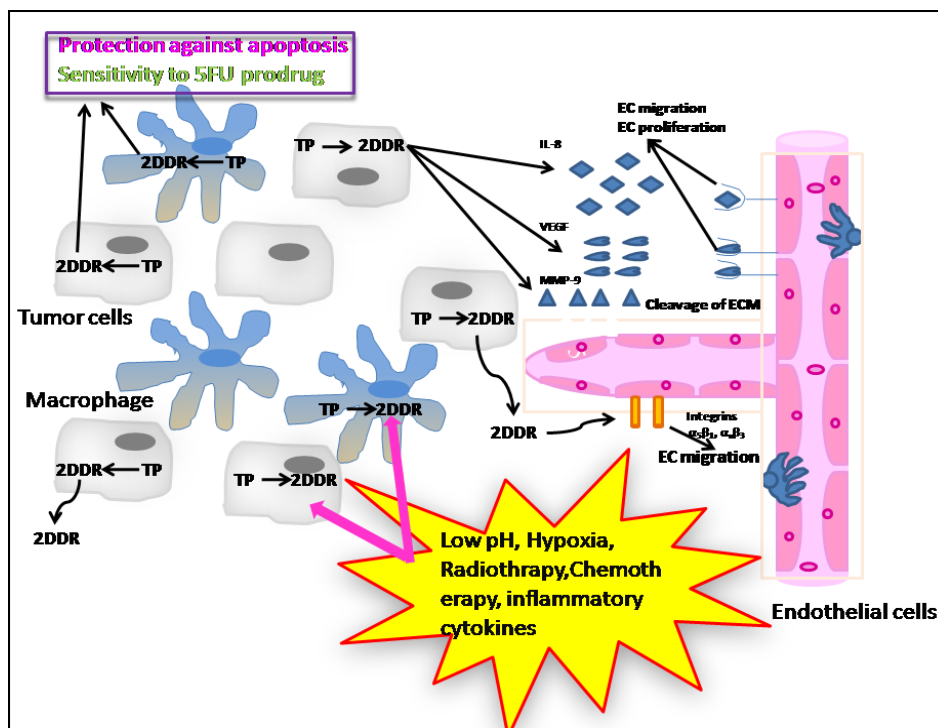


Figure 5. The function of thymidine phosphorylase and 2-deoxy-D-ribose in tumour development – a schematic representation⁸²

Unlike other angiogenic molecule, TP shows some exceptional characteristic features. Firstly, it exerts its angiogenic effect by staying inside of the cells whereas most angiogenic factors are released into the extracellular space to activate endothelial cells. This is probably due to its deficiency of amino-terminal hydrophobic leader sequence required for cell secretion⁷¹. However, some tumour cell lines such as the epidermoid carcinoma A431 and stomach cancer MKN74 cell lines secrete this protein into the cell culture medium. Although, TP is mostly confined inside the cell, its metabolite 2DDR diffuses out of the cell and exerts its biological effects on other cells. Secondly, in mammalian cells, TP and 2DDR are most likely able to induce angiogenesis through a nonreceptor-mediated mechanism whereas other angiogenic factors usually bind to a specific cell surface receptor followed by a transduction cascade that exerts biological response of the cell.

The mechanism by which TP induces angiogenesis is not fully understood, and a receptor for TP has not yet been identified. Several reports suggested that the angiogenic activity of TP is depending on its enzymatic activity. Among the metabolites of thymidine generated by TP, 2DDR is expected to be responsible for the angiogenic activity of TP. TP produces monosaccharide 2DDR-1P as a metabolic by-product, which is converted to 2DDR by the nonenzymatic dephosphorylation. This 2DDR is then secreted from the cell to exhibit the angiogenic effect *via* direct and indirect pathway (Figure 5).

Hotchkiss et al.¹²² revealed that 2DDR can directly affect endothelial cell migration through the activation of focal adhesion kinase (FAK) and focal adhesion formation by regulating the association with components of FAK (integrins $\alpha 5\beta 1$ and vinculin) on the cellular surface in human umbilical vein endothelial cells (HUVECs).

Indirectly, it also stimulates the secretion or expression of other angiogenic factors like VEGF, interleukin-8, and MMPs in tumour microenvironments. Following thymidine treatment of TP-overexpressing human bladder carcinoma RT112 cells showed an elevated expression of heme oxygenase-1 (HO-1), producing an oxidative stress which induces the expression and/or secretion of other angiogenic factors^{123, 124}. In addition, Brown et al.¹²⁴ suggested that 2DDR is a strongly reducing sugar that may generate oxygen radical species during the early stages of protein glycation. Thus, through the formation of 2DDR, TP may induce oxidative stress in TP-overexpressing tumour cells causing these cells to secrete angiogenic factors, such as VEGF.

- Metastasis

Many clinical studies have reported that the elevated TP expression is correlated to invasion and metastasis of gastric, colorectal, renal, pancreatic, non-small cell lung, and ovarian cancers. The metastasis effects of TP are confirmed by the fact that the elevated metastasis in TP-overexpressing cells can be dramatically inhibited by the TP inhibitor **TPI** or by 2-deoxy-L-ribose (2DLR), a stereoisomer of 2DDR^{125,126}. Moreover, it was observed that the lung colonization and spontaneous metastasis in mice, xenografted with the human melanoma cancer cell line A-07 were inhibited by treatment with neutralizing antibodies against TP¹²⁷.

- Protection of cancer cells against apoptosis

It was also established that TP reduced apoptotic index in colon¹²⁸, gastric¹²⁹, esophageal¹³⁰, ovarian¹³¹, and oral squamous cell carcinomas¹³². Uchimiya et al reported that the apoptotic index in KB/TP tumours was significantly lower than that in KB/CV tumours demonstrating TP could protect cells against apoptosis¹¹⁸. It was

postulated that 2DDR would inhibit numerous hypoxia-induced pro apoptotic events, such as activation of caspase 3 and 9, mitochondrial cytochrome c release, loss of mitochondrial transmembrane potential, phosphorylation of p38 mitogen-activated protein kinase, and downregulation of the anti-apoptotic proteins Bcl-2 and Bcl-xl^{133,134}. Furthermore, 2DDR also inhibits the upregulation of the transcription factor HIF-1a¹³³. Besides hypoxia-induced apoptosis, TP was reported to suppress the apoptosis induced by Fas, microtubule-interfering, and DNA damage-inducing agents such as cisplatin¹³⁵⁻¹³⁹.

1.2.4 Thymidine phosphorylase inhibitors

From the above literature review, it can be postulated that inhibition of thymidine phosphorylase in cancer cells may be viewed as a plausible strategy to control angiogenesis stimulation and apoptosis inhibition. In addition, TP inhibitors may also serve as adjuvant agent to enhance the bioavailability and therapeutic efficacy of co-administered anticancer drugs that belong to the deoxynucleosides *viz.* trifluorothymidine (TFT) that is rapidly metabolized by TP. Therefore, TP serves as an interesting target for the development of chemotherapeutic agents and thus many laboratories have synthesized various chemical classes of TP inhibitors which have been tested preclinically and clinically. However, up to now, no compound has been approved yet for clinical use. In the next few paragraphs, selected TP inhibitors will be discussed and representative example of different classes (according to their mode of enzyme inhibition) of TP inhibitors are tabulated in table 1.

For more than 30 years, the prototypic TP inhibitors were 6-aminothymine (6AT) and the derivatives of 6-aminouracil such as 6-amino-5-chlorouracil (6A5CU) and 6-amino-5-bromouracil; all of which possessed IC₅₀ values in the micro molar range¹⁴⁰.

When it was revealed that TP is directly or indirectly involved in angiogenesis, interest was raised to synthesize novel TP inhibitors which might prevent tumour progression. Such efforts resulted in the generation of compounds such as AEAC which demonstrated improved solubility and activity compared to parent 6A5BU¹⁴¹. In 1998, Balzarini et al developed the first purine derivative, 7-deazaxanthine (7-DX) as a potential inhibitor against a pyrimidine nucleoside phosphorylase (i.e. TP) based on three-dimensional structure of *E. coli* TP¹⁴². This inhibitor was designed by including an additional second ring on the pyrimidine base of 6-aminothymine, in order to create extra stabilising interactions. It was reported that 7-DX was able to efficiently inhibit the neovascularization in the CAM assay¹⁴². In addition, inhibitors having 6-methylenepyridinium and 6-(phenylalkylamino) uracil have been investigated and evaluated as well^{143,144}. Efforts to develop novel TP inhibitors in order to improve the potency of antitumor 2'-deoxynucleosides, led to the investigation of 6-methylene linked pyrrolidinyl and imidazolyl uracil analogues that exhibited potent competitive inhibitory effect on TP. In 2000, Fukushima et al identified 5-chloro-6-[1-(2-iminopyrrolidinyl)methyl] uracil hydrochloride (TPI) as the most potent inhibitor of human TP so far, with an IC₅₀ value of 35 nM¹⁴⁵. TPI inhibited the migration and basement membrane invasion of TP-overexpressing KB cells *in vitro* and TP induced angiogenesis in the mouse dorsal air sac assay¹⁴⁶. It also significantly reduced the tumour growth rate and increased apoptotic index of KB/TP xenografted tumours. In addition, it suppressed liver metastases of KB/TP cells xenografted into nude mice¹⁴⁷. Therefore, TPI has been considered for combination therapy with trifluorothymidine (TFT), an anti-tumoral agent that is rapidly inactivated by TP. An oral combination therapy of TFT and TPI (at a molar ratio of 1:0.5), called TAS-102, is currently developed and evaluated in phase I studies for

patients with solid tumours¹⁴⁸. The concurrent application of thymidine phosphorylase inhibitor (TPI) increases the bioavailability and *in vivo* efficacy of TFT. In addition, TPI exerts antiangiogenic effects by inhibiting thymidine phosphorylase (TP). A phase I clinical trial demonstrated that TAS-102 was active against heavily pre-treated metastatic breast cancers¹⁴⁹. However, TAS-102 showed no significant response in patients with solid (mostly colorectal) tumours¹⁵⁰. In order to selectively deliver TP inhibitors, a series of prodrugs of known TP inhibitors were designed, synthesized and tested^{151,152}. These compounds exhibited their inhibitory effects after bioreductive activation by xanthin oxidase (XO) in hypoxic tumour microenvironments.

A series of N1-alkylphosphonouracil derivatives has been synthesized and tested as multisubstrate inhibitors of *E. coli* TP. These compounds are designed based on structural features of TP. These inhibitors contain a thymine base that would interact at the nucleoside binding site, a spacer of 6 to 9 atoms, and a phosphonate moiety that could interact at the phosphate binding site. Further modification of these compounds by replacing the thymine ring by 6-A5BU or 7-deazaxanthine afforded compounds TP64 and TP65 respectively, which exhibit IC₅₀ values against *E. coli* or human TP in the micro molar range¹⁵³. Detailed kinetic experiments revealed that these compounds inhibited TP in a purely competitive or mixed fashion¹⁵⁴. It is reported that TP65 completely inhibited TP-induced formation of microvascular sprouts from endothelial cell aggregates in a three-dimensional fibrin gel, and TP induced angiogenesis in the CAM assay¹⁵⁵.

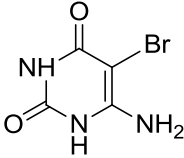
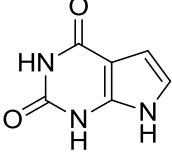
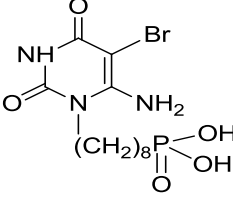
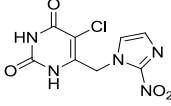
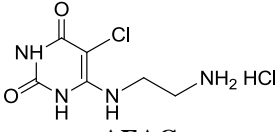
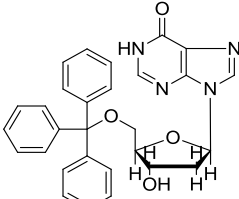
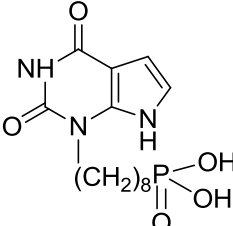
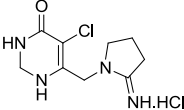
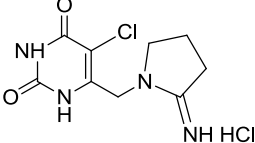
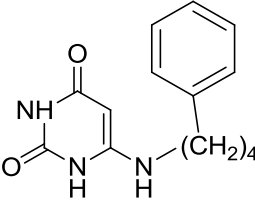
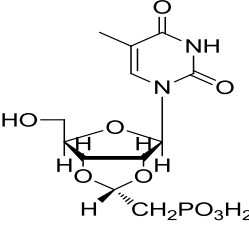
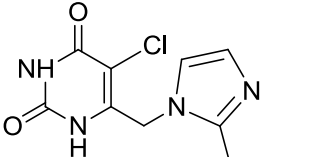
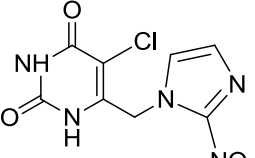
Recently, a series of novel, multisubstrate, bicyclic pyrimidine nucleoside inhibitors of human thymidine phosphorylase (TP) was synthesized and tested¹⁵⁶. Another multisubstrate inhibitor, 5-aryl-1-[2-(phosphonomethoxy)ethyl]uracil derivative was

designed based on an assumption that the potential hydrophobic effect of the aryl groups might modify the inhibitory effect towards this enzyme and they may also demonstrate cytostatic activity¹⁵⁷.

In addition, a different purine derivative KIN59 (5'-*O*-tritylinosine) was synthesized and tested against human and bacterial recombinant TP and TP-induced angiogenesis. The kinetic study suggested that this inhibitor exerted its inhibition in a non-competitive manner in the presence of both thymidine and phosphate as the variable substrate. In addition, KIN59 has been found to inhibit angiogenesis in the chorioallantoic membrane assay. The data suggested that TP triggered angiogenesis may not solely be directed through its functional substrate binding sites, but other regulatory (allosteric) site(s) may be playing a crucial role to exert this biological property, which is still to be explored^{158,159}. Recently, the purine ring and ribose moiety of the lead compound KIN59 was modified and it is demonstrated that this kind of modification resulted in improvement of inhibitory activity¹⁶⁰.

Within the last few years, extensive research work in this field generated many inhibitors having diverse molecular structure including 5,6-disubstituted uracil derivatives¹⁶¹, pyrimidine 1-[2-(phosphonomethoxy)propyl] derivatives¹⁶², N³-substituted thymine acyclic nucleoside phosphonate derivatives¹⁶³ and schiff bases of 3-formylchromone¹⁶⁴ that show promising inhibitory activity against TP. It was also demonstrated that a few glycosides isolated from plant origin *viz.* symplocomoside and symponoside exhibit anti-TP activity and also inhibit TP-associated angiogenesis¹⁶⁵.

Table 1. Representative examples of different types of TP inhibitors

Competitive inhibitors	Non-competitive, non-substrate inhibitors	Multi-substrate inhibitors	Prodrugs of TP
 <p>6A5BU IC₅₀- 17μM¹⁴¹</p>	 <p>7DX IC₅₀- 40μM¹⁰²</p>	 <p>POABrU (TP64) IC₅₀- 20 μM¹⁰¹</p>	 <p>5C6-NIMU IC₅₀- 22μM¹⁵¹</p>
 <p>AEAC IC₅₀- 0.25μM¹⁴¹</p>	 <p>KIN59 IC₅₀- 44μM¹⁶⁷</p>	 <p>PODX (TP65)¹⁰¹</p>	 <p>2-deoxo-TPI¹⁵²</p>
 <p>TPI IC₅₀- 0.035μM¹⁴⁵</p>	 <p>PBAU IC₅₀- 30μM¹⁴³</p>	 <p>PFP IC₅₀- 0.24μM¹⁵⁶</p>	
 <p>6-2'AIMU IC₅₀- 0.020μM¹⁵²</p>			
 <p>5C6-2'NIMU IC₅₀- 20μM¹⁵²</p>			

6A5BU (6-amino-5-bromouracil), **AEAC** (6-(2-aminoethylamino)-5-chlorouracil), **5C6-2'AIMU** (5-chloro-6-(2'-aminoimidazol-1'-yl)methyluracil), **5C6-2'-NIMU** (2-chloro-6-(2'-nitroimidazol-1'-yl)methyluracil)- prodrug of 5C6-2'AIMU, **7DX** (7-deazaxanthine), **KIN59** (5'-O-trityl-inosine), **PBAU** (6-(4-phenylbutylamino)uracil), **POABrU** (1-(8-phosphonoctyl)-6-amino-5-bromouracil), **PODX** (1-(8-phosphonoctyl)-7-deazaxanthine), **PFP** ([4-hydroxymethyl-6-(5-methyl-2,4-dioxo-3,4-dihydro-2H-pyrimidin-1-yl)-tetrahydro-furo[3,4-d][1,3]dioxol-2-ylmethyl]-phosphonic acid)

A number of studies has demonstrated that 2-deoxy-L-ribose (2DLR), a stereoisomer of 2-deoxy-D-ribose, does not inhibit the enzymatic activity of TP but it suppresses the angiogenesis activity of TP. Indeed, it inhibits 2-deoxy-D-ribose-induced endothelial cell migration in a Boyden chamber, tube formation in collagen gel, and invasion of KB cells overexpressing TP (KB/TP) into matrigel. 2DLR has been shown to be able to abrogate TP-induced angiogenesis in a rat corneal assay and in the mouse dorsal air sac assay¹¹⁸. Moreover, it significantly reduces the 2-deoxy-D-ribose stimulated VEGF, IL-8 and MMP-9 expression^{126,166}. In contrast to TP inhibitors, 2-deoxy-L-ribose abrogates the biological activities of TP without affecting its enzymatic activity and therefore this may offer advantages for its use in combination therapy with 5FU prodrug that requires activation by TP.

1.2.5 Thymidine phosphorylase mediated activation of anticancer prodrug

It is mentioned earlier that due to low substrate specificity of TP, it can recognize various pyrimidine deoxynucleoside analogues possessing anti-tumour or anti-viral properties. Therefore, it plays a crucial role in the activation of chemotherapeutic drugs such as 5-fluorouracil (5-FU) and its prodrugs such as 1-(tetrahydro-2-furanyl)-5-fluorouracil (Tegafur), 4-N-pentyloxy-carbonyl-5'-deoxy-5-fluorocytidine (capacetabine), 5-fluoro-2'-deoxyuridine (FdUrd, floxuridine) and doxifluridine (5'-deoxy-5'-fluorouridine, DFUR). 5FU, an antimetabolite, has been used for the treatment of colorectal carcinoma for more than a decade. In systemic circulation, it is converted to FUTP and incorporated into replicating RNA and thus exerts cytotoxicity effects. Alternatively, in the presence of sufficient co-substrate, 2-deoxyribose-1-phosphate TP may convert 5FU to FdUrd, which is then phosphorylated to FdUMP by TK. The FdUMP can inhibit thymidylate synthase

resulting in thymidine depletion for DNA synthesis¹⁶⁸. However, it is reported that the clinical efficiency of 5FU is unsatisfactory due to its rapid degradation by DPD and poor oral absorption. Therefore, significant research has been carried out to develop prodrug of 5FU. Doxifluridine (DFUR) and capecitabine are thus designed as prodrugs of 5FU to improve poor pharmacokinetic profile of the parent drug¹⁶⁹. It should also be mentioned that capecitabine after converting to DFUR by enzymatic process in intestine and liver, is metabolized to 5FU by TP, which is up-regulated in tumour microenvironment compared to normal cells resulting in lower toxicity to normal tissues (Figure 6)¹⁷⁰. Therefore, the metabolism of capecitabine by TP is considered as the rate limiting step for cytotoxicity effects of this prodrug and this has led to the hypothesis that a combination of TP-inducible chemotherapy (i.e., cyclophosphamide and taxanes) and TP-targeted treatment (i.e., DFUR and capecitabine) may improve the effectiveness of anti-cancer therapy¹⁷¹. Based on this, several combination chemotherapy of capecitabine with standard TP inducible chemotherapy is in phase-III trials and the outcomes suggested that this type of combination therapy shows increased response rate, survival time compared to standard treatment alone⁶⁹.

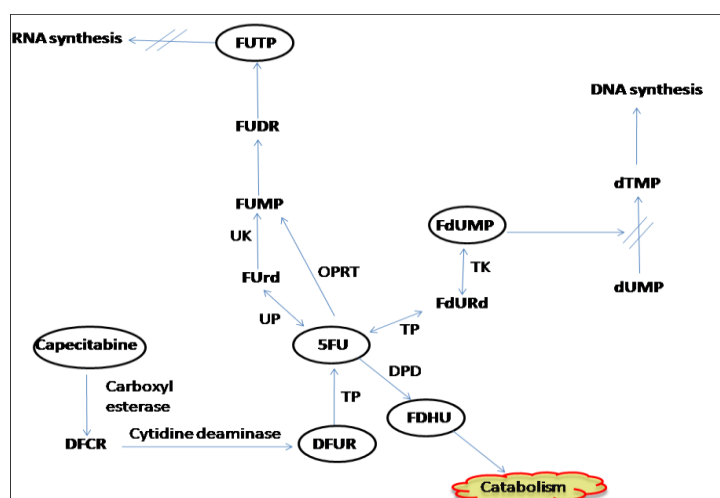


Figure 6. Metabolic conversion and mode of action of 5FU, an anticancer drug, and its prodrugs¹⁷²

1.2.6 Structural aspect and crystal structure of human thymidine phosphorylase

Due to the failure of many crystallization trials in producing well-diffracting crystals, it took several years to solve the structure of human TP¹⁷³. Spraggon et al¹⁷⁴ reported the crystals of human TP using a synchrotron X-ray source in which diffraction was limited to 3.5 Å resolution. In 2004, the crystal structure of human thymidine phosphorylase complexed with **TPI**¹⁷³ was elucidated. In this crystal, TP was found as a dimer with similar orientation as observed in *E. coli* TP. It was also deduced that **TPI** appeared to mimic the substrate transition state and bind to the enzyme as a zwitterions. The 5-chlorouracil moiety of **TPI** was found to form strong hydrogen bonds with R202, S217 and H116 and contribute to the tight binding of TPI to the active site. In addition, the chlorine atom in the 5-chlorouracil moiety was accommodated in a hydrophobic pocket formed by V208 and I214 of the α domain and L148 and V241 of the α/β domain in the enzyme. The 2-iminopyrrolidinyl moiety of **TPI** was found to make two hydrogen bonds with the active site; one of which interacted with the carbonyl oxygen of S117 and another to a water molecule (W) (Figure 7). However, in this structure several amino acid residues (amino acids 409 and 410) were missing as it was subjected to limited proteolysis with trypsin to grow crystal as a result the loop formed by amino acid residues 405–416 was disordered.

In 2006, El Omari et al¹⁷⁵ solved a complete, good quality diffracting crystal structure of unproteolyzed human TP at 2.3 Å resolution in presence of thymidine. Surprisingly, the product thymine was found to be present in three of the four monomers of the asymmetric unit instead of thymidine, which was added during crystallization. Results from the kinetic studies of *E. coli* TP have suggested an ordered binding mechanism in which phosphate is the first substrate that binds to TP

whereas 2DDR-1P dissociates last from the enzyme. Therefore, this finding suggests that thymine, a non-competitive inhibitor of TP, may associate with the unoccupied enzyme, and induce domain closure and stabilize the closed conformation after product release, and thus explaining the mechanism of noncompetitive inhibition. This work also suggested the presence of higher electron density closer to residues Ser117, Gly152 and Tyr199 that could be further explored in drug design by incorporating some suitable substituent to an inhibitor, which might form strong hydrogen bonds with these residues. In 2009, Mitsiki et al¹⁷⁶ reported the crystal structure of recombinant human TP complexed with 5-iodouracil (5IUR) at 3.0 and 2.5 Å resolutions, respectively. This study provides some information about the role of specific residues in the enzymatic activity of TP *via* mutagenesis and kinetic studies.

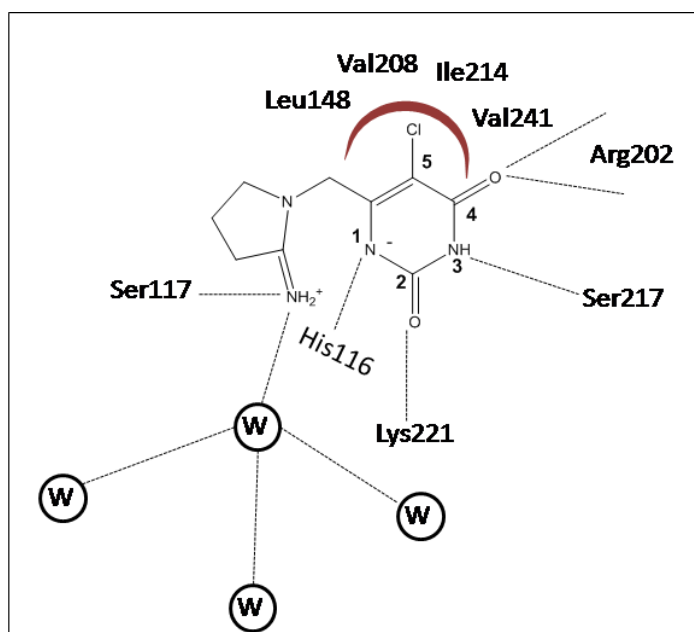


Figure 7. Schematic representation of the human TP active site and important interactions with TPI¹⁷³

1.3 CoMFA, a 3D-QSAR method, as a means of lead optimization

Drug discovery is considered as a long term and expensive process. It is mostly the result of accidental discovery and intensive screening of large libraries of synthesized or naturally occurring compounds. The most important step in drug design is to identify a lead, which can be discovered by *in vitro* screening of large libraries of compounds. It is noteworthy that after lead identification, it takes quite long time in lead optimization process to finally derive a commercial drug. A lead may demonstrate a low affinity for the target receptor, can be unstable in nature, possess high toxicity, exhibit poor pharmacokinetic properties or can be expensive to synthesize in large quantities. To make the lead compound suitable for commercialization, computer-aided drug design has been employed. The availability of three-dimensional (3D) structural information of biological receptors and their complexes with various ligands can be extremely useful in improving the affinity of the lead towards the target. Whenever, detailed structural information of target molecule is not available, the drug design process will follow a more indirect quantitative structure-activity relationship (QSAR) approach¹⁷⁷. This approach basically creates a reliable statistical model using physicochemical properties of chemical substances and their biological activities for prediction of the activities of new chemical compounds. In classical QSAR studies, the biological end points are correlated with a range of atomic, group or molecular properties such as lipophilicity, polarizability, electronic and steric properties^{178,179}. However, such studies have exhibited their limitations for designing a new molecule due to the lack of consideration of the 3D structure of the molecules.

Nowadays, 3D-QSAR has emerged as a natural extension to the classical QSAR approaches pioneered by Hansch and Free-Wilson. In these approaches, the three-dimensional properties of the ligands are exploited to predict their biological activities using robust chemometric techniques such as PLS, gPLS, ANN etc. In the absence of adequate structural information of the biological target, the drug design process has been adopted indirect 3D QSAR approach that uses molecular alignment of atoms, pharmacophores, volume, or fields to generate a virtual receptor. However, when the receptor structure is known, it is possible to investigate the ligand-receptor interactions and derive 3D-QSAR models from the corresponding parameters. In 1987, Cramer developed the 3D-approaches named as DYnamic Lattice-Oriented Molecular Modeling System (DYLOMMS) that use PCA to calculate vectors from the molecular interaction fields, which are then correlated with biological activities. Subsequently, it was modified by including the two existing techniques, GRID and PLS, to develop a powerful 3D-QSAR methodology, known as Comparative Molecular Field Analysis (CoMFA)¹⁸⁰. Today CoMFA is considered as leading 3D-QSAR methods.

The primary objective of CoMFA study is to derive a correlation between the 3D shape and biological activity of a series of molecules in a superimposed conformation. These conformations are presumed to be the biologically active structures, overlaid in their common binding mode. From these conformations, the molecular fields *viz.* electrostatic and steric (van der Waals interactions) are calculated. The fields, usually, are measured at the lattice points of a regular Cartesian 3D grid; the lattice spacing is typically set to 2 Å. The interaction between the molecule and a probe atom (a sp^3 -hybridized carbon with +1 charge) is measured. In addition, CoMFA uses a partial least-squares (PLS) analysis to predict activity from energy values at the grid points.

1.4 Summary

In summary, this introductory chapter has described various practical approaches for the construction of the 1,3,5-triazin-2,4-dione derivatives. In addition, several ways to convert triazolo fused 1,3,5-triazin-2,4-dione and its thioxo analogues are discussed. Depending on the starting reagents and reaction condition, different derivatives of 1,2,4-triazolo[1,5-*a*][1,3,5]triazin-5,7-dione and its thioxo analogues can be synthesized. In particular, substitutions at position C2, N3, C5 and N6 can be introduced with the use of differently substituted starting reagents. Similar observations are seen in the pyrazolo[1,5-*a*][1,3,5]triazin-2,4-dione analogues. In addition, a brief overview of TP and its reported inhibitors was described. Furthermore, attention was given to computer aided drug design based on CoMFA analysis.

The brief literature review suggested that although 1,3,5-triazin-2,4-dione and its fused analogues exhibited wide range of biological properties, the activity of these scaffolds against thymidine phosphorylase (TP) has not yet been investigated. Therefore, the major part of this thesis is concerned with the synthesis and exploration of TP associated bioactivities of the said scaffolds. Moreover, a pharmacophore based 3D-QSAR model will be generated using CoMFA analysis to predict the activity of novel TP inhibitor. Therefore, it is assumed that these research activities may be able to fill the gaps of previous research and it may have significant impact on the advancement of cancer chemotherapy management protocols by inhibiting TP.

Chapter 2

The Study Proposal - Hypotheses and Objectives

2.1 Importance of the development of thymidine phosphorylase inhibitors as a novel antiangiogenic agents

The diagnosis of cancer is often accompanied by the staging of the cancer development. The type and staging of cancer determine the treatment to be prescribed. In order to provide good clinical outcomes in chemotherapy of cancer patients, there is still room to develop new treatment strategies that target at various stages of cancer growth and development. Considerable evidence has identified angiogenesis as one of the processes in cancer development that can be interrupted as it promotes tumour growth and metastasis¹⁸¹⁻¹⁸³. Therefore, in 1971, Folkman postulated that anti-angiogenesis could be an effective strategy to be adopted in chemotherapy¹⁸⁴. Since then, interests for developing anti-angiogenic factors have increased. Among 30 pro-angiogenic factors identified, the family of vascular endothelial cell growth factor (VEGF) receptors is considered as potential targets for drug development as it is often expressed in various malignant tumours¹⁸⁵⁻¹⁸⁷. A humanized anti-VEGF monoclonal antibody, bevacizumab was developed and it was approved by the US Food and Drug Administration (FDA) for use in combination with standard chemotherapy for the treatment of metastatic colorectal, non-small cell lung and breast cancers. Thereafter, many other potential anti-VEGF monoclonal antibodies were developed. However, this anti-angiogenic adjunct therapy suffers from several serious problems. Firstly, selection of the most effective combination of anti-angiogenic agents with chemotherapeutic agents is always challenging. Secondly, anti-angiogenic therapy has been demonstrated in some cases to show resistance to response¹⁸⁸⁻¹⁹⁰. Although an increased dose can overcome such problem, but higher doses are likely to adversely affect the vascula of normal tissue. Some clinical studies have reported that bevacizumab shows an increased risk of arterial thromboembolic events and

hypertension¹⁹¹. Lastly, anti-angiogenic therapy may also create hypoxic conditions and obstruct drug delivery to the tumour. This hypoxic tumour microenvironment may promote upregulation of chemokines and other angiogenic factors from stromal cells, including tumour associated macrophages and carcinoma-associated fibroblasts¹⁹². Therefore, there is a need to explore alternative targets for further development of angiogenic inhibitors to overcome the said limitations of traditional anti-angiogenic therapy. From the literature review, it is evident that the enzyme thymidine phosphorylase (TP) induces tumour vascularisation, promotes tumour growth and metastasis by inducing the secretion and/or expression of the angiogenic agents⁸². Therefore, TP may serve as an alternative target for the development of new anti-angiogenic therapy.

Thymidine phosphorylase (TP, EC 2.4.2.4), also known as platelet derived endothelial cell growth factor (PD-ECGF) and gliostatin⁷³, is involved in the catalysis of the reversible phosphorolysis of thymidin-2'-deoxyuridine, and its analogues into 2-deoxy-alpha-D-ribose-1-phosphate (2DDR-1P) and the respective bases⁶². It also acts in the salvage pathway of pyrimidine nucleotides by transferring the deoxyribosyl moiety to form new nucleoside⁶³. TP is overexpressed in many solid tumours¹⁰⁰ including oesophageal, gastric, pancreatic, ovarian, breast, renal, bladder and non-small cell lung cancers^{101, 102}. It is reported that this enzyme and its metabolite 2DDR-1P stimulate the secretion and/or expression of the angiogenic agents and involve in the induction of endothelial cell migration^{124,193-195}. In addition, increased level of TP is associated with protection of the tumour against apoptosis^{135, 196} and enhancement of metastatic potential¹²⁷ that may influence tumour progression. Therefore, inhibition of thymidine phosphorylase may be viewed as a plausible strategy to overcome its pathological effects. In addition, TP inhibitors may also serve as adjuvant to enhance

the bioavailability and therapeutic efficacy of co-administered anticancer drugs that belong to the deoxynucleosides¹⁹⁷.

Pioneering work in this field have generated several potent thymidine phosphorylase inhibitors, most of which are derivatives of pyrimidin-2,4-dione, with only a few that are fused bicyclic heterocycles possessing the homophthalimide moiety which is believed to be essential for binding to the active site of TP¹⁹⁸. In 2000, Fukushima et al synthesized 5-chloro-6-[1-(2-iminopyrrolidinyl) methyl]uracil hydrochloride (TPI), the most potent human TP inhibitor known so far, which has an IC₅₀ value of 35 nM and K_i of 20 nM¹⁴⁵. In addition, Balzarini et al (1998)¹⁴² designed a fused bicyclic TP inhibitor, 7-deazaxanthine (**7-DX**) based on three-dimensional structure of *E. coli* TP (Figure 8).

Among the bioactive 1,3,5-triazines, derivatives of 1,3,5-triazin-2,4-dione have been known for their wide application in agricultural field. In contrast, fused 1,2,4-triazolo[1,5-*a*][1,3,5]triazines have shown bioactivities such as selective adenosine receptor antagonism^{47,49} and xanthine oxidase inhibition⁵⁰. Beside these activities, this fused scaffold also exhibits anti-inflammatory, antioxidant, antiproliferative, antibacterial, and antifungal properties⁹. In addition, its closely related fused pyrazolo[1,5-*a*][1,3,5]triazine derivatives are also known for their diverse medicinal applications as reported over the past few decades. Due to the close resemblance with purine, derivatives of pyrazolo[1,5-*a*][1,3,5]triazine are known to modulate various enzymes and G-protein coupled receptors that are involved in purine metabolism and are therefore used in treatment of several pathological conditions¹⁰. However, inhibitory activity of 1,3,5-triazin-2,4-dione and its fused bicyclic analogues against TP has not yet been explored. Therefore, its potential interaction with TP is worth investigating.

2.2 Hypotheses and objectives

The most potent TP inhibitor TPI contains a pyrimidin-2,4-dione nucleus, hence it is hypothesized that the 1,3,5-triazin-2,4-dione having the essential homophthalimide moiety (O=C-NH-C=O), should be able to interact with the enzyme. In addition, it is postulated that structural modification of 7-deazaxanthine (7-DX) (Figure 8), a bicyclic TP inhibitor, by replacing the two carbon atoms at positions C9 and C5 with nitrogen would generate new compounds *viz.* 1,2,4-triazolo[1,5-*a*][1,3,5]triazine (Figure 8b) and pyrazolo[1,5-*a*][1,3,5]triazine (Figure 8c) would also demonstrate TP inhibitory activity. Furthermore, it is assumed that these compounds would demonstrate the TP associated anti-angiogenic property by attenuating the expression of various downstream angiogenic mediators and exhibited antiproliferative activity.

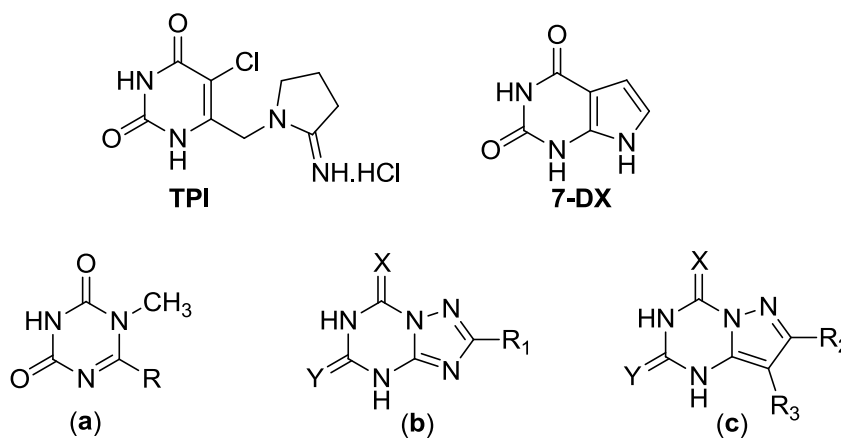


Figure 8. Structures of known TP inhibitor (**TPI** and **7-DX**) and target compounds (**a**, **b** and **c**)

To test these hypotheses, the following objectives have been considered in this study.

- (i) To develop a practical synthetic methodology for preparing a library of various substituted 1,3,5-triazin-2,4-dione derivatives. The strategy for the synthesis of these monocyclic target compounds will include ring transformation reactions. In addition, molecular diversity of 1,3,5-triazin-

2,4-dione scaffolds will be achieved by introducing different groups at the position C6 of the core ring structures.

- (ii) To synthesize bicyclic analogues that carry the 1,2,4-triazolo[1,5-*a*][1,3,5]triazine and pyrazolo[1,5-*a*][1,3,5]triazine scaffolds via intramolecular heterocyclization. In addition, work will be carried out to investigate the optimal interactions and explore the chemical space of the binding site of the enzyme. The positions of C5 and C7, and the positions of C2 and C4 of the respective triazolo and pyrazolo fused triazine scaffold would be modified to include a carbonyl, a thiocarbonyl and a thiomethyl group. While the position C2 of 1,2,4-triazolo[1,5-*a*][1,3,5]triazine and C7, C8 of pyrazolo[1,5-*a*][1,3,5]triazine scaffolds would be modified by inserting different aromatic group and longer flexible side chain. Moreover, the structures of the target compounds and intermediates would be characterized, with an aim to understand the mechanism and regiochemistry of the reaction process.
- (iii) To evaluate the TP inhibition potential of the synthesized compounds by using an *in vitro* enzyme assay. This assay would be used to estimate the inhibition kinetic behaviour of the active target compounds. To quantify the TP inhibitory activity, a spectrophotometric assay method would be adopted. In this assay, recombinant human thymidine phosphorylase would be used together with thymidine as the substrate.
- (iv) To evaluate the structure activity relationship of the synthesized compounds by 3D-QSAR model based on the enzyme inhibition study. The 3D-QSAR study would be conducted based on comparative molecular field analysis (CoMFA).

- (v) To evaluate cellular responses *viz.* antiproliferative and antimetastasis potential of these compounds using cell viability assay and cell migration assay respectively. The MTT colorimetric assay would be employed to determine the cell viability while the cell invasion property would be estimated by using a ThinCert cell culture inserts with 8 μ M polycarbonate filters coated with BD Matrigel matrix of the synthesized compounds on breast cancer cell line, MDA-MB-231.
- (vi) To evaluate anti-angiogenesis effect *via* estimation of the expression of MMP-9, VEGF, IL-8 in breast cancer cell line. The gelatine zymography would be used to determine MMP expression on the same cell line whereas to quantify VEGF and IL-8 expression, a colorimetric enzyme-linked immunosorbent assay (ELISA) method would be adopted.

2.3 Significance of the study

The outcome of this study will demonstrate the utility of some of the reported methodologies for the synthesis of 1,3,5-triazin-2,4-dione, 1,2,4-triazolo[1,5-*a*][1,3,5]triazine and pyrazolo[1,5-*a*][1,3,5]triazine scaffold. Although, the synthetic methodologies for the construction of the monocyclic and fused bicyclic 1,3,5-triazine derivatives are based on previously described schemes, extensive structural modifications by incorporating a wide range of substituents around different positions of the core scaffolds have never been synthesized nor have their regiochemistry been investigated. Therefore, most of the compounds reported in this thesis will be new. Moreover, the investigation of the influencing factors in regioselectivity of the reaction processes will help to generate new derivatives of these scaffolds. Furthermore, the inhibition potential of these compounds against TP and their

inhibition kinetic behaviour have not been elucidated and reported. Therefore, it will be a first attempt. The set up of a 3D-QSAR study based on CoMFA analysis will provide the important structural pre-requisites for the interaction with TP. To demonstrate the potential significance of these new compounds in anticancer therapy, this study will also explore the inhibitory effect of these new TP inhibitors against tumour vascularisation, tumour growth, and metastasis. Overall, this study will be helpful in laying the foundation for further design and optimization of the new bicyclic TP inhibitors. Even though it is evident from literature review that these scaffolds exhibit diverse biological activities, this project mainly focuses on specific biological aspects of these compounds. A complete evaluation of all the possible biological activities is beyond the scope of this study.

In the subsequent chapters, detail descriptions on the experimental design, results and discussion of the synthesis, biological evaluations and QSAR study of 1,3,5-triazin-2,4-dione and its fused analogues will be provided.

Chapter 3

The Preliminary Studies - Establishing Lead Compounds through Synthesis and Bioassay

3.1 Synthesis of 1,3,5-triazin-2,4-dione and their fused analogues to explore lead inhibitor compounds of thymidine phosphorylase

Functionalization of the 1,3,5-triazine scaffold with suitable substituents can generate a large number of biologically active compounds having exciting range of medicinal values. However, few derivatives of 1,3,5-triazin-2,4-dione have exhibited in their pharmaceutical uses. The compounds bearing this scaffold have a long history in their agricultural applications such as fungicides, insecticides and herbicides⁴⁵. In contrast, fused 1,2,4-triazolo[1,5-*a*][1,3,5]triazines and pyrazolo[1,5-*a*][1,3,5]triazines are well known for their diverse medicinal applications^{9,10}. As a result, the synthesis of 1,2,4-triazolo and/or pyrazolo fused 1,3,5-triazine continues to draw considerable attention of the organic and medicinal chemists. Derivatives of 1,2,4-triazolo[1,5-*a*][1,3,5]triazine have been of special interest due to their biological activities such as adenosine receptor inhibition^{47,49} and xanthine oxidase antagonism⁵⁰. This scaffold with appropriate substituents is known for its antiinflammatory, antioxidant, antiproliferative, antibacterial, and antifungal properties⁹. On the other hand, the derivatives of the pyrazolo[1,5-*a*][1,3,5]triazine scaffold are known to target enzymes involved in the metabolism of biogenic purines including xanthine oxidase (XO), type 2 cyclin-dependent kinase (CDK2), phosphodiesterase (PDE), DNA gyrase etc. Furthermore, some derivatives of this scaffold also modulate the activities of G-protein coupled purinergic signalling receptors *viz.* adenosine, P2Y₁, corticotrophin-releasing factor, neuropeptide Y, 5-HT, cannabinoid and angiotensin receptors, thus resulting in diverse biological outcomes. To date, on-going efforts are being made in exploiting the therapeutic potential of developing the 1,3,5-triazine and its fused analogues. With regards to our interest in the synthesis of 1,3,5-triazine derivatives with potential biological activity, our laboratory has reported some synthetic aspects

as well as medicinal properties of the 4,6-diamino-1,3,5-triazines¹⁹⁹⁻²⁰¹. The success of this project has encouraged us to extend 1,3,5-triazin-2,4-dione and its fused analogues expected to have interesting medicinal and biological properties. As stated, although significant efforts have been made to explore wide range of biological activities of 1,3,5-triazine and its fused analogues, no unequivocal study on inhibitory activity of this scaffold against thymidine phosphorylase (TP) is currently available despite large number of TP inhibitors with wide range of structural diversity has been investigated. Obviously, an investigation of 1,3,5-triazin-2,4-dione and its fused analogues for TP inhibition is worthy of an attempt.

Significant research works in exploring novel TP inhibitors have identified 5-chloro-6-[1-(2-iminopyrrolidinyl) methyl] uracil hydrochloride (**TPI**) and 7-deazaxanthine (**7-DX**) as leading TP inhibitor candidate¹⁴⁵. Herein, it was assumed that monocyclic 1,3,5-triazin-2,4-dione and bicyclic 1,2,4-triazolo[1,5-*a*][1,3,5]triazine and pyrazolo[1,5-*a*][1,3,5]triazine would exhibit anti-thymidine phosphorylase activity due to their close resemblance to **TPI** and **7-DX** structural motifs (Figure 8).

To address these hypotheses, a library of compounds bearing 1,3,5-triazin-2,4-dione and its fused analogues was synthesized and the compounds were screened for their TP inhibitory activity to explore potential lead inhibitors against thymidine phosphorylase. In an attempt to determine the pharmacophoric requirements and to explore the chemical space of the active site of the enzyme, the fused scaffolds were modified by introducing a carbonyl, a thiocarbonyl and a thiomethyl group. In addition, the respective position C2 and C7 of these two fused analogues was modified by inserting aromatic or aliphatic groups. Moreover, further modification at the position C2 of the 1,2,4-triazolo[1,5-*a*][1,3,5]triazine scaffold was made by

incorporating one methylene bridge in between the fused skeleton and lipophilic aromatic moiety. Similar approach was adapted to modify the position C8 of the pyrazolo[1,5-*a*][1,3,5]triazine scaffold. Analogous synthetic methodology allowed the introduction of additional thiourea moiety at position C7 of the same scaffold. In this preliminary study, the target compounds to be synthesized are provided in Figure 9.

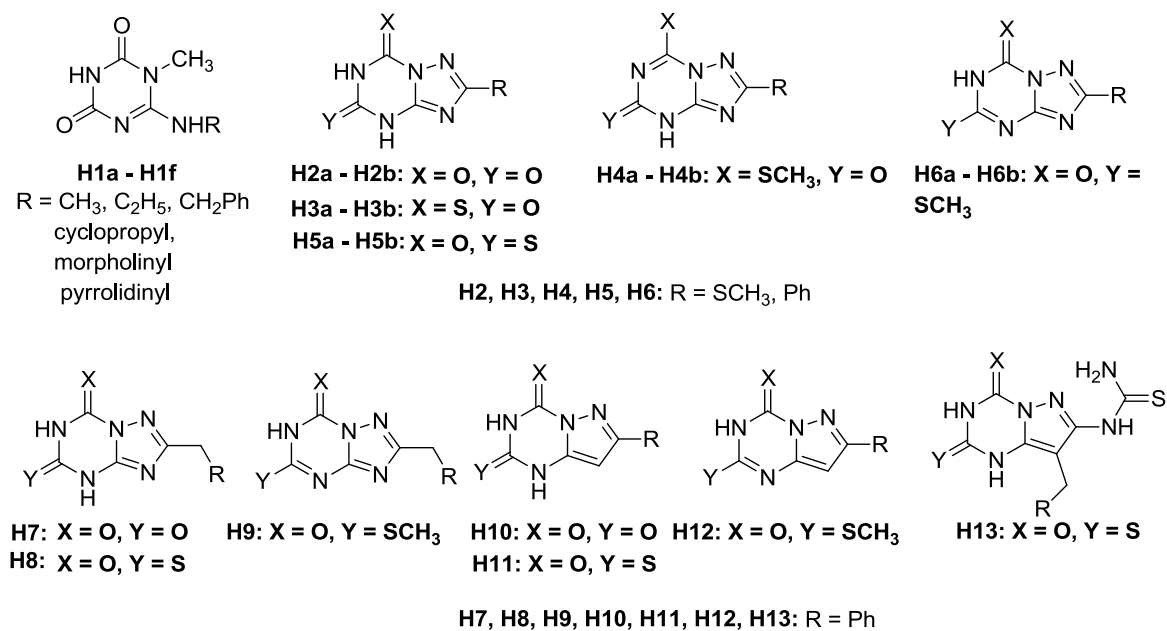


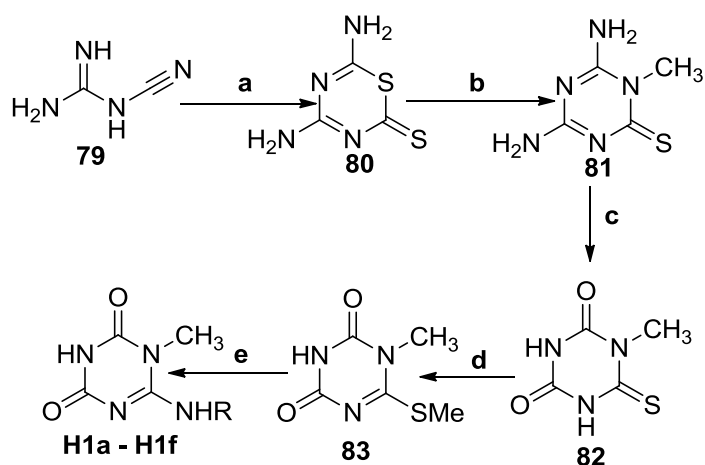
Figure 9. Structures of target compounds to be synthesized in the preliminary study

3.2 Chemistry

3.2.1 Synthesis of 1,3,5-triazin-2,4-diones derivatives

Several methods for the synthesis of 1,3,5-triazin-2,4-diones have been reported in the literature. These include, for example, the condensation of biurets with orthoester²⁰², the reaction of urea derivatives with an isocyanate etc⁷. Alternatively, Kantlehner et al⁸ developed a method to synthesize this scaffold *via* the reaction of aromatic or aliphatic isocyanates with N,O-bis(trimethylsilyl)acetamide followed by desilylation using alcohol.

In an attempt to synthesize monocyclic 1,3,5-triazin-2,4-dione derivatives (**H1a** – **H1f**) with potential anti-TP activity, a multi-step synthetic approach has been developed (Scheme 15).



Reagents and conditions: (a) CS₂, acetone, r.t., acetic acid (b) CH₃NH₂, DMF, r.t. 2 M NaOH (c) Reflux in 6M HCl (d) MeI, 2.5M NaOH, r.t. (e) RNH₂, reflux in MeOH

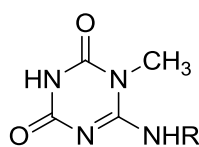
Scheme 15. Synthesis of monocyclic 1,3,5-triazin-2,4-dione derivatives (**H1a**–**H1f**)

Although, previously disclosed methods were modified to construct the desired compounds, the compounds reported here are new. The adopted synthetic scheme 15 allowed the reactive methyl mercaptan group of compound **83** to be substituted by

primary and secondary amines *via* single step that led to the formation of various target compounds (**H1a-H1f**). The compounds were characterized by NMR and mass spectroscopic analysis. The reaction yields and melting points of the compounds were also determined and presented in Table 2.

The synthesis of 1-methyl-6-methylthio-1,3,5-triazin-2,4-dione (**83**) reported here has been successfully accomplished *via* four steps. The first step of the process began with the preparation of the 4,6-diamino-2-mercapto-1,3,5-thiadiazine (**80**), which was promptly obtained as previously described by Birtwell (1948)²⁰³. In this step, the cyclocondensation of cyanoguanidine (**79**) with carbon disulphide in presence of potassium hydroxide afforded an intermediate, dipotassium ω-cyanoguanidinodithiocarbonate, which upon ring closure in the presence of acetic acid has led to the formation of **80**. The reaction was very straight forward and proceeded with satisfactory yield (55%). The main features in the ¹H NMR spectrum of **80** consisted of four singlets located at around 8.03, 8.30, 8.67 and 8.81 ppm and each singlet corresponded to one proton of the four H of the two NH₂ groups. This splitting of the two -NH₂ group was probably due to restricted rotation of N-C bond resulted from charge delocalization from the ring onto exocyclic amino group. In the second step, the successful synthesis of 1-methyl-4,6-diamino-1,3,5-triazin-2(1*H*)-thione (**81**) was achieved by a previously reported method, with some modifications²⁰⁴. In brief, in a suspension of **80** in DMF, methylamine was added to react for 30 min and followed by addition of 2M NaOH solution allowed to ring close in one-pot reaction. The appearance of the N-Me peak at about 3.68 and 35.5 ppm in ¹H NMR and ¹³C NMR respectively indicated the formation of **81**. To synthesize 6-thio-1,3,5-triazin-2,4-dione (**82**), initially, the previous described method was adopted²⁰⁵. However, due to the prolonged reaction time in acidic medium, the

hydrolytic step afforded 1-methyl-[1,3,5]triazin-2,4,6-trione instead. The structure of this compound was confirmed by the use of ^{13}C NMR spectroscopy. The three carbonyl carbons appeared in 149.2 and 150.6 ppm respectively in ^{13}C NMR spectra. Thereafter, to optimize the reaction condition in order to achieve the desired compound **82**, the reaction time was shortened to 2 hours using the same concentration of hydrochloric acid (6M) and this condition indeed afforded the desirable product. The appearance of the peak of thiocarbonyl carbon atom in ^{13}C NMR at about 179.4 ppm indicated the formation of compound **82**. In the subsequent step, the corresponding 6-methylthio derivative (**83**) was prepared by the reaction of **82** with iodomethane in alkali. Due to presence of several nucleophilic centers in **82**, the methyl group of iodomethane could attack at different positions under different reaction conditions and afforded a mixture of products. However, the condition²⁶ adopted here, produced thermodynamically most stable compound **83** exclusively with reasonably good yield (60%). The appearance of a sharp singlet at 2.50 ppm corresponding to the three protons of SMe in the ^1H NMR spectrum confirmed the structure of the product. In the final step, compound **83** was employed to synthesize substituted 1,3,5-triazin-2,4-diones (**H1a-H1g**) *via* nucleophilic substitution with different primary and secondary amines. Simple reflux in methanol for duration between 3-5 hr was employed as the reaction condition. The products were obtained in a range of yields (23-85%) (Table 2).

Table 2. Synthesis of 6 substituted 1,3,5-triazin-2, 4-diones**H1a - H1f**

Entry	Cpd	R	Yield (%)	mp (°C)
1	H1a	CH ₃	66	305-307
2	H1b	C ₂ H ₅	76	263-265
3	H1c	CH ₂ Ph	53	297-298
4	H1d	cyclopropyl	61	259
5	H1e	morpholinyl	85	240-242
6	H1f	pyrrolidinyl	23	220

3.2.2 Synthesis of fused 1,2,4-triazolo[1,5-*a*][1,3,5]triazin-5,7(4*H*,6*H*)-dione and its thioxo-bioisosteres

As mentioned in the literature review, the synthesis of 1,2,4-triazolo[1,5-*a*][1,3,5]triazine could be successfully achieved by several reported methods and these methods can be broadly categorized as: A) annulation of the 1,3,5-triazine ring onto a 1,2,4-triazole scaffold; B) annulation of the 1,2,4-triazole ring onto a 1,3,5-triazine scaffold; C) concurrent formation of both the 1,3,5-triazine and 1,2,4-triazole ring; (D) synthesis *via* ring transformation reactions. Herein, the synthesis of 1,2,4-triazolo[1,5-*a*][1,3,5]triazin-5,7(4*H*,6*H*)-dione and their thioxo-bioisosteres was performed *via* annulation of 1,3,5-triazine ring onto a 1,2,4-triazole scaffold. The adopted synthetic methodology allowed the synthesis of different derivatives of this fused scaffold with modification at the position C2 conveniently. Strategically, the position C2 of the 1,2,4-triazolo[1,5-*a*][1,3,5]triazin-5,7(4*H*,6*H*)-dione and their

thioxo-bioisosteres was modified by introducing substituents which are either directly attached with the fused ring or *via* methylene bridge respectively (Scheme 16 and 17).

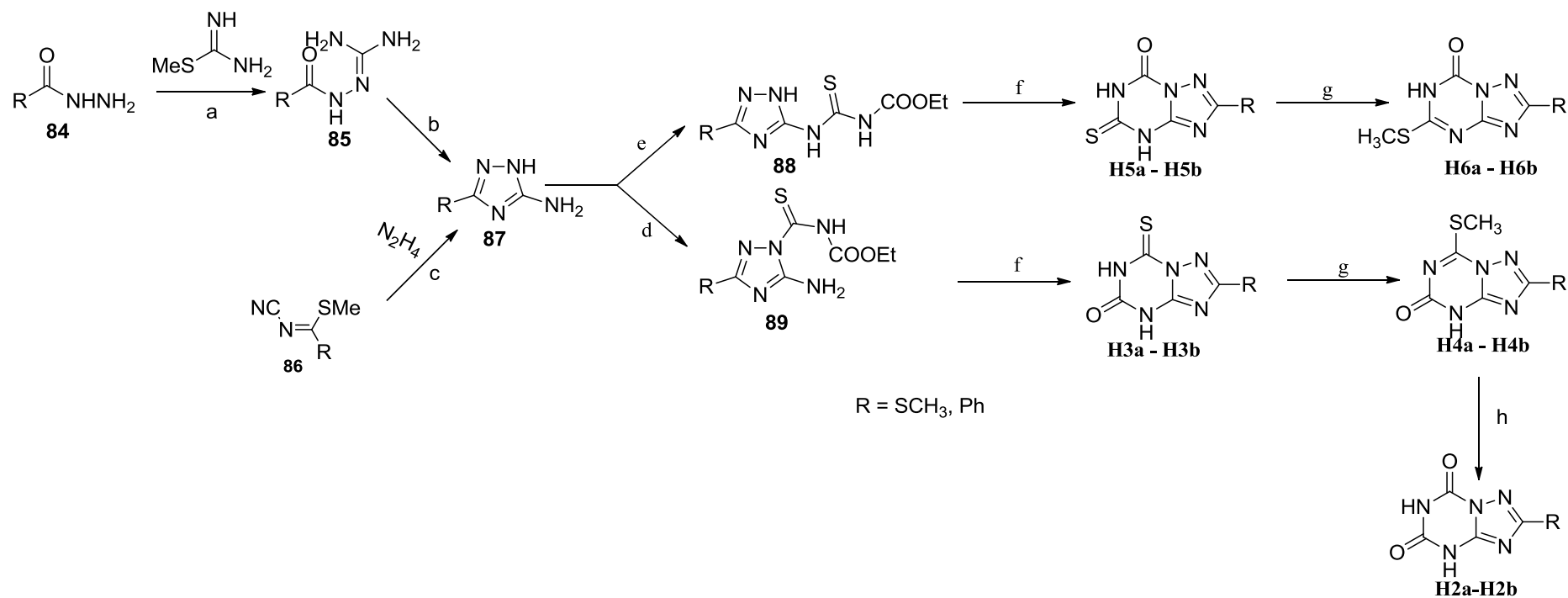
- **Synthesis of derivatives modified at the position C2 (substituents directly attached with fused ring)**

In these reaction methods, 5-amino-1,2,4-triazoles bearing -C-N-C appendage (carbethoxylthiocarbamoyl) at N1 or 1,2,4-triazoles having N-C-N-C at N(5)3 underwent intramolecular heterocyclization resulting in formation of target compounds (**H2-H6**). Before synthesis of 1,2,4-triazolo[1,5-*a*][1,3,5]triazine, two general methods which were previously developed by our group and other lab²⁰⁶⁻²⁰⁸, were adopted to synthesize the key intermediate, 3(5)-amino-1,2,4-triazoles (**87**) (Scheme 16). In the first method, the reaction of benzhydrazide (**84**) with *S*-methyl isothiurea in basic condition afforded arylamidoguanidines (**85**) which underwent cyclocondensation in microwave irradiation, and subsequently afforded 3(5)-amino-1,2,4-triazoles (**87**) in water. It gave quantitative yield and excellent purity of the products. In the second method, the reaction of dimethyl-*N*-cyanodithiocarbonimidate (**86**) with hydrazine produced 3-(methylthio)-amino-1,2,4-triazoles (**87**). Therefore, these two methods provided scope to introduce aromatic and aliphatic substituents at C2 of the fused ring respectively.

Due to the presence of several nucleophilic centres, different regioisomeric products could be produced from the reactions of 3(5)-amino-5(3)-aryl-1,2,4-triazoles (**87**) with ethoxycarbonyl isothiocyanate and the regioselectivity of the reaction depended on the conditions used for the reactions. For example, in DMF, ethoxycarbonyl isothiocyanate attacked the exocyclic nitrogen of 3(5)-amino-1,2,4-triazoles (**87**) resulting in the formation of the thermodynamically more stable products *N*-(3(5)-

aryl-1,2,4-triazol-5(3)-yl)-*N'*-carbethoxythioureas (**88**) exclusively with good yields. Due to mesomeric effect, probably the lone pair electron of N(1)H was withdrawn by substitutions attached at the position C3(5) resulting in decrease of the nucleophilicity of N(1)H and consequently addition product **88** was exclusively isolated in DMF. However, the reaction of 3(5)-amino-5(3)-aryl-1,2,4-triazoles (**87**) with ethoxycarbonyl isothiocyanate in anhydrous acetone afforded a separable mixture of two regioisomeric products (**88** and **89**). The 5-amino-1-carbethoxylthiocarbamoyl-1,2,4-triazole (**89**) was thermodynamically unstable isomer and it was readily converted to the more stable *N*-(1,2,4-triazol-5(3)-yl)-*N'*-carbethoxythioureas (**88**) in DMSO or at higher temperature.

The synthesis of target compounds **H5a-H5b** and **H3a-H3b** was achieved by intramolecular heterocyclization of *N*-(1,2,4-triazol-5(3)-yl)-*N'*-carbethoxythioureas (**88**) and 5-amino-1-carbethoxylthiocarbamoyl-1,2,4-triazole (**89**) respectively in an alkaline medium ²⁶ as illustrated in scheme 16. This approach afforded products of high yields and purity. The compounds **H4** and **H6**, corresponding methylthio derivatives of **H3** and **H5** respectively, were prepared *via* the treatment of parent compounds with iodomethane in aqueous alkaline medium and this method afforded generally good yields (61-67%) of products. These methylthio derivatives **H4a-H4b** were converted subsequently to compounds **H2a-H2b** by the treatment of a mild oxidizing agent, hydrogen peroxide, in an alkaline medium and this reaction afforded highly pure products with satisfactory yields (54-68%) (Table 3).



Reagents and conditions: (a) NaOH, r.t, 72 h, (b) Water, MW irradiation, 180 °C, 10 min (c) MeOH, 40 °C, 5 h (d) Ethoxycarbonyl isothiocyanate, acetone, r.t. (e) Ethoxycarbonyl isothiocyanate, DMF, r.t. (f) NaOH, 80% ethanol (aq.), 100 °C. (g) MeI, NaOH, water, r.t. (h) H₂O₂, NaOH, water, 60-70 °C.

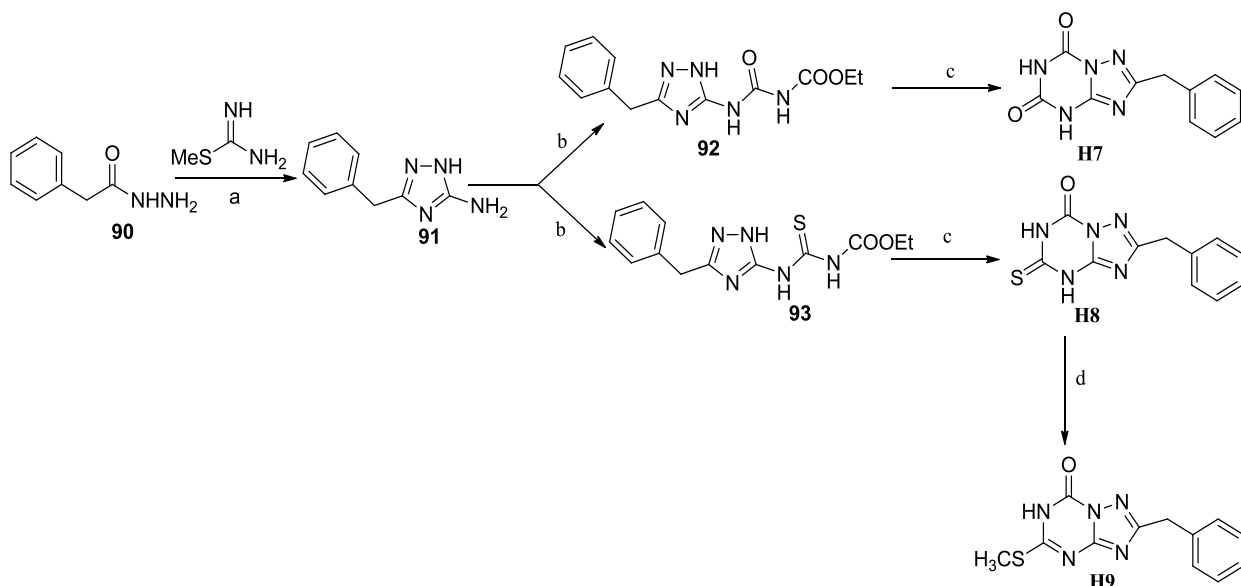
Scheme 16. Synthesis of 2-substituted-1,2,4-triazolo[1,5-*a*][1,3,5]triazin-5,7(4*H*,6*H*)-dione and its derivatives (**H2**, **H3**, **H4**, **H5** and **H6**)

All the synthesized compounds were characterized by melting points, ^1H NMR, ^{13}C NMR spectroscopy and mass spectrometry. The purity of compounds was determined by reverse phase HPLC. Interestingly, the structures of compounds **H2-H6** were readily distinguished and confirmed by the use of ^{13}C NMR spectroscopy. The ^{13}C peak of the thiocarbonyl (C=S) carbon of **H5b** appeared at around 175.8 ppm; while this group showed peaks at about 170.8 ppm for **H3b**. The two signals of the carbonyl (C=O) groups of compound **H2a** appeared at about 152.5 and 162.2 ppm in ^{13}C NMR spectra. The appearance of the peak at about 11.8 and 13.9 ppm assigned to SMe in the ^{13}C NMR spectrum indicated the formation of product **H4b** and **H6b** respectively. The purity of all compounds was satisfactory (above 95%).

- **Synthesis of derivatives with benzyl group at the position C2 (substituents attached with fused ring *via* methylene bridge)**

Analogously, the synthesis of 2-benzyl-[1,2,4]triazolo[1,5-*a*][1,3,5]triazin-5,7(4*H*,6*H*)-dione and its derivatives (**H7**, **H8**, and **H9**) was successfully achieved by a ring annulation reaction (Scheme 17). Although the general synthetic route for the base catalyzed annulations of triazine ring is based on chemistry developed by Bokaldere and co-workers²⁶, this study described for the first time, a simple and efficient method for the preparation of related compounds having 1,2,4-triazolo fused triazine structure with one methylene bridge at position 2. The synthesis started from the preparation of building block, benzyl substituted 1,2,4-triazole (**91**) *via* the reaction of 2-phenylacetohydrazide (**90**) with *S*-methyl isothiourea in an aqueous alkaline medium which was previously established in our lab²⁰⁶. The reagent 2-phenylacetohydrazide would provide the methylene bridge at the position C2 of target compounds. The treatment of **91** with ethoxy carbonyl isothiocyanate and ethyl

isocyno formate in DMF afforded the corresponding thiourea and urea derivatives (**92** and **93**) which underwent intramolecular heterocyclization in presence of base resulting in formation of target compounds (**H7** and **H8**) respectively in 47-55% yield (Table 3). In alkali medium, compound **H8** was subjected to treatment with iodomethane to produce **H9**.



Reagents and conditions: (a) NaOH, r.t, 72 h (b) Ethoxycarbonyl isothiocyanate, or ethyl isocyanocarbonyl methyl sulfide, DMF, r.t. 5 h (c) NaOH, 80% ethanol (aq.), 100 °C. (d) MeI, NaOH, water, r.t.

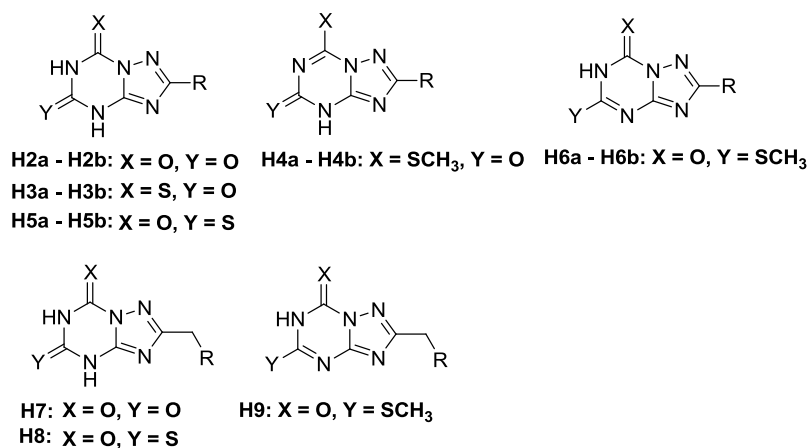
Scheme 17. Synthesis of 2-benzyl-[1,2,4]triazolo[1,5-*a*][1,3,5]triazin-5,7(4*H*,6*H*)-dione and its derivatives (**H7**, **H8** and **H9**)

The prepared compounds were characterized by ¹H, ¹³C NMR and mass spectroscopy. The ring closure of **H8** was evident by the disappearance of triplet around 1.24 ppm and quartet at around 4.19 ppm corresponding to the CO₂Et signal and singlet at around 13.52 and 13.78 ppm corresponding to tautomeric NH signal of intermediate **93** in the ¹H NMR spectra when the spectra was recorded in DMSO-*d*₆. In addition, a low field movement of the signal corresponding to the aromatic proton was observed when the spectrum of open (**93**) to the close analogues (**H8**) was compared. In ¹³C NMR, the sharp signal of carbonyl (C=O) and thiocarbonyl (C=S) appearing at

around 165.0 and 175.8 ppm respectively indicated the formation of desired compounds (**H8**). In contrast, two sharp peaks at around 152.1 and 164.8 ppm corresponding to two carbonyl (C=O) carbon were observed in ^{13}C NMR spectra for compound **H7**.

The characteristic signal of methyl group appeared at around 2.50 and 34.4 ppm in ^1H NMR and ^{13}C NMR respectively suggested formation of compound **H9**. The purity of all compounds determined by HPLC was above 95 %.

Table 3. Synthesis of 1,2,4-triazolo[1,5-*a*][1,3,5]triazin-5,7(4*H*,6*H*)-dione and its derivatives



Entry	Cpd	R	% Yield	mp (°C)	Entry	Cpd	R	% Yield	mp (°C)
1	H2a	SCH ₃	68	284-286	8	H5b	Ph	78	258-259
2	H2b	Ph	54	318-319	9	H6a	SCH ₃	54	241-243
3	H3a	SCH ₃	72	254-256	10	H6b	Ph	58	292-294
4	H3b	Ph	59	285-287	11	H7	Ph	47	>75-
5	H4a	SCH ₃	67	274-276	12	H8	Ph	55	246
6	H4b	Ph	61	300-301	13	H9	Ph	54	96-98
7	H5a	SCH ₃	64	263					

3.2. 3 Synthesis of pyrazolo[1,5-*a*][1,3,5]triazin-2,4(1*H*,3*H*)-dione and its thioxo bioisostere

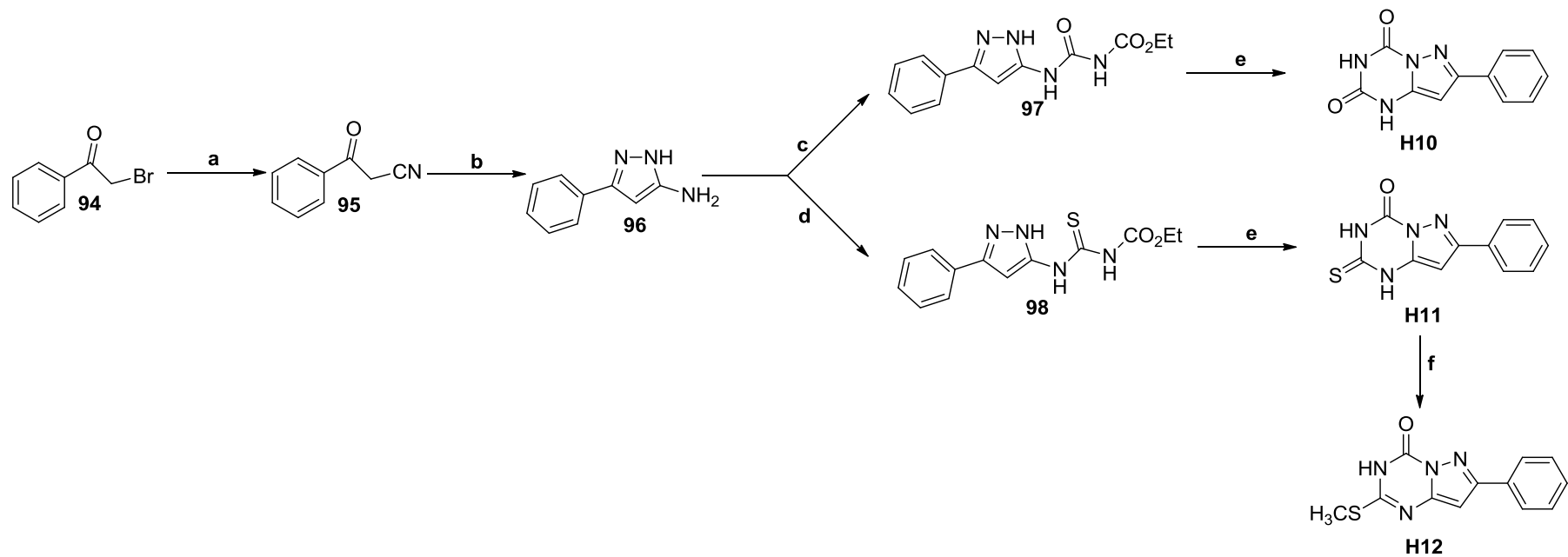
Similarly, we adopted reported method and modified it to construct pyrazolo[1,5-*a*][1,3,5]triazin-2,4(1*H*,3*H*)-dione and their thioxo-bioisosteres **H10-H13**^{41,44}. The synthesis of these target compounds was achieved *via* annulation of the triazine ring onto a pyrazole motif. In this synthetic pathway, pyrazole ring having a N-C-N-C appendage at C3(5) underwent intramolecular heterocyclization in alkaline medium to afford the desired compounds **H10-H13**. By adopting this synthetic methodology, various substitutions could be introduced at the position C7 and C8 of the fused ring system depending on the starting materials used which are available commercially. Initially, the C7 of fused ring was modified by inserting substituent which was directly attached with the core structure. Moreover, an attempt was made to include substituents at the positions C7 and C8 of the fused ring using similar reaction condition.

- **Synthesis of derivatives modified at the position C7 (substituent directly attached with fused ring)**

To generate the target compounds **H10-H12**, initially, the key intermediate, aminopyrazole (**96**) was synthesized *via* two convenient practical steps (Scheme 18). In the first step, the bromoacetophenone (**94**) was converted to cyanoacetophenone (**95**) by sodium cyanide in aqueous ethanol in the presence of dilute hydrochloric acid^{209,210}. Consequently, the cyanoacetophenone (**95**) was subjected to microwave irradiation in the presence of hydrazine hydrate to afford the aminopyrazole²¹¹. Following these steps, the nucleophilic reaction between the synthesized aminopyrazole and ethoxycarbonyl isocyanate or ethoxycarbonyl isothiocyanate in

DMF resulted in the formation of the addition product *viz.* compound **97** and **98** respectively with good yields. The compounds **97** and **98** having carbethoxycarbamoyl and carbethoxylthiocarbamoyl moiety underwent intramolecular cyclization to afford desired compounds **H10** and **H11** respectively when heated in presence of the sodium hydroxide with acceptable yield and purity. The corresponding thiomethyl derivative **H11** was synthesized by treating **H12** with methyl iodide in alkaline medium. It is reported that the compounds **H11** and **H12** were successfully synthesized *via* similar reaction condition in different solvent system^{44a}. However, this reaction took prolong time to complete.

The structures of the synthesized compounds were determined using different analytical tools including ¹H NMR, ¹³C NMR, and mass spectroscopy whereas the purity of the compounds was evaluated using reverse phase HPLC. Analysis of the ¹³C NMR spectral data of these compounds revealed that two sharp signals of carbonyl (C=O) and thiocarbonyl (C=S) carbon of compound **H11** were appeared at around 155.9 and 173.6 ppm respectively while two peaks corresponding to carbonyl (C=O) moiety of compound **H10** were found at around 148.3 and 155.0 ppm in ¹³C NMR spectral data. Moreover, the appearance of sharp peaks at around 13.6 ppm assigned for thiomethyl moiety confirmed the formation of compound **H12**.

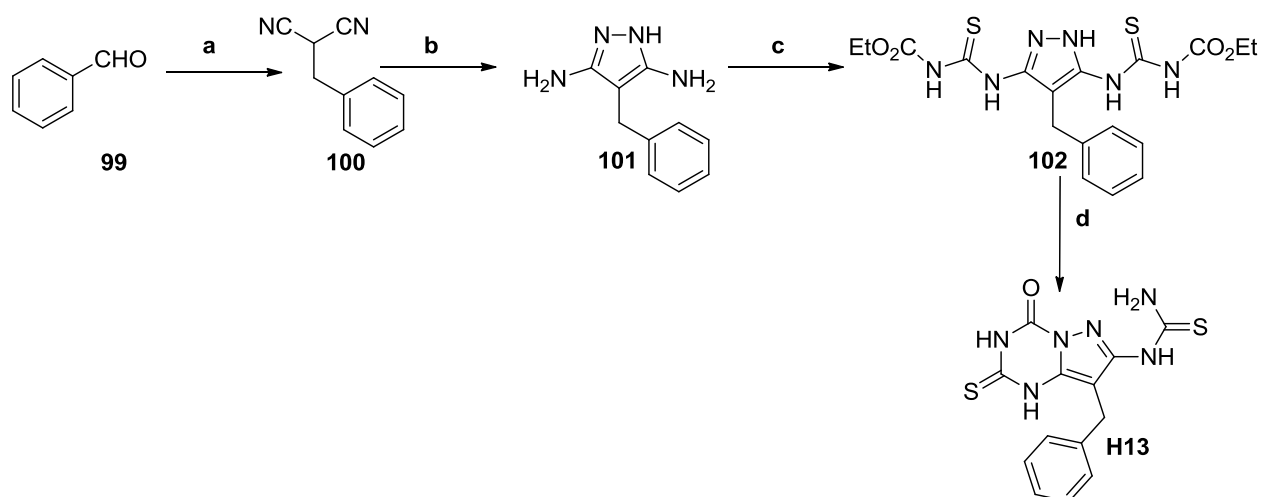


Reagents and conditions: (a) NaCN, HCl, aq-ethanol, r.t. (b) NH₂NH₂·H₂O, Methanol, MW, 140 °C, (c) EtO₂CN=O, DMF, r.t., 5 h (d) EtO₂CN=S, DMF, r.t., 5 h (e) NaOH, 80% ethanol (aq.), 100 °C. (f) MeI, NaOH, water, r.t., 30 min, 2.5 M HCl.

Scheme 18. Synthesis of 7-phenyl-pyrazolo[1,5-*a*][1,3,5]triazin-2,4(1*H*,3*H*)-dione and its derivatives (**H10**, **H11** and **H12**)

- **Synthesis of derivatives modified at the positions C7 (introduction of thiourea moiety) and C8 (introduction of benzyl moiety)**

Introduction of substituents at both C7 and C8 of the pyrazolo fused triazine scaffold was achieved by using 4-substituted-1*H*-pyrazol-3,5-diamine as a building block, which upon treatment with ethoxycarbonyl isothiocyanate afforded corresponding thiourea derivatives. The intramolecular heterocyclization of thiourea derivative in the presence of base led to the formation of target compounds (**H13**) (Scheme 19).



Reagents and conditions: (a) Malononitrile, aq-ethanol, NaBH₄, HCl, r.t. (b) NH₂NH₂.H₂O, ethanol, reflux, 5-8 h (c) Ethoxycarbonyl isothiocyanate, DMF, r.t., 5 h (d) NaOH, 80% ethanol (aq.), 100 °C

Scheme 19. Synthesis of (8-benzyl-4-oxo-2-thioxo-1,2,3,4-tetrahydro pyrazolo[1,5-*a*][1,3,5]triazin-7-yl)-thiourea (**H13**)

The diamino pyrazole (**101**) was synthesized *via* a practical two-step procedure starting from benzaldehyde (**99**). The first step of the process comprised of the synthesis of monosubstituted malononitriles (**100**) *via* the reductive alkylation of malononitrile with benzaldehyde (**99**) which readily converted to di-amino pyrazole (**101**) through simple reflux in ethanol with hydrazine hydrate. To synthesize the monosubstituted malononitrile (**100**), reported method was adopted that afforded

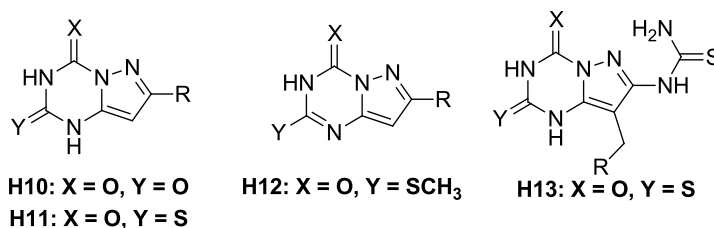
clean and high yield of products. This reaction process consisted of two steps including condensation of malononitrile and benzaldehyde in aqueous-ethanol medium followed by reduction of intermediate dicyanoalkene in the presence of sodium borohydride in the same pot²¹². The monosubstituted malononitriles formed in the reaction mixture were isolated *via* filtration or extraction process. Following this step, the reaction of **100** with hydrazine hydrate was carried out by conventional reflux in ethanol for 5-8 h which proceeded to 4-substituted-1*H*-pyrazol-3,5-diamine (**101**) with satisfactory yield²¹³. In the subsequent step, the nucleophilic addition reaction of 4-substituted-1*H*-pyrazol-3,5-diamine (**101**) with ethoxycarbonyl isothiocyanate in DMF, afforded product **102** in good yield.

Heating of thiourea derivative (**102**) in aqueous-ethanol in the presence of a base resulted in the hydrolysis of ethoxycarbonyl group from one of the carbethoxythiourea chains while the other underwent subsequent (6 + 0) heterocyclization to give target compound **H13** (Scheme5). The heterocyclization was found to proceed regioselectively (1,5-*a* ring junction) resulting in the formation of target compound **H13** exclusively. The structures of the target compound were confirmed by using ¹H and ¹³C NMR and mass spectral data. The characteristic signal of carbonyl carbon (C=O) was observed at 151.9 ppm, whereas the two sharp peaks of thiocarbonyl moiety (C=S) appeared around 173.5 and 179.8 ppm respectively in ¹³C NMR spectra. The results are in agreement with those obtained in our previously synthesized structurally related compounds.

The appearance of two sharp singlets at 8.94 and 9.07 ppm that corresponded to one proton each of the NH₂ group of the thiourea chain in ¹H NMR spectrum of **H13** indicated restricted rotation of NH proton around N-C bond. The satisfactory purity of

the compound (above 95%) was assessed by HPLC method. In addition, the physicochemical properties including yield and melting point of compound **H13** were determined and tabulated in table 4.

Table 4. Synthesis of pyrazolo[1,5-*a*][1,3,5]triazin-2,4(1*H*,3*H*)-dione and its thioxo-derivatives



Entry	Cpd	R	%Yield	mp (°C)	Entry	Cpd	R	%Yield	mp (°C)
1	H10	Ph	55	312-314	3	H12	Ph	46	240-242
2	H11	Ph	72	286-288	4	H13	Ph	73	239-241

3.3 Evaluation of anti-thymidine phosphorylase (Anti-TP) activity

The thirteen groups of compounds (**H1-H13**) were evaluated for *in vitro* TP inhibitory activity by a spectrophotometric assay that used recombinant human thymidine phosphorylase, expressed in *E. coli* (T2807- Sigma Aldrich). The original method developed by Krenitsky (Krenitsky et al, 1979)²¹⁴ was modified and adopted. Briefly, in this assay, the change of absorbance of thymidine (dThd) at 290 nm due to enzymatic reaction was monitored after 4, 8, 12, 16, and 20 min and the initial reaction rate was determined from the slope of change in absorbance. For calculation of enzyme inhibition, the initial rate of change in absorbance at different concentrations of the test compound were converted to percentage inhibition of enzyme, and plotted against inhibitor concentration using Graphpad Prism vs 4.0 to obtain the IC₅₀ values. Preliminary screening of enzyme inhibition was carried out at 100 μM of each compound. The results of inhibitory potency of each compound

evaluated were expressed in terms of IC_{50} values, and was compared with that of **7-DX** (Table 5).

Unexpectedly, compounds **H1a-H1f**, having the homophthalimide moiety did not show any inhibitory potential at 100 μ M. From the x-ray crystal structure of TP complexed with **TPI**, it was revealed that **TPI** appeared to mimic the substrate transition state and bound to the enzyme as zwitterions (Figure 7). The nucleotide base interacted with residues Ser217, Arg202, Lys221 and His116 *via* hydrogen bonds while electron withdrawing chlorine atom at C5 projected into a lipophilic pocket formed by residues Leu148, Val208, Ile214 and Val24. In addition, the NH_2 group of the iminopyrrolidine ring formed two hydrogen bonds with an oxygen atom of S117 and with a water molecule of the bound phosphate group.

Compounds **H1a-H1f**, bearing the homophthalimide moiety, were predicted to bind in a similar orientation to the uracil moiety of **TPI** in the active site. However, these compounds exhibited no inhibitory effect, which could be attributed to many reasons. Firstly, the synthesized compounds have N-Me group instead of electron-withdrawing substituent at the C-5 position of the uracil ring. It is important to mention that 5-chloro group at C5 of **TPI** accommodated in a hydrophobic pocket of active site. In addition, this chloro group, attributed to the increased acidity of the N1 of **TPI**, resulting in a better mimic of the zwitterionic resonance and tighter binding to the active site. Secondly, our synthesized compounds compared to **TPI** lack a methylene bridge and therefore, they could not interact with important amino acid residues in the active site as a consequence of steric constraints arising from inflexibility of substitutions at C6. Lastly, compared to **TPI**, there is an absence of (protonated)

amino group in the structure of compounds **H1a-H1f**, and therefore it could not form the hydrogen bonds with the water pocket associated with phosphate.

Analogously, fused 1,2,4-triazolo[1,5-*a*][1,3,5]-triazin-2,4-dione *viz.* compound **H2a**, **H2b** having the aliphatic (SCH₃) and aromatic (Ph) substituent at the position C2 respectively, did not show any inhibitory potential at 100 μM. This result was not consistent with the previous report indicating that the homophthalimide group was a pharmacophoric requirement to impart inhibitory activity against TP¹⁹⁸. The modification of **H2a-H2b** by replacing the oxygen atom at C7 with the bioisosteric sulphur exhibited no improvement in the activity. In addition, the introduction of thiomethyl group at C7 and consequently the removal of one active hydrogen at C6 in compounds **H4a** and **H4b** showed no activity, just like in the case of **H2a-H2b**. Interestingly, with further modification of **H3a** and **H3b** by switching the positions of the carbonyl and thiocarbonyl moieties, affording 5-thioxo-5,6-dihydro-4*H*-[1,2,4]triazolo[1,5-*a*][1,3,5]triazin-7-one analogues (**H5a** and **H5b**), exhibited moderate to weak TP inhibitory activity (IC₅₀ value = 51.67 and 39.56 μM respectively). Further modification of **H5a** and **H5b**, by replacing thio-oxo moiety by thiomethyl group at the position C5 resulting in subsequent elimination of active hydrogen atom from N4, led to dramatic decrease in inhibition property as observed in compound **H6a** and **H6b** (IC₅₀ = > 100 and 95.05 μM respectively). The IC₅₀ values of the test compounds were compared with the positive control, 7-deazaxanthine, that exhibited IC₅₀ value of 42.63 μM in the same experimental conditions which was found to be in accordance with previous reported results¹⁰². Therefore, from the preliminary screening of different derivatives, it was revealed that a particular orientation of the C(=S)NHC(=O) moiety would be required to impart the inhibitory activity. In addition, it was also observed that lipophilic aromatic group was

compatible with higher binding affinity compared with aliphatic substitutions. These data clearly suggested that **H5a** and **H5b** could interact with binding site of the enzyme and thus exhibited inhibition property. It was assumed that the carbonyl group at C7, and its adjacent NH(6) group of **H5a** and **H5b** would form strong hydrogen bonding contacts with the binding site. Moreover, thiocarbonyl moiety at C5 and substitution at C2 may place themselves into some hydrophobic space in the interaction site. It was postulated from the experimental data that the hydrogen bonds in between amino acid residue and carbonyl group at C7 and the hydrophobic interaction with the thiocarbonyl moiety at C5 played a crucial role in inhibitory action. This explains why the modification of compounds **H5a** and **H5b** by switching the positions of the thiocarbonyl and carbonyl groups (in compounds **H3a-H3b**) and their corresponding thiomethyl compound (in compounds **H4a-H4b**) resulted in lowering inhibitory action. In addition, in compounds **H2a-H2b**, although the carbonyl group was retained at C7, the carbonyl group at C5 could not be properly accommodated in huge hydrophobic space due to its smaller atomic size as well as high polarity which may lead to misalignment of entire compound. The postulation of TP inhibitory activity of different 1,3,5-triazine and its fused analogues is based on the physicochemical properties of the different bioisosteric substituent (*viz.* C and S) present in the core ring structure. However, this postulation will still need to be further validated by modeling.

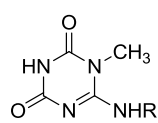
To improve inhibitory effect of compounds **H5b** and **H6b**, further modification of lead structure was made by adopting two strategies. Firstly, in order to impart flexibility and subsequently removal of steric constraints in the lead structure, a methylene bridge was introduced in between aromatic phenyl and fused ring. It is noteworthy that recently 6-methylene bridged uracil derivatives was reported as

novel, orally active, TP inhibitors including TPI, most potent TP inhibitor, so far. Secondly, for the purpose of structural optimization, the N3 of **H5b** and **H6b** was replaced with carbon atom, led to synthesis of pyrazolo[1,5-*a*][1,3,5]triazine. These two strategies resulted in generation of compounds **H10-H13**.

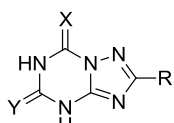
Biological evaluation of these compounds with respect to TP inhibitory activity suggested that compound **H8** ($IC_{50} = 43.32 \mu\text{M}$) and **H11** ($IC_{50} = 48.39 \mu\text{M}$) were not able to improve binding affinity compared to lead **H5b**. Therefore, it can be concluded that the introduction of methylene bridge in order to impart flexibility in lead structure and consequently removal of steric constrain could not enhance binding interaction for the enzyme. In addition, the presence of N3 moiety in **H5b** was proven to be essential as it could provide its lone pair of electron for hydrogen bond formation with amino acid residues of enzyme resulting in stronger inhibition pattern with respect to **H11**.

The exploration of TP inhibitory activity of compound **H9** and **H12**, the corresponding thiomethyl derivatives of **H8** and **H11** respectively, suggested that both of them exhibited lower inhibitory profile than their parent compound **H8** and **H11**. Surprisingly, **H12** ($IC_{50} = 71.01 \mu\text{M}$) showed better inhibitory activity than **H6b**. Interestingly, although two newly generated series did not display improvement of relative potency of **H5b**, there are several general structure-activity similarities, including the following: (1) introduction of the homophthalimide moiety in each series resulted in a complete loss of inhibitory potency, (2) isosteric replacement of carbonyl moiety at C5 or C2 by the thiocarbonyl moiety significantly enhanced inhibitory potency, and (3) incorporation of a thiomethyl moiety in C5 or C2 of fused ring decreases inhibitory activity compared to parent compound.

Table 5. Thymidine phosphorylase inhibitory activity of the synthesized compounds (H1-H13)



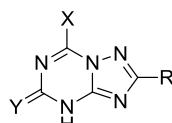
H1a - H1f



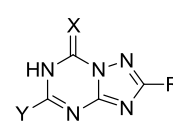
H2a - H2b: X = O, Y = O

H3a - H3b: X = S, Y = O

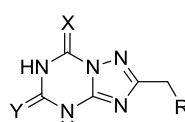
H5a - H5b: X = O, Y = S



H4a - H4b: X = SCH₃, Y = O

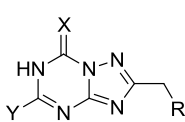


H6a - H6b: X = O, Y = SCH₃

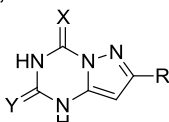


H7: X = O, Y = O

H8: X = O, Y = S

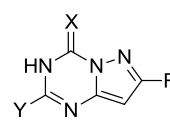


H9: X = O, Y = SCH₃

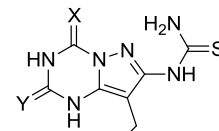


H10: X = O, Y = O

H11: X = O, Y = S



H12: X = O, Y = SCH₃



H13: X = O, Y = S

Entry	Cpd	R	TP Inhibition activity ^b IC ₅₀ (μM) (95% CI) ^a
1	H1a	CH ₃	> 100
2	H1b	C ₂ H ₅	> 100
3	H1c	CH ₂ Ph	> 100
4	H1d	cyclopropyl	> 100
5	H1e	morpholinyl	> 100
6	H1f	pyrrolidinyl	> 100
7	H2a	SCH ₃	> 100
8	H2b	Ph	> 100
9	H3a	SCH ₃	> 100
10	H3b	Ph	> 100
11	H4a	SCH ₃	> 100
12	H4b	Ph	> 100
13	H5a	SCH ₃	51.67 (45.75 to 58.36)
14	H5b	Ph	39.56 (38.32 to 40.84)
15	H6a	SCH ₃	> 100
16	H6b	Ph	95.05 (91.97 - 98.23)
17	H7	Ph	>100
18	H8	Ph	43.32 (39.91 - 47.02)
19	H9	Ph	>100
20	H10	Ph	> 100
21	H11	Ph	48.93 (46.54 - 51.44)
22	H12	Ph	71.01 (64.64 - 77.99)
23	H13	Ph	29.92 (25.74 - 34.77)
24	7-DX	-	42.63 (39.07-46.50)

^aconfidence interval, ^bexperiments carried out at least in duplicate.

In order to explore further, the structure of pyrazolo[1,5-*a*][1,3,5]triazine was modified by introducing substitutions at both C7 and C8 using analogous synthetic methodology that resulted in generation of new di-substituted lead compound **H13**. The TP inhibitory property assessment of this compound identified it as most potent lead compound among all the synthesized compounds ($IC_{50} = 29.92 \mu\text{M}$). It was believed that the newly introduced thiourea moiety would form strong hydrogen bond with amino acid residues of the binding site of enzyme, whereas, benzyl group could impart some hydrophobic interaction resulting in augmentation of inhibitory potential of compound **H13** (Table 5).

3.4 Summary

To summarize, an inexpensive and efficient method was optimized for the synthesis of 1,3,5-triazin-2,4-dione derivatives (**H1a-H1f**) with good yields. In addition, the use of intramolecular heterocyclization to generate the target compounds (**H2-H13**) was a practical synthetic approach. This preliminary study revealed that compounds having 1,3,5-triazin-2,4-dione and its fused analogues bearing homophthalimide moiety surprisingly did not exhibit the inhibitory potential against TP. It is believed that due to the structural alteration of the lead compounds (**TPI** and **7-DX**) by the insertion of the N moieties, the target compounds, in spite of having homophthalimide group, did not demonstrate any inhibitory activity. However, among the fused analogues, compounds having thiocarbonyl group and carbonyl group in particular orientation *viz* 5-thioxo-5,6-dihydro-4*H*-[1,2,4]triazolo[1,5-*a*][1,3,5]triazin-7-one, 2-thioxo-2,3-dihydropyrazolo[1,5-*a*][1,3,5]triazin-4(1*H*)-one and their thiomethyl derivatives showed inhibitory activity against thymidine phosphorylase. The compound **H13**, (8-benzyl-4-oxo-2-thioxo-1,2,3,4-tetrahydro-pyrazolo[1,5-*a*][1,3,5]triazin-7-yl)-thiourea,

was identified as most active lead compound among all the synthesized compounds ($IC_{50} = 29.92 \mu M$). Herein, the derivatives having triazolo and/or pyrazolo fused triazines scaffold were established as a new class of potential thymidine phosphorylase inhibitors that might provide more leads in drug design and optimization of fused-ring TP inhibitors. In addition, it is revealed from the preliminary study that one aromatic ring is essential to impart better biological effect and with the introduction of flexible chain in between aromatic and fused ring motif, compound can exhibit inhibitory property. Based on these promising results, further efforts are made to synthesize compounds with diverse structural modifications on the leads to enhance biological activities, and the results obtained from these efforts are reported and discussed in the following chapters.

Chapter 4

Lead Optimization for more Active Inhibitors of Thymidine Phosphorylase

4.1 Craig plot directed structural optimization of the lead compounds and the evaluation of their anti-thymidine phosphorylase activity

In the previous chapter, selected 1,3,5-triazin-2,4-dione and its fused bicyclic analogues *viz.* 1,2,4-triazolo[1,5-*a*][1,3,5]triazine and pyrazolo[1,5-*a*][1,3,5]triazine were synthesized and evaluated for their anti-TP potential. This preliminary study revealed that monocyclic 1,3,5-triazin-2,4-dione derivatives surprisingly did not exhibit inhibitory property against TP. However, the fused bicyclic analogues of this monocyclic 1,3,5-triazine have demonstrated moderate TP inhibitory effects. Among the fused bicyclic analogues, 5-thioxo-5,6-dihydro-4*H*-[1,2,4]triazolo[1,5-*a*][1,3,5]triazin-7-one and 2-thioxo-2,3-dihydropyrazolo[1,5-*a*][1,3,5]triazin-4(1*H*)-one showed inhibitory activity against thymidine phosphorylase. Particularly, compounds **H5b** ($IC_{50} = 39.56 \mu\text{M}$), **H8** ($IC_{50} = 43.32 \mu\text{M}$), **H11** ($IC_{50} = 48.93 \mu\text{M}$), and **H13** ($IC_{50} = 29.92 \mu\text{M}$) were identified as key lead structures with moderate inhibitory activity against TP (Figure 10). Therefore, further structural optimization of the lead compounds may lead to better enzyme inhibition activity.

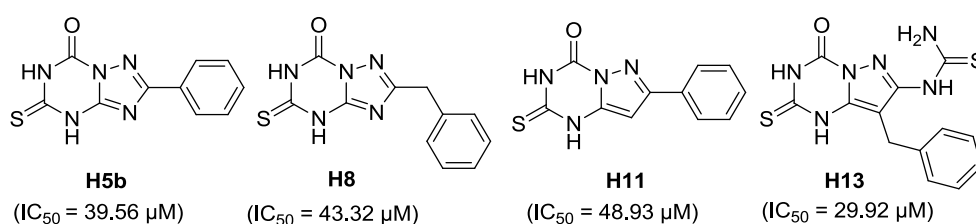


Figure 10. Structures of lead compounds and their IC_{50} values

Several strategies can be employed in the process of lead optimization in medicinal chemistry. These strategies often may involve the synthesis of derivatives containing a range of substituents on an aromatic or heteroaromatic ring or derivatising accessible functional groups that can modify the physicochemical properties of lead

compound resulting in alteration of the distribution, metabolism, or receptor binding interactions. There are an infinite number of possible analogues or derivatives that can be made, using several substituents and combination of substituents having different physicochemical properties in terms of their electronic, steric and hydrophobic properties and thus selection of substituents to synthesize analogues in lead optimization process is always challenging. However, Craig plot guided optimization²¹⁵ approach has often been employed to decide on the substituents to be selected for the study and such method has been proven to be extremely useful in tackling this stage of drug development.

It is evident from the preliminary study that all the lead compounds possess one phenyl ring directly or indirectly (*via* a methylene bridge) attached to the fused ring. It is important to mention that the phenyl ring of compound **H5b** ensured better hydrophobic interaction into the active site resulting in improved activity compared to aliphatic substituted analogues **H5a**. Herein, it is assumed that Craig plot directed structural modification of the phenyl ring of the lead compounds (**H5b**, **H8**, **H11** and **H13**) would exhibit improved inhibition properties against TP.

Therefore, the objective of this section was to synthesize derivatives of **H5b**, **H8**, **H11** and **H13** having different substituents on the phenyl ring (Figure 11). An evaluation of the influence of physicochemical properties of the substituents on TP inhibitory activity would be conducted. The libraries of the modified lead compounds were synthesized based on selected substituents found on the Craig plot. Substituents with a range of electronic properties, shapes and hydrophobicity were selected that are scattered around all four Craig plot quadrants. Guided by the Craig plot, representatives of substituents (F, Cl, Br, CF₃) with increased hydrophobicity and

electron withdrawing properties ($+\pi$, $+\sigma$), substituents (OCH_3 , OH) with more hydrophilic and electron donating properties ($-\pi$, $-\sigma$), substituents (CH_3) with positive hydrophobicity and negative σ values ($+\pi$, $-\sigma$), substituents (CN) with negative hydrophobicity and positive σ values ($-\pi$, $+\sigma$) were chosen for this study.

In this study, an array of 28 aromatic acid chlorides was selected as starting materials to generate a small library of 5-thioxo-5,6-dihydro-4*H*-[1,2,4]triazolo[1,5-*a*][1,3,5]triazin-7-one derivatives. These acid chlorides carried different substituents of varying hydrophobicity constant and Hammett constant at *meta* and/or *para* position in the phenyl ring. Analogous attempt was made to build 18 analogues of **H11** and **H13** starting from different substituted bromoacetophenone and aromatic aldehyde respectively. Consequently, the compounds synthesized were evaluated for *in vitro* enzyme assay.

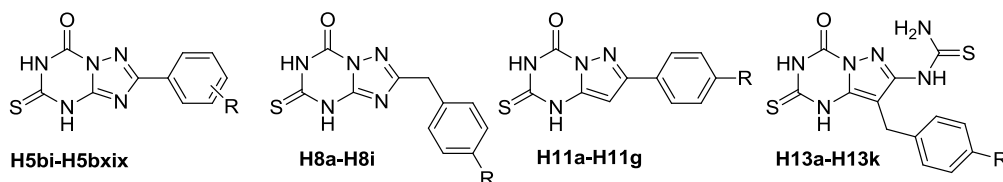


Figure 11. Planned Craig plot guided structural modification of lead compounds **H5b**, **H8**, **H11** and **H13**

4.1.1 Chemistry

4.1.1.1 Synthesis of 5-thioxo-5,6-dihydro-4*H*-[1,2,4]triazolo[1,5-*a*][1,3,5]triazin-7-one analogues

Target compounds, **H5b-H5bxix** and **H8a-H8i**, were prepared *via* (6+0) intramolecular heterocyclization of 1,2,4-triazoles having N-C-N-C appendages at N(5)₃ as described in scheme 20. For the synthesis of the desired compounds, the synthetic methodology adopted here a four-step reaction sequence. The synthesis

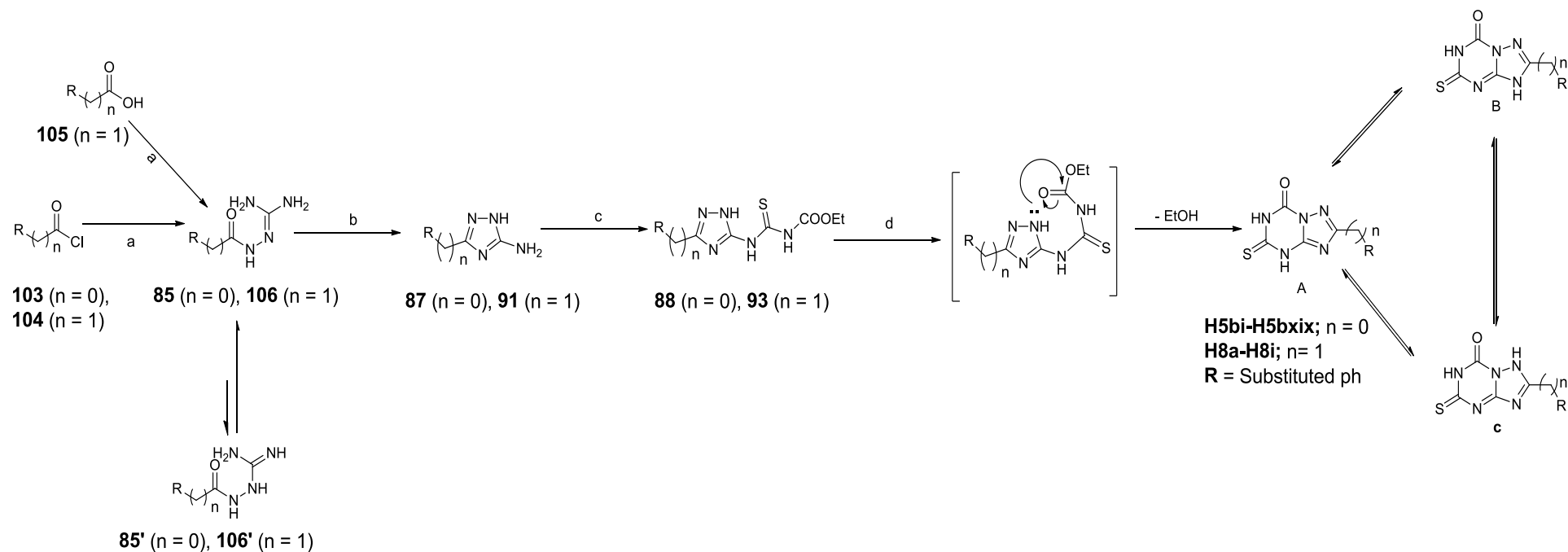
started from the aryl acid chloride (**103** and **104**) or aryl acetic acid (**105**) derivatives which were reacted with aminoguanidine hydrochloride to yield arylamidoguanidine and its derivatives (**85** and **106**) which upon microwave irradiation led to the synthesis of the key intermediates, 1,2,4-triazole derivatives (**87** and **91**). The treatment of **87** and **91** with ethoxycarbonyl isothiocyanate in DMF afforded the corresponding thiourea derivatives (**88** and **93**). In the presence of a base, the carbethoxythioureas underwent intramolecular heterocyclization, *via* an intermediate, resulting in the formation of the target compounds **H5bi-H5bxix** and **H8a-H8i**²⁶. The compounds synthesized were fully characterized by ¹H and ¹³C NMR spectroscopy and mass spectrometry. The yield and melting points of compounds were evaluated and reported in Table 6. The purity of compounds was accessed by the use of HPLC. The purity of all compounds was above 95 %.

By using different 3(5) substituted 1,2,4-triazole, this annulation reaction allowed a convenient means to introduce different substituents (substituted phenyl or benzyl) at the position C2 of the 1,2,4-triazolo fused triazine scaffold. The synthesis of 3(5) substituted 1,2,4-triazoles (**87** and **91**) was started by adopting the previously reported methods established in our laboratory^{206,207}. This method comprised of two steps reaction sequences. In the first step, the synthesis of arylamidoguanidines (**85** and **106**) was achieved from the reaction of corresponding hydrazides and *S*-methyl isothiurea. Following this step, 1,2,4-triazoles (**87** and **91**) were prepared from **85** and **106** by using microwave irradiation in aqueous medium. Although the second step reaction was found to be clean and afforded almost quantitative yield with satisfactory purity of products, the first step of this method had several disadvantages. For example, this reaction needed prolonged reaction time to complete (3 days) and often afforded only low yield of the products because of a complicated workup during

the isolation of the products from the reaction mixture. Moreover, this reaction could not successfully proceed for all the different substituted hydrazide used. Thereafter, continuous efforts were employed to overcome the disadvantages of this reaction. Initially, attempts were made to synthesize arylamidoguanidines by heating acid chloride and aminoguanidine bicarbonate in refluxing water or aqueous-ethanol medium. However, this reaction condition was not successful to afford the desired product. Alternatively, heating of acid chloride and aminoguanidine bicarbonate at 180 °C without using any solvent was attempted. In this reaction condition, the *para*-substituted nitro arylacid chloride was readily converted to the corresponding triazole. However, the reaction with other substituted acid chlorides was unsuccessful. Interestingly, by using aminoguanidine hydrochloride, the desired products were achieved successfully. In other words, arylamidoguanidines (**85** and **106**) could be formed by fusion of aryl acid chloride (**103** and **104**) with aminoguanidine hydrochloride at 180 °C for 20 minutes. Some acid chlorides were readily cyclised to 1,2,4-triazole under this reaction condition and therefore arylamidoguanidines were not isolated. In addition, it was observed that few substituted acid chlorides afforded a mixture of arylamidoguanidines and 1,2,4-triazole. The scope of the reaction was further explored using substituted (4-MeO, 4-NO₂, 4-Me, 4-CN, 4-OH, 4-CF₃, 4-Br and 3,4-di Cl) phenyl acetic acid (**105**) and it was observed that the reactions proceeded to give the desired product with excellent yield and purity. Theoretically, two possible tautomeric forms (**85** and **106**) and (**85'** and **106'**) for the arylamidoguanidines were observable (Scheme 20). The two signals of NH₂ groups in ¹H NMR spectra of compounds demonstrated that tautomeric form (**85** and **106**), rather than form (**85'** and **106'**), was preferred in DMSO solution. This phenomenon was reported earlier²⁰⁶. The intermediate arylamidoguanidines and its derivatives were

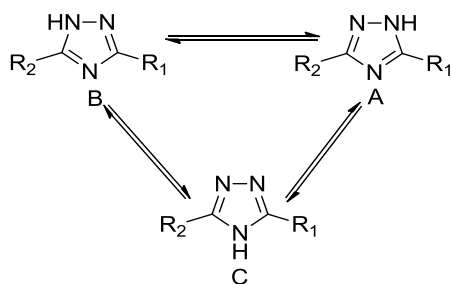
cyclised in the subsequent step upon microwave irradiation to afford the desired 1,2,4-triazoles.

Theoretically three annular tautomeric forms (A, B and C) are possible for prepared 1,2,4-triazoles (**87,91** and **88, 93**) (Scheme 21)²⁰⁷. However, tautomeric study of the 1, 2, 4-triazoles by ¹H NMR revealed that forms A and B existed in the DMSO solution, while form C was not observed under the experimental conditions. Due to annular tautomerism, target compounds **H5bi-H5bxix** and **H8a-H8i** could also exist in dynamic equilibrium of A) 4-, B) 3- and C) 1*H*- forms (Scheme 20). The prototropic interconversion between these tautomeric forms resulted in broadening of the 4-N(H) signal in the ¹H NMR spectra of compounds in DMSO. On heating, the broad signal disappeared due rapid exchange of this NH proton.



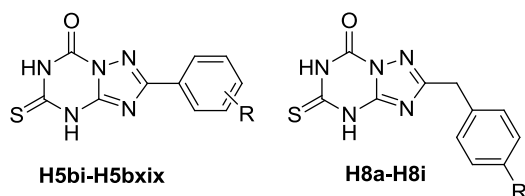
Reagents and conditions: (a) Aminoguanidine hydrochloride, fusion at 180 °C, 20 min, 5M NaOH (b) Water, MW irradiation, 180 °C, 10 min (c) Ethoxycarbonyl isothiocyanate, DMF, r.t. (e) NaOH, 80% ethanol (aq.), 100 °C.

Scheme 20. Synthesis of 5-thioxo-5,6-dihydro-4*H*-[1,2,4]triazolo[1,5-*a*][1,3,5]triazin-7-one (**H5bi-H5bxix** and **H8a-H8i**)



Scheme 21. Tautomerism of 1,2,4-triazoles

Table 6. Synthesis of 5-thioxo-5,6-dihydro-4*H*-[1,2,4]triazolo[1,5-*a*][1,3,5]triazin-7-one analogues

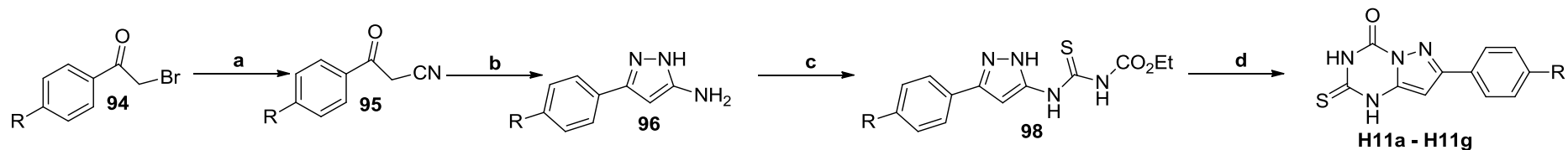


Entry	Cpd	R	% Yield	mp (°C)	Entry	Cpd	R	% Yield	mp (°C)
1	H5bi	3-NO ₂	80	246-248	15	H5bxv	4-MeO	63	270-271
2	H5bii	3-CF ₃	81	268-270	16	H5bxvi	4-CN	69	>300
3	H5biii	3-Cl	65	266-267	17	H5bxvii	(3,4)-Cl ₂	74	271-273
4	H5biv	3-Br	75	262-264	18	H5bxviii	(3,4)-F ₂	68	267-269
5	H5bv	3-F	72	283-285	19	H5bxix	3-Me, 4-Br	77	278-281
6	H5bvi	3-Me	80	259-261	20	H8a	4-CF ₃	67	280-281
7	H5bvii	3-MeO	90	260	21	H8b	4-Cl	64	241-243
8	H5bviii	3-CN	67	>300	22	H8c	4-Br	65	238-240
9	H5bix	4-NO ₂	65	>300	23	H8d	4-F	72	260-262
10	H5bx	4-CF ₃	69	280	24	H8e	4-Me	72	244-246
11	H5bxi	4-Cl	66	281-282	25	H8f	4-MeO	78	243-244
12	H5bxii	4-Br	73	292-293	26	H8g	4-OH	65	268-270
13	H5bxiii	4-F	67	262	27	H8h	4-CN	60	>300
14	H5bxiv	4-Me	78	296-297	28	H8i	(3,4)-Cl ₂	57	265-267

4.1.1.2 Synthesis of 2-thioxo-2,3-dihydro-1*H*-pyrazolo[1,5-*a*][1,3,5]triazin-4-one analogues

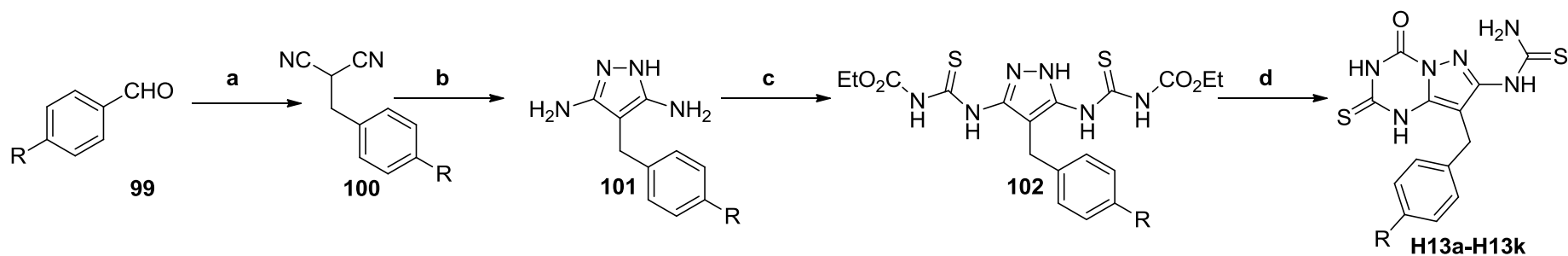
To synthesize the target molecules, **H11a-H11g** and **H13a-H13k**, the two highly efficient and high yielding synthetic approaches (scheme 22 and 23 respectively) were adopted, that involved the heterocyclization of the pyrazole derivatives having attached with N-C-N-C appendages^{41, 44}. These practical methods for the synthesis of the target compounds have generally proceeded with a four-step reaction sequence.

In the synthesis of compounds **H11a-H11g**, the key intermediate, 3-substituted aminopyrazoles were synthesized *via* a two step reaction. In the first step, the synthesis of substituted cyanoacetophenone (**95**) from corresponding bromoacetophenone (**94**) was achieved *via* the reaction with sodium cyanide in aqueous ethanol in presence of dilute hydrochloric acid^{209,210}. This reaction remained unsuccessful for 4-nitro substituted derivatives. Consequently, the cyanoacetophenones were treated with hydrazine hydrate in microwave irradiation to produce the key intermediate, aminopyrazole (**96**)²¹¹..



Reagents and conditions: (a) NaCN, HCl, aq-ethanol, r.t. (b) NH₂NH₂·H₂O, methanol, MW, 140 °C, (c) Ethoxycarbonyl isothiocyanate, DMF, r.t., 5 h (d) NaOH, 80% ethanol (aq.), 100°C.

Scheme 22. Synthesis of 2-thioxo-2,3-dihydro-1*H*-pyrazolo[1,5-*a*][1,3,5]triazin-4-one analogues (**H11a-H11g**)



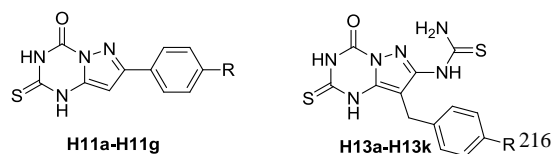
Reagents and conditions: (a) Malononitrile, aq-ethanol, NaBH₄, HCl, r.t. (b) NH₂NH₂·H₂O, ethanol, reflux, 5-8 h (c) Ethoxycarbonyl isothiocyanate, DMF, r.t., 5 h (d) NaOH, 80% ethanol (aq.), 100 °C

Scheme 23. Synthesis of (8-benzyl-4-oxo-2-thioxo-1,2,3,4-tetrahydro-pyrazolo[1,5-*a*][1,3,5]triazin-7-yl)-thiourea analogues (**H13a-H13k**)

Analogously, the compounds **H13a-H13k**, were synthesized by preparing building block, 4-benzyl-1*H*-pyrazole-3,5-diamine (**101**) *via* a two-step process. The first step of the process comprised of the synthesis of monosubstituted malononitriles (**100**) *via* reductive alkylation of malononitrile with aromatic aldehydes (**99**) which were readily converted to di-amino pyrazole (**101**) through simple reflux in ethanol in presence of hydrazine hydrate^{212, 213}. The compounds (**100** and **101**) synthesized were characterized by using ¹H NMR spectroscopy. The signals of methylene and methine proton appeared at around 3.33 and 5.11 ppm respectively and their splitting pattern in ¹H NMR spectra suggested the formation of compound (**100**) while, the two amino groups of **101** observed at 4.25 ppm in the ¹H NMR spectra as one broad signal.

The reaction of 5-aminopyrazole (**96**) and 3,5-diaminopyrazole (**101**) with ethoxycarbonyl isothiocyanate afforded corresponding thiourea derivatives which underwent subsequent cyclization in presence of base affording target compounds **H11a-H11g** and **H13a-H13k**. The structures of prepared compounds were assigned by ¹H, ¹³C NMR and mass spectroscopy. The satisfactory purity (above 95%) was assessed by HPLC method. In addition, the physicochemical properties including % yield and melting points of each compound were determined and tabulated in table 7.

Table 7. Synthesis of 2-thioxo-2,3-dihydro-1*H*-pyrazolo[1,5-*a*][1,3,5]triazin-4-one analogues



Entry	Cpd	R	% Yield	mp (°C)	Entry	Cpd	R	% Yield	mp (°C)
1	H11a	4-Cl	69	290-292	10	H13c	4-Br	82	222-224
2	H11b	4-Br	66	>300	11	H13d	4-F	65	221-223
3	H11c	4-F	74	270-272	12	H13e	Ph	70	239-241
4	H11d	4-Me	65	286-288	13	H13f	OPh	81	210-212
5	H11e	4-MeO	68	292-294	14	H13g	4-Me	76	254-256
6	H11f	4-CN	61	>300	15	H13h	4-Et	73	228-230
7	H11g	(3,4)-Cl ₂	63	287-289	16	H13i	4-MeO	69	252-254
8	H13a	4-CF ₃	71	189-191	17	H13j	4-OH	80	219-221
9	H13b	4-Cl	78	243-245	18	H13k	4-CN	62	259-262

4.1.2 Evaluation of anti-thymidine phosphorylase (Anti-TP) activity

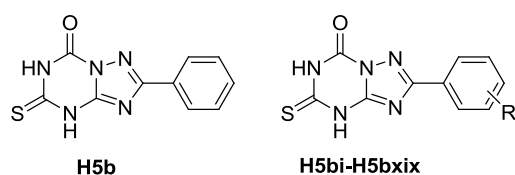
The compounds synthesized were spectroscopically tested for inhibitory activity against recombinant (expressed in *E. coli*) human thymidine phosphorylase. The inhibitory property of each tested compound was expressed in terms of IC₅₀ values and compared with that of **7-DX** (Tables 8, 9 and 10).

- **Thymidine phosphorylase activity of H5bi - H5bxix**

As shown in Table 8, the analogues of the lead **H5b** demonstrated a varying degree of TP inhibitory activities exhibiting a range of IC₅₀ values (10.84 to 48.54 μM). The results also suggested that among the compounds **H5bi-H5bxix**, except *meta*-fluoro and *meta*-cyano substituted compounds (compound **H5bv** and **H5bviii** respectively),

the inhibitory activity of all compounds, no matter having electron-withdrawing or electron-donating substituents, were better compared to the lead **H5b** (IC₅₀ value = 39.56 μM) and the reference TP inhibitor, **7-DX** (IC₅₀ value = 42.63 μM). Interestingly, di-substituted analogues of **H5b** viz. compounds **H5bxvii**, **H5bxviii** and **H5bxix** showed improved activity pattern than the analogues with mono substitutions on phenyl ring. For example, compounds **H5bxix** constituted with electron-withdrawing and electron donating substituents exhibited improved inhibitory activity with IC₅₀ value 13.09 μM. In addition, compounds **H5bxvii** (IC₅₀ = 10.84 μM) having Cl substituent in both *meta* and *para* position on the phenyl ring led to a 3.6 and 3.9-fold improvement in activity as compared to non substituted compound, **H5b** (IC₅₀ = 39.56 μM) and **7-DX**. The compound **H5bxvii** was identified as the most active inhibitor of this series.

The results also demonstrated that the compounds with electron-donating and - π hydrophobicity exhibited better activity compared to the compounds with electron-donating and + π hydrophobic substituents for both *meta* and *para* substituted compounds. In other words, the compounds **H5bvii** and **H5bxv** having a methoxy group imparted better activity than compounds **H5bvi** and **H5bxiv** which possessed a methyl substituent. However, among the compounds having (+ π , + σ) substituents, compounds **H5bii** and **H5bx** with trifluoromethyl moiety exhibited improved inhibitory potential. This observation indicated that compounds having electron-withdrawing substituents with higher lipophilicity were compatible with improved hydrophobic interactions into the binding site.

Table 8. Thymidine phosphorylase inhibitory activity of **H5bi - H5bxix**

Entry	Cpd	R	TP Inhibition activity ^b IC ₅₀ (μM) (95% CI) ^a
1	H5b	-	39.56 (38.32 - 40.84)
2	H5bi	3-NO ₂	22.63 (19.26 - 26.58)
3	H5bii	3-CF ₃	22.14 (19.91 - 24.61)
4	H5biii	3-Cl	30.29 (26.67 - 34.41)
5	H5biv	3-Br	31.78 (29.37 - 34.40)
6	H5bv	3-F	48.24 (41.98 - 55.42)
7	H5bvi	3-Me	34.42 (32.23 - 36.77)
8	H5bvii	3-MeO	23.18 (19.42 - 27.66)
9	H5bviii	3-CN	48.54 (46.65 - 50.51)
10	H5bix	4-NO ₂	36.56 (34.00 - 39.32)
11	H5bx	4-CF ₃	22.68 (20.20 - 25.47)
12	H5bxi	4-Cl	25.98 (23.09 - 29.23)
13	H5bxii	4-Br	22.06 (19.16 - 25.41)
14	H5bxiii	4-F	32.21 (29.00 - 35.77)
15	H5bxiv	4-Me	31.58 (29.46 - 33.84)
16	H5bxv	4-MeO	21.91 (20.37 - 23.56)
17	H5bxvi	4-CN	33.06 (31.87 - 34.29)
18	H5bxvii	(3,4)-Cl ₂	10.84 (9.03 - 13.02)
19	H5bxviii	(3,4)-F ₂	21.90 (17.32 - 27.69)
20	H5bxix	3-Me, 4-Br	13.09 (11.85 to 14.47)
21	7-DX	-	42.63 (39.07-46.50)

^aconfidence interval, ^bexperiments carried out at least in duplicate.

- **Thymidine phosphorylase activity of H8a - H8i and H11a - H11g**

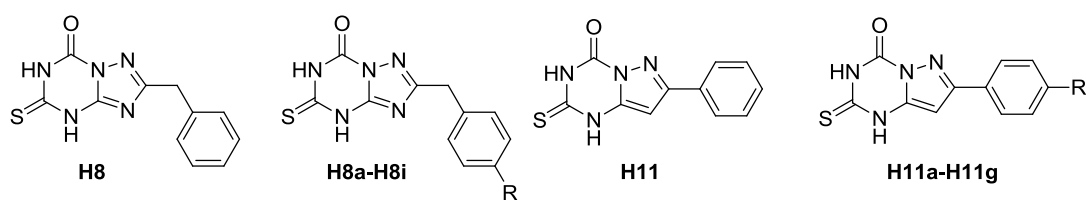
The preliminary screening identified compounds **H8** and **H11** as potential new leads (IC₅₀ values being 43.32 μM and 48.93 μM respectively). In an attempt to improve the inhibitory potency of leads **H8** and **H11**, the modification of the *para*-position of

phenyl ring using various substituents from all four quadrants of the Craig plot was employed.

The results of compound **H8** series demonstrated that, except for cyano substituted compound **H8h**, inhibitory activity was improved with all substituents, irrespective of their electron-withdrawing or electron-donating properties, as compared to the leads **H8** and **H5b**. As shown in table 9, the results suggested that compounds with substituents having electron-donating and less hydrophobic ($-\pi$) property, exhibited lower activity compared to compounds with electron-donating and more hydrophobic ($+\pi$) substituents. In other words, the compound **H8e** having Me group imparted better activity than compound **H8f** and **H8g** bearing MeO and OH substituents respectively. This behaviour was not consistent as observed in compounds of **H5b** series. Therefore, it could be possible that with introduction of flexible methylene bridge MeO and OH moieties could impart steric effects resulting in reduction of binding affinities. In addition, among the compounds having $+\pi$ and $+\sigma$ substituents, compound **H8a** (with CF_3) moiety exhibited improved inhibitory potential (IC_{50} value = 9.92 μM). It is noteworthy that within compounds **H8a-H8d**, except for compound **H8b**, the inhibitory effect on TP was decreasing in descending order of hydrophobicity of the substitutions at the *para* position of the phenyl ring. These observations indicated that hydrophobicity played an important role to impart high binding interaction and improved inhibitory activity. Interestingly, di-chloro substituted analogues of **H8a**, compound **H8i** was found to be the most potent inhibitor of this series with IC_{50} value 2.95 μM that showed 14.7, 13.4 and 14.5 fold enhancement of inhibitory activity compared to lead **H8a**, **H5b** and **7-DX** respectively. The similar trend of inhibitory activity was observed in disubstituted analogues of **H5b**.

Within the **H11** series, all the compounds substituted with varied range of electron-donating and electron-withdrawing groups demonstrated improved inhibition property compared to the lead **H11**. In contrast to **H8** series, the compounds with electron donating group having positive and negative hydrophobicity showed reverse pattern of TP inhibition profile. In other words, **H11d** ($IC_{50} = 39.5 \mu\text{M}$) bearing Me group showed almost 2 fold decreased in activity compared to **H11e** that have a methoxy substituent. Compounds **H11a-H11c** with $+\pi$ and $+\sigma$ substituents exhibited hydrophobicity dependent ascending order of inhibition profile. Analogously, di-chloro substituted compound **H11g** exhibited the highest inhibitory activity with an IC_{50} value of $13.07 \mu\text{M}$.

In general, the di-chloro substituted analogues **H5b**, **H8** and **H11** demonstrated improved inhibitory activity compared to the mono-substituted derivatives. In addition, the structural modification in **H5b** by replacing one of the N atoms with carbon atom (giving rise to **H11**) resulted in no significant improvement in activity. Therefore, it is concluded that both N and C atoms are not crucial for better interaction with the enzyme.

Table 9. Thymidine phosphorylase inhibitory activity of **H8a - H8i** and **H11a - H11g**

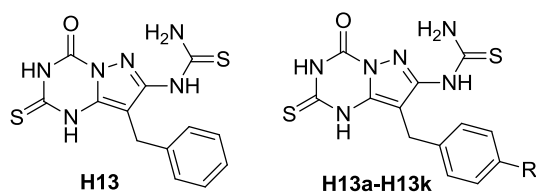
Entry	Cpd	R	TP Inhibition activity ^b IC ₅₀ (μM) (95% CI) ^a
1	H8	-	43.32 (39.91 - 47.02)
2	H8a	4-CF ₃	9.92 (8.03 - 12.25)
3	H8b	4-Cl	8.54 (7.29 - 9.99)
4	H8c	4-Br	13.71 (10.71 - 17.54)
5	H8d	4-F	22.43 (20.61 to 24.41)
6	H8e	4-Me	19.80 (15.98 - 24.54)
7	H8f	4-MeO	33.95 (29.02 - 39.73)
8	H8g	4-OH	33.78 (32.63 - 34.97)
9	H8h	4-CN	64.33 (60.32 - 68.62)
10	H8i	(3,4)-Cl ₂	2.95 (2.47 - 3.52)
11	H11	-	48.93 (46.54 - 51.44)
12	H11a	4-Cl	36.69 (32.76 - 41.08)
13	H11b	4-Br	26.54 (21.72 - 32.42)
14	H11c	4-F	46.45 (44.11 - 48.91)
15	H11d	4-Me	39.50 (32.88 - 47.45)
16	H11e	4-MeO	21.60 (18.09 - 25.79)
17	H11f	4-CN	30.32 (28.45 - 32.32)
18	H11g	(3,4)-Cl ₂	13.07 (12.22 - 13.96)
19	7-DX	-	42.63 (39.07-46.50)

^aconfidence interval, ^bexperiments carried out at least in duplicate.

• Thymidine phosphorylase activity of H13a-H13k

In a similar way, the lead structure **H13** was modified by inserting different substituents to *para*-position of phenyl ring guided by Craig plot optimization approach. The results of the TP inhibitory activity of **H13** analogues showed that all compounds suppressed the enzymatic reaction with IC₅₀ values ranging in between 52

μM to $3 \mu\text{M}$ (Table 7). The most pronounced TP inhibition (IC_{50} value = $3.82 \mu\text{M}$) was observed for compound **H13a**, which contains a trifluoromethyl group at the *para* position of the phenyl ring. As shown in Table 7, except compounds bearing substituents from third and fourth quadrant of Craig plot, inhibitory activity was improved with all substituents, no matter having electron-withdrawing and electron-donating group, as compared to the lead **H13**. In other words, compounds **H13i**, **H13j**, and **H13k** having substituents with negative hydrophobic constant ($-\pi$) exhibited lower inhibitory activity compared to non substituted **H13** (IC_{50} value = $29.92 \mu\text{M}$). The results also demonstrated that compounds with electron-donating substituent having positive hydrophobic constant showed improved activity as compared to **H13**. Among them, compound **H13h** (IC_{50} value = $12.56 \mu\text{M}$) having ethyl moiety exhibited inhibitory activity slightly better than compound **H13g** (IC_{50} = $19.98 \mu\text{M}$) having methyl substituent. In addition, it was evident from the results that among the compounds with ($+\pi$, $+\sigma$) substituents, compound **H13a** bearing CF_3 moiety was proven to be the most potent member in this series. It is interesting to note that substituent CF_3 imparted higher hydrophobicity among other substitutions selected from first quadrant of Craig plot. Therefore, the above mentioned observations indicated that substitution with $+\pi$ hydrophobicity at the *para* position of the phenyl ring seemed to play an important role in the binding interactions led to improved anti-TP effect of the compounds. Encouraged by these exciting findings, we were prompted to modify the compound **H13** by introducing some hydrophobic substituents including biphenyl and phenoxyphenyl groups. Interestingly, such efforts generated compounds **H13e** and **H13f** and their anti-TP evaluation demonstrated a 4.9 and 6.7 fold improvement in inhibitory activity over **H13** respectively.

Table 10. Thymidine phosphorylase inhibitory activity of **H13a-H13k**

Entry	Cpd	R	TP Inhibition activity ^b IC ₅₀ (μM) (95% CI) ^a
1	H13	-	29.92 (25.74 - 34.77)
2	H13a	4-CF ₃	3.82 (3.31 to 4.41)
3	H13b	4-Cl	7.54 (5.97 - 9.51)
4	H13c	4-Br	14.78 (13.52 - 16.15)
5	H13d	4-F	22.65 (19.60 - 26.17)
6	H13e	Ph	6.11 (5.55 - 6.72)
7	H13f	OPh	4.46 (4.17 - 4.77)
8	H13g	4-Me	19.98 (16.04 - 24.90)
9	H13h	4-Et	12.56 (11.53 - 13.69)
10	H13i	4-MeO	51.44 (48.73 - 54.31)
11	H13j	4-OH	37.38 (32.80 - 42.60)
12	H13k	4-CN	51.53 (49.66 - 53.46)
13	7-DX	-	42.63 (39.07-46.50)

^aconfidence interval, ^bexperiments carried out at least in duplicate.

4.2 Further miscellaneous structural modifications

As discussed in previous chapter, 2-(methylthio)-5-thioxo-5,6-dihydro-[1,2,4]triazolo[1,5-*a*][1,3,5]triazin-7(4*H*)-one **H5a** exhibited moderate inhibitory activity against recombinant human thymidine phosphorylase (IC₅₀ value = 51.67 μM). However, replacing the thiomethyl group at the position C2 of this fused ring with aromatic phenyl ring led to an improvement of TP inhibitory activity, suggesting that the bulky lipophilic moiety may increase the hydrophobic interactions of compound **H5b** (IC₅₀ value = 39.56 μM) in the binding site and thus the inhibitory activity of compound **H5b** against TP enzyme was augmented. Therefore, it was hypothesized that replacing the thiomethyl group by benzylthio, substituents with

higher flexible alkyl chain, and hydrophobic moiety at the position C2 might serve as a lipophilicity modulator that might facilitate improvement of interaction of lead compound with the binding site of enzyme. In addition, based on the structure of **TPI**, where the heterocycle pyrrolidine is attached to the pyrimidin-2,4-dione ring, it is assumed that heterocycle substituted fused ring scaffold would also fit well in the active site. Moreover, moderate TP inhibitory potential exerted by **H11** ($IC_{50} = 48.93 \mu\text{M}$) and **H13** ($IC_{50} = 29.92 \mu\text{M}$), has led to the postulation that C8 substituted pyrazolo fused triazine scaffold would also exhibit anti-TP property.

Therefore, the objective of the study was to synthesize a small series of compounds with phenylalkylthio groups introduced at the position C2 of 5-thioxo-5,6-dihydro-[1,5-*a*][1,3,5]triazin-7(4*H*)-one ring and to evaluate whether the increasing alkyl chain length will be able to enhance binding affinity to TP. As continuous efforts to develop potent TP inhibitors, lead compounds **H5b** and **H11** were modified further by inserting a diphenyl group and *t-butyl* moiety at the position C2 and C7 respectively as a lipophilic modulator. In addition, various heterocycles were introduced in the lead structures **H5b** and **H13** by replacing phenyl ring using analogous synthetic methodology. Moreover, further modification of **H11** was carried out by switching the position of phenyl ring from C7 to C8 in order to test above mentioned hypothesis.

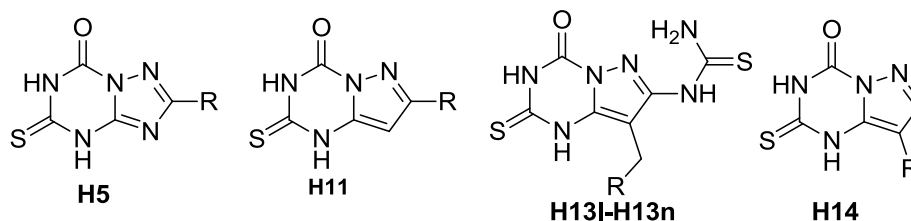
4.2.1 Chemistry

The synthesis of all the target compounds (**H5ai-H14**) (Table 8) were conveniently achieved by a ring annulation reaction of carbethoxythioureas derivatives (**88**, **93**, **98**, and **102**) having N-C-N-C appendages in alkali medium (Scheme 16, 17, 18 and 19). The nucleophilic reaction of ethoxycarbonyl isothiocyanate with various 1,2,4-

triazoles (**87** and **91**) and pyrazole (**96** and **101**) having exocyclic amino group afforded corresponding carbethoxythioureas derivatives with good yield in DMF.

Herein, to synthesize 1,2,4-triazoles (**87** and **91**) and pyrazole (**96** and **101**) derivatives, several methods were adopted. For example, reported method was followed to prepare 5-phenylalkylthio substituted-1,2,4-triazols by alkylation of 3-amino-5-sulfanyl-1,2,4-triazole with benzyl bromide and its longer alkyl chain derivatives in DMF²⁰⁸. The furyl, thienyl and pyridyl substituted aminotriazole was synthesized *via* the preparation of (het)arylamidoguanidines from the reaction of appropriate hydrazides with *S*-methyl isothiourea in basic condition. Consequently, the cyclocondensation of (het)arylamidoguanidines in microwave irradiation led to formation of corresponding 1,2,4-triazoles with excellent yield and purity. For compound **H5g**, corresponding amino-1,2,4-triazole was synthesized by adopting alternative pathway of synthesis of arylamidoguanidines by using aryl acid chloride reacted with aminoguanidine hydrochloride and resulting product upon microwave irradiation led to synthesis of key intermediate 1,2,4-triazoles. In addition, to synthesize 4-substituted-pyrazol-3,5-diamine as a building block for preparation of **H13l**, **H13m** and **H13o**, the scheme 19 was directly utilized, starting from corresponding aromatic aldehyde. All other compounds (**H5f**, **H11h** and **H14**) were prepared by using commercially available aminotriazole or aminopyrazoles. The synthesized compounds were characterized by their % yield and melting points (Table 11). The structures of these compounds were confirmed by using NMR spectroscopy and mass spectroscopy; while the purity (above 95 %) was determined by reverse phase HPLC.

Table 11. Synthesis of target compounds (derivatives of **H5**, **H11**, **H13** and compound **H14**)



Entry	Cpd	R	% Yield	mp (°C)	Entry	Cpd	R	% Yield	mp (°C)
1	H5ai	SCH ₂ Ph	89	249	8	H5g	CH(Ph) ₂	63	210-212
2	H5aii	S(CH ₂) ₂ Ph	94	232-234	9	H11h	C(Me) ₃	55	268-270
3	H5aiii	S(CH ₂) ₃ Ph	69	220-221	10	H13l	2-furyl	74	227-229
4	H5c	2-furyl	62	292-294	11	H13m	2-thienyl	72	242-244
5	H5d	2-thienyl	64	273	12	H13n	1-naphthyl	63	230-233
6	H5e	2-pyridyl	63	280-282	13	H14	Ph	60	222-224
7	H5f	H	54	>300					

4.2.2 Evaluation of anti-thymidine phosphorylase (Anti-TP) activity

The potency of the inhibition of thymidine phosphorylase (TP) by the synthesized compounds was spectrophotometrically evaluated *via in vitro* enzyme assay method. From the percentage of the enzymatic activity inhibition, IC₅₀ values were calculated and reported in Table 12. The IC₅₀ values of reference compound, **7-DX** was determined under the same experimental conditions and the value was compared with our synthesized compounds.

The preliminary study demonstrated that compounds **H5a** and **H5b** having 5-thioxo-5,6-dihydro-4H-[1,2,4]triazole[1,5-*a*][1,3,5]triazin-7-one scaffold exhibited weak to moderate TP inhibitory activity. Herein, additional variation in substitution at C2 of the **H5a** and **H5b** was carried out *via* introducing phenyl ring through flexible alkyl chain and inserting heterocyclic rings instead of phenyl ring. The resultant compounds

(**H5ai-H5aiii**) and (**H5c-H5e**) showed varying degrees of TP inhibition with IC_{50} values ranging between 22 and 38 μM (Table 12). The modification of compounds **H5a** and **H5b** by introducing longer flexible side chain and higher spacer length at the position C2 suggested that activity was increased with such kind of attempts. To illustrate, it should be mentioned that the compound **H5ai**, **H5aii** and **H5aiii** showed better binding interactions ($IC_{50} = 38.19, 33.04, 27.64 \mu\text{M}$ respectively) with respect to **H5a** and **H5b** ($IC_{50} = 51.67, 39.56 \mu\text{M}$ respectively). The replacement of phenyl ring with other aromatic ring like furan, thiophene and pyridyl motif produced compounds **H5c**, **H5d** and **H5e** that also exhibited improvement in enzyme affinity. In other words, the IC_{50} values of compounds **H5c**, **H5d** and **H5e** were 22.84 μM , 30.95 μM and 24.53 μM respectively that were lower than the IC_{50} value of **H5b**. As depicted in the Table 9, compounds with aromatic substituents at the position C2 demonstrated better interactions than the unsubstituted compound **H5f** which is considered as most structurally similar to the lead compound **7-DX** ($IC_{50} = 42.63 \mu\text{M}$). Compound **H5c**, 2-(furan-2-yl)-5-thioxo-5,6-dihydro-[1,2,4]triazolo[1,5-*a*][1,3,5]triazin-7(4*H*)-one, was found to be the most active member of this series ($IC_{50} = 22.84 \mu\text{M}$).

The previous experimental data demonstrated that hydrophobicity of the substituents played an important role in enhancing inhibitory activity. Encouraged by this fact, bulky di-phenyl moiety and *t-butyl* group were introduced instead of phenyl ring at the position C2 and C7 of the lead compound **H5b** and **H11** respectively. However, it could not able to impart significant improvement in inhibition potency suggesting such bulky group might present negative steric hindrance on the interaction to the binding site of the enzyme.

In addition, optimization of lead **H13** was further extended by replacing phenyl ring by some aromatic heterocycles namely 2-furyl and 2-thienyl and naphthoyl substituents resulting in synthesis of compound **H13l**, **H13m** and **H13n**. Such effort demonstrated that although, compound **H13n** exhibited 6.8 fold enhancement of inhibition potential, **H13m**, **H13n** did not show any significant improvement of activity compared to lead **H13**. It was further proven that hydrophobicity of substituents might play significant role in improving interactions of compounds in the binding site. Moreover, it was observed that when the orientation of phenyl ring of pyrazolo[1,5-*a*][1,3,5]triazine was changed from C7 to C8, the enzyme affinity was augmented. In other word, the compound **H14** showed lower IC₅₀ value than all lead compounds identified (**H5a**, **H5b**, **H8**, **H11** and **H13**). Therefore, a further structural modification of this compound is strongly recommended.

Table 12. Thymidine phosphorylase inhibitory activity of the synthesized compounds (derivatives of **H5**, **H11**, **H13** and compound **H14**)

Entry	Cpd	R	TP Inhibition activity ^b IC ₅₀ (μM) (95% CI) ^a
1	H5ai	SCH ₂ Ph	38.19 (33.37 to 43.71)
2	H5aai	S(CH ₂) ₂ Ph	33.04 (28.31 to 38.56)
3	H5aiii	S(CH ₂) ₃ Ph	27.64 (23.21 to 32.91)
4	H5c	2-furyl	22.84 (20.25 to 25.78)
5	H5d	2-thienyl	30.95 (26.88 to 35.65)
6	H5e	2-pyridyl	24.53 (21.30 to 28.25)
7	H5f	H	40.45 (32.36 to 50.57)
8	H5g	CH(Ph) ₂	36.37 (33.49 - 39.50)
9	H11h	C(Me) ₃	55.70 (52.19 - 59.45)
10	H13l	2-furyl	36.72 (31.70 - 42.52)
11	H13m	2-thienyl	27.69 (24.99 - 30.68)
12	H13n	1-naphthyl	4.29 (3.714 - 4.953)
13	H14	Ph	26.30 (28.3-24.3)
14	7-DX	-	42.63 (39.07-46.50)

^aconfidence interval, ^bexperiments carried out at least in duplicate

4.3 Summary

To summarize, several compounds having 1,2,4-triazolo[1,5-*a*][1,3,5]triazine and pyrazolo[1,5-*a*][1,3,5]triazine ring structures were synthesized and their anti-TP effect was evaluated. The biological evaluation identified a number of new TP inhibitors bearing 5-thioxo-5,6-dihydro[1,2,4]triazolo[1,5-*a*][1,3,5]triazin-7(4*H*)-one, 2-thioxo-2,3-dihydro-1*H*- pyrazolo [1,5-*a*][1,3,5]triazin-4-one scaffold. Among them, compounds **H5bxvii** and **H8i**, **H11g** and **H13a** exhibited the most promising inhibitory property against TP with low micromolar IC₅₀ values (IC₅₀ values = 10.84, 2.95 and 13.07, 3.82 μM respectively). This study also provided evidence that the

potency of the active compounds strongly depends on physicochemical properties particularly on hydrophobic properties of the substituents at the different position of the phenyl ring. In addition, the biological evaluation demonstrated that several compounds of this series have shown significant TP inhibitory activity, in particular those that bear disubstitutions on the phenyl ring. Moreover, di-substituted pyrazolo [1,5-*a*][1,3,5]triazine derivatives, including **H13e**, **H13f** and **H13n**, demonstrated attractive inhibition property against TP.

In general, when the structural features of all fused 1,3,5-triazine compounds were considered with respect to their TP activity, a qualitative structure-activity relationship has emerged. Even though **TPI** and **7-DX** were used as the leads for the design of this study, the structures of the new TP inhibitors from this study have deviated significantly from the lead compounds. As depicted in Figure 12, the bicyclic fused 1,3,5-triazines, having the homophthalimide group did not exhibit TP inhibitory activity. However, its replacement with the isosteric group -NH(S=S)NH(C=O) gave rise to good TP inhibitory activity in some derivatives. In addition, the incorporation of a thiomethyl group at either C5 or C2 of the fused ring scaffold, has led to a dramatic decrease in activity. It is evident from the data that a range of aromatic and aliphatic substituents ($\text{R} = \text{Ph}$, SCH_3 , CH(Ph)_2 , NH(C=S)NH_2) and various aromatic heterocycles could be accommodated by the enzyme and exhibited good inhibitory effects. However, results also suggested that aromatic substitutions are essential for better inhibitory effect. The binding pocket of the enzyme appeared to tolerate substitutions such as the phenyl or benzyl group at C8/N3 and exhibited inhibitory effects. Moreover, the inhibitory potency of these synthesized compounds suggested that the introduction of different atoms including C or N at C8/N3 did not significantly alter the inhibitory effect.

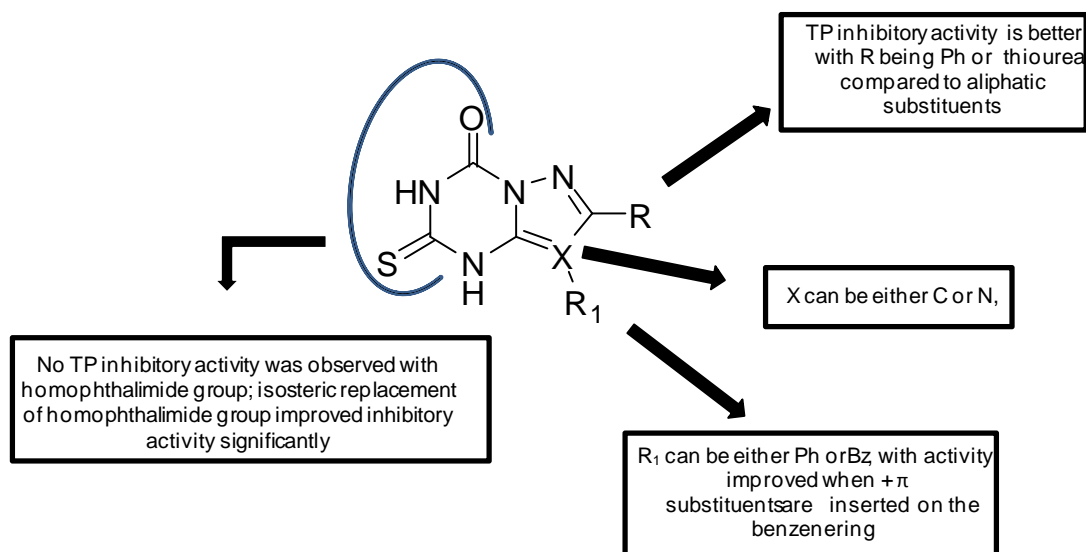


Figure 12. A schematic diagram describing the structure-TP inhibitory activity relationship of the 1,2,4-triazolo and pyrazolo fused triazines

Overall, the interesting TP inhibitory activity of the synthesized compounds make them suitable leads for further development of new chemical entities for potential use in the treatment of disease associated with TP. It is important to mention that the synthesis of these target compounds was achieved *via* intramolecular heterocyclization of key intermediate *viz.* substituted triazole and pyrazole derivatives. In this reaction pathway, it was noticed that these intermediates could generate different regioisomeric products depending on reaction conditions used. Therefore, in the following chapter, the regiochemistry of the synthetic intermediates will be described.

Chapter 5

Structural Investigation – Regiochemistry of Synthetic Intermediates

5.1 Synthesis and tautomerism study of the key intermediates, 3(5)-amino/carbethoxythiourea-5(3)-aryl-1,2,4-triazoles

The derivatives of 1,2,4-triazolo[1,5-*a*][1,3,5]triazine constitute an important class of heterocycles found in many compounds that are used in medicine and agriculture²¹⁷. Therefore, the synthesis of 1,2,4-triazolo fused 1,3,5-triazine analogues and the exploration of their diverse bioactivities draw increasing interest to organic and medicinal chemists. In an attempt to investigate the new biological properties of this scaffold, thio-oxo derivatives of 1,2,4-triazolo[1,5-*a*][1,3,5]triazine were established as potential TP inhibitors for the first time as described in previous chapter. The synthesis of these biologically active compounds was achieved *via* intramolecular heterocyclization of 1,2,4-triazoles having N-C-C-N appendage at C3(5) *viz.* *N*-(3(5)-aryl-1,2,4-triazol-5(3)-yl)-*N'*-carbethoxythioureas which were generated from the reaction of substituted 3(5)-amino-1,2,4-triazoles and ethoxy carbonyl isothiocyanate. Therefore, 3(5)-amino-1,2,4-triazoles and *N*-(3(5)-aryl-1,2,4-triazol-5(3)-yl)-*N'*-carbethoxythioureas were considered as valuable intermediates for the construction of desirable thio-oxo analogues of 1,2,4-triazolo[1,5-*a*][1,3,5]triazine. In this synthetic pathway, it was observed that depending on reaction conditions used, the substituted 1,2,4-triazole could afford different regioisomeric products. Among the different factors, the tautomerism is often considered as the most influencing factors in regioselectivity of reactions. Therefore, knowledge of the tautomeric preferences of intermediate compounds and the factors affecting the tautomeric equilibrium is essential to achieve desired compounds in chemical processes.

Due to annular prototropic tautomerism, 1,2,4-triazole without substituents on the ring nitrogen atoms, can exist in three forms. Although several theoretical reports have

been published in the area of tautomerism in 1,2,4-triazole, the precise experimental data on the annular tautomerism in 1,2,4-triazoles is limited^{218, 219}. Previously, our research group reported the annular tautomerism study of 3(5)-amino-5(3)-aryl-1,2,4-triazoles²⁰⁷ and established a good correlation between the relative energies of individual tautomeric preferences and electronic property using limited number of *para*-substituted 3(5)-amino-5(3)-phenyl-1,2,4-triazoles. Herein, in continuation of our investigation on annular tautomerism, the tautomeric aspects of 3(5)-amino-1,2,4-triazoles and related structure *viz.* *N*-(3(5)-aryl-1,2,4-triazol-5(3)-yl)-*N'*-carbathoxythioureas, considering a wide range of substitutions is studied in solutions (Figure 13). In addition, the various methods used to introduce different substituents at 3(5) position of 1,2,4-triazole will be summarized and the effects of nucleophilicity of different substituents of 3(5)-amino-1,2,4-triazole on reaction processes will be discussed.

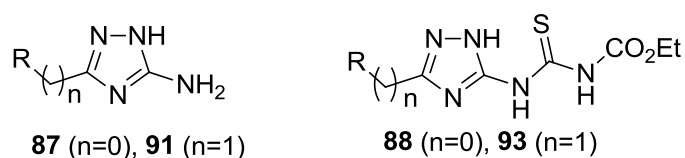
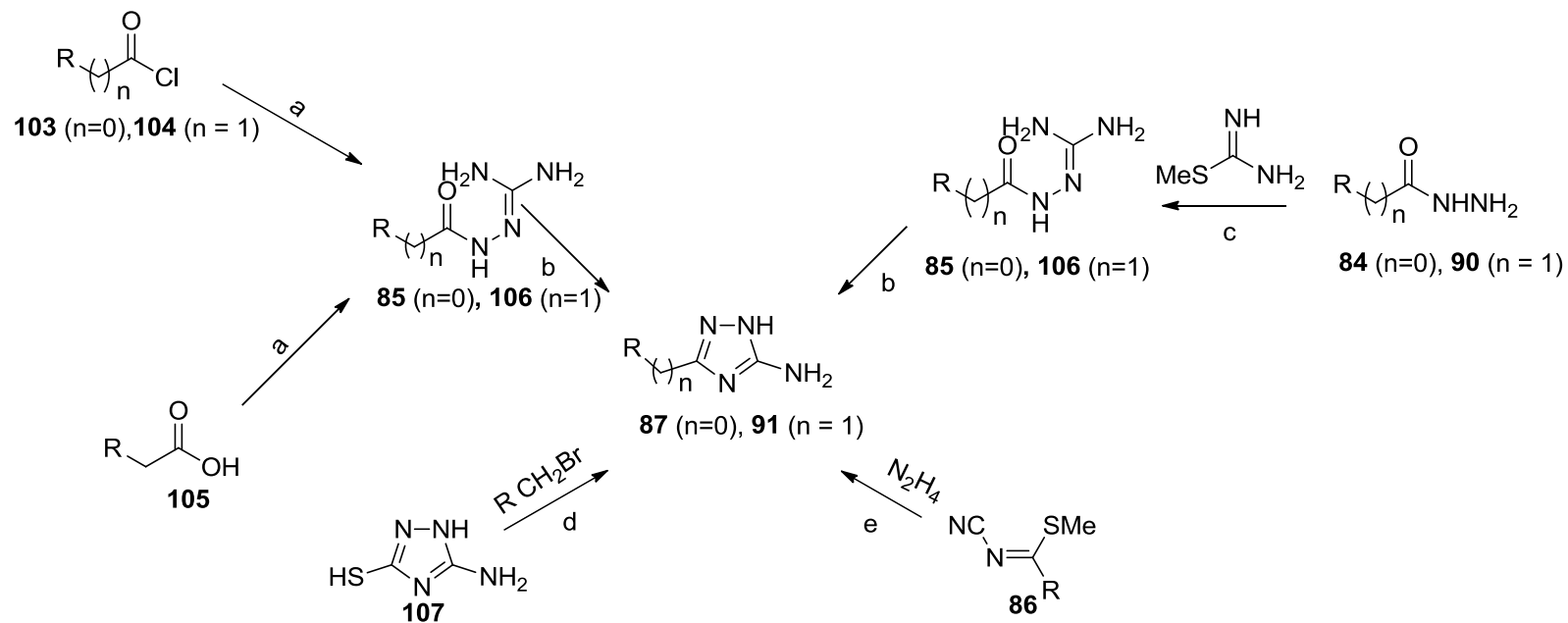


Figure 13. Structures of 1,2,4-triazole derivatives

5.1.1 Synthesis of 3(5)-amino-5(3)-(het)aryl-1,2,4-triazoles (**87**, **91**)

The synthesis of 3(5)-amino-5(3)-(het)aryl-1,2,4-triazoles (**87**, **91**) was achieved by adopting some environment friendly synthetic methods in which solvents like water and ethanol were selected for use, the energy was effectively utilized and the formation of by-products were minimized. The 5(3)-substituted-3(5)-amino-1,2,4-triazoles (**87**, **91**) were prepared by using four different reaction processes (Scheme 24). Firstly, the condensation of substituted aryl hydrazide and *S*-methyl isothiurea

produced arylaminoguanidines (**85**, **106**) in alkali medium which upon microwave irradiation afforded 3(5)-amino-1,2,4-triazoles (**87**, **91**)^{206, 207}. The first step of this method had several limitations including prolonged reaction time and complicated work-up process that often led to decrease in the yield of the products. Alternatively, these (het)arylamidoguanidines (**85**, **106**) were synthesized through the fusion of aminoguanidine hydrochloride with substituted benzoyl chloride (**103**, **104**) by heating at high temperature (above 175 °C) followed by basification using 5M NaOH. The (het)arylamidoguanidines (**85**, **106**) thus obtained were cyclised using microwave irradiation in water and subsequently afforded 3(5)-amino-5(3)-(het)aryl-1,2,4-triazoles (**87**, **91**). It gave quantitative yield and excellent purity of the products. The synthesis of compound **85**, **106** was also achieved by the reaction of substituted (4-MeO, 4-NO₂, 4-Me, 4-CN, 4-OH, 4-CF₃, 4-Br and 3,4-di Cl) phenyl acetic acid (**105**) and aminoguanidine hydrochloride and the products were proceeded successfully to afford corresponding benzyl substituted 3(5)-amino-1,2,4-triazoles upon microwave irradiation with excellent yield and purity. Thirdly, the reaction of dimethyl-N-cyanodithiocarbonimidate (**86**) with hydrazine produced 3(methylthio)-amino-1,2,4-triazoles²⁰⁶. Lastly, previously reported method was adopted to synthesize 5-phenylalkylthio substituted-1,2,4-triazols *via* alkylation of commercially available 3-amino-5-sulfanyl-1,2,4-triazole (**107**) with benzyl bromide and its longer alkyl chain derivatives in DMF²⁰⁸.



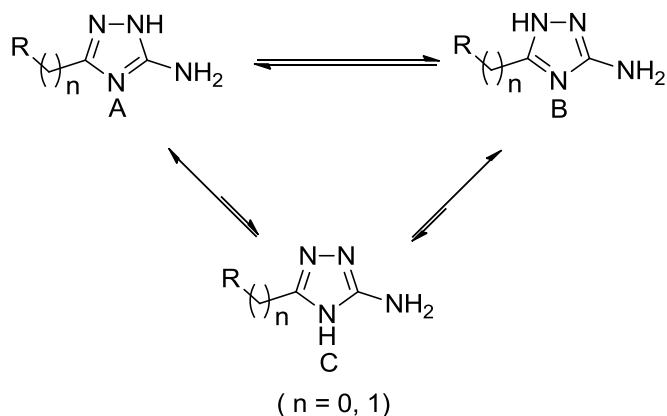
Reagents and conditions: (a) Fusion at 180 °C, 20 min, 5M NaOH (b) Water, MW irradiation, 180 °C, 10 min (c) NaOH, r.t, 72 h (d) DMF, Et₃N, r.t., 4 h (e) MeOH, 40 °C, 5h.

Scheme 24. Synthesis of 3(5)-amino-5(3)-(het)aryl-1,2,4-triazoles (**87**, **91**)

5.1.2 Tautomerism study of 3(5)-amino-5(3)-(het)aryl-1,2,4-triazoles

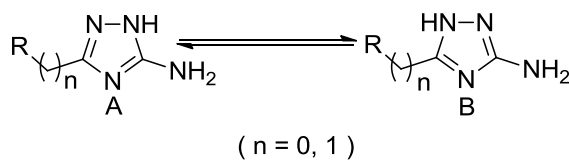
Tautomerism is an intriguing phenomenon with a long history of investigation and the tautomerism in azoles has been a subject of discussion for many years^{218, 219}. Theoretically three annular tautomeric forms are possible for prepared 3(5)-amino-5(3)-(het) aryl-1,2,4-triazoles (Scheme 25)²⁰⁷. The structures of these compounds, in particular their tautomerism were investigated using NMR spectroscopy, which is considered to be the most informative and accurate method for solutions. The tautomeric study by ¹H NMR of the 1, 2, 4-triazoles revealed that forms A and B were exist in the DMSO solutions, while form C was not observed under the experimental conditions. The equilibrium between the tautomers was established rapidly and the compositions did not change with time. The identical spectra for the tautomeric system A and B was observed on dissolving the samples and after equilibration of the solution overnight.

The tautomeric equilibrium constant (K_T) was determined by integrating the characteristic NH and/or NH₂ signals of tautomers A and B in the ¹H NMR spectra and subsequently, the Gibbs free energies (ΔG_{298}) of individual tautomers were calculated using equation, $\Delta G_{298} = -RT \ln K_T$ (Table 13). The 5-amino-1,2,4-triazoles (A) was identified as dominant in the equilibrium while form B was found to be minor. The substituents exhibited important role on the equilibrium. The study demonstrated that the ratio of predominant and thermodynamically most stable form A to form B was influenced by the electronic property of substituents present.



Scheme 25. Tautomers of 3(5)-amino-1,2,4-triazoles

It was observed that the K_T and ΔG_{298} values correlated well with the Hammett constants²²⁰ of substituents on the phenyl or benzyl moiety of triazole, $-\Delta G_{298} = 4.462\sigma + 5.217$, $R^2 = 0.981$ and $-\Delta G_{298} = 1.768\sigma + 3.415$, $R^2 = 0.972$ (Figure 14A and 14B respectively). Therefore, the thermodynamic stability of form A in comparison with B increased together with the electron-withdrawing properties of the substituents. Analogously, the tautomeric equilibrium constant and Gibbs free energy of individual tautomer were determined for some heterocyclic, that is, 2pyridyl, 3-pyridyl, 4-pyridyl, 2-thienyl and 2-furyl substituents at C3(5) of the 1,2,4-triazole ring. However, experimental results for these compounds were outside this correlation. In addition, the correlation could not be extended for compound **87j**, **87r** and **87zd**. The calculated $K_{T(A/B)}$ for **87a** and **87v** was found 16.8 and 19.01 whereas the ΔG_{298} was equal to 6.98 and -7.28 KJ/mol respectively. It was observed that introduction of longer flexible chain attached with sulphur moiety reduced electron donating property of this C3(5) position and thus form B was disfavoured and consequently the $K_{T(A/B)}$ values decreased gradually.

Table 13. Tautomerism in 3(5)-amino-1,2,4-triazoles in DMSO-*d*₆ solution

Entry	Cpd	R	n	¹ H NMR signal in DMSO- <i>d</i> ₆ (ppm)				K _T	-ΔG ₂₉₈
				Tautomer B		Tautomer A			
				3(5)-NH ₂	N(1)-H	3(5)-NH ₂	N(1)-H		
1	87a	CH ₃ S	0	5.29	12.67	6.04	11.91	16.84	6.98
2	87b	Ph	0	5.35	13.24	6.12	12.08	7.75	5.06
3	87c	3-NO ₂ C ₆ H ₄	0	5.47	13.60	6.26	12.34	27.62	8.21
4	87d	3-CF ₃ C ₆ H ₄	0	5.45	13.50	6.23	12.29	19.84	7.39
5	87e	3-ClC ₆ H ₄	0	5.38	13.35	6.16	12.20	15.82	6.83
6	87f	3-BrC ₆ H ₄	0	5.40	13.35	6.17	12.22	15.67	6.81
7	87g	3-FC ₆ H ₄	0	5.42	13.38	6.19	12.21	13.91	6.51
8	87h	3-MeC ₆ H ₄	0	5.45	13.16	6.09	12.08	6.47	4.62
9	87i	3-MeOC ₆ H ₄	0	5.39	13.22	6.09	12.08	10.23	5.75
10	87j	3-CNC ₆ H ₄	0	5.37	13.34	6.12	12.14	14.25	6.57
11	87k	4-NO ₂ C ₆ H ₄	0	5.54	13.69	6.30	12.45	33.33	8.67
12	87l	4-CF ₃ C ₆ H ₄	0	5.53	13.55	6.24	12.32	22.42	7.69
13	87m	4-ClC ₆ H ₄	0	5.43	13.33	6.17	12.18	13.25	6.39
14	87n	4-BrC ₆ H ₄	0	5.40	13.33	6.15	12.17	13.50	6.44
15	87o	4-FC ₆ H ₄	0	5.36	13.24	6.13	12.10	10.30	5.77
16	87p	4-MeC ₆ H ₄	0	5.32	13.14	6.08	12.02	5.86	4.37
17	87q	4-MeOC ₆ H ₄	0	5.27	13.02	6.04	11.94	4.99	3.97
18	87r	4-CNC ₆ H ₄	0	5.50	13.60	6.26	12.37	25.58	8.02
19	87s	(3,4)-diClC ₆ H ₃	0	5.43	13.42	6.21	12.28	22.78	7.73
20	87t	(3,4)-diFC ₆ H ₃	0	5.41	13.33	6.19	12.21	18.28	7.19
21	87u	3Me,4BrC ₆ H ₃	0	5.35	13.27	6.11	12.15	12.06	6.16
22	87v	C ₆ H ₅ CH ₂ S	0	5.19	12.69	6.08	11.96	19.01	7.28
23	87w	C ₆ H ₅ (CH ₂) ₂ S	0	5.37	12.66	6.06	11.95	14.03	6.53
24	87x	C ₆ H ₅ (CH ₂) ₃ S	0	5.21	12.66	6.03	11.90	13.04	6.35
25	87y	2-Furyl	0	5.39	13.28	6.17	12.15	11.90	6.13
26	87z	2-Thienyl	0	5.40	13.26	6.19	12.09	13.76	6.48
27	87za	2-Pyridyl	0	5.45	13.55	6.22	12.41	1.68	1.29
28	87zb	3-Pyridyl	0	5.52	13.51	6.29	12.34	19.92	7.40
29	87zc	4-Pyridyl	0	5.53	13.65	6.28	12.42	29.15	8.34
30	87zd	(Ph) ₂ CH-	0	5.42	12.62	5.92	11.75	7.27	4.91
31	91a	C ₆ H ₅	1	5.08	12.52	5.85	11.68	3.70	3.23
32	91b	4-CF ₃ C ₆ H ₄	1	5.16	12.55	5.88	11.74	5.75	4.33
33	91c	4-NO ₂ C ₆ H ₄	1	5.14	12.62	5.92	11.78	6.70	4.70
34	91d	4-ClC ₆ H ₄	1	5.09	12.48	5.84	11.68	4.61	3.78
35	91e	4-BrC ₆ H ₄	1	5.11	12.47	5.83	11.67	5.01	3.98
36	91f	4-FC ₆ H ₄	1	5.10	12.51	5.87	11.70	4.41	3.67
37	91g	4-MeC ₆ H ₄	1	5.05	12.46	5.82	11.64	3.36	3.00
38	91h	4-MeOC ₆ H ₄	1	5.11	12.43	5.81	11.65	3.47	3.07
39	91i	4-OHC ₆ H ₄	1	5.10	12.53	5.76	11.57	2.99	2.71
40	91j	4-CNC ₆ H ₄	1	5.25	12.54	5.89	11.76	6.64	4.68
41	91k	(3,4)-DiClC ₆ H ₃	1	5.14	12.51	5.90	11.74	6.06	4.46

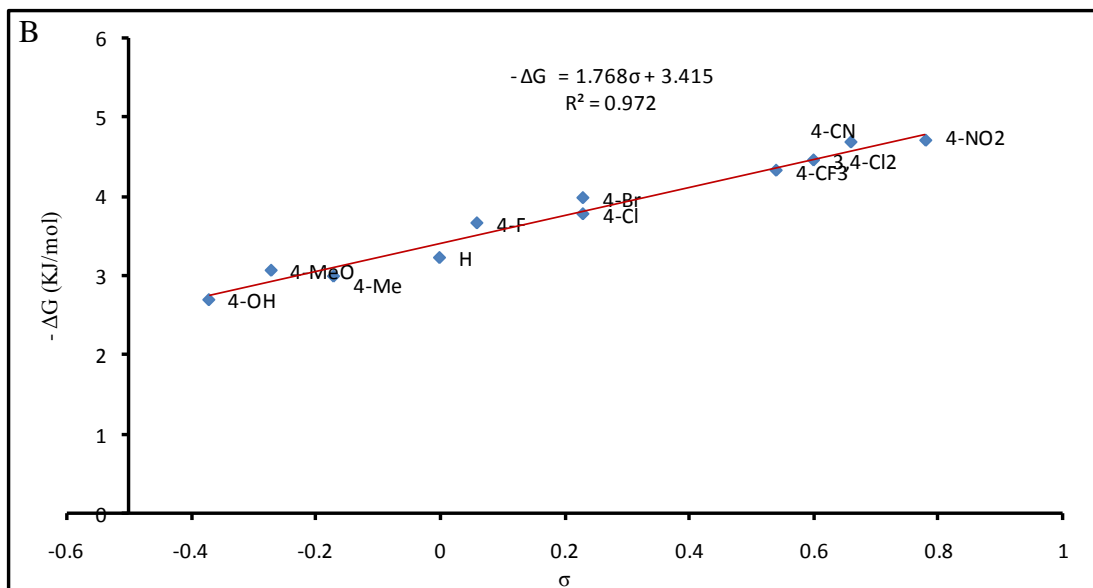
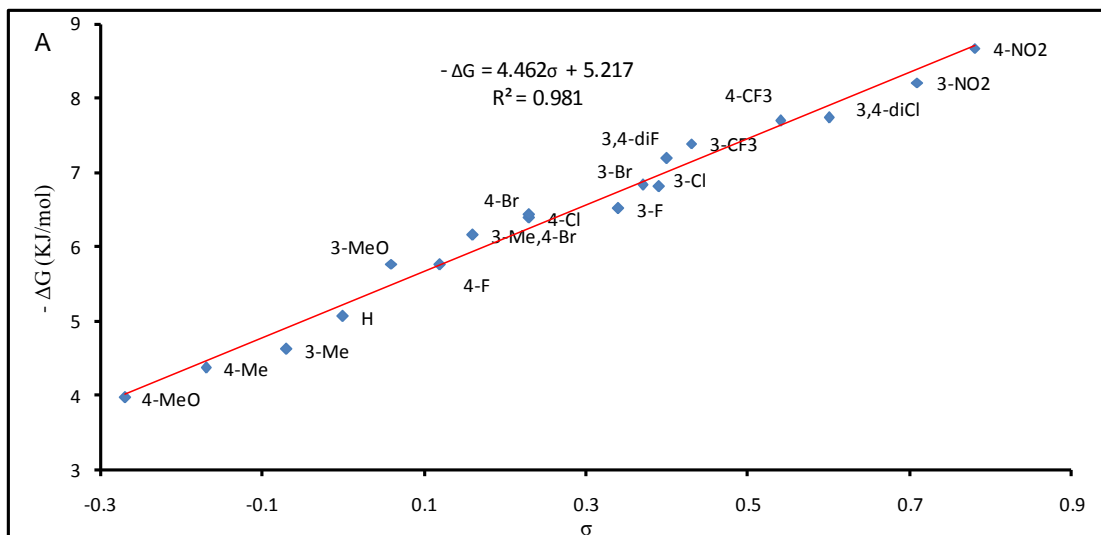
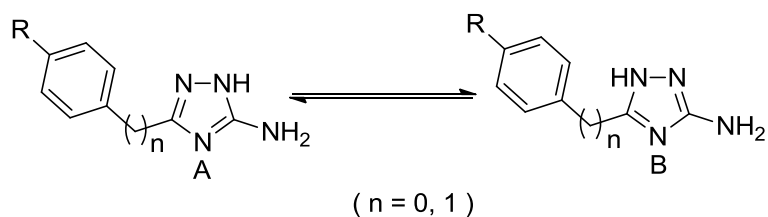
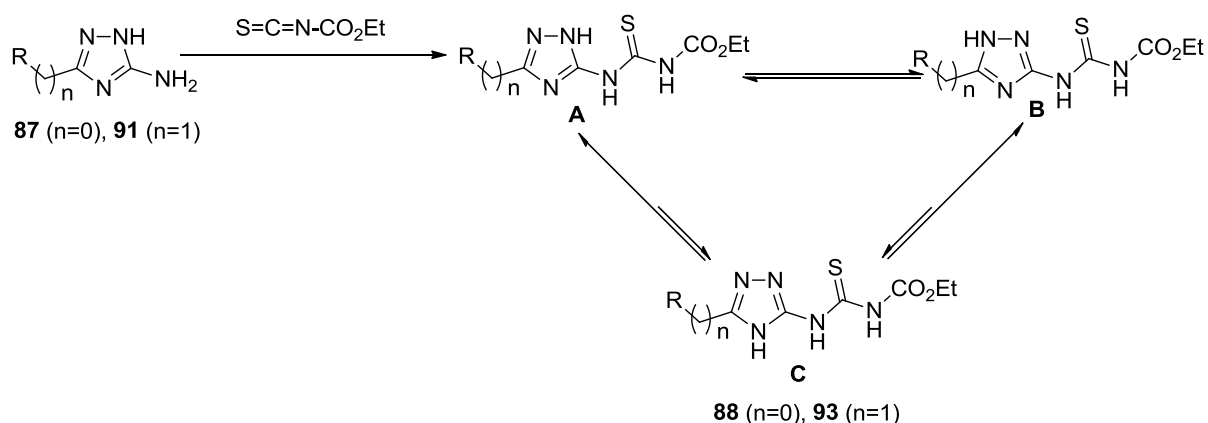


Figure 14. Correlation of ΔG for the tautomeric equilibrium of 3(5)-amino-1,2,4-triazoles (**87**, **91**) (A. phenyl, B. benzyl moiety) with the Hammett constant (σ) of the R group

5.1.3 Synthesis of *N*-(3(5)-aryl-1,2,4-triazol-5(3)-yl)-*N'*-carbethoxythioureas (**88**, **93**)

The nucleophilic reaction of ethoxycarbonyl isothiocyanate with various heterocyclic compounds having exocyclic amino group afforded addition product with good yield in polar aprotic solvent²²¹⁻²²³. It was found that variations in substrate or reaction conditions produced isomeric derivatives of product²²⁴. Herein, to synthesize *N*-(3(5)-aryl-1,2,4-triazol-5(3)-yl)-*N'*-carbethoxythioureas and their derivatives (**88**, **93**), the reactions of various substituted 3(5)-amino-5(3)-aryl-1,2,4-triazoles with ethoxy carbonyl isothiocyanate in dry DMF were performed and it was observed that at room temperature the reaction always preceded smoothly with satisfactory yield and purity (Scheme 26).



Scheme 26. Synthesis of *N*-(3(5)-aryl-1,2,4-triazol-5(3)-yl)-*N'*-carbethoxythioureas (**88**, **93**)

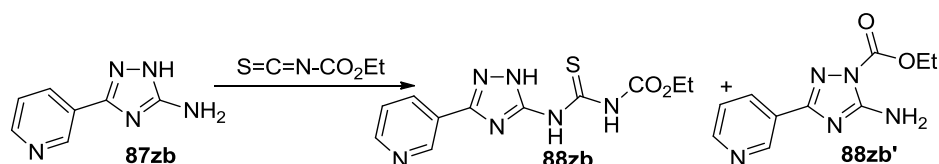
Interestingly, although there are several nucleophilic centres available in **87** and **91**, ethoxycarbonyl isothiocyanate attacked to exocyclic nitrogen and compounds (**88**, **93**) were isolated exclusively and with good yields except some heterocycles substituted 3(5)-amino-1,2,4-triazoles. For example, the reaction of 3(5)-amino-5(3)-3-pyridyl-1,2,4-triazoles (**87zb**) with ethoxy carbonyl isothiocyanate in the same reaction condition afforded corresponding thiourea derivative (**88zb**) (yield 45 %) and 5-

amino-3-pyridin-3-yl-[1,2,4]triazole-1-carboxylic acid ethyl ester (**88zb'**) (yield 40 %) after 5 hr. The formation of this two compounds (**88zb** and **88zb'**) clearly indicated that the nucleophilic reactions of **87zb** took place at the two electrophilic centres *viz.* isothiocyanato and carbonyl carbon atoms of ethoxycarbonyl isothiocyanate and resulted in addition reactions of isothiocyanato moiety with exocyclic amino group and nucleophilic substitution of carbonyl carbon atom at N(1)H of (5)-amino-5(3)-3-pyridyl-1,2,4-triazoles. Due to the strong electron-attracting power of alkoxycarbonyl group enhances the reactivity of the adjacent isothiocyanato-function and promotes the nucleophilic addition at strong nucleophilic centre *viz.* exocyclic amino moiety of **87zb**, whereas, the weak electrophile carbonyl carbon atom attack to weaker nucleophilic centre *viz.* at N(1)H resulting in formation of **88zb** and **88zb'** respectively.

To isolate compound **88zb** exclusively from reaction mixture, several other reaction conditions were attempted using a wide range of polar aprotic solvents and varying reaction temperature. Initially, various polar solvents including dry acetonitrile, acetone, toluene and THF instead of DMF were used as reaction medium at room temperature. The reaction in acetonitrile (monitored by TLC) was found to complete after 24 hours. The products obtained from the reaction in dry acetone, were not pure enough and yield was also less. In addition, the reaction carried out in toluene and THF did not yield any products. Thereafter, to explore further, the reaction was carried out in both hot (100 °C) and cold condition (0 °C) in DMF. In both case the yields of product was unsatisfactory. Therefore, except the reaction in DMF at r.t., several other reaction conditions resulted in unsatisfactory, giving poor yield, or an impure product or both (Table 14). Although the attempt to optimize the reaction condition was unsuccessful, the reaction of entry 1 gave the highest yield for **88zb** and

this condition was used further. The separation of two products was achieved by column chromatography using hexane:ethyl acetate (1:1) as eluent.

Table 14. Optimization of reaction condition of N-(3(5)-3-pyridyl-1,2,4-triazol-5(3)-yl)-N'-carbethoxythioureas

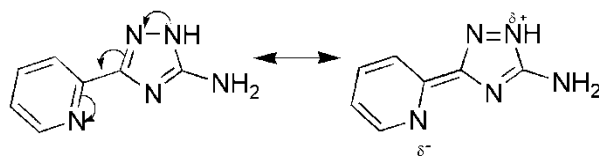


Entry	Solvent	Temp.	Time (hr.)	% yield 88zb	% yield 88zb'
1	DMF	r.t	5 hr.	45	40
2	Acetonitrile	r.t	24 hr.	29	11
3	Acetone	r.t	12hr.	30	16
4	THF	r.t	12hr.	-	-
5	Toluene	r.t	24 hr.	-	-
6	DMF	100	3hr.	15	12
7	DMF	0	12hr.	18	17

To explore further, the reaction condition of entry 1 was applied on 3(5)-amino-5(3)-2-pyridyl-1,2,4-triazoles (**87za**) and 3(5)-amino-5(3)-4-pyridyl-1,2,4-triazoles (**87zc**). Interestingly, although there are several nucleophilic centres available in **87za**, ethoxycarbonyl isothiocyanate attacked to exocyclic nitrogen *viz.* compounds **88za** were isolated exclusively and with good yields (84%). The corresponding product **88za** obtained from the reaction of 3(5)-amino-5(3)-4-pyridyl-1,2,4-triazoles (**87zc**) and ethoxycarbonyl isothiocyanate in DMF could not be characterized due to its poor solubility.

In case of 3(5)-amino-5(3)-2-pyridyl-1,2,4-triazoles, due to mesomeric effect (Scheme 27), probably the lone pair electron of N(1)H was withdrawn by nitrogen atom of 2-pyridyl moiety resulted in transmission of δ^+ and δ^- charge at N(1)H and

pyridyl nitrogen respectively. Therefore, the nucleophilicity of N(1)H of **87za** is decreased dramatically in respect to **87zb** that leads to exclusively addition product **88za** in the reaction of 3(5)-amino-5(3)-2-pyridyl-1,2,4-triazoles and ethoxycarbonyl isothiocyanate in DMF.



Scheme 27. Nucleophilicity of 3(5)-amino-5(3)-2-pyridyl-1,2,4-triazoles

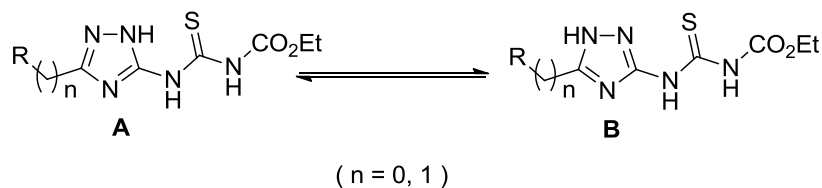
5.1.4 Tautomerism study of *N*-(3(5)-aryl-1,2,4-triazol-5(3)-yl)-*N'*-carbethoxythioureas (**88**, **93**)

The tautomerism aspect of thiourea derivatives of 1,2,4-triazole was evaluated by the use of ^1H NMR spectroscopy. This tool is believed to provide most reliable and comprehensive structural information in solution. Due to annular tautomerism, there is theoretical possibility for existence of three tautomeric forms *viz.* *N*-carbethoxy-*N'*-(3-phenyl-1*H*-1,2,4-triazol-5-yl)thioureas (A), *N*-carbethoxy-*N'*-(5-phenyl-1*H*-1,2,4-triazol-3-yl)thioureas (B), *N*-carbethoxy-*N'*-(3-phenyl-4*H*-1,2,4-triazol-5-yl)thioureas (C) (Scheme 26). To study tautomeric aspect of compounds (Table 15) in solution, DMSO-*d*6 was used as a solvent to disfavour a potential intramolecular hydrogen bonding in the compounds due to the presence of C=S and CO₂Et hydrogen acceptors. Similarly to our results²⁰⁷ obtained previously for 3(5)-amino-5(3)-aryl-1,2,4-triazoles, forms A and B were found to be present in the solutions of triazoles (**88**, **93**) while form C was not observed under the experimental conditions (Scheme 26). The equilibrium between the tautomers was established rapidly and the compositions did not change with time. The identical spectra of the tautomeric system A-B were

observed instantaneously on dissolving the samples and after equilibration of the solution overnight.

The N(1)H signals of tautomers A and B in the ^1H NMR spectra in DMSO-*d*₆ were quite distinct allowing calculation of K_T values (Table 15). In comparison with parent 5-amino-1,2,4-triazoles (**87**, **91**), compounds (**88**, **93**) had the mesomeric electron donating effect of amino group compromised by the thiocarbonyl attached, that resulted in rather similar electronic properties of the aryl and carbethoxythiourea groups. Therefore, electronic properties of the substituents on the phenyl ring changed the predominant tautomeric form. Thus, form B was predominant for R = MeO, Me, and H while form A is major in case of more electronegative R (Cl, Br, CF₃ and NO₂). The K_T and ΔG_{298} values correlated well with the Hammett constant²⁰⁶ of the substituents on the phenyl ring of (**88**, **93**) (Figure 15). Therefore, the thermodynamic stability of form A in comparison with B increased proportionally with increasing electron-withdrawing properties of the substituents R. This relation was not fit well for compound **88j**, **88r** and **88zd**. The anomalous thermodynamic stability of tautomeric forms in solution for these compounds could not be explained properly by this limited study. Therefore, a detail investigation of the factors affecting tautomeric preference of these compounds is strongly recommended.

Table 15. Tautomerism of N-(3(5)-aryl-1,2,4-triazol-5(3)-yl)-N'-carbethoxythioureas in DMSO-*d*₆ solution



Entry	Cpd	R	n	¹ H NMR signal in DMSO- <i>d</i> ₆ (ppm)					KT	ΔG ₂₉₈
				Tautomer A			Tautomer B			
				NH	NH	N(1)H	2NH	N(1)H		
1	88a	CH ₃ S	0	11.82	12.00	13.79	11.41; 11.52	13.93	1.01	-0.02
2	88b	Ph	0	11.87	12.16	13.93	11.56	14.47	1.35	-0.74
3	88c	3-NO ₂ C ₆ H ₄	0	11.89	12.13	14.18	11.61	14.81	0.42	2.15
4	88d	3-CF ₃ C ₆ H ₄	0	11.89	12.13	14.11	11.56	14.69	0.57	1.39
5	88e	3-ClC ₆ H ₄	0	11.91	12.16	14.06	11.58	14.59	0.72	0.81
6	88f	3-BrC ₆ H ₄	0	11.89	12.14	14.05	11.57	14.57	0.74	0.75
7	88g	3-FC ₆ H ₄	0	11.89	12.15	14.04	11.58	14.59	0.78	0.62
8	88h	3-MeC ₆ H ₄	0	11.88	12.18	13.90	11.57	14.42	1.60	-1.16
9	88i	3-MeOC ₆ H ₄	0	11.88	12.16	13.93	11.56	14.48	1.48	-0.97
10	88j	3-CNC ₆ H ₄	0	11.87	12.11	14.12	11.56	14.62	0.64	1.09
11	88k	4-NO ₂ C ₆ H ₄	0	11.89	12.13	14.25	11.58	14.86	0.32	2.82
12	88l	4-CF ₃ C ₆ H ₄	0	11.88	12.12	14.13	11.57	14.74	0.47	1.87
13	88m	4-ClC ₆ H ₄	0	11.87	12.16	14.00	11.62	14.55	0.81	0.52
14	88n	4-BrC ₆ H ₄	0	11.86	12.13	14.00	11.59	14.55	0.79	0.58
15	88o	4-FC ₆ H ₄	0	11.85	12.10	13.92	11.52	14.44	1.08	-0.19
16	88p	4-MeC ₆ H ₄	0	11.86	12.13	13.85	11.53	14.24	1.89	-1.58
17	88q	4-MeOC ₆ H ₄	0	11.82	12.05	13.77	11.54	14.24	2.56	-2.33
18	88r	4-CNC ₆ H ₄	0	11.87	12.10	14.18	11.56	14.77	0.41	2.18
19	88s	(3,4)-diClC ₆ H ₃	0	11.89	12.12	14.11	11.56	14.62	0.51	1.67
20	88t	(3,4)-diFC ₆ H ₃	0	11.87	12.13	14.04	11.60	14.54	0.57	1.39
21	88u	3Me,4BrC ₆ H ₃	0	11.87	12.13	13.97	11.55	14.49	0.90	0.26
22	88v	C ₆ H ₅ CH ₂ S	0	11.79	11.98	13.85	11.55	14.02	1.02	-0.05
23	88w	C ₆ H ₅ (CH ₂) ₂ S	0	11.81	12.01	13.83	11.56	14.01	1.07	-0.16
24	88x	C ₆ H ₅ (CH ₂) ₃ S	0	11.81	11.99	13.80	11.41-11.53	14.03	1.03	-0.06
25	88y	2-Furyl	0	11.78	12.01	14.00	11.70	14.50	1.10	-0.25
26	88z	2-Thienyl	0	11.85	12.07	13.90	11.47-11.55	14.45	0.86	0.37
27	88za	2-Pyridyl	0	11.81	12.09	14.06	11.52	14.76	8.95	-5.42
28	88zb	3-Pyridyl	0	11.87	12.11	14.10	11.56	14.66	0.56	1.45
29	88zc	4-pyridyl	0	-	-	-	-	-	-	-
30	88zd	(Ph) ₂ CH-	0	11.80	12.11	13.65	11.47	13.90	1.47	-0.96
31	93a	Ph	1	11.76	12.06	13.54	11.46	13.80	2.94	-2.67
32	93b	4-CF ₃ C ₆ H ₄	1	11.80	12.08	13.61	11.47	13.86	1.95	-1.65
33	93c	4-NO ₂ C ₆ H ₄	1	11.80	12.07	13.64	11.46	13.88	1.65	-1.23
34	93d	4-ClC ₆ H ₄	1	11.79	12.04	13.55	11.42	13.78	2.29	-2.05
35	93e	4-BrC ₆ H ₄	1	11.79	12.03	13.55	11.42	13.78	2.30	-2.06
36	93f	4-FC ₆ H ₄	1	11.78	12.05	13.54	11.44	13.78	2.55	-2.31
37	93g	4-MeC ₆ H ₄	1	11.78	12.05	13.49	11.42	13.75	3.11	-2.81
38	93h	4-MeOC ₆ H ₄	1	11.77	12.06	13.49	11.43	13.73	3.32	-2.96
39	93i	4-OHC ₆ H ₄	1	11.77	12.03	13.46	11.41	13.69	3.92	-3.38
40	93j	4-CNC ₆ H ₄	1	11.76	12.03	13.62	11.46	13.85	1.92	-1.62
41	93k	(3,4)-DiClC ₆ H ₃	1	11.77	12.03	13.60	11.43	13.80	2.04	-1.76

The signals of N(1)H in the ^1H NMR spectra appeared at the same range and had similar line widths for some heterocyclic, that is 3-pyridyl, 2-pyridyl, and 2-thienyl, 2-furyl substituent at C3(5) of the 1,2,4-triazole ring. The experimental results suggested that for compounds **88zb** and **88z**, form A was favoured whereas, for compounds **88y**, **88za** with 2-furyl and especially 2-pyridyl substituents at C3(5) of the 1,2,4-triazole ring, form B was predominant. Initially, it was believed that this observation could be attributed to possible intramolecular hydrogen bonding between N1–H and the nitrogen atom of the pyridyl and the oxygen atom of the furyl moieties [N1–H---X (X = O, N)] would prevent movement of the tautomeric equilibrium toward form A. However, this explanation was no longer existed by detailed analysis of further experiments. At elevated temperature, compounds **88za** (with potential intramolecular hydrogen bonding) did not disfavour systems stabilized by intramolecular hydrogen bonding and did not change its K_T value. Similar results were observed for compound **88b** (without potential intramolecular hydrogen bonding). The signals of the tautomers A and B appeared clearly in the ^1H NMR spectra in DMSO-*d*6 solution and coalesced only on heating. With the introduction of S moiety in between triazole and benzyl moiety decrease electron donating property of this C3(5) position, disfavour B form. Similar tautomeric preference was observed in compound **88a**.

Replacement of benzyl group at C3(5), the tautomeric form B was predominated, and an attempt to establish a relation between the electronic properties (σ) of substituents and relative Gibbs free energy (ΔG) of tautomeric preference demonstrated that there is a good correlation between two parameters with R^2 value 0.96 (Figure 15b).

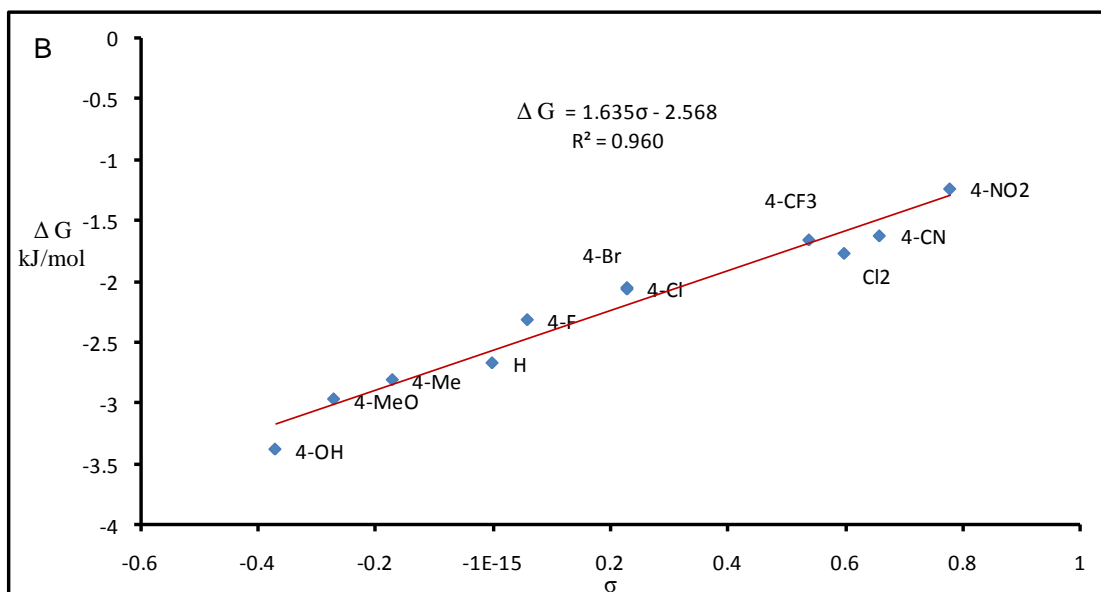
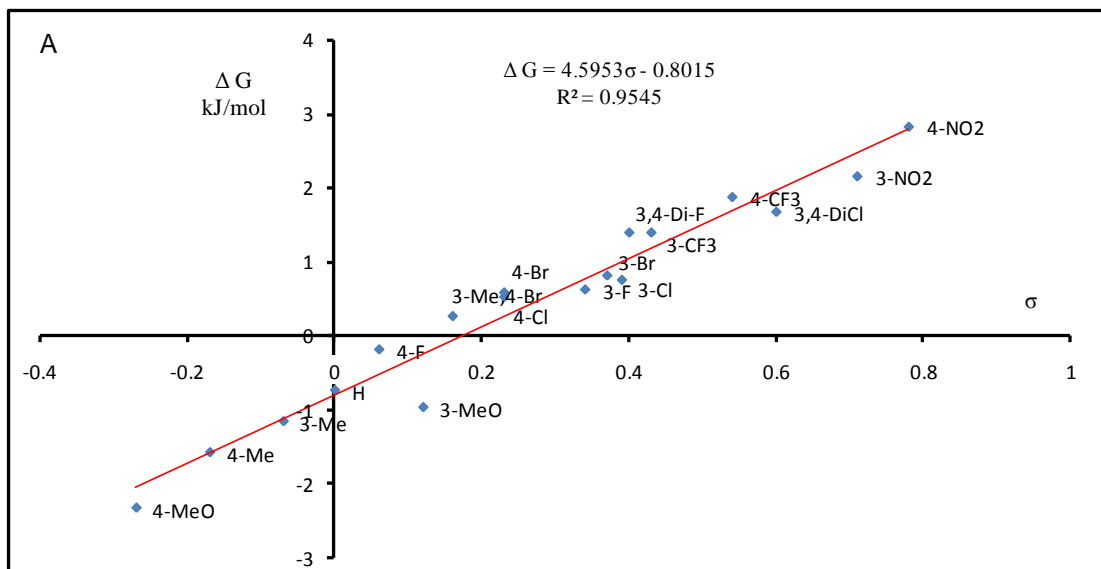
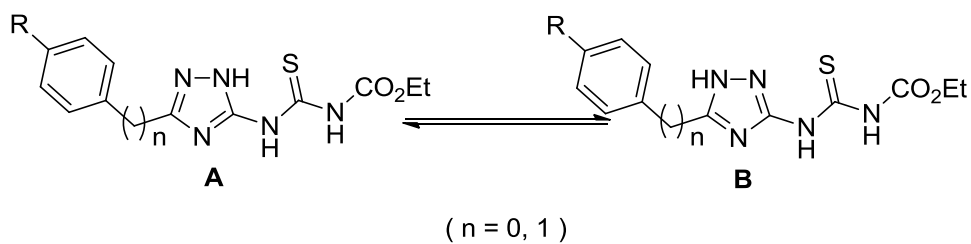


Figure 15. Correlation of ΔG for the tautomeric equilibrium of N-(3(5)-aryl-1,2,4-triazol-5(3)-yl)-N'-carboethoxythioureas (**88**, **93**) (A. phenyl, B. benzyl moiety) with the Hammett constant (σ) of the R group

5.2 Synthesis of 4-carbethoxy-1-[4-(*N,N*-dimethylamino)benzoyl]thiosemicarbazide

To broaden the scope of nucleophilic substitution reaction of ethoxycarbonyl isothiocyanate with heterocyclic compounds and to observe the preferable site of electrophilic attachment, a similar reaction condition was performed using 4-(*N,N*-dimethylamino)benzhydrazide (**108**) as starting material in DMF. In this reaction, it was observed that the ethoxycarbonyl isothiocyanate attacked to hydrazino amino group and resulted in the formation of 4-carbethoxy-1-[4-(*N,N*-dimethylamino)benzoyl]thiosemicarbazide (**109**) exclusively (yield 89 %) (Scheme 28)²²⁵.



Scheme 28: Synthesis of 4-carbethoxy-1-[4-(*N,N*-dimethylamino)benzoyl]thiosemicarbazide (**109**)

The crystal structure of 4-carbethoxy-1-[4-(*N,N*-dimethylamino)benzoyl]thiosemicarbazide suggested that the structure is stabilized by intramolecular N-H---O=C hydrogen bonding arranged in an S(6) graph-set motif. In this crystal, the inversion dimers were connected *via* intermolecular N-H---S=C hydrogen bonds [$R^2_2(8)$ graph-set motif] for sheets parallel to the ($\bar{1}21$) plane. The dimers were also formed by the molecules *via* weak intermolecular N-H---S=C hydrogen bonds [$R^2_2(10)$ graph-set motif] connecting the sheets (Figure 16).

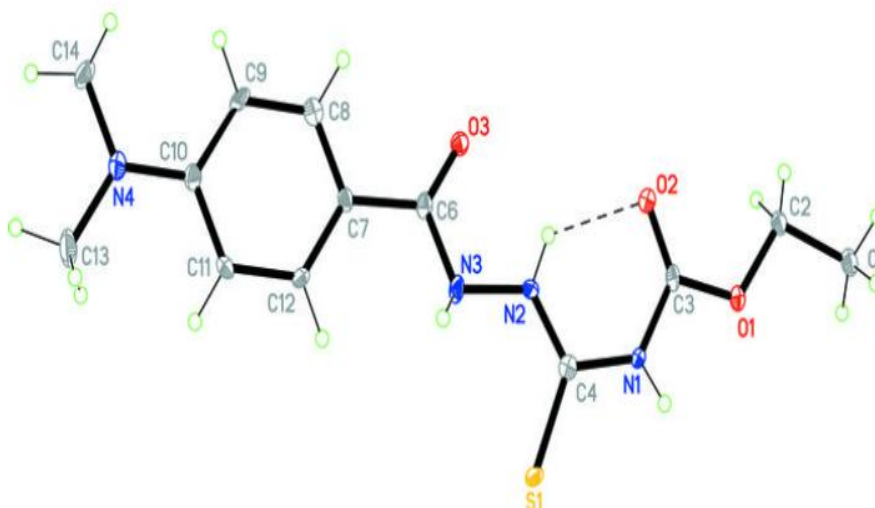


Figure 16. X-ray structure of 4-carbethoxy-1-[4-(N,Ndimethylamino)benzoyl]thiosemicarbazide

5.3 Summary

To summarize, various optimized and highly efficient conditions to synthesize 3(5)-amino-1,2,4-triazoles and *N*-(3(5)-aryl-1,2,4-triazol-5(3)-yl)-*N'*-carbethoxythioureas were discussed and some aspect of the tautomerism of these compounds have been investigated using NMR spectroscopy. The triazoles were found to exist in equilibrium of 1H and 2H-forms whereas the 4H-form was not identified in solution. In addition, the tautomeric equilibrium of triazoles was greatly influenced by electronic properties of substituents presents, however, some exceptions from the established relationship were observed. Following this study, continuous investigation has been employed to explore pharmacophoric requirement of our synthesized TP inhibitors, and the results obtained from these efforts will be reported and discussed in the due course.

Chapter 6

A Quantitative Structure Activity Relationship (QSAR) Study

6.1 CoMFA based 3D-QSAR study of synthesized TP inhibitors

Many laboratories, including our own, have devoted significant efforts in the design and synthesis of a variety of TP inhibitors. Most of the inhibitors generated by this process are mainly the analogues of its natural substrate and primarily belong to the uracil type molecules with various substituents at C-5 and / or C-6 positions. Among them, **TPI** was identified as the most potent inhibitor, so far, exhibiting a substantial suppression of the tumour growth by inhibiting angiogenesis. Moreover, based upon the crystal structure of *E. coli* TP, purine based compounds *viz.* **7-DX** has been investigated for TP inhibition. In addition, multisubstrate inhibitors have designed and evaluated as well. Meanwhile, *N*-phenyl homophthalimide derivatives and purine derivative (5'-*O*-tritylinosine) were identified as mixed and noncompetitive inhibitors of TP respectively¹⁰¹.

In the search for promising TP inhibitors, we have synthesized a few series of thio-oxo analogues of 1,2,4-triazolo[1,5-*a*][1,3,5]triazines and pyrazolo[1,5-*a*][1,3,5]triazines bearing aromatic or aliphatic side chains as TP inhibitors. Structural diversity was generated by modifying aromatic phenyl ring using a range of substituents scattered over different quadrants of the Craig plot. Furthermore, it was revealed that modification of the lead structure with introduction of methylene bridge in between the lipophilic aromatic and the fused ring system resulted in an improvement of TP inhibitory activity. An attempt to investigate the effects of di-substitution (C7 and C8) in the pyrazolo[1,5-*a*][1,3,5]triazine scaffold demonstrated their propensity to better inhibition property. Among different compounds synthesized, compounds **H5bxvii**, **H5bxix**, **H11i**, **H8g**, and **H13a** exhibited excellent inhibition potential towards TP with recorded IC₅₀ values in the low micro molar

range. At this stage of investigation, the exploration of structural requirements of these new fused TP inhibitors in order to improve the inhibitory activity is needed.

Quantitative structure activity relationship (QSAR) studies are examples of the application of chemometrics, to collect useful information for the design of new compounds acting on specific targets. QSAR study attempts to derive meaningful relationship between biological activity and molecular properties. Thus, QSAR models can be used to predict the activity of new compounds and many successful applications in medicinal chemistry have proven its importance in drug discovery and development. There are several meaningful approaches available to relate chemical structure to biological activity in quantitative terms²²⁶. Nowadays, comparative molecular field analysis (CoMFA), a 3D-QSAR method, is widely used tool as it provides information on structural complementarity between the ligand and its binding site, in a 3D arrangement of all relevant molecular properties essential for specific interaction¹⁸⁰. As the derivatives of 1,2,4-triazolo[1,5-*a*][1,3,5]triazines and pyrazolo[1,5-*a*][1,3,5]triazines were identified as novel thymidine phosphorylase inhibitors, it is assumed that 3D-QSAR study would be able to investigate the structural requirements for the future development of promising TP inhibitors.

Therefore, to elucidate a ligand-based pharmacophore and in order to fine-tune the structural requirements, a 3D-QSAR approach using CoMFA analysis was adopted. In addition, same experimental data was analyzed for better understanding of the structural basis for activity particularly for positions 2(C)/ C(7) and 3(N)/ C(8) of the 1,2,4-triazolo[1,5-*a*][1,3,5]triazine and pyrazolo[1,5-*a*][1,3,5]triazine template respectively. In this study, the compounds possessing aromatic phenyl ring attached

directly or indirectly to the fused ring were used in the experiment. To-date, no QSAR report using CoMFA is available on this class of compounds as a TP inhibitor.

6.2 3D-QSAR study design

6.2.1 Dataset

A total of 43 structurally related compounds (training set) were selected and used to generate a CoMFA model. They consisted of six classes of fused bicyclic compounds. Among them, 5-thioxo-5,6-dihydro-[1,2,4]triazolo[1,5-*a*][1,3,5]triazin-7-(4*H*)-one (**H5**) and its derivatives, 5-(methylthio)-[1,2,4]triazolo[1,5-*a*][1,3,5]triazin-7(6*H*)-one (**H6**), 2-thioxo-2,3-dihydro-pyrazolo[1,5-*a*][1,3,5]triazin-4(1*H*)-one (**H11**) and its derivatives, 2-(methylthio)-pyrazolo[1,5-*a*][1,3,5]triazin-4(3*H*)-one (**H12**), 1-(8-phenyl-4-oxo-2-thioxo-1,2,3,4-tetrahydro-pyrazolo[1,5-*a*][1,3,5]triazin-7-yl)thiourea (**H13**) and its derivatives and 8-phenyl-2-thioxo-2,3-dihydro-pyrazolo[1,5-*a*][1,3,5]triazin-4(1*H*)-one (**H14**), all of which bearing phenyl moiety were selected as training set. On the other hand, to examine the predictability of the model generated from training set, 2-benzyl-5-thioxo-5,6-dihydro-[1,2,4]triazolo[1,5-*a*][1,3,5]triazin-7-(4*H*)-one (**H8**) and its derivatives and its related compounds were considered as testing set (Figure 17)

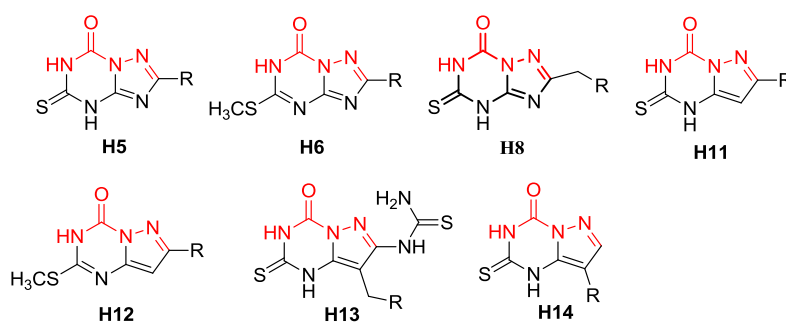


Figure 17. Structures of synthesized TP inhibitors used in CoMFA study (red portion indicated common structural feature)

The rationale behind selecting seven different groups of derivatives for our QSAR study was based on three main considerations: (1) these groups of compounds comprise similar bicyclic 1,2,4-triazolo and pyrazolo fused 1,3,5-triazine ring which are planar in shape; (2) these derivatives share similar substituents at the corresponding C2/C7 position of the bicyclic nuclei such as (un)substituted phenyl ring (ph), (un)substituted benzyl moiety (PhCH₂), and benzylthio groups (PhCH₂S) allowing investigation on the significance of steric and electrostatic effects; (3) most importantly, the majority of these compounds bear a similar (C=O)NH(C=S) motif. This last aspect enables the evaluation of importance of the (C=O)NH(C=S) motif to exhibit inhibitory activity against TP, which represents the first attempt to identify the structural requirements for bicyclic inhibitors of TP.

6.2.2 Preparation of dataset

The CoMFA analysis was performed using SYBYL-X 1.3 molecular modeling software. The partial atomic charges required for the electrostatic interaction were computed using the Gasteiger-Huckel method. The structures were then energy minimized using the standard Tripos force field with a distance dependent dielectric function until a root mean square (rms) deviation of 0.001 kcal/mol Å was achieved.

6.2.3 Alignment

The superimposition of the molecules is considered as the most crucial step in CoMFA analysis. The alignment of the molecules was performed by the database alignment method implemented in SYBYL-X 1.3. The most active compound (**H13a**) was chosen as the template molecule and shared backbone or core structure was identified on which rest of the molecules were aligned.

6.2.4 CoMFA analysis

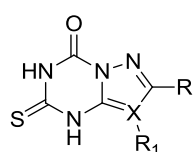
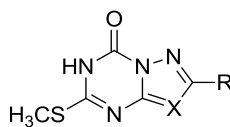
The CoMFA steric and electrostatic interaction fields were calculated at each lattice intersection point of a regularly spaced grid of 2.0 Å. The grid pattern, generated automatically by the Sybyl/CoMFA routine, extended 4.0 Å units in X, Y and Z directions beyond the dimensions of each molecule. The steric term that represented van der Waals (Lennard-Jones) interaction, and the coulombic term, which represented electrostatic interactions, were calculated with the standard Tripos force field. A sp^3 carbon atom with a van der Waals radius of 1.52 Å and +1.0 charge was used as the probe to calculate the steric and electrostatic fields. The values of the steric and electrostatic fields were truncated at 30 kcal/mol. The SYBYL default energy cut-off of 30 kcal mol⁻¹ was used. The minimum sigma (column filtering) was set to 2.0 kcal/mol to improve the signal to noise ratio by eliminating those points whose energy variation was below this threshold.

To generate statistically significant 3D QSAR models, partial least squares (PLS) regression analysis was used. In this analysis, the CoMFA descriptors were used as independent variables, whereas the pIC₅₀ (nM) values were considered as dependent variables. Initially, the optimal number of components was determined by using cross-validation analysis accomplished with the leave-one-out (LOO) methodology that produced q^2 (r^2_{cv}) values that indicate the predictive power of the models. Subsequently, using this optimum number of components, a final QSAR model was derived that yielded the conventional correlation coefficient (r^2), and its standard error (s) of estimation. Finally, the CoMFA results were graphically represented by field contour maps. In addition, the CoMFA model generated from training set was applied to predict the pIC₅₀ of test set.

6.3 Results and discussion

The results of the CoMFA analysis are presented in Tables 16, 17 and 18. To evaluate the predictive power of QSAR model, several statistical parameters including cross-validated correlation coefficient (q^2), non-cross-validated correlation coefficient (r^2), and standard error of estimate, F -statistic values as well as the optimum number of components were determined.

As depicted in Table 17, the cross-validated PLS analysis of training set produced a correlation with q^2 (cross-validated r^2) value of 0.545 with optimum component number of 8. The high value of these two parameters indicated a proper internal predictive capacity of the model. Thereafter, the non-cross-validated PLS analysis was conducted using this optimum number of components to generate an r^2 of 0.960. The r^2 value, which tended to one suggested self-consistency in the study. Moreover, the relatively small estimated standard error of 0.063 and a high F -test value of 100.95 produced from the non-cross-validated analysis also indicated a high degree of confidence in the analysis. In term of the relative contributions, the steric and electrostatic field accounts for 46.5% and 53.5% contributions respectively for the compounds in the training set demonstrated that the electrostatic property was relatively more predominant for the optimal interaction of these inhibitors to the binding site of TP.

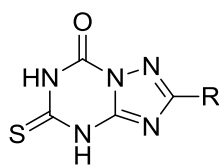
Table 16. Training set compounds with observed and predicted pIC₅₀ values**H5, H11, H13, H14**
and their derivatives**H6b and H12**

Entry	Cpd	R	R ₁	X	pIC ₅₀ value (nM)		
					Observed	Predicted	Residual
1	H5a _{iii}	S(CH ₂) ₃ Ph	-	N	4.559	4.595	0.036
2	H5b	Ph	-	N	4.403	4.283	-0.120
3	H5b _i	3-NO ₂ C ₆ H ₄	-	N	4.645	4.677	0.032
4	H5b _{ii}	3-CF ₃ C ₆ H ₄	-	N	4.655	4.601	-0.054
5	H5b _{iii}	3-ClC ₆ H ₄	-	N	4.519	4.546	0.027
6	H5b _{iv}	3-BrC ₆ H ₄	-	N	4.498	4.525	0.027
7	H5b _v	3-FC ₆ H ₄	-	N	4.317	4.376	0.059
8	H5b _{vi}	3-MeC ₆ H ₄	-	N	4.463	4.516	0.053
9	H5b _{vii}	3-MeOC ₆ H ₄	-	N	4.635	4.574	-0.061
10	H5b _{viii}	3-CNC ₆ H ₄	-	N	4.314	4.376	0.062
11	H5b _{ix}	4-NO ₂ C ₆ H ₄	-	N	4.437	4.489	0.052
12	H5b _x	4-CF ₃ C ₆ H ₄	-	N	4.644	4.667	0.023
13	H5b _{xi}	4-ClC ₆ H ₄	-	N	4.585	4.589	0.004
14	H5b _{xii}	4-BrC ₆ H ₄	-	N	4.656	4.629	-0.027
15	H5b _{xiii}	4-FC ₆ H ₄	-	N	4.492	4.497	0.005
16	H5b _{xiv}	4-MeC ₆ H ₄	-	N	4.501	4.544	0.043
17	H5b _{xv}	4-MeOC ₆ H ₄	-	N	4.659	4.684	0.025
18	H5b _{xvi}	4-CNC ₆ H ₄	-	N	4.481	4.536	0.055
19	H5b _{xvii}	(3,4)-Cl ₂ C ₆ H ₃	-	N	4.965	4.826	-0.139
20	H5b _{Xviii}	(3,4)-F ₂ C ₆ H ₃	-	N	4.660	4.597	-0.063
21	H5b _{xix}	3-Me, 4-BrC ₆ H ₃	-	N	4.883	4.835	-0.048
22	H6b	Ph	-	N	4.022	4.023	0.001
23	H11	Ph	H	C	4.310	4.204	-0.106
24	H11a	4-ClC ₆ H ₄	H	C	4.436	4.512	0.076
25	H11b	4-BrC ₆ H ₄	H	C	4.576	4.528	-0.048
26	H11c	4-FC ₆ H ₄	H	C	4.333	4.435	0.102
27	H11d	4-MeC ₆ H ₄	H	C	4.403	4.453	0.050
28	H11e	4-MeOC ₆ H ₄	H	C	4.666	4.614	-0.051
29	H11f	4-CNC ₆ H ₄	H	C	4.518	4.481	-0.037
30	H11g	(3,4)-Cl ₂ C ₆ H ₃	H	C	4.884	4.878	-0.006
31	H12	Ph	H	C	4.149	4.133	-0.016
32	H13	H ₂ N(C=S)NH-	PhCH ₂	C	4.524	4.592	0.068
33	H13a	H ₂ N(C=S)NH-	4-CF ₃ C ₆ H ₄ CH ₂	C	5.418	5.430	0.012
34	H13c	H ₂ N(C=S)NH-	4-BrC ₆ H ₄ CH ₂	C	4.830	4.768	-0.062
35	H13d	H ₂ N(C=S)NH-	4-FC ₆ H ₄ CH ₂	C	4.645	4.594	-0.051
36	H13e	H ₂ N(C=S)NH-	4-PhC ₆ H ₄ CH ₂	C	5.214	5.214	0.000
37	H13f	H ₂ N(C=S)NH-	4-OPhC ₆ H ₄ CH ₂	C	5.351	5.382	0.031
38	H13g	H ₂ N(C=S)NH-	4-MeC ₆ H ₄ CH ₂	C	4.699	4.743	0.044
39	H13h	H ₂ N(C=S)NH-	4-EtC ₆ H ₄ CH ₂	C	4.901	4.827	-0.074
40	H13i	H ₂ N(C=S)NH-	4-OMeC ₆ H ₄ CH ₂	C	4.289	4.302	0.013
41	H13j	H ₂ N(C=S)NH-	4-OHC ₆ H ₄ CH ₂	C	4.427	4.501	0.074
42	H13k	H ₂ N(C=S)NH-	4-CNC ₆ H ₄ CH ₂	C	4.288	4.235	-0.053
43	H14	H	Ph	C	4.580	4.622	0.042

Table 17. Statistical results from CoMFA analysis

Parameters	Statistical values
No. of compounds	43
No. of optimal components	8
$q^2(r^2_{cv})$	0.545
r^2	0.960
<i>F</i> -test	100.95
<i>p</i> -value	<0.001
Standard error of estimate	0.063
Steric contribution	0.465
Electrostatic contribution	0.535

Although high value of q^2 derived from internal validation *via* cross-validation is considered as necessary requisite, it is not sufficient to confirm the high predictive power of model. In fact, external validation is considered fundamental to establish a reliable QSAR model. Therefore, to verify the efficacy of the CoMFA model generated, thirteen compounds of 2-benzyl-5-thioxo-5,6-dihydro-[1,2,4]triazolo[1,5-*a*][1,3,5]triazin-7-(4*H*)-one (**H8**) analogues and its related compounds were included as external validated set which were not used in the training set during the model development. The actual and predicted TP activities for this external testing set were shown in Table 18. Consistently, the CoMFA model has shown a reasonable predictability of the test set compounds. As shown in Table 18, except compound **H8**, **H8h** and **H8i**, the residual values of all compounds are below 0.5, which further confirmed the reliability of the model.

Table 18. Test set compounds with observed and predicted pIC₅₀ values

Entry	Cpd	R	pIC ₅₀ value (nM)		
			Observed	Predicted	Residual
44	H8	C ₆ H ₅ CH ₂	4.363	4.896	0.533
45	H8a	4-CF ₃ -C ₆ H ₅ CH ₂	5.004	4.978	-0.026
46	H8b	4-Cl-C ₆ H ₅ CH ₂	5.069	4.939	-0.130
47	H8c	4-Br-C ₆ H ₅ CH ₂	4.863	4.922	0.059
48	H8d	4-F-C ₆ H ₅ CH ₂	4.649	4.965	0.316
49	H8e	4-Me-C ₆ H ₅ CH ₂	4.703	4.875	0.172
50	H8f	4-MeO-C ₆ H ₅ CH ₂	4.469	4.921	0.452
51	H8g	4-OH-C ₆ H ₅ CH ₂	4.471	4.953	0.482
52	H8h	4-CN-C ₆ H ₅ CH ₂	4.192	5.049	0.857
53	H8i	(3,4)-Cl ₂ C ₆ H ₅ CH ₂	5.530	4.905	-0.625
54	H5ai	SCH ₂ Ph	4.418	4.812	0.394
55	H5aii	S(CH ₂) ₂ Ph	4.481	4.822	0.341
56	H5g	CH(Ph) ₂	4.439	4.920	0.481

The CoMFA results are usually represented as 3D ‘coefficient contour’ maps. They usually indicate the regions where the variation of steric and electrostatic nature in the structural features of the different training set molecules lead to increase or decrease in the biological activity. The overall graphical representations of the analysis comprising both the electrostatic and steric contour plots were depicted in Figure 18 and to aid visualization, compound **H13a** (most active compound in training set) and **H6b** (least active compound in training set) is displayed in the maps. For CoMFA steric contour, the green colour indicates the region where the bulky groups are associated with enhanced enzyme interaction while the yellow contour suggested the region where increased steric bulk is unfavourable for activity. In the case of electrostatic contour, the regions where more positive charge is favourable to

inhibitory activity are indicated in blue, while those where increased negative charge is favourable to activity were indicated in red.

As shown in Figures 18c and 18e, the biggest yellow contour surrounding the R and R₁ substituents, suggests that the modification of the compounds with the bulky group in this region would lead to decrease in activity. The yellow colour near R₂ indicated that bulky group was not compatible for this region. The IC₅₀ values of **H6b** and **H12** supported this finding. It is noteworthy that with the introduction of the bulky group at R₂, **H6b** and **H12** exhibited dramatic decrease of inhibition potential compared to parent **H5b** and **H11**. However, a small green contour near the *para* and *meta* substituents of the phenyl ring of **H5b** and **H13** series also suggests that bulkiness is indeed favoured to certain extent. Thus, the size of substituent at this site should be neither too large nor too small. This finding is supported by the high activity of compound **H5bxix** bearing bromo and methyl group at *para* and *meta* position of phenyl ring.

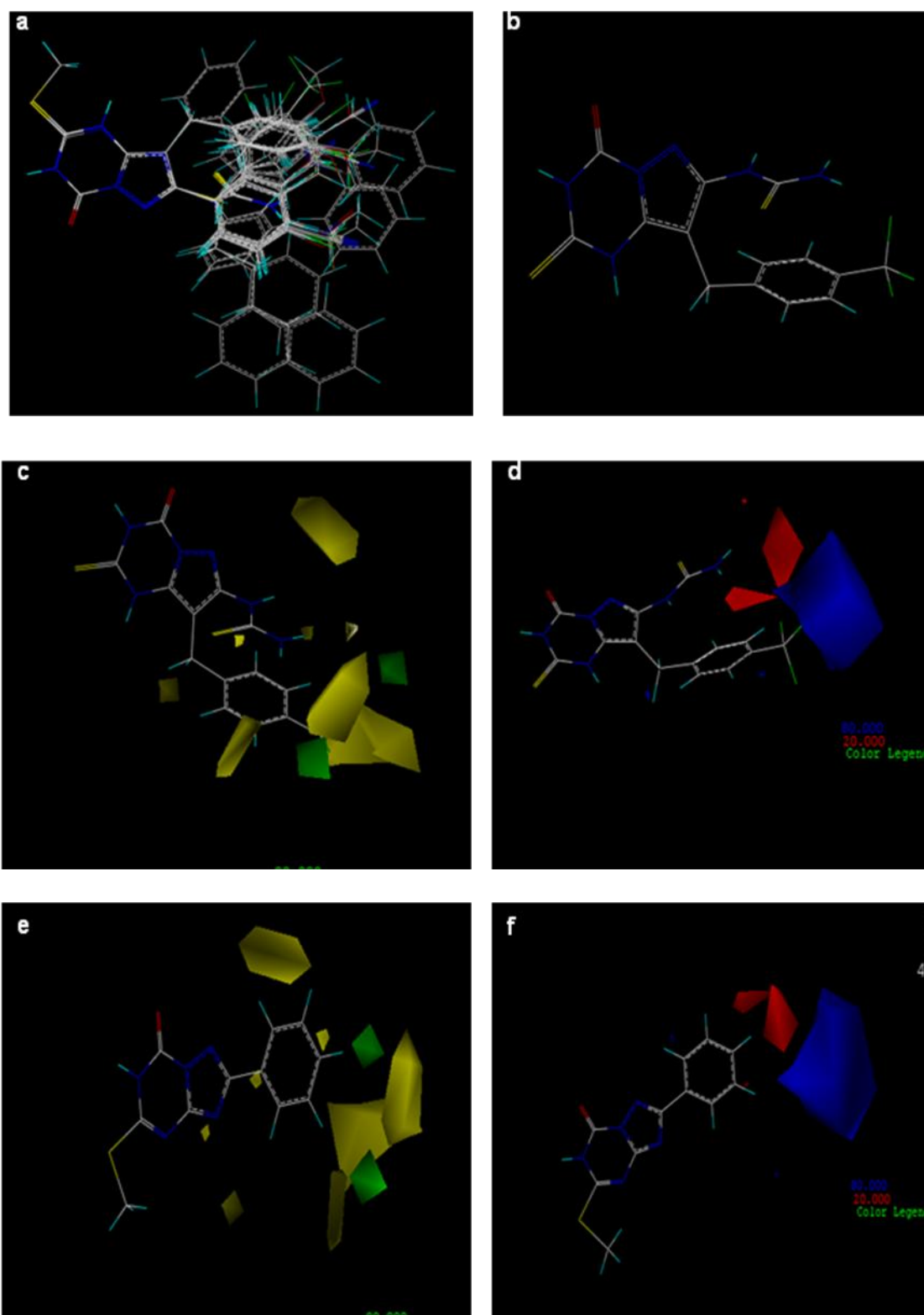


Figure 18. CoMFA analysis. (a). structural alignments of all compounds. (b). structure of the template compound **H13a**. (c, e and d, f). steric and electrostatic contour plots of compounds **H13a** and **H6b** . Green areas correspond to favoured steric bulk, yellow areas indicate bulky groups are disfavoured, blue contours refer to regions where electron-donating groups are favoured; red contours indicate regions where electron-withdrawing groups are favoured.

On the other hand, the blue contour near the atom connecting R₁, indicates that a more electropositive or in other words a lesser electronegative atom at this site will enhance the activity of the molecules. This finding is clearly supported by the improved activity of compounds **H13f** having OPh moiety compared to compound **H13e** bearing Ph group at the site in question. The red contour surrounding the thiourea moiety and connected to R substituent and *para* position of phenyl ring of **H5b** and **H11** series suggested that greater electron density at this site is important for improvement of enzyme affinity.

6.4 Summary

To summarize, the CoMFA analysis was conducted to study the effect of steric and electrostatic properties of the different substituents on TP inhibition exhibited by the series of 1,2,4-triazolo[1,5-*a*][1,3,5]triazine and pyrazolo[1,5-*a*][1,3,5]triazine derivatives. The electrostatic descriptor of the molecules was found to be the more predominant factor for optimal TP interaction. Moreover, this study derived QSAR model with good predictive capacity for TP inhibition exerted by the new fused triazine analogues with acceptable accuracy; therefore, it has provided structural requirements for the development of newer TP inhibitors. The results may aid in designing new TP inhibitors with improved biological potencies. The CoMFA study together with the SAR study from Chapter 4 provided good evidence that with appropriate substitution on the pyrazolo and triazolo triazine, TP inhibitory activity can be better than **7-DX** which is also a bicyclic heterocycle. Following this study, further investigation has been conducted to explore TP associated biological activities of synthesized compounds, which will be reported and discussed in next chapter.

Chapter 7

Biological Characterization of the Active Thymidine Phosphorylase Inhibitors

7.1 Investigation of enzyme inhibition kinetics and TP associated antiangiogenic activity of synthesized compounds

Intensive research has been devoted to the development of TP inhibitors with diverse structures. Consequently, numerous TP inhibitors disclosed over the past few years were found to be mainly competitive inhibitors. However, limited number of compounds was designed as multi-substrate, mixed-type competitive type and non-competitive inhibitors of TP. Although, several potent inhibitors were generated and have been tested preclinically and clinically, to-date, there is no TP inhibitor clinically available. It is believed that the development of TP inhibitors with potent antiangiogenic activity may improve future TP-targeted therapy.

In this thesis, continuous efforts in exploring new TP inhibitors have identified thio-oxo analogues of 1,2,4-triazolo[1,5-*a*][1,3,5]triazine and pyrazolo[1,5-*a*][1,3,5]triazine scaffolds as new lead compounds exhibiting promising TP inhibition profiles. Among them, compounds **H5bxvii**, **H5bxix**, **H8i**, **H11g**, **H13a**, **H13e**, **H13f** and **H13n** have demonstrated good inhibitory activities against TP with IC₅₀ values in the low micro molar range (Figure 19). The good inhibitory profile of the compounds has prompted the need to investigate the enzyme inhibition kinetics in order to determine the interaction mechanism against the enzyme. In addition, the exciting outcome from the *in vitro* enzyme assay has led to the question of whether these novel inhibitors would inhibit the TP associated downstream mediation of various angiogenic factors such as matrix metalloproteinase (MMPs), interleukins (IL) and vascular endothelial growth factor (VEGF). If the new inhibitors were to exhibit such functions, it would mean that these compounds might exhibit antiangiogenic property. At the same time, the likelihood of these compounds exhibiting antiproliferative and

antimetastatic properties would be evaluated so as to determine their potential use in chemotherapy.

To investigate these potentials, the experiments that demonstrate inhibition of the expression of MMP-9, VEGF, IL-8 in breast cancer cell line, MDA-MB-231, were performed. In addition, to verify their antiproliferative and antimetastatic properties, the cell viability and migration assay were employed respectively. In this study, initial investigation was tested on selected compounds from the **H5b** series. The compounds, which exhibited attractive *in vitro* TP enzyme inhibition profile with IC₅₀ values less than 30 μ M, were screened for their antiproliferative and MMP-9 inhibitory activity. Based on the results of these experiments, compounds which showed positive response were chosen for further investigations. Similarly, selected compounds from libraries **H8**, **H11**, and **H13** were subjected to the same screens for their effects on specific biological assays as were tested on the **H5b** series compounds. Moreover, the enzyme kinetic study was performed to evaluate the inhibitory mechanism of the synthesized compounds using the most active compounds from each series.

In this study, the gelatine zymography was employed to determine MMP expression on the said cell line whereas to quantify VEGF and IL-8 expression colorimetric enzyme-linked immunosorbent assay (ELISA) method was adopted. In addition, the MTT colorimetric assay and the cell invasion assay were conducted using the same cell line in order to determine the cytotoxicity and antimetastatic properties of selected compounds respectively. Furthermore, *in vitro* enzyme assay was performed to study the inhibition kinetics. The statistical significance between treatment and control groups was analyzed using ANOVA test. The values of $p < 0.05$ were considered statistically significant.

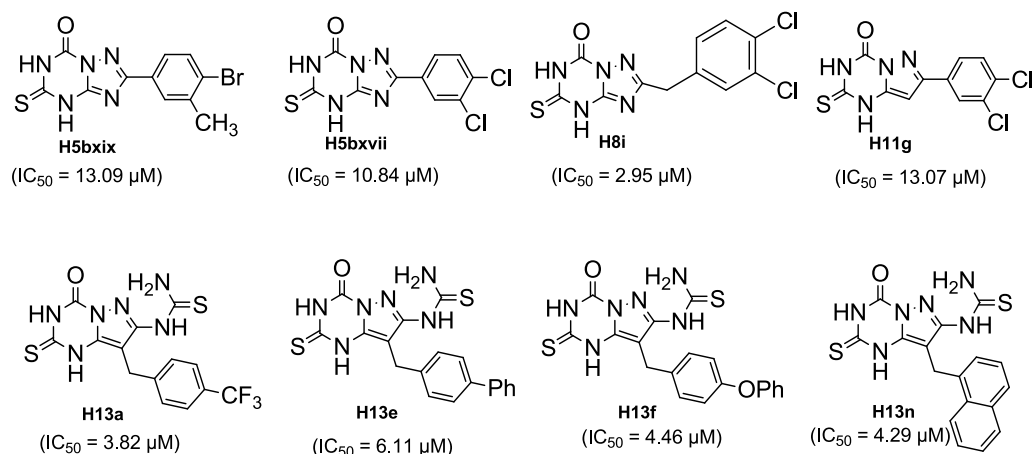


Figure 19. Structures of synthesized TP inhibitors with low micromolar IC_{50} values

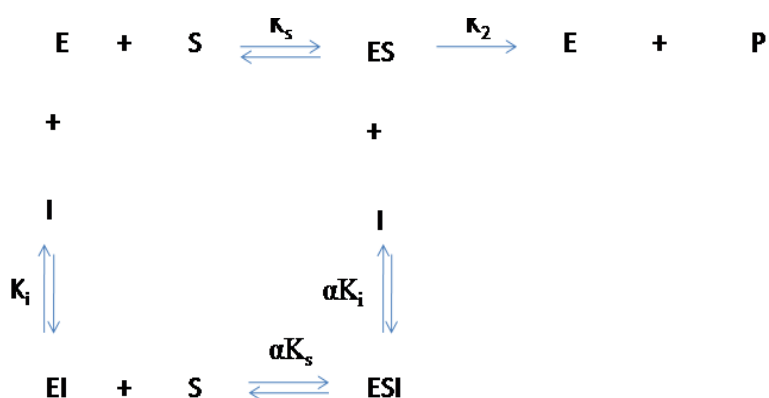
7.2 Results

7.2.1 Enzyme inhibition kinetics characterization

To elucidate the mechanism of enzyme inhibition, a kinetic study was attempted using compound **H5bxix** at different inhibitor concentrations (0, 2, 15, 20, 30 μM) in the presence of variable thymidine (dThd) and phosphate (kpi) concentration. In this study, both thymidine and phosphate are considered as substrates because the structural features of *E. coli* TP suggests that there are two distinct places namely the nucleoside and the phosphate binding sites in the active pocket of the enzyme. The data obtained was analyzed by the Lineweaver–Burk plot (the double reciprocal plot) (Figure 20). The results demonstrated that compound **H5bxix** exhibited mixed type inhibition for both dThd and kpi as a variable substrate (Figure 20a and 20b) since the straight lines corresponding to different concentrations of the inhibitor intersected in the second quadrant of the reciprocal plot. This was further confirmed by the fact that increasing inhibitor concentration was accompanied by the increase of K_m values whereas the V_{max} values decreased gradually (Figure 20). Therefore, the compound could directly interact with enzyme as well as enzyme-substrate complex by weak

bonds at, near, or inside the active site which inactivated the enzyme but does not affect the binding of substrate. Similar pattern of enzyme inhibition kinetics was observed for the other selected compounds *viz.* **H5bxvii**, **H8i**, **H11g** and **H13a** in the presence of varying concentration of thymidine and phosphate as substrates (Figures 21, 22, 23, and 24 respectively).

As the compounds exhibited mixed type enzyme inhibition pattern, it was expected that these inhibitors would bind to the free enzyme, E, as well as to the enzyme-substrate complex, ES. For mixed-type inhibitors, the following model is adopted (Scheme 29):



Scheme 29. Mixed type inhibition model

The enzyme-inhibitor complex (EI) has lower affinity for substrate (S) than free enzyme (E) ($\alpha > 1$), and ESI would be non productive.

In order to analyze the mixed type inhibition kinetics, the Lineweaver-Burk equation in double reciprocal form can be presented as following equations

$$\frac{1}{v} = \frac{K_m}{V_{max}} \left[1 + \frac{[I]}{K_i} \right] \frac{1}{[S]} + \frac{1}{V_{max}} \left[1 + \frac{[I]}{\alpha K_i} \right]$$

Where,

$$Slope = \frac{K_m}{V_{max}} + \frac{K_m [I]}{V_{max} K_i}$$

$$Intercept = \frac{1}{V_{max}} + \frac{[I]}{V_{max} \alpha K_i}$$

where K_m is the Michaelis constant, V_{max} is the maximum enzymatic reaction velocity, $[S]$ is the substrate concentration, $[I]$ is the concentration of inhibitors, K_i is the inhibition constant for free enzyme and inhibitor, and αK_i represents the inhibition constant for enzyme-substrate complex and inhibitor. Replots of slopes and intercepts of the double reciprocal plot with inhibitor concentrations yielded K_i and αK_i values (Table 19).

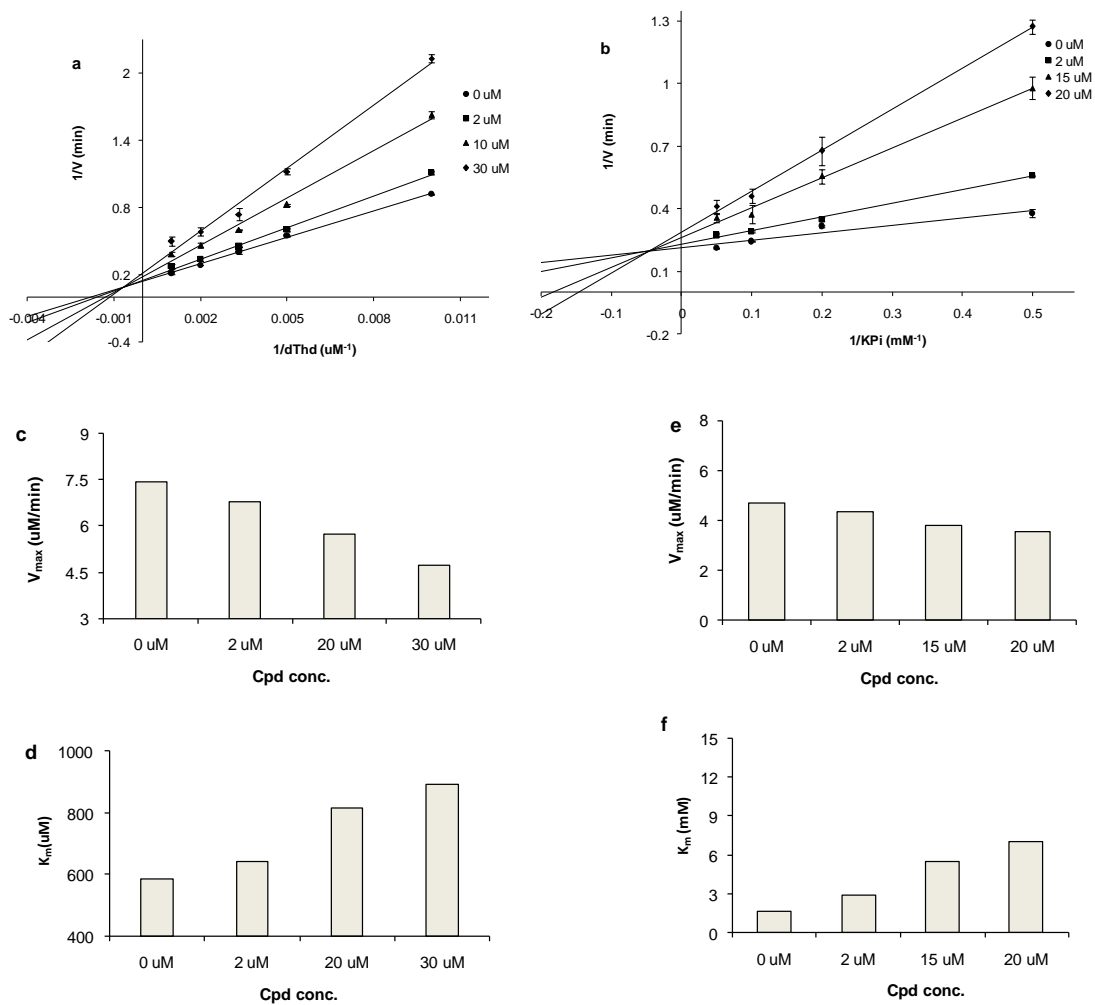


Figure 20. Lineweaver-Burk plots of TP inhibition by **H5bxix**, in the presence of variable concentrations of dThd (**a**) and phosphate (**b**) demonstrating mixed type enzyme inhibition and response of kinetic parameters V_{max} and K_m with increasing concentration of **H5bxix** in variable concentrations of dThd (**c**, **d**) and phosphate (**e**, **f**). Experiments carried out at least in triplicate.

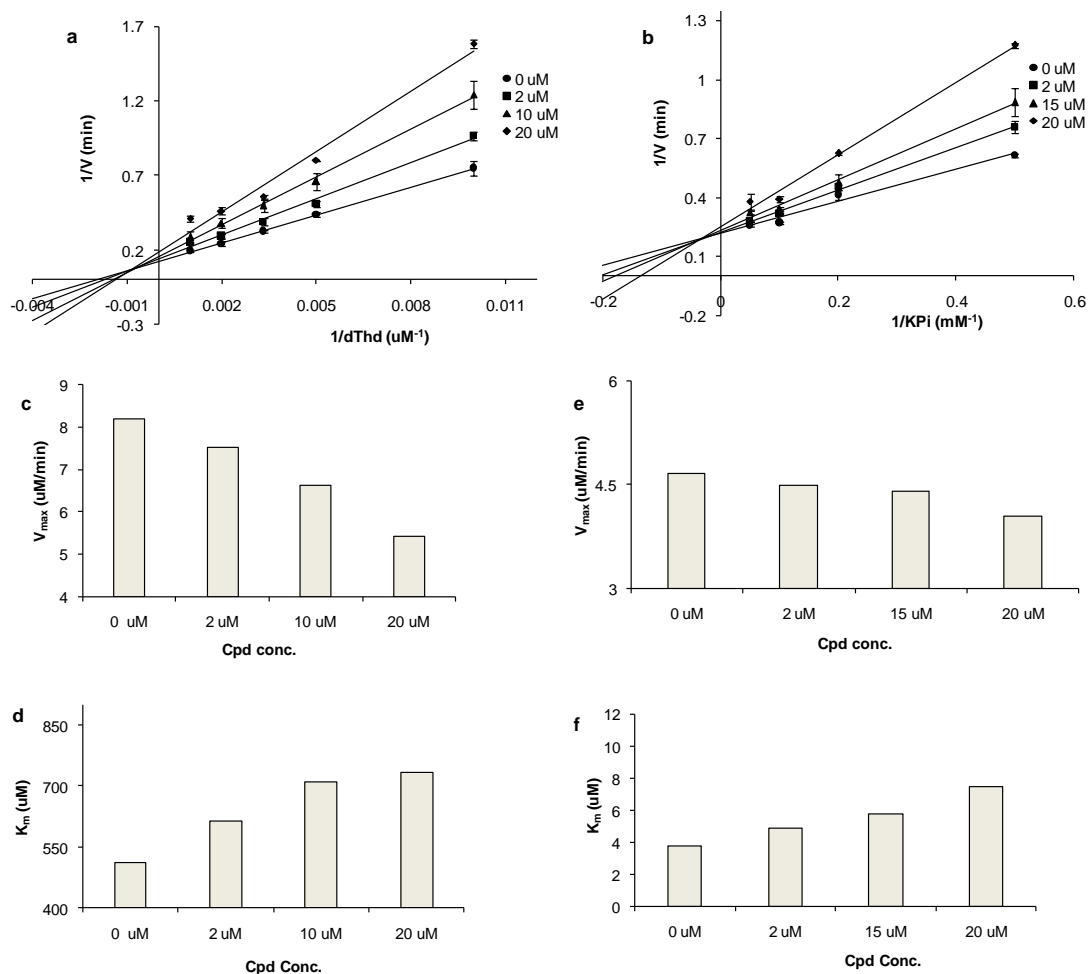


Figure 21. Lineweaver-Burk plots of TP inhibition by **H5bxvii**, in the presence of variable concentrations of dThd (a) and phosphate (b) demonstrating mixed type enzyme inhibition and response of kinetic parameters V_{max} and K_m with increasing concentration of **H5bxvii** in variable concentrations of dThd (c, d) and phosphate (e, f). Experiments carried out at least in triplicate.

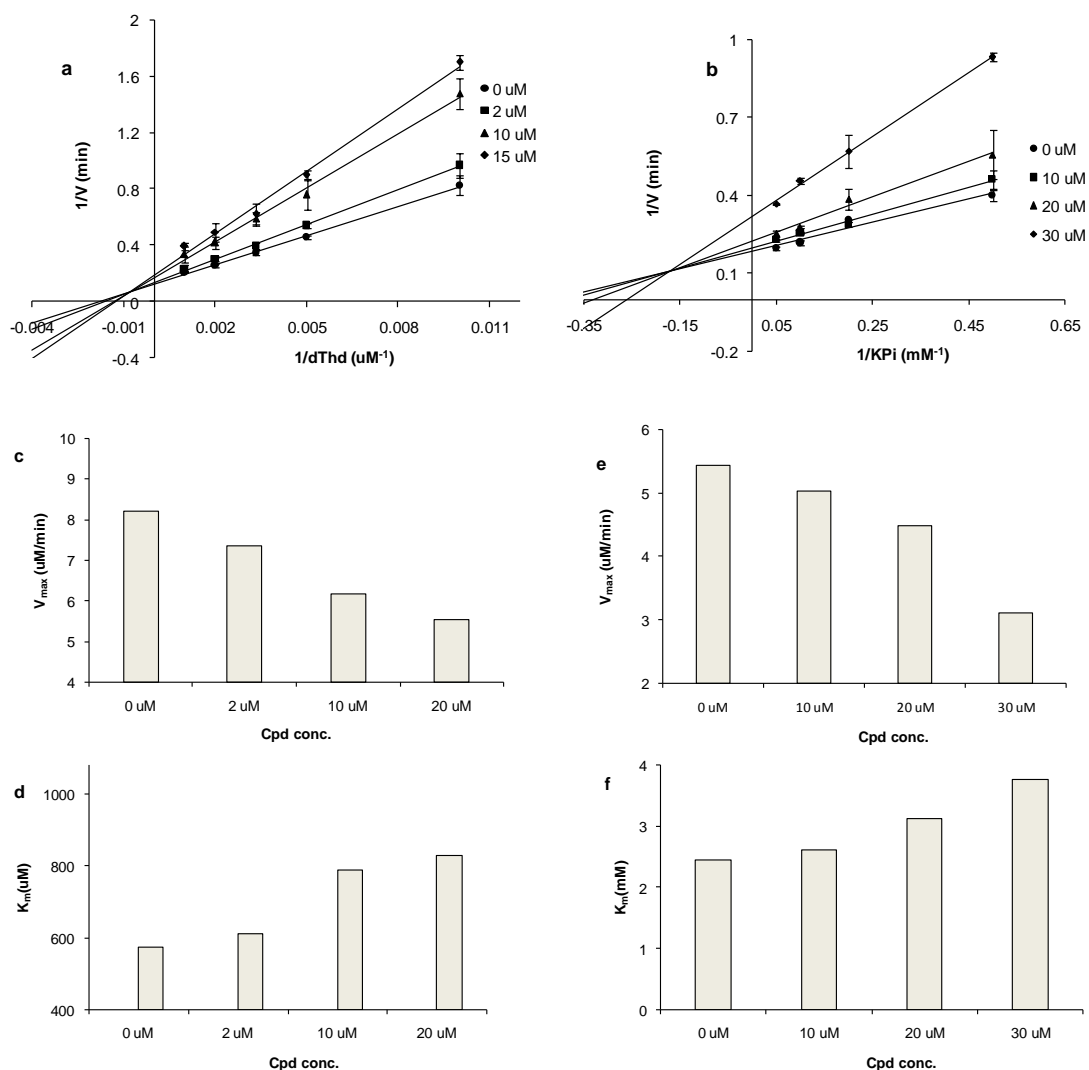


Figure 22. Lineweaver-Burk plots of TP inhibition by **H8i**, in the presence of variable concentrations of dThd (a) and phosphate (b) demonstrating mixed type enzyme inhibition and response of kinetic parameters V_{max} and K_m with increasing concentration of **H8i** in variable concentrations of dThd (c, d) and phosphate (e, f). Experiments carried out at least in triplicate.

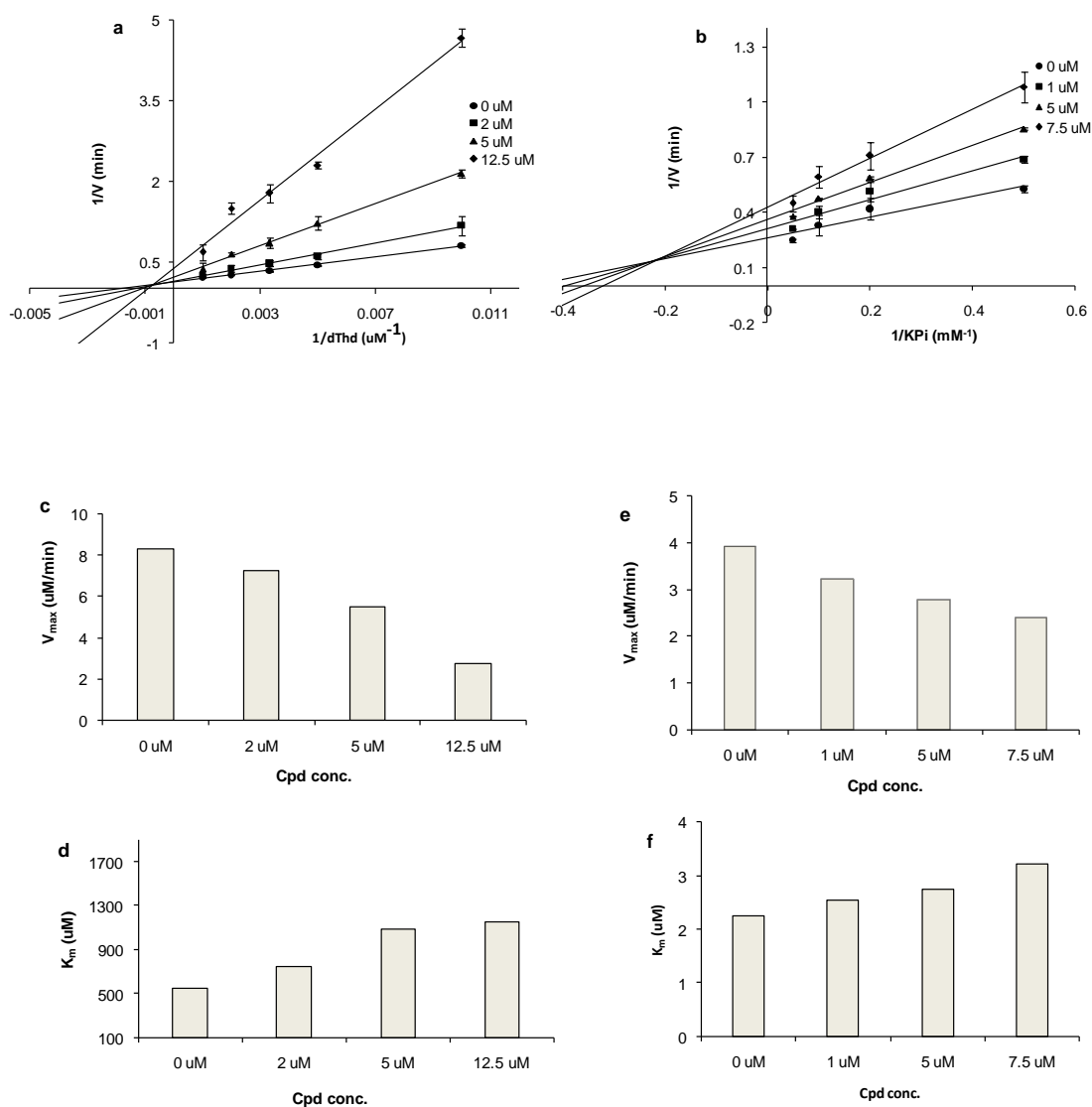


Figure 23. Lineweaver-Burk plots of TP inhibition by **H11g**, in the presence of variable concentrations of dThd (**a**) and phosphate (**b**) demonstrating mixed type enzyme inhibition and response of kinetic parameters V_{max} and K_m with increasing concentration of **H11g** in variable concentrations of dThd (**c, d**). and phosphate (**e, f**). Experiments carried out at least in triplicate.

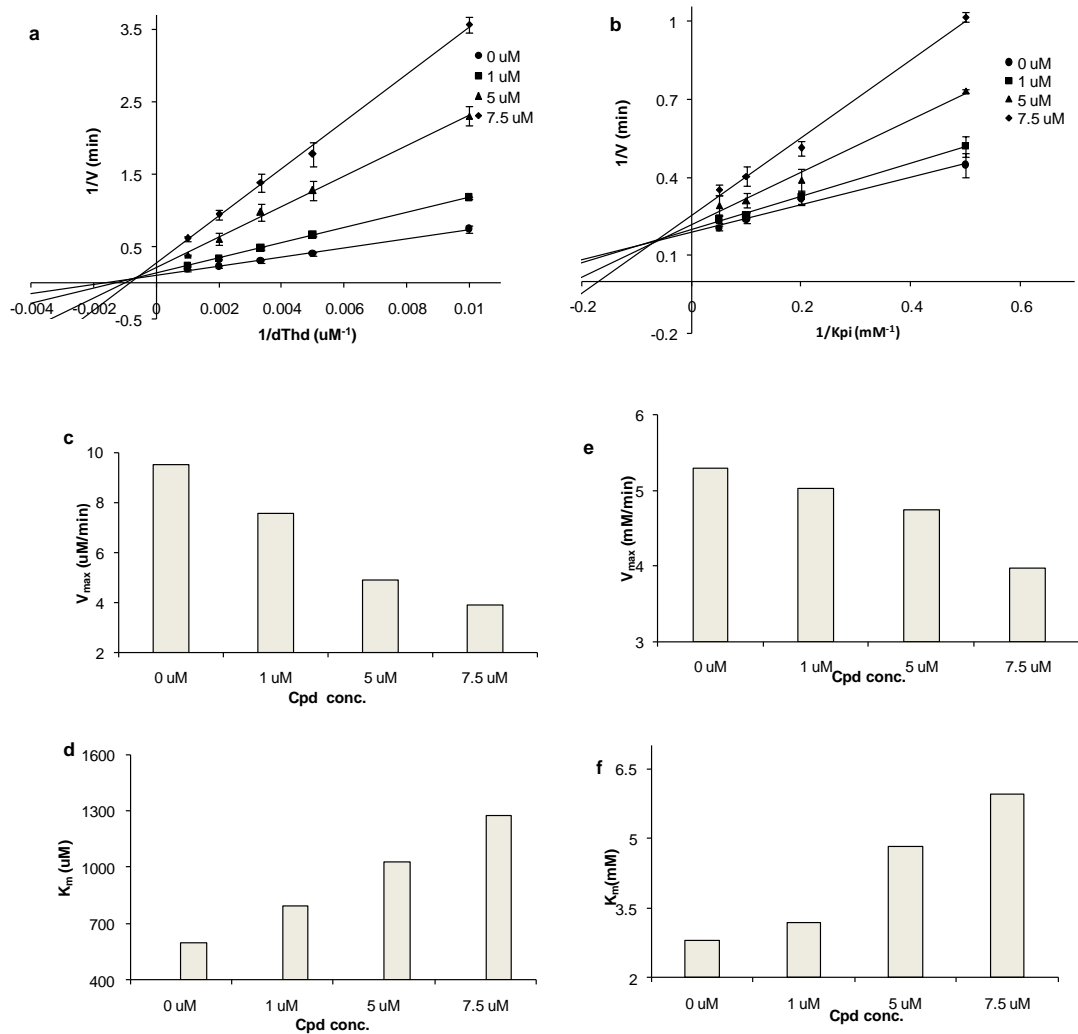


Figure 24. Lineweaver-Burk plots of TP inhibition by **H13a**, in the presence of variable concentrations of dThd (**a**) and phosphate (**b**) demonstrating mixed type enzyme inhibition and response of kinetic parameters V_{max} and K_m with increasing concentration of **H13a** in variable concentrations of dThd (**c**, **d**) and phosphate (**e**, **f**). Experiments carried out at least in triplicate.

Table 19. A summary of the enzyme inhibition kinetics parameters

Cpd	Substrate	K _i value (μM)	α	Type of inhibition
H5bxix	dThd	24.21 ± 0.53	2.48	Mixed type
	KP _i	5.58 ± 0.91	15.47	Mixed type
H5bxvii	dThd	20.09 ± 1.25	2.12	Mixed type
	KP _i	21.12 ± 1.18	9.47	Mixed type
H8i	dThd	19.57 ± 5.62	5.41	Mixed type
	KP _i	14.52 ± 4.178	2.74	Mixed type
H11g	dThd	2.00 ± 0.37	1.57	Mixed type
	KP _i	7.08 ± 1.68	1.94	Mixed type
H13a	dThd	1.19 ± 0.13	3.07	Mixed type
	KP _i	4.14 ± 0.85	5.94	Mixed type

7.2.1 Antiangiogenic activity determination

- Compounds inhibited PMA-stimulated MMP-9 secretion and expression in breast cancer cell

The MMP-9 and MMP-2 have been reported to play key roles in the degradation and remodelling of the basement membrane, and therefore they promote tumour cell invasion, migration, and metastasis. MMPs have been shown to be up regulated by the activity of TP²²⁷. To demonstrate inhibition profile towards MMP-9 by the synthesized TP inhibitors, the test compounds were subjected to gelatine zymography screening using MDA-MB-231 cells. Initially, the exploration of TP associated biological activities was started with the **H5** series compounds. The thirteen

compounds from **H5** series, which showed promising TP inhibitory activity with IC_{50} values less than 30 μ M, were selected. The cells were treated with 100 and 200 μ M of the test compounds along with PMA (80 nM) for 24h. The conditioned medium from the cell culture was collected and the secreted form of MMP-9 was analysed using gelatine zymography. As shown in Figure 25a, the proteolytic activity of MMP-9 (band corresponded to the MW of 92 kDa) was not significantly inhibited by any of the test compounds at concentration of 100 μ M. Interestingly, an obvious change in band intensity, compared to vehicle control, was detected for compounds **H5bii**, **H5bxvii** and **H5bxix** at 200 μ M indicating inhibition of proteolytic activity of MMP-9 at a higher concentration (Figure 25b). Therefore, identified compounds **H5bii**, **H5bxvii** and **H5bxix** were subjected to further investigations.

To study the dose response of extracellular expression of MMP-9, the conditioned medium of MDA-MB-231 cells exposed to PMA and different doses of the selected test compounds was examined and the results suggested that a PMA-induced elevation of MMP-9 expression was attenuated dose dependently by all compounds tested (Figure 26a). It is noteworthy that by visual inspection of the results, **TPI**, the most potent TP inhibitor reported so far and **7-DX**, reference TP inhibitor, did not show significant reduction in the activity of MMP-9 even at 200 μ M. When the band intensities of gelatine zymography of the corresponding doses were quantified by using the Image Gauge 4.0 software and subsequent densitometric analysis of these results revealed that compounds **H5bxvii** and **H5bxix** at 100 and 200 μ M significantly ($p < 0.05$) inactivated the MMP-9 activity. Moreover, compounds **H5bxix** and **H5bxvii** exhibited 43 and 32 fold stronger inhibition profile towards MMP-9 expression at 200 μ M compared to **TPI** respectively (Figure 26b). However, the proteolytic activity of MMP-2 (band corresponded to the MW of 62 kDa) was not

significantly affected by combining treatment with the synthesized compounds and PMA using lung cancer cell line A549 (Data not shown here).

Using similar technique, a total of twenty compounds from the **H8**, **H11** and **H13** series that showed TP inhibition with IC_{50} values of less than 30 μ M was examined for inhibitory effects of MMPs production. They were subjected to gelatine zymography screening at 100 μ M for 24 h using the same cell line. The level of MMP-9 expression was determined from the conditioned media. Interestingly, the visual analysis of the zymograms (Figure 27a) revealed that the basal MMP-9 secretion levels were significantly inhibited by **H11g**, **H8i**, **H13a**, **H13e**, **H13f** and **H13n** at 100 μ M compared with the control. Therefore, to study the dose response on PMA-induced MMP-9 activity, compounds **H11g**, **H8i**, **H13a**, **H13e**, **H13f** and **H13n** were selected. The treatment of the compounds (from 25 to 100 μ M) decreased the expression level of MMP-9 in MDA-MB-231 cell line in a dose-dependent fashion (Figure 27b). The densitometric analysis of the band intensity of the corresponding dose of compounds suggested that except for compounds **H8i** and **H13a**, all the other selected compounds significantly inhibited the MMP-9 expression at 50 and 100 μ M ($p < 0.05$) (Figures 28a and 28b). It is noteworthy that even though compounds **H8i** ($IC_{50} = 2.95 \mu$ M) and **H13a** ($IC_{50} = 3.82 \mu$ M) were identified as most active TP inhibitors in their corresponding series, they did not show promising inhibitory potential on MMP-9 expression.

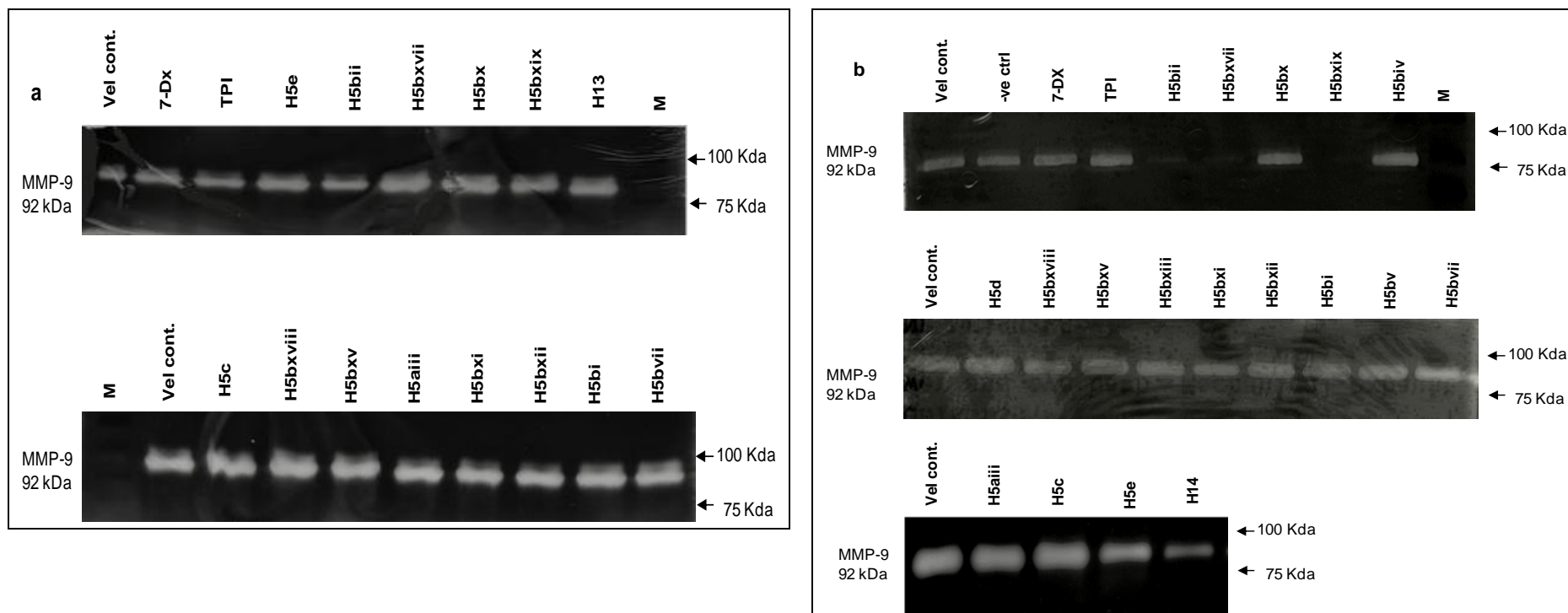


Figure 25. Screening of compounds ($IC_{50TP} < 30 \mu M$) (series **H5** and reference compounds) based on their inhibitory effect of MMP expression on breast cancer cell line, MDA-MB-231 (**a**). screening of inhibitory potential of compounds (series **H5**, compound **H14** and reference compounds) towards PMA induced MMP-9 expression after 24 h treatment at 100 μM (**b**). screening of inhibitory potential of compounds (series **H5**, compound **H14** and reference compounds) towards PMA induced MMP-9 expression after 24 h treatment at 200 μM .

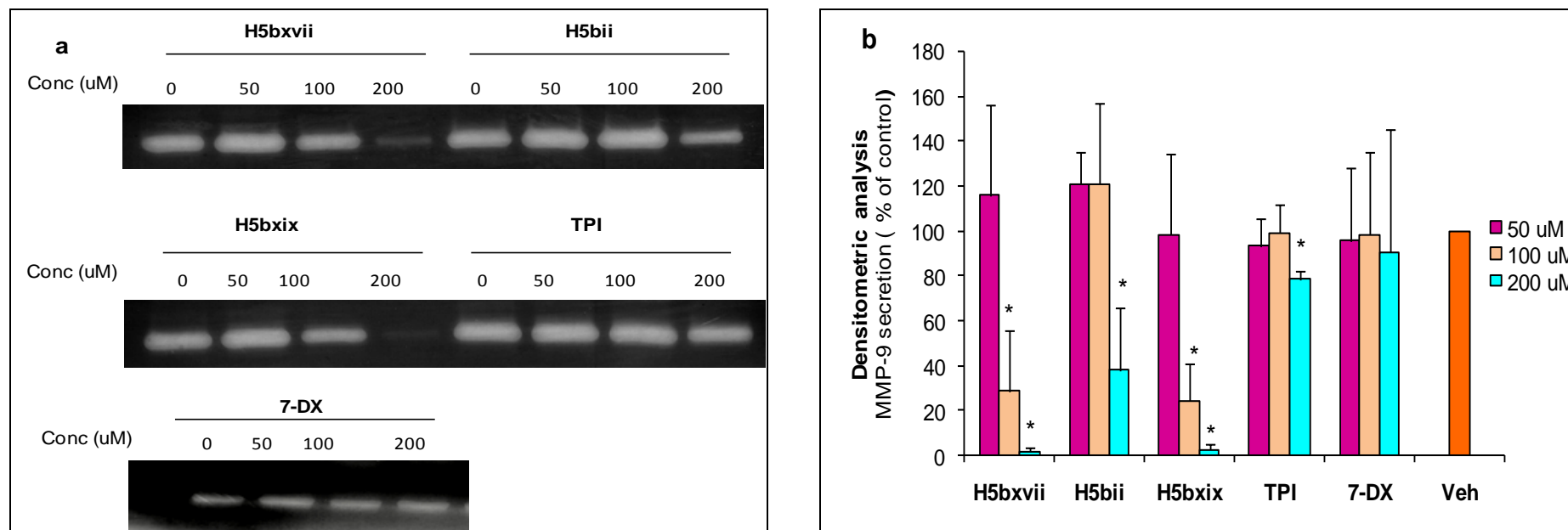


Figure 26. Antiangiogenic effect (MMP-9 expression) of compounds (series **H5** and reference compounds) on breast cancer cell line (**a**). suppressive effects of selected compounds (**H5bxix**, **H5bii**, **H5bxvii**, **TPI** and **7-DX**) on PMA-induced MMP-9 expression and their dose response. (**b**). densitometry analysis of band intensities of corresponding dose of compounds, normalized to respective vehicle controls. Results are presented as means \pm SD; SD denoted by error bars (Experiments carried out at least in triplicate). * $p < 0.05$.

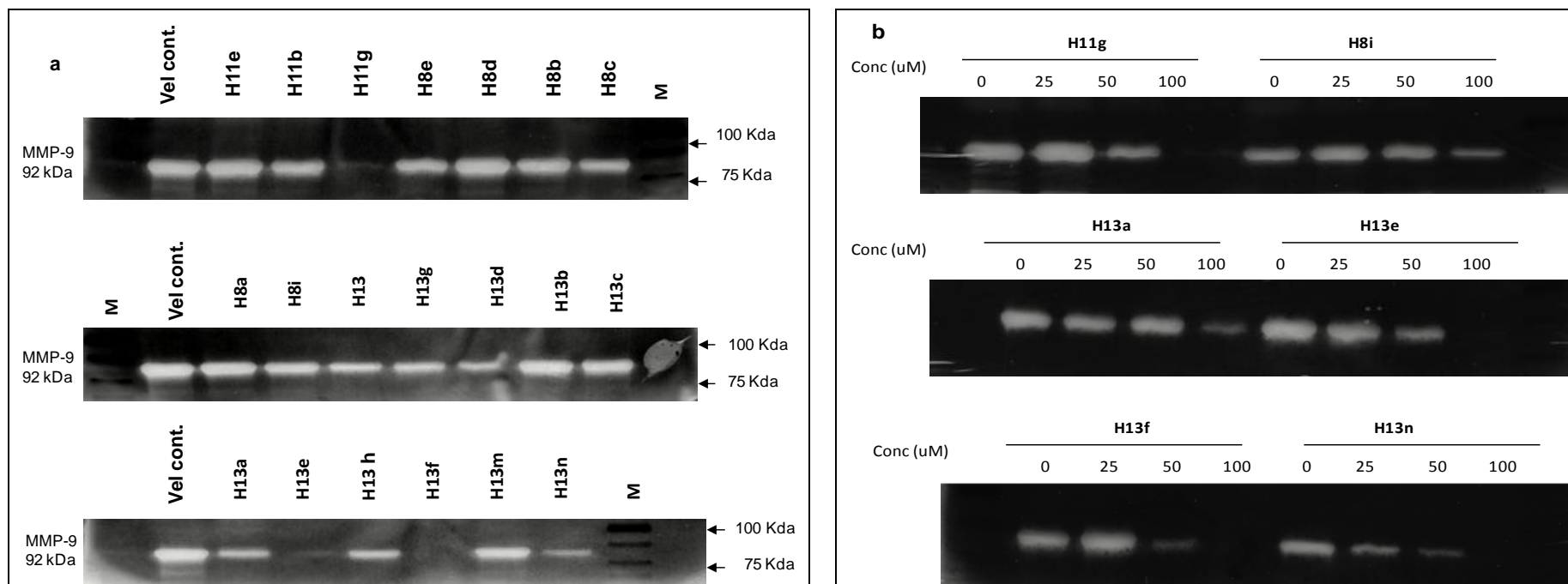


Figure 27. Antiangiogenic potential (MMP expression) of selected synthesized compounds (series **H11**, **H8** and **H13**) on breast cancer cell line (**a**). screening of inhibitory potential of compounds ($IC_{50TP} < 30 \mu M$) (series **H11**, **H8** and **H13**) towards PMA induced MMP-9 expression after 24 h treatment at $100 \mu M$ (**b**). suppressive effects of selected compounds (**H11g**, **H8i**, **H13a**, **H13e**, **H13f** and **H13n**) on PMA-induced MMP-9 expression and their dose response

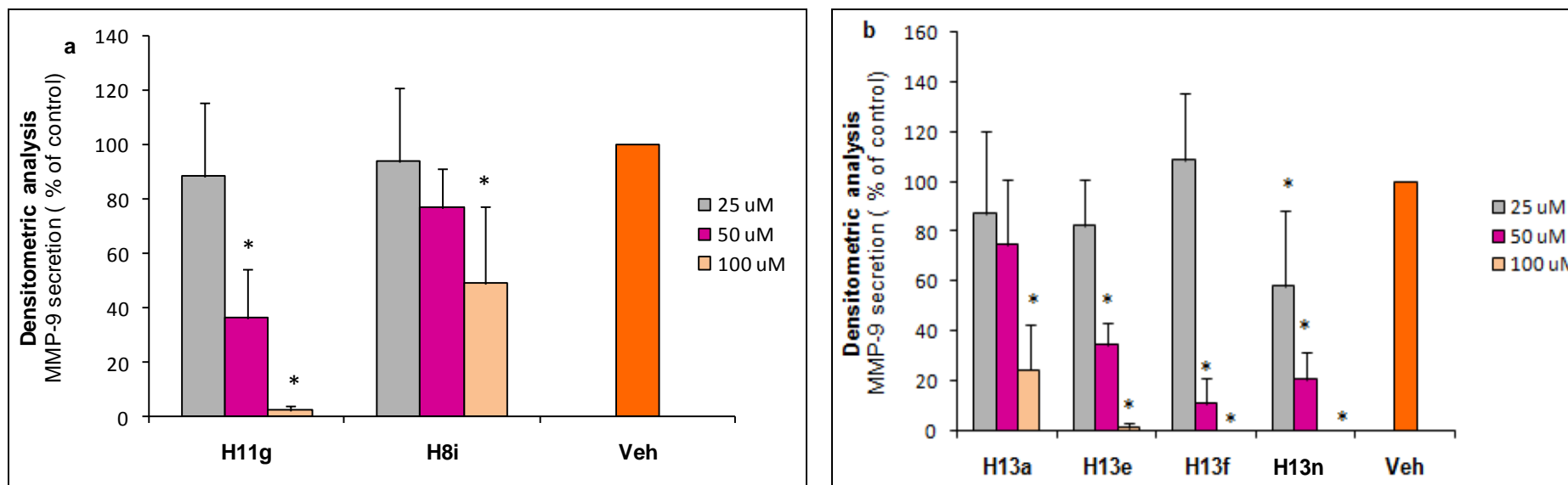


Figure 28. Densitometry analysis of MMP expression of selected synthesized compounds (series **H11**, **H8** and **H13**) on breast cancer cell line (a). compound **H11g** and **H8i**. (b). compound **H13a**, **H13e**, **H13f** and **H13n**. Results are presented as means \pm SD; SD denoted by error bars (Experiments carried out at least in triplicate). * $p < 0.05$.

- Compounds inhibited VEGF secretion and expression in breast cancer cell

Several studies suggested that TP and its metabolite 2DDR stimulate the secretion and/or expression of the angiogenic molecules VEGF and induce endothelial cell migration. The effect of compounds **H5bii**, **H5bxvii** and **H5bxix** on vascular endothelial growth factor (VEGF) protein secretion was determined by treating MDA-MB-231 cells for 24 hours either without the test compounds or in the presence of the indicated dose of the compounds (10, 25, 50, 100, and 200 μ M). The expression of VEGF protein levels in the conditioned cell medium was measured using an enzyme linked immunosorbent assay. As shown in Figure 29, all compounds at dose ranging between 25 μ M to 200 μ M markedly inhibited VEGF expression compared to vehicle control ($p < 0.05$). The secretion of the protein normalized to the corresponding number of cells seeded after treatment with **H5bxix** was inhibited in a dose dependent manner (Figure 29a).

Similarly, an attempt to study the effects of the synthesized compounds **H11g**, **H8i**, **H13a**, **H13e**, **H13f** and **H13n** on VEGF expression in the breast cancer cells was conducted using the ELISA technique. After a 24-hour treatment of this cell line with the test compounds at concentrations of 10, 25, 50 and 100 μ M, the assay revealed a significant suppression of VEGF protein secretion ($p < 0.05$) (Figure 29b and 29c).

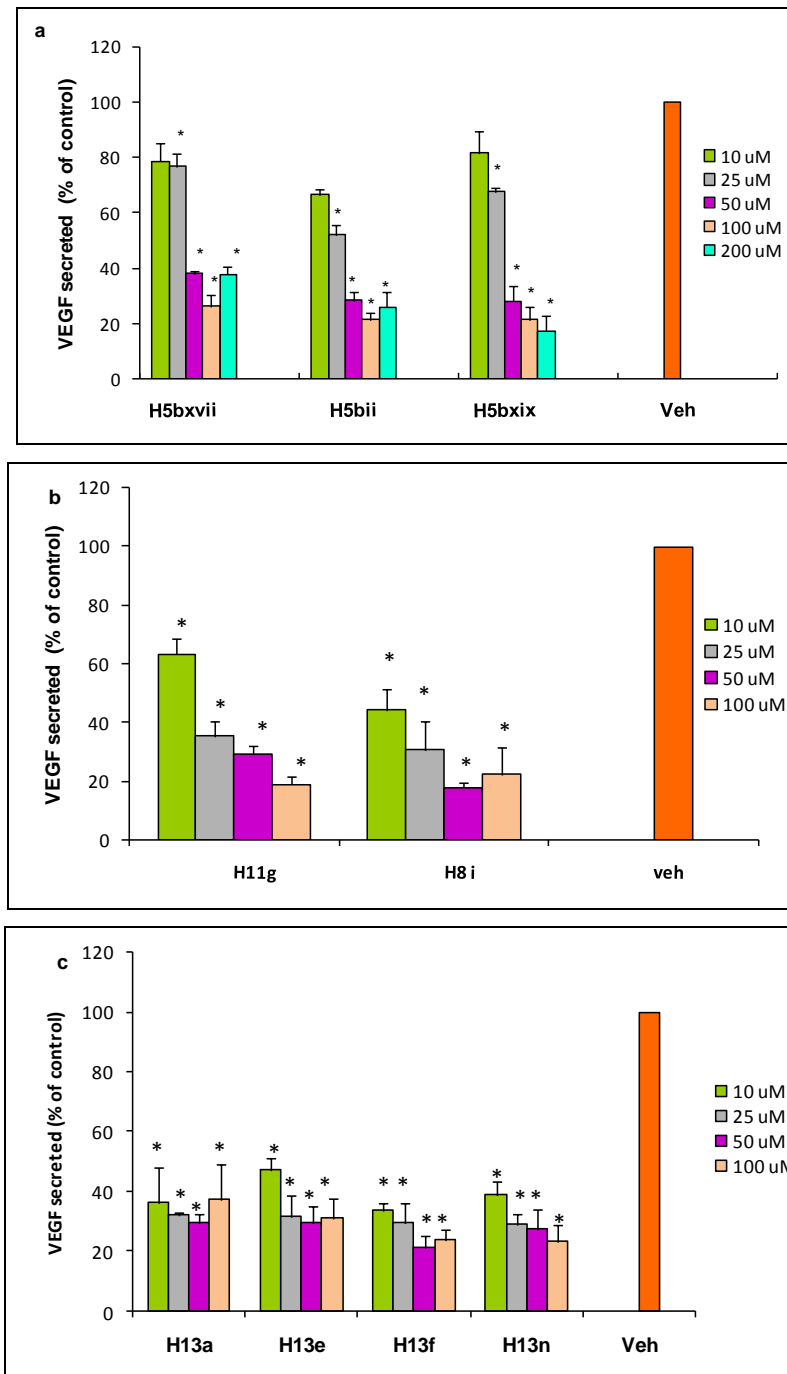


Figure 29. Antiangiogenic potential (VEGF expression) of selected synthesized compounds on breast cancer cell line (a). effect of selected compounds (**H5bxix**, **H5bii** and **H5bxvii**) on VEGF expression in indicated dose on MDA-MB-231 cells after 24 h treatment. (b and c). effect of selected compounds (**H11g**, **H8i**, **H13a**, **H13e**, **H13f** and **H13n**) on VEGF expression in indicated dose on MDA-MB-231 cells after 24h treatment. Results are presented as means \pm SD; SD denoted by error bars (Experiments carried out at least in triplicate). * $p < 0.05$.

7.2.2 Antimetastasis activity determination

- Compounds did not inhibit *in vitro* breast cancer cell invasion and induce IL-8 secretion and expression in breast cancer cell

The significant inhibitory effect against MMP-9 and VEGF expression demonstrated by some of the test compounds encouraged further exploration of other biological effects of the active compounds. To correlate the functional relevance of MMP-9 expression and cell invasion, the invasive capability of MDA-MB-231 cells that were treated with different doses of compounds **H5bii**, **H5bxvii** and **H5bxix** was investigated. The *in vitro* effect of the selected compounds on cell migration was assessed by using Matrigel-coated, porous polycarbonate filters. Figure 30a indicated that compounds were not able to suppress FBS-induced invasiveness of MDA-MB-231 even at 200 μ M, thus demonstrating that the test compounds did not have *in vitro* antiinvasive effects.

The inability to exhibit anti-invasive effects by compounds **H5bii**, **H5bxvii** and **H5bxix** prompted further exploration of IL-8 expression *via* enzyme linked immunosorbent assay. The IL-8 protein expression in MDA-MB-231 cells, upon exposure to different concentrations of the test compounds, is shown in Figure 30b. Pre-treatment with the test compounds for 24 hour was found to gradually induce IL-8 protein expression in a dose-dependent manner. Therefore, the study concerning the exploration of antimetastatic properties and IL-8 protein expression was not attempted for compounds from other series.

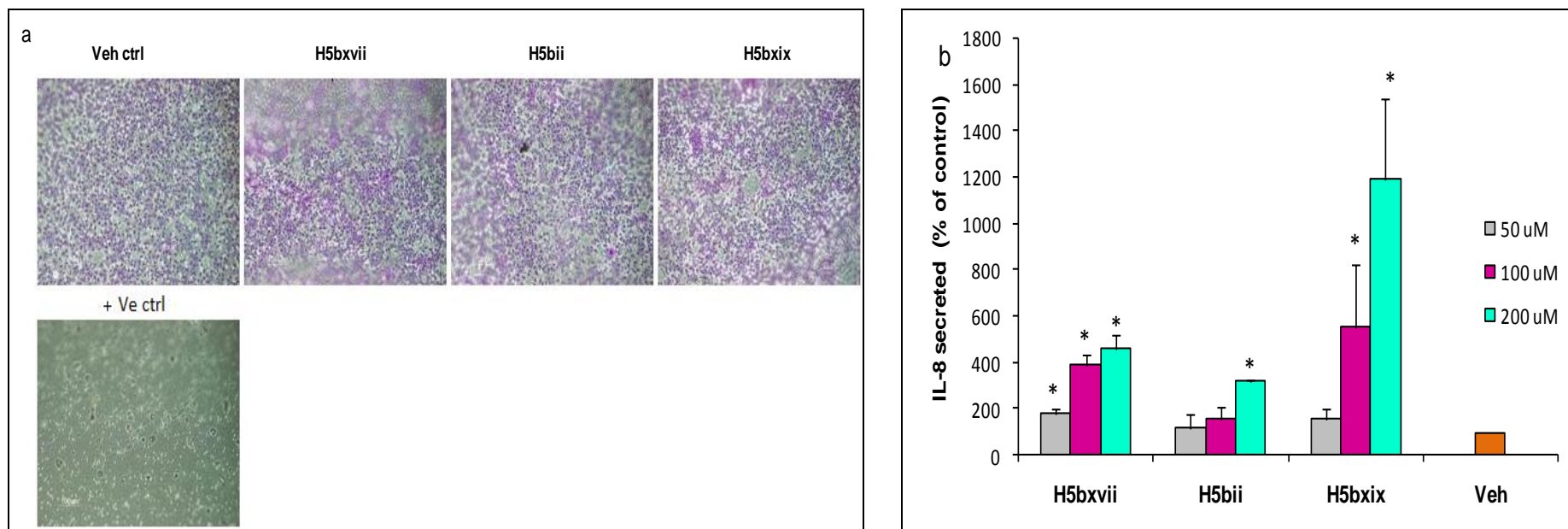


Figure 30. Antimetastasis potential of selected synthesized compounds on breast cancer cell line (**a**). effect of compounds (**H5bxix**, **H5bii** and **H5bxvii**) (at 200 μ M) on MDA-MB-231 cell invasion. (**b**). effect of IL-8 induction on MDA-MB-231 cell after 24 h treatment with different dose of selected compounds (**H5bxix**, **H5bii** and **H5bxvii**). Results are presented as means \pm SD; SD denoted by error bars (Experiments carried out at least in duplicate). * $p < 0.05$.

7.2.3 Antiproliferative activity determination

In order to ascertain the inhibition of MMP-9 and VEGF expression by the compounds on breast cancer cell was not the consequence of its cytotoxic effect, the inhibitory effect of the test compounds on MDA-MB-231 cell growth was determined by means of the MTT assay. Using the analogous basis of selecting compounds for MMP-9 screening, the compounds were chosen for the cell viability assay.

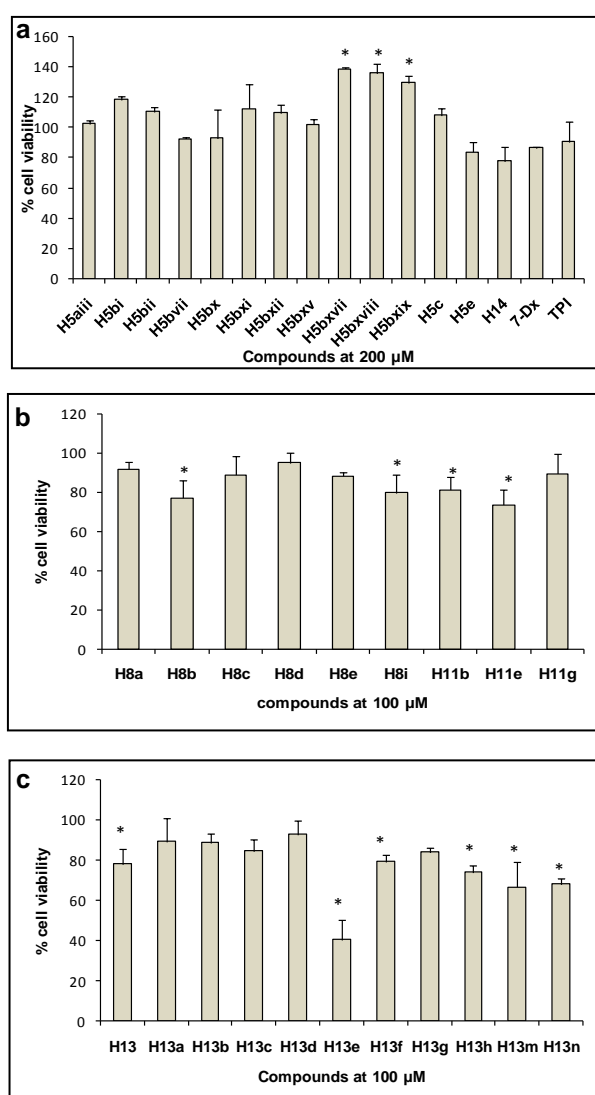


Figure 31. Antiproliferative effect of the test compounds on breast cancer cell line (a). cell viability (%) of MDA-MB-231 cells after 72 h treatment of the test compounds (series H5) exhibiting TP inhibition ($IC_{50} < 30 \mu M$) and reference TP inhibitors (TPI and 7-DX) at concentration of $200 \mu M$. (b and c). cell viability of MDA-MB-231 cells after 72 h treatment of compounds (series H8, H11 and H13) exhibiting TP inhibition ($IC_{50} < 30 \mu M$) at concentration of $100 \mu M$. Results are presented as means \pm SD; SD denoted by error bars (Experiments carried out at least in duplicate). * $p < 0.05$.

As shown in Figure 31, except for some compounds from series **H13**, all compounds exhibited cell viability at around 80-100 % after 72 h exposure. In particular, only compound **H13e**, exhibited attractive cell viability (40.30 ± 10.35 %) compared to vehicle control ($p < 0.05$).

7.3 Discussion

Breast carcinoma is the leading cause of cancer-related death in world. Due to the rapid advancement in cancer diagnosis and therapy options, the life expectancy and survival rate of cancer patients have shown improvement, however, the overall clinical outcome of breast cancer is still unsatisfactory for its highly invasive and metastatic properties. The exact molecular mechanism associated with metastatic nature of this cancer remains largely unclear. However, several studies demonstrated that thymidine phosphorylase (TP), an angiogenic protein, is overexpressed in many solid tumours including breast cancer and it is believed that TP would play a crucial role in breast cancer angiogenesis and metastasis^{228, 229}. TP exerts angiogenesis *via* release of metabolic product 2-deoxy-D-ribose that stimulates the secretion and or expression of many angiogenic factors *viz.* MMP-9, MMP-2, VEGF, IL-8 and others resulting in endothelial cell migration, angiogenesis accompanied by tumour growth and metastasis. Pioneering research in this field has generated several potent TP inhibitors having pyrimidin-2,4-dione as core structure including TPI, which mostly binds at the substrate active site of the target enzyme and exert competitive inhibition with respect to natural substrate.

In this study, thio-oxo analogues of 1,2,4-triazolo[1,5-*a*][1,3,5]triazine and pyrazolo[1,5-*a*][1,3,5]triazine scaffolds were discovered as new TP inhibitors and among these derivatives, compounds **H5bxvii**, **H5bxix**, **H8i**, **H11g**, **H13a**, **H13e**,

H13f and **H13n** exhibited exciting TP inhibition profiles (Figure 19). Therefore, in this section, attempts were made to evaluate the enzyme inhibition kinetics of the most active candidates from each series. In addition, TP-induced anti-angiogenic activity of the synthesized bicyclic TP inhibitors was also investigated. The anti-angiogenesis property of the compounds was assessed *via* their inhibitory potential against the expression of different angiogenic markers in the breast cancer cell line, MDA-MB-231. Moreover, the antimetastatic and antiproliferative activities of these compounds were determined as well.

In the experiments conducted, the most active TP inhibitors **H5bxvii**, **H5bxix**, **H8i**, **H11g** and **H13a** were found to demonstrate mixed type of enzyme inhibition kinetics in the presence of varying concentrations of thymidine and phosphate as the substrates. Therefore, this inhibition pattern suggested that these compounds would interact with the free enzyme (E) and/or enzyme substrate (ES) complex. The values of dissociation constants (K_i and αK_i) (Table 19) indicated that the inhibitor has stronger affinity towards the free enzyme than enzyme substrate complex ($\alpha > 1$). Moreover, the enzyme-inhibitor complex would exhibit lower affinity for substrate compared to free enzyme ($\alpha > 1$) (Scheme 29). The mixed-type inhibitors of enzymes may offer some advantages when compared to compounds interacting at the substrate-binding site. The mixed inhibitors may be safer and more efficacious by overcoming selectivity issues and substrate competition. In addition, by interacting with both free enzyme and enzyme-substrate complex, it could make both E and ES complex non-productive. Indeed, the kinetic results demonstrated that the synthesized compounds exhibited different kinetic pattern compared to **TPI** and **7-DX**. It is interesting to mention that, **TPI** behaved as competitive inhibitors with respect to thymidine¹⁴⁵ as substrate, while **7-DX** exhibited non-competitive inhibition with respect to phosphate

and competitive or mixed type inhibition in presence of variable thymine/thymidine concentration¹⁵⁴. The difference in enzyme inhibition kinetic behaviour with respect to **TPI** and **7-DX** is probably due to the structural modification of the core ring structure *via* the introduction of additional nitrogen atoms and the incorporation of other substituted functional groups around the fused ring system. Therefore, it is believed that the modified molecule might interact with the enzyme differently and consequently demonstrated mixed type inhibition.

The studies that were intended to explore the anti-angiogenic properties showed that the test compounds exhibited inhibitory effect on PMA induced MMP-9 expression of the MDA-MB-231 breast carcinoma cells. Among the selected compounds tested, compounds **H11g**, **H13e**, **H13f** and **H13n** having pyrazolo[1,5-*a*][1,3,5]triazine scaffold, demonstrated higher inhibition against MMP-9 suggesting that pyrazolo[1,5-*a*][1,3,5]triazine analogues were suitable for better activity than compounds having 1,2,4-triazolo[1,5-*a*][1,3,5]triazine ring. It is noteworthy that with the introduction of substitutions at positions C7 and C8, as evident in series **H13**, the inhibitory activity against MMP-9 was improved compared to mono substituted (at C7 only) pyrazolo[1,5-*a*][1,3,5]triazine analogues (**H11g**). Particularly, the compounds **H13e**, **H13f** and **H13n**, having lipophilic bulky group at the position C8, demonstrated almost complete attenuation of MMP-9 expression and activity at 100 μ M. On the other hand, although compounds **H8i** and **H13a** identified as the most active TP inhibitors ($IC_{50} = 2.95 \mu$ M and 3.82μ M respectively) in their corresponding series, could not establish themselves as the most active candidates in reducing MMP-9 expression. This observation could suggest that MMP-9 expression was not directly correlated to the potency of *in vitro* anti-TP activity. Analysis of gelatine zymography of **TPI** ($IC_{50} = 35$ nM), the most potent TP inhibitor, revealed that under the condition

of PMA stimulation, MMP-9 activity was not significantly inhibited by **TPI** even at concentration of 200 μ M. Analogously, the prototype TP inhibitor, **7-DX** did not demonstrate any inhibition of MMP-9 expression under similar experimental condition as well.

Most reported TP inhibitors including **TPI** are substituted uracil analogues that compete mostly with the substrate binding site of TP. However, based on the structural features, the synthesized compounds represented very unusual TP inhibitors. Therefore, it is assumed that these compounds might interact with a completely different site at the enzyme, which would abrogate the angiogenic (MMP-9) activity of TP. The kinetic behaviour of these compounds also strongly supported this assumption.

Matrix metalloproteinase 9 (MMP-9), a Zn^{+2} dependent endopeptidase, is involved in the breakdown of extracellular matrix surrounding tumour and endothelial cells facilitating tumour cell invasion, migration, and metastasis²³⁰. Several studies have suggested that MMP-9 expression is well correlated with cancer cell migration and invasion and agents that down-regulate MMP-9 have also been demonstrated to inhibit tumour invasion²³¹. In addition, the experimental data provided evidence that in the selected breast cancer cell line, TP was associated with higher levels of activated MMP-9²²⁷. Indeed, in the study, the synthesized compounds being TP inhibitors exhibited down-regulation of the MMP-9 expression and therefore, these compounds would serve as promising anti-angiogenic lead compound for future development.

Another important finding of this study was that selected compounds inhibited VEGF expression in the breast cancer cell line. It is reported that most of the solid tumour

cells overexpressed vascular endothelial growth factor (VEGF) which plays a crucial role in tumour angiogenesis by inducing endothelial cell proliferation, migration and survival²³². As depicted in Figure 29, all compounds irrespective of having 1,2,4-triazolo[1,5-*a*][1,3,5]triazine and pyrazolo[1,5-*a*][1,3,5]triazine scaffold exhibited similar pattern of inhibition profile at higher dose (200 μ M, 100 μ M, and 50 μ M). However, in lower doses (25 μ M and 10 μ M) the inhibition rates among the selected compounds were significantly varied. In addition, compounds **H5bxix**, **H5bii**, **H5bxvii** and **H11g** demonstrated around three fold differences in response between lower and higher dose. It is important to indicate that all these compounds possess an aromatic ring directly attached to the fused ring system. In contrast, the difference of VEGF suppressive effect exhibited by lower and higher dose was reduced to around 1.5 fold for compound **H8i**, **H13a**, **H13f** and **H13n**. It is noteworthy that for all these compounds the aromatic ring attached with fused ring *via* a methylene bridge. It is important to mention that there is a significant correlation between expression of VEGF and TP in many solid tumours. Various studies suggested that both pro-angiogenic factors share same transcription site^{81, 233}.

Indeed, the synthesized TP inhibitors showed anti-angiogenic property, through inhibition of MMP-9 and VEGF expression. Therefore, it is expected that compounds would inhibit the growth of tumour by cessation of several biomarkers. For example, it could prevent the extracellular matrix degradation essential for cancer cell migration and prevent the formation of new blood vessels leading to cessation of supply of necessary oxygen and nutrients to malignant cells. In addition, these compounds inhibit the TP enzyme activity.

Encouraged by the promising MMP-9 and VEGF expression inhibition potential, an attempt to investigate the invasive ability of **H5bxix**, **H5bii** and **H5bxvii** on the same cell line using a cell invasion assay kit was carried out. However, the results indicated that these compounds were not able to exhibit anti-invasive property even at 200 μ M concentration. To explore further, the effect of IL-8 expression pattern after treating by different doses of compound **H5bxix**, **H5bii** and **H5bxvii** were investigated. Interestingly, the experimental data suggested that the compounds induced the expression of IL-8 in a dose dependent manner.

It was established by a different studies that human mononuclear phagocytes (macrophage cells) regulate the remodelling of extracellular matrix by producing metalloproteinases including MMP-9 as well as the tissue inhibitor of metalloproteinases (TIMP)²³⁴. In addition, several evidences suggested that interleukin and other inflammatory cytokines released from activated T lymphocytes co-ordinately suppress metalloproteinase biosynthesis in macrophages without affecting TIMP production²³⁵. Therefore, from the data presented in this report, it is assumed that the synthesized compounds could activate T lymphocytes resulting in elevated expression of IL-8 leading to attenuation of MMP-9 activity. Furthermore, an increasing number of studies have implicated that cytokines and growth factors including interleukins induce the transcription of many intracellular protein involved in cell cycle progression, apoptosis, and tumour cell invasion^{236, 237}. Hence, it is postulated that the inability of the active test compounds to show anti-invasive potential is a consequence of their induction of IL-8 expression. However, further investigation to explore the exact mechanism in molecular level to explain the diverse biological effects exerted by our compounds is strongly recommended.

The viability study demonstrated that most of these compounds showed weak cytotoxic effects towards breast cancer cell. Some compounds from series **H13** significantly reduced the cell viability at the concentration of 100 μ M. Among them, compound **H13e** bearing lipophilic biphenyl moiety exhibited lowest cell viability. Therefore, these compounds could be used as template compounds for future development of anti-angiogenic agent, which exert inhibition towards angiogenic marker without producing substantial cytotoxicity.

7.4 Summary

In summary, the series of experiments conducted has provided general information on the biological characteristics of the active TP inhibitors. Firstly, it was demonstrated that the new bicyclic fused triazines exhibited mixed type of enzyme inhibition kinetics with respect to both substrates. It is noteworthy that structural modification of lead compound **7-DX** by inserting additional nitrogen atom in core ring structure and incorporating different substituents around the fused ring scaffolds have led to TP inhibitors that could interact with the enzyme in different orientations and exhibit mixed type inhibition kinetics. Secondly, some of the compounds reduced VEGF and MMP-9 expression without exhibiting significant cytotoxicity in breast cancer cell line, which would explain the potential anti-angiogenesis effect of the test compounds. However, **TPI** and **7-DX** did not demonstrate significant antiangiogenic property with respect to attenuation of MMP-9 expression. Therefore, it is postulated that the synthesized compounds bearing different structural features compared to lead compound **7-DX**, may interact distinctly with TP and which is sufficient for suppression of angiogenic property exerted by TP. Interestingly, compounds **H8i** and **H13a** that exhibited 14.5 and 11.2 fold improvement in TP inhibitory property with

respect to **7-DX**, were identified as the most active compounds in their corresponding series. Moreover, compounds **H13e**, **H13f** and **H13n** having di-substituted pyrazolo[1,5-*a*][1,3,5]triazine scaffold, demonstrated antiangiogenic effect by suppressing expression of MMP-9 and VEGF in breast cancer cell line. Since, these compounds showed inhibition towards multiple targets including TP and important angiogenic markers, they might be very useful for the design of efficacious anticancer drugs. However, further studies are necessary to reveal the detail mechanism of action of these compounds at the molecular level.

Chapter 8

Conclusion and Future work

8.1 Conclusion

The derivatives of 1,3,5-triazine and its fused analogues *viz.* 1,2,4-triazolo[1,5-*a*][1,3,5]triazine and pyrazolo[1,5-*a*][1,3,5]triazine are commonly found in several biologically active chemical compounds. Despite a wide spectrum of biological activities exhibited by 1,3,5-triazine derivatives and the compounds having 1,2,4-triazolo and pyrazolo fused triazine scaffolds, no unequivocal study has been conducted to explore their activity associated with TP inhibition. Therefore, the focus of this thesis was to synthesize different types of 1,3,5-triazin-2,4-diones and their fused analogues and investigate their thymidine phosphorylase inhibitory activity. In addition, the inhibitory effect of the selected compounds towards MMP-9 and VEGF expression on breast cancer cell line was also determined. This project also dealt with the exploration of cell migration and relevant IL-8 expression pattern exerted by the target compounds. Moreover, pharmacophore elucidation for new series of TP inhibitors was performed *via* comparative molecular field analysis-based quantitative structure activity relationship studies. The motivation of conducting this whole project came from the gaps of previous works reported in the literature. An increasing number of studies discovered several potent thymidine phosphorylase inhibitors, most of which are derivatives of pyrimidin-2,4-dione with only a few that are fused bicyclic heterocycles having homophthalimide moiety assumed to be essential for binding to the active site of this enzyme. Among the previously disclosed TP inhibitors, **TPI** and **7-DX** have emerged as leading TP inhibitor candidates. Although **TPI** and **7-DX** were identified as prototypic TP inhibitors in long back, further extensive structural exploration by isosteric replacement in different positions of the core structures along with introduction of different substituents has never been synthesized nor have their antiproliferative activity, inhibitory effect of MMP-9, VEGF and IL-8 expression as

well as anti-metastasis activity been investigated before. Collectively, the significant gaps from pioneering studies have led us to investigate the hypothesis that derivatives of 1,3,5-triazin-2,4-dione and its fused analogues *viz.* substituted 1,2,4-triazolo[1,5-*a*][1,3,5]triazines and pyrazolo[1,5-*a*][1,3,5]triazines would exhibit TP inhibitory activity.

To address the hypotheses, a total of eighty-two compounds having the 1,3,5-triazin-2,4-dione, 1,2,4-triazolo[1,5-*a*][1,3,5]triazine and pyrazolo[1,5-*a*][1,3,5]triazine as the core scaffold were synthesized. The use of ring transformation and intra-molecular annulation of appropriately substituted starting material to afford the target compounds was found to be practical and flexible. Undoubtedly, the objective of developing convenient synthetic methodologies to generate target compounds was successfully achieved. Among the different scaffolds synthesized, 5-thioxo-5,6-dihydro-4*H*-[1,2,4]triazolo[1,5-*a*][1,3,5]triazin-7-one and 2-thioxo-2,3-dihydropyrazolo[1,5-*a*][1,3,5]triazin-4(1*H*)-one and their corresponding thiomethyl derivatives showed TP inhibitory activity. Therefore, these findings proved the hypothesis to be true.

In this study, it was revealed that compounds having homophthalimide moiety did not exhibit TP inhibition property which turned out to be inconsistent with previous reported studies¹⁰¹. However, the compounds having keto group (C=O) and thioketo group (C=S) in particular orientation demonstrated inhibitory activity. This study also suggested that the introduction of flexible chain in between aromatic and fused ring system imparted better biological effects towards TP inhibition. In addition, structural modification by incorporating substituents at the both C8 and C7 of pyrazolo[1,5-*a*][1,3,5]triazine exhibited improvement of inhibitory potential as evident in series **H13**. Furthermore, structural diversity of compounds generated based on Craig plot

optimization, suggested that hydrophobicity and electronic effects of substituent are important influencing factors for improvement of inhibition property. The TP active compounds exhibited varying degree of thymidine phosphorylase inhibitory activity with IC_{50} values recorded in the range of 3 - 95 μ M. Compounds **H5bxvii**, **H5bxix**, **H8i**, **H11g**, and **H13a** were identified as most active TP inhibitors in their respective series, exhibiting low micromolar IC_{50} values (IC_{50} = 10.84, 13.09, 2.95, 13.07 and 3.82 μ M respectively).

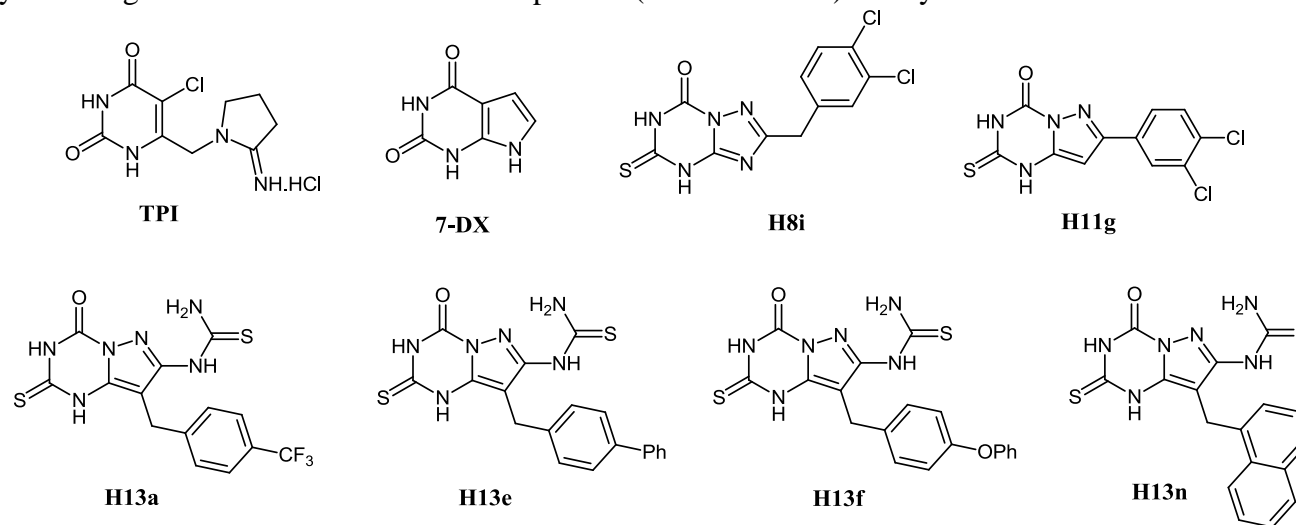
With the aim to clarify the structural basis, the 3D-QSAR studies based on CoMFA method was employed on a series of 1,2,4-triazolo and pyrazolo fused triazine derivatives that showed different extent of anti-TP activity, with IC_{50} values ranging from 2.95 μ M to 95.05 μ M. The models turned out satisfactorily based on the statistical validation results and contour map analysis. Moreover, the excellent predictive abilities of these model observed for the test set of compounds suggested that these CoMFA models could be successfully employed for predicting the IC_{50} values of other TP inhibitors. Furthermore, the CoMFA contour maps provided enough information to understand the structure–activity relationship and identify structural features influencing the inhibitory activity.

In order to investigate the inhibition mechanism of these test compounds, enzyme inhibition kinetics studies of selected compounds were conducted and it was revealed that these compounds exhibited mixed type inhibition against the enzyme in the presence of variable substrates concentrations. It was believed that due to unique structural features, these compounds would interact with the enzyme in different pattern and hence, it demonstrated different enzyme kinetic behaviour compared to **TPI** and **7-DX**. This finding has led to an important assumption that these compounds

would exhibit TP associated anti-angiogenic property *via* interacting in different orientation. To prove these postulations, the experiments were carried out to explore anti-angiogenic effects of the selected compounds and it was found that these compounds demonstrated TP associated antiangiogenic potential as they attenuate the expression of VEGF and MMP-9 in breast cancer cell line without exerting cytotoxicity. Therefore, the hypothetical statements were proven to be true. It is noteworthy that the compounds did not inhibit cell migration as a consequence of their interleukin induction.

Overall, this study has established the fused bicyclic triazolo and pyrazolo triazines and their derivatives to be a new class of potential thymidine phosphorylase inhibitors, which demonstrated mixed type enzyme inhibition kinetics with respect to thymidine and phosphate as substrate. As depicted in Table 20, the difference in kinetic behaviour compared to reference compounds is probably due to structural alteration of core ring structure of synthesised TP inhibitors.

Table 20. A summary of biological activities of reference compounds (**TPI** and **7-DX**) and synthesized TP inhibitors



Cpd	IC ₅₀ (μM)	Anti-TP effect	Antiangiogenic effects ^a		Antiproliferative effects ^b
		Kinetic behaviour	MMP-9 expression (%)	VEGF expression (%)	(% cell viability)
TPI	0.035	competitive	insignificant	-	90.48
7-DX	42.63	competitive/mixed	insignificant	-	86.73
H8i	2.95	mixed	48.97	22.27	79.82
H11g	13.07	mixed	2.29	18.95	89.66
H13a	3.82	mixed	24.58	37.36	89.27
H13e	6.11	mixed	1.61	31.15	40.30
H13f	4.46	mixed	0	23.99	74.10
H13n	4.29	mixed	0	23.29	68.21

^acomparison of antiangiogenic effects (MMP-9 and VEGF expression (%)) with respect to Veh. ctrl (100 %) at 100 μM, ^bcell viability (%) of **TPI** and **7-DX** at 200 μM and others at 100 μM

Although, the synthesized compounds exhibited weaker inhibition activity against TP compared to **TPI**, these inhibitors would provide some added advantages as they demonstrated mixed type of enzyme kinetic behaviour. Firstly, in the presence of sufficiently high concentration of substrate, the effectiveness of mixed inhibitors could not alter significantly in contrast to competitive inhibitors. Secondly, as the mixed inhibitors would bind to both free enzyme and enzyme substrate complex, these inhibitors could make the enzyme non-productive by forming EI and ESI complex. In addition, these synthesized TP inhibitors suppress the expression of some biological markers including MMP-9 and VEGF that are closely associated with angiogenesis whereas the reference compounds did not exhibit significant inhibitory effects (Table 20). Moreover, compound **13e** exhibited significant antiproliferative effect (% cell viability = 40.30) which is better compared to lead compounds, **7-DX** and **TPI**. It is important to mention that compounds having pyrazolo[1,5-*a*][1,3,5]triazine scaffold exhibited better inhibition response against all these assays compared to the compounds bearing 1,2,4-triazolo[1,5-*a*][1,3,5]triazine ring. It was also evident that di-substituted compounds **H13e**, **H13f** and **H13n** having lipophilic bulky group at the position C8, significantly attenuated the expression of angiogenic markers including MMP-9 and VEGF and also exhibited remarkable inhibitory property against TP. Therefore, these compounds would be used as lead for future development of potent TP inhibitors. Moreover, CoMFA model established in this investigation would contribute molecular basis in designing novel fused TP inhibitors. Therefore, this dissertation demonstrated the foundation for further design and optimization of fused-ring TP inhibitors that may lead to development of chemotherapeutic agents, as it can overcome the pathological effects of TP such as tumour progression *via* angiogenesis.

8.2 Future work

Although this comprehensive study has shown some promising results, there is still room for further improvement of this project and thus the following studies need to be investigated.

Undoubtedly, this study has revealed that the compounds having 1,2,4-triazolo[1,5-*a*][1,3,5]triazine and pyrazolo[1,5-*a*][1,3,5]triazine exhibited anti-TP and anti-angiogenic effects. However, most of the compounds did not demonstrate antiproliferative property except for compound **H13e** that showed around 40 % cell viability at 100 μ M. It is assumed that the bi-phenyl group of compound **H13e** attached at the position C8 of fused ring is responsible for this property. Therefore, further structural modification of this compound by introducing bulky lipophilic groups with an aim to generate TP inhibitor with antiproliferative potential is crucial.

In order to investigate the anti-angiogenic effects, the synthesized compounds were found to inhibit the expression and/or activity of MMP-9 and VEGF. However, the molecular mechanism through which these TP inhibitors exert these biological effects is still largely unclear. Therefore, to identify the detailed signal transduction cascades inhibited by the synthesized TP inhibitors, more research needs to be performed. In addition, to prove potency of the synthesized compounds in angiogenesis, *in vivo* experiments of angiogenesis and detailed exploration of inhibitory potential toward other angiogenic biomarkers are still to be revealed. This knowledge would help rational development of strategies to inhibit the protumoral actions of TP.

In this study, the identified mixed type TP inhibitors, which are structurally entirely unrelated to the natural substrates of the enzyme, has opened up interesting perspectives for further development of new classes of TP inhibitors. As part of the lead finding and optimization program in our laboratory, continuous efforts with a view to enhancing the biological activity, will be employed to modify the lead compounds **H14** ($IC_{50} = 26.30 \mu\text{M}$). In addition, it is believed that introduction of thiourea chain in compound **H14** would generate some potent inhibitors of TP. Taking these hypotheses into consideration, a series of compounds is proposed to be synthesized where flexibility can be made by using different R group to generate a range of libraries and thereafter it will be evaluated for the TP inhibitory activity to explore better lead in drug design against TP (Figure 32). Such compounds may also be employed to reveal TP associated angiogenesis and other biological processes such as apoptosis and tumour cell metastasis.

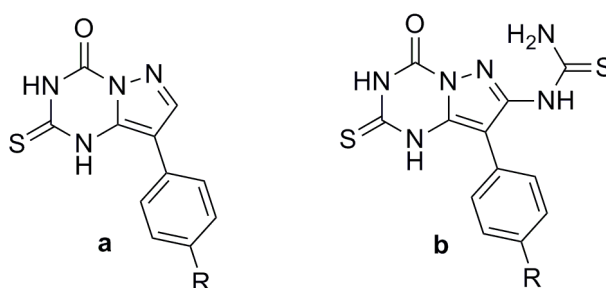


Figure 32. Structures of proposed compounds

Structures could be further improved by another QSAR study using a wider range of molecular properties. The results obtained after QSAR study could be helpful in designing new series of fused analogues as novel TP inhibitors. The study can be extended with advanced techniques including CoMSIA, 3-D-QSAR method, and docking *etc* which may further lead to design of novel and potent TP inhibitors having better therapeutic index with low toxicity, higher oral bioavailability and solubility.

It is very interesting and encouraging that the most potent TP inhibitor, TPI has now entered clinical trials in the combination with TFT, designated as TAS-102¹⁵⁰. The outcome of these studies will be extremely helpful to establish the clinical relevance of a potent TP inhibitor. Similarly, it is essential to establish the synergism of our synthesized compounds with TFT for applications in cancer therapy.

The potential use of TP inhibitors is not limited to cancer as TP is also involved in many inflammatory diseases, such as rheumatoid arthritis⁸². Therefore, it is worth-trying to explore the potential effects in TP associated inflammatory diseases using our synthesized compounds.

Chapter 9
Materials and Methods

9.1 Chemistry

9.1.1 Reagents and general methods

All reagents were purchased from Sigma-Aldrich or Alfa Aesar and were used without further purification. Melting points were determined on a Gallenkamp melting point apparatus and were uncorrected. The ^1H NMR and ^{13}C NMR spectra were recorded on a Bruker DPX-300 spectrometer at 300 MHz and 75 MHz respectively using $\text{DMSO-}d_6$ as solvent and TMS as internal standard. Mass spectra were obtained on a Finnigan MAT LCQ LC-MS mass spectrometer using electrospray ionization (ESI) mode. Reactions were monitored by TLC on silica gel (60 F₂₅₄) coated aluminium plate.

- HPLC

HPLC analysis was carried out using Hewlett-Packard series 1050 HPLC system equipped with a HP-1050 quaternary pump, a degasser, diode array detector, a HP-1100 autosampler, and a LiChrosorb reversed phase C18 (5 μm) column (4.6 \times 250 mm). All the samples were prepared by dissolving them in methanol to form a 25 $\mu\text{g/ml}$ solution. The analysis was performed at 30°C using isocratic elution with a suitable mobile phase, consisting of water (50%) and acetonitrile (50%) (method A) or methanol (50%) and acetonitrile (50%) (method B). The total run time was set for 20 minutes. In addition, another two gradient elution methods (method C and D) were adopted to determine the purity of compounds. In method C, the analysis was started with a mobile phase composition of 95:5 (aqueous phase (0.1% acetic acid):acetonitrile) and it gradually changed to 60:40 within first 10 min. For the next 30 min, the composition of the mobile phase was changed from 60:40 to 0:100.

Alternatively, another mobile phase system composed of water (with 0.1 % formic acid) and acetonitrile (with 0.1 % formic acid) was selected for method D. In this method, the experiment started using mobile phase composition of 95:5 (aqueous phase :acetonitrile) which gradually changed to 0:100 within 7 minutes. The flow rate was set at 1 ml/ minute and the ultraviolet detection was made at wavelength 254 nm. The injection volume was 5 μ L.

9.1.2 General procedure for the synthesis of 1,3,5-triazin-2,4-dione (H1a-H1f)

- General procedure for the synthesis of 4,6-diamino-[1,3,5]-thiadiazine-2-thione (80)²⁰³

In well-stirred suspension of cyanoguanidine (8.4 g, 10 mmol) in acetone (70 ml), potassium hydroxide pellets (11 g, 20 mmol) and carbon disulphide (6.64 ml, 11 mmol) were added at -10 to -5 °C. The temperature was then allowed gradually to rise to 15 °C and stirring was continued for another 3.5 hours. The yellow coloured intermediate dipotassium ω -cyanoguanidinodithiocarbonate was filtered off, washed with acetone and dried. This intermediate was dissolved in water, and acetic acid added to make it neutral. The precipitated product was filtered off, washed with water, and dried.

Yield 55%; mp > 300°C; ¹H NMR (300 MHz, DMSO-*d*6): δ 8.03 and 8.30 (two s, 2H, NH₂), 8.67 and 8.81 (two s, 2H, NH₂); ¹³C NMR (75 MHz, DMSO-*d*6): δ 162.6 (C-4), 171.8 (C-6), 191.6 (C-2).

- General procedure for the synthesis of 1-methyl-4,6-diamino-1,3,5-triazin-2(1*H*)-thione (**81**)²⁰⁵

4, 6-Diamino-2*H*-1,3,5-thiadiazine-2-thione (1.6 g, 10 mmol) was suspended in dimethylformamide (DMF, 5 ml). To it, methylamine (1.3ml, 10 mmol) was added and stirred the reaction mixture for 30 minutes. 10 ml of 2M NaOH solution was then added and allowed it to stand at room temperature for 1 day. The precipitated product was filtered, washed well with water and dried.

Yield 44%; mp 275°C; ¹H NMR (300 MHz, DMSO-*d*6): δ 3.68 (s, 3H, NMe), 6.85 and 7.11 (two s, 2H, NH₂), 7.55 (s, 2H, NH₂); ¹³C NMR (75 MHz, DMSO-*d*6): δ 35.5 (NMe), 158.1 (C-6), 161.1 (C-4), 184.4 (C-2).

- General procedure for the synthesis of 1-methyl-6-thioxo-1,3,5-triazin-2,4-dione (**82**)²⁰⁴

A suspension of 1-methyl-4,6-diamino-1,3,5-triazin-2-thione (314 mg, 2 mmol) in 50 ml of 6N hydrochloric acid on heating under reflux for 2 hours gave a clear solution, which upon cooling deposited a solid. The acidic filtrate obtained after removing the solid, on concentration and cooling afforded another solid, which upon recrystallization from water gave 1-methyl-6-thioxo-1,3,5-triazin-2,4-dione.

Yield 15%; mp 272-270°C (water); ¹H NMR (300 MHz, DMSO-*d*6): δ 3.68 (s, 3H, NMe), 11.86 (s, 1H, NH), 12.55 (s, 1H, NH); ¹³C NMR (75 MHz, DMSO-*d*6): δ 35.8 (NMe), 147.0 (C-4), 148.9 (C-2), 179.4 (C-6).

- General procedure for the synthesis of 1-methyl-6-methylthio-1,3,5-triazin-2,4-dione (**83**)²⁶

To a stirred solution of 1-methyl-6-thio-1,3,5-triazin-2,4-dione (1.6 g, 10 mmol) in 8 ml of 2.5 M NaOH, iodomethane (933 μ l, 15 mmol) was added, the stirring was continued for 30 minutes. A solid precipitate was afforded by acidification (pH 1-3) with 2.5 M HCl of resulting reaction mixture. The precipitated solid was filtered, washed with ice cold water and recrystallized from water-ethanol system.

Yield 60%; mp 220-222°C (water-ethanol); ¹H NMR (300 MHz, DMSO-*d*6): δ 2.50 (s, 3H, SMe), 3.27 (s, 3H, NMe), 11.42 (s, 1H, NH); ¹³C NMR (75 MHz, DMSO-*d*6): δ 15.1 (SMe), 30.4 (NMe), 147.0 (C-4), 148.9 (C-2), 179.4 (C-6).

- General procedure for the synthesis of 1-methyl-6-substituted-1,3,5-triazin-2,4-dione (**H1a- H1f**)

In methanolic (30 ml) suspension of 1-methyl-6-methylthio-1,3,5-triazin-2,4-dione (865 mg, 5 mmol) , a secondary amine (10 mmol) or a primary amine (7.5 mmol) was added. The reaction mixture was heated under reflux for 3-5 hours. The products were obtained by removing the solvent under vacuum and recrystallizing the residue with ethanol.

1-Methyl-6-(methylamino)-1,3,5-triazin-2,4(1H,3H)-dione (H1a)

Yield 66%; mp 305-307°C (ethanol); ESI-MS *m/z* 157.0 (M-1)⁺; ¹H NMR (300 MHz, DMSO-*d*6): δ 2.78 (s, 3H, NHMe), 3.16 (s, 3H, NMe), 7.63 (s, 1H, NHMe), 10.65 (s, 1H, NH). ¹³C NMR (75 MHz, DMSO-*d*6): δ 28.4 (NHMe), 28.9 (NMe), 151.4 (C-2), 155.0 (C-4), 156.7 (C-6).

6-(Ethylamino)-1-methyl-1,3,5-triazin-2,4(1H,3H)-dione (H1b)

Yield 76%; mp 263-265°C (Ethanol); ESI-MS m/z 170.9 (M-1)⁺; ¹H NMR (300 MHz, DMSO-*d*6): δ 1.11 (t, 3H, CH₂CH₃, J = 7.1 Hz), 3.16 (s, 3H, NMe), 3.32 (q, 2H, CH₂, J = 6.9 Hz), 7.61 (s, 1H, NHCH₂), 10.62 (s, 1H, NH). ¹³C NMR (75 MHz, DMSO-*d*6): δ 14.8 (Me), 28.39 (NMe), 36.7 (NHCH₂), 151.5 (C-2), 155.1 (C-4), 156.1 (C-6).

6-(Benzylamino)-1-methyl-1,3,5-triazin-2,4(1H,3H)-dione (H1c)

Yield 53%; mp 297-298°C (Ethanol); ESI-MS m/z 233.1 (M-1)⁺; ¹H NMR (300 MHz, DMSO-*d*6): δ 3.25 (s, 3H, NMe), 4.53 (s, 2H, -CH₂Ph), 7.21-7.33 (m, 5H, Ph), 8.20 (s, 1H, NHCH₂), 10.71 (s, 1H, NH). ¹³C NMR (75 MHz, DMSO-*d*6): δ 28.6 (NMe), 44.7 (NHCH₂), 127.4 (C'4), 127.6 (C'2 & C'6), 128.7 (C'3 & C'5), 139.1 (C'1), 151.5 (C-2), 155.1 (C-4), 156.7 (C-6).

6-(Cyclopropylamino)-1-methyl-1,3,5-triazin-2,4(1H,3H)-dione (H1d)

Yield 61%; mp 259°C (Ethanol); ESI-MS m/z 183.3 (M-1)⁺; ¹H NMR (300 MHz, DMSO-*d*6): δ 0.61-0.71 (m, 4H, two H-2' and H-3'), 2.78 (s, 1H, H-1'), 3.13 (s, 3H, NMe), 7.53 (s, 1H, NH), 10.69 (s, 1H, NH). ¹³C NMR (75 MHz, DMSO-*d*6): δ 6.5 (C-2' and 3'), 25.3 (C-1'), 26.6 (NMe), 151.4 (C-2), 155.1 (C-4), 157.8 (C-6).

1-Methyl-6-(morpholino)-1,3,5-triazin-2,4(1H,3H)-dione (H1e)

Yield 85%; mp 240-242°C (Ethanol); ESI-MS m/z 212.9 (M-1)⁺; purity > 95%; ¹H NMR (300 MHz, DMSO-*d*6): δ 3.21 (s, 3H, NMe), 3.32-3.36 (m, 4H, two H-2' and H-6'), 3.65-3.68 (m, 4H, two H-3' and H-5'), 10.98 (s, 1H, NH); ¹³C NMR (75 MHz, DMSO-*d*6): δ 34.7 (NMe), 48.7 (C-2' and C-6'), 66.0 (C-3' and C-5'), 153.0 (C-2), 154.9 (C-4), 161.7 (C-6).

1-Methyl-6-(pyrrolidin-1-yl)-1,3,5-triazin-2,4(1*H*,3*H*)-dione (H1f)

Yield 23%; mp 220°C (Ethanol); purity > 95%; ¹H NMR (300 MHz, DMSO-*d*₆): δ 1.81-1.85 (m, 4H, two H-3' and H-4'), 3.26 (s, 3H, NMe), 3.49-3.52 (m, 4H, two H-2' and 2H-3') 10.63 (s, 1H, NH). ¹³C NMR (75 MHz, DMSO-*d*₆): δ 25.6 (C-3' and C-5'), 33.8 (NMe), 50.6 (C-2' and C-5'), 153.0 (C-2), 154.7 (C-4), 158.9 (C-6).

9.1.2 General procedure for the synthesis of 1,2,4-triazolo[1,5-*a*][1,3,5]triazine (H2-H6)

- General procedure for the synthesis of 3(5)-amino-1,2,4-triazoles (**87**)

Method A ^{206,207} In well-stirred suspension of *s*-methylisothiourea sulfate (2.8 g, 10 mmol) in 20 ml 1M NaOH, corresponding hydrazides (3.0 g, 20 mmol) was added at 0 °C. The stirring was continued for 48 hours at room temperature. The reaction mixture was allowed to heat at 50 °C for another 3 hours. After cooling, the precipitated product was filtered, washed with ice cooled water and recrystallized from water. The obtained (het)arylamidoguanidines (5mmol) were heated with fixed microwave irradiation power (100W) using water (10 ml) as solvent for 3 to 5 minutes. After cooling, the precipitated products were filtered, washed with ice-cold water and recrystallized.

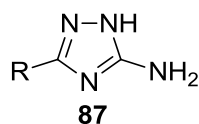
Method B: A mixture of aryl acid chloride (10 mmol) and aminoguanidine HCl (20 mmol) were heated in an oil bath for 20 minutes to at 180-185 °C. After cooling, water (25 ml) was added with continuous stirring to make a homogeneous suspension. To it, 2 ml 5 M NaOH was added to basify the suspension. The precipitated products ((het)arylamidoguanidines) was filtered, washed with water and dried. The (het)arylamidoguanidines (5 mmol) were treated with microwave irradiation power

(100W) for 5 to 8 minutes in water. After cooling, the precipitated products were filtered off, washed with ice-cold water and recrystallized by ethanol or aqueous-ethanol.

Method C ²⁰⁸ To a stirred suspension of 3-amino-5-sulfanyl-1,2,4-triazole 1 (1.8 g, 15.5 mmol) in DMF (25 ml), Et₃N (2.2 ml, 17 mmol) was added drop wise and stirred for few minutes. To this mixture, benzyl bromide and its longer chain analogue (17 mmol) was added, and the mixture was stirred at room temperature for 4 hours. The resulting reaction mixture was partitioned between ethyl acetate (150 ml) and water (100 ml). The organic layer was washed with brine (50 ml), dried by using magnesium sulphate (MgSO₄). The resulting organic layer was concentrated under reduced pressure and recrystallized with suitable solvent.

Method D ²⁰⁶: To a stirred solution of dimethyl-N-cyanodithiocarbonimidate (2.9 g, 20 mmol) in methanol (20 ml), hydrazine hydrate (98%, 1.1 ml, 22 mmol) was added. The stirring was continued for 5 hours at 40 °C. After stirring, the solvent was removed under vacuum. The solid was recrystallized from ethyl acetate.

- Synthesis of 3(5)-amino-1,2,4-triazoles and their ¹H NMR spectral data (* signals of the minor tautomeric form 3-amino-1,2,4-triazoles).



3-(Methylthio)-1H-1,2,4-triazole-5-amine (87a)

Yield 68 % (method D); mp 123-125°C (EA); ¹HNMR (300 MHz, DMSO-*d*₆): δ 2.42 (s, 3H, SMe), 5.29* and 6.04 (s, 2H, NH₂), 11.91 and 12.67* (s, 1H, NH).

3-Phenyl-1*H*-1,2,4-triazole-5-amine (87b)

Yield 97 % (method A); mp 186-187 °C (water); ¹H NMR (300 MHz, DMSO-*d*₆): δ 5.35* and 6.11 (two s, 2H, NH₂), 7.31-7.90 (m, 3H, H-3', H-4' and H-5'), 7.91 (d, 2H, H-2' and H-6', *J* = 7.1 Hz), 12.08 and 13.24* (two s, 1H, NH).

3-(3-Nitrophenyl)-1*H*-1,2,4-triazole-5-amine (87c)

Yield 94 % (method B); mp 268 °C (water-ethanol); ¹H NMR (300 MHz, DMSO-*d*₆): δ 5.47* and 6.26 (two s, 2H, NH₂), 7.73 (t, 1H, H-5', *J* = 7.9 Hz), 8.21 (dd, 2H, H-4' and H-6', *J* = 8.2, 1.5 Hz), 8.65 (s, 1H, H-2'), 12.34 and 13.60* (two s, 1H, NH).

3-(3-(Trifluoromethyl)phenyl)-1*H*-1,2,4-triazole-5-amine (87d)

Yield 93 % (method B); mp 208-210 °C (water-ethanol); ¹H NMR (300 MHz, DMSO-*d*₆): δ 5.45* and 6.23 (two s, 2H, NH₂), 7.62-7.77 (m, 2H, H-4' and H-5'), 8.14-8.25 (m, 2H, H-2' and H-6'), 12.29 and 13.50* (two s, 1H, NH).

3-(3-Chlorophenyl)-1*H*-1,2,4-triazole-5-amine (87e)

Yield 93 % (method B); mp 192 °C (water-ethanol); ¹H NMR (300 MHz, DMSO-*d*₆): δ 5.38* and 6.16 (two s, 2H, NH₂), 7.38-7.47 (m, 2H, H-4' and H-5'), 7.83-7.7.87 (m, 2H, H-6' and H-2'), 12.20 and 13.35* (two s, 1H, NH).

3-(3-Bromophenyl)-1*H*-1,2,4-triazole-5-amine (87f)

Yield 92 % (method B); mp 199-200 °C (water-ethanol); ¹H NMR (300 MHz, DMSO-*d*₆): δ 5.40* and 6.17 (two s, 2H, NH₂), 7.38 (t, 1H, H-5', *J* = 7.8 Hz), 7.54 (d, 1H, H-4', *J* = 7.8 Hz), 7.87-7.93 (m, 1H, H-6'), 8.04 (s, 1H, H-2'), 12.22 and 13.35* (two s, 1H, NH).

3-(3-Fluorophenyl)-1*H*-1,2,4-triazole-5-amine (87g)

Yield 92 % (method B); mp 189-190 °C (water-ethanol); ¹H NMR (300 MHz, DMSO-*d*₆): δ 5.42* and 6.19 (two s, 2H, NH₂), 7.14-7.22 (m, 1H, H-5'), 7.46 (dd, 1H, H-4', *J* = 14.2, 7.9 Hz), 7.76 (d, 1H, H-2', *J* = 7.8 Hz), 7.74-7.78 (m, 1H, H-6'), 12.21 and 13.38* (two s, 1H, NH).

3-(3-Methylphenyl)-1*H*-1,2,4-triazole-5-amine (87h)

Yield 80 % (method B); mp 147-148 °C (water-ethanol); ¹H NMR (300 MHz, DMSO-*d*₆): δ 2.34 (s, 3H, Me), 5.45* and 6.09 (two s, 2H, NH₂), 7.15 (d, 1H, H-4', *J* = 7.0 Hz), 7.29 (t, 1H, H-5', *J* = 7.5 Hz), 7.71 (d, 1H, H-6', *J* = 7.6 Hz), 7.75 (s, 1H, H-2'), 12.08 and 13.16* (two s, 1H, NH).

3-(3-Methoxyphenyl)-1*H*-1,2,4-triazole-5-amine (87i)

Yield 83 % (method A); mp 166-168 °C (water); ¹H NMR (300 MHz, DMSO-*d*₆): δ 3.79 (s, 3H, OMe), 5.39* and 6.09 (two s, 2H, NH₂), 6.92 (d, 1H, H-4', *J* = 7.5 Hz), 7.32 (t, 2H, H-5', *J* = 7.9 Hz), 7.44 (s, 1H, H-2'), 7.49 (d, 1H, H-6', *J* = 7.5 Hz), 12.08 and 13.22* (two s, 1H, NH).

3-(3-Cyanophenyl)-1*H*-1,2,4-triazole-5-amine (87j)

Yield 75 % (method B); mp 246-248 °C (water-ethanol); ¹H NMR (300 MHz, DMSO-*d*₆): δ 5.37* and 6.12 (two s, 2H, NH₂), 7.39-8.60 (m, 4H, Ar-H), 12.14 and 13.34* (two s, 1H, NH).

3-(4-Nitrophenyl)-1*H*-1,2,4-triazole-5-amine (87k)

Yield 98 % (method B); mp 263-265 °C (water-ethanol); ¹H NMR (300 MHz, DMSO-*d*₆): δ 5.54* and 6.30 (two s, 2H, NH₂), 8.15 (d, 2H, H-3' and H-5', *J* = 9.0 Hz), 8.29 (d, 2H, H-2' and H-6', *J* = 9.0 Hz), 12.45 and 13.69* (two s, 1H, NH).

3-(4-(Trifluoromethyl)phenyl)-1*H*-1,2,4-triazole-5-amine (87l)

Yield 93 % (method B); mp 207-208 °C (water-ethanol); ¹H NMR (300 MHz, DMSO-*d*₆): δ 5.53* and 6.24 (two s, 2H, NH₂), 7.78 (d, 2H, H-3' and H-5', *J* = 8.1 Hz), 8.13 (d, 2H, H-2' and H-6', *J* = 8.0 Hz), 12.32 and 13.55* (two s, 1H, NH).

3-(4-Chlorophenyl)-1*H*-1,2,4-triazole-5-amine (87m)

Yield 94 % (method B); mp 229-230 °C (water-ethanol); ¹H NMR (300 MHz, DMSO-*d*₆): δ 5.43* and 6.17 (two s, 2H, NH₂), 7.47 (d, 2H, H-3' and H-5', *J* = 8.0 Hz), 7.92 (d, 2H, H-2' and H-6', *J* = 8.5 Hz), 12.18 and 13.33* (two s, 1H, NH)

3-(4-bromophenyl)-1*H*-1,2,4-triazole-5-amine (87n)

Yield 98 % (method B); mp 213-215 °C (water-ethanol); ¹H NMR (300 MHz, DMSO-*d*₆): δ 5.40* and 6.15 (two s, 2H, NH₂), 7.60 (d, 2H, H-3' and H-5', *J* = 8.5 Hz), 7.85 (d, 2H, H-2' and H-6', *J* = 8.5 Hz), 12.17 and 13.33* (two s, 1H, NH).

3-(4-Fluorophenyl)-1*H*-1,2,4-triazole-5-amine (87o)

Yield 95 % (method B); mp 188-189 °C (water-ethanol); ¹H NMR (300 MHz, DMSO-*d*₆): δ 5.36* and 6.13 (two s, 2H, NH₂), 7.23 (t, 2H, H-3' and H-5', *J* = 8.7 Hz), 7.94 (dd, 2H, H-2' and H-6', *J* = 8.7, 5.6 Hz), 12.10 and 13.24* (two s, 1H, NH).

3-(4-Methylphenyl)-1*H*-1,2,4-triazole-5-amine (87p)

Yield 98 % (method B); mp 209 °C (water-ethanol); ¹H NMR (300 MHz, DMSO-*d*₆): δ 2.32 (s, 3H, Me), 5.32* and 6.08 (two s, 2H, NH₂), 7.20 (d, 2H, H-3' and -5', *J* = 7.8 Hz), 7.80 (d, 2H, H-2' and -6', *J* = 8.1 Hz), 12.02 and 13.14* (two s, 1H, NH).

3-(4-Methoxyphenyl)-1*H*-1,2,4-triazole-5-amine (87q)

Yield 96 % (method B); mp 226 °C (water-ethanol); ¹H NMR (300 MHz, DMSO-*d*₆): δ 3.78 (s, 3H, OMe), 5.27* and 6.04 (two s, 2H, NH₂), 6.96 (d, 2H, H-3' and -5', *J* = 8.4 Hz), 7.83 (d, 2H, H-2' and -6', *J* = 8.8 Hz), 11.94 and 13.02* (two s, 1H, NH).

3-(4-Cyanophenyl)-1*H*-1,2,4-triazole-5-amine (87r)

Yield 76 % (method B); mp 226 °C (water-ethanol); ¹H NMR (300 MHz, DMSO-*d*₆): δ 5.50* and 6.26 (two s, 2H, NH₂), 7.88 (d, 2H, H-3' and H-5', *J* = 8.3 Hz), 8.07 (d, 2H, H-2' and H-6', *J* = 8.5 Hz), 12.37 and 13.60* (two s, 1H, NH).

3-(3,4-Dichlorophenyl)-1*H*-1,2,4-triazole-5-amine (87s)

Yield 94 % (method B); mp 243-245 °C (water-ethanol); ¹H NMR (300 MHz, DMSO-*d*₆): δ 5.43* and 6.21 (two s, 2H, NH₂), 7.67 (d, 1H, H-5', *J* = 8.4 Hz), 7.86 (dd, 1H, H-6', *J* = 8.4, 1.9 Hz), 8.03 (d, 1H, H-2' *J* = 1.6 Hz), 12.28 and 13.42* (two s, 1H, NH).

3-(3,4-Difluorophenyl)-1*H*-1,2,4-triazole-5-amine (87t)

Yield 92 % (method B); mp 189-190 °C (water-ethanol); ¹H NMR (300 MHz, DMSO-*d*₆): δ 5.41* and 6.19 (two s, 2H, NH₂), 7.41-7.53 (m, 1H, H-5'), 7.70-7.84 (m, 2H, H-2' and -6'), 12.21 and 13.33* (two s, 1H, NH).

3-(4-Bromo-3-methylphenyl)-1*H*-1,2,4-triazole-5-amine (87u)

Yield 96 % (method B); mp 185-187 °C (water-ethanol); ¹H NMR (300 MHz, DMSO-*d*₆): δ 2.39 (s, 3H, Me), 5.35* and 6.11 (two s, 2H, NH₂), 7.58-7.86 (m, 2H, H-5' and -6'), 7.86 (s, 1H, H-2'), 12.15 and 13.27* (two s, 1H, NH).

3-(Benzylthio)-1*H*-1,2,4-triazole-5-amine (87v)

Yield 80 % (method C); mp 85-87 °C (EA-hexane); ¹H NMR (300 MHz, DMSO-*d*₆): δ 4.23(s, 2H, CH₂), 5.19* and 6.08 (s, 2H, NH₂), 7.10-7.47 (m, 5H, Ph), 11.96 and 12.69*(S, 1H, NH).

3-(Phenethylthio)-1*H*-1,2,4-triazole-5-amine (87w)

Yield 82 % (method C); mp 103 °C (EA-hexane); ¹H NMR (300 MHz, DMSO-*d*₆): δ 2.93 (t, 2H, CH₂Ph, *J* = 8.0 Hz), 3.20 (t, 2H, SCH₂, *J* = 7.2 Hz), 5.37* and 6.06 (s, 2H, NH₂), 7.20-7.31 (m, 5H, Ph), 11.95 and 12.66* (s, 1H, NH).

3-((Phenylpropyl)thio)-1*H*-1,2,4-triazole-5-amine (87x)

Yield 82 % (method C); mp 103 °C (EA-hexane); ¹H NMR (300 MHz, DMSO-*d*₆): δ 1.92 (q, 2H, CH₂CH₂CH₂, *J* = 7.4 Hz), 2.67 (t, 2H, CH₂Ph, *J* = 7.5 Hz), 2.94 (t, 2H, SCH₂, *J* = 7.2 Hz), 5.21* and 6.03 (s, 2H, NH₂), 7.14-7.32 (m, 5H, H-4', Ph), 11.90 and 12.66* (s, 1H, NH).

3-(Furan-2-yl)-1*H*-1,2,4-triazole-5-amine (87y)

Yield 95 % (method B); mp 211-212 °C (EA-hexane); ¹H NMR (300 MHz, DMSO-*d*₆): δ 5.39* and 6.17 (two s, 2H, NH₂), 6.46-6.64 (m, 1H, H-4'), 6.65-6.91 (m, 1H, H-3'), 7.56-7.87 (m, 1H, H-5'), 12.15 and 13.28* (two s, 1H, NH).

3-(Thiophen-2-yl)-1H-1,2,4-triazole-5-amine (87z)

Yield 97 % (method B); mp 211-212 °C (water-ethanol); ¹H NMR (300 MHz, DMSO-*d*₆): δ 5.40* and 6.19 (two s, 2H, NH₂), 7.09 (t, 1H, H- 4', *J* = 4.3 Hz), 7.44 (d, 1H, H-3', *J* = 3.1 Hz), 7.47 (d, 1H, H-5', *J* = 5.0 Hz), 12.09 and 13.26* (two s, 1H, NH).

3-(Pyridin-2-yl)-1H-1,2,4-triazole-5-amine (87za)

Yield 92 % (method A); mp 220-221 °C (water-ethanol); ¹H NMR (300 MHz, DMSO-*d*₆): δ 5.45* and 6.22 (two s, 2H, NH₂), 7.37-7.44 (m, 1H, H-5'), 7.86-7.98 (m, 2H, H-3' and H-4'), 8.63-8.64 (m, 2H, H-6'), 12.41 and 13.55* (two s, 1H, NH).

3-(Pyridin-3-yl)-1H-1,2,4-triazole-5-amine (87zb)

Yield 98 % (method A); mp 224-225 °C (water-ethanol); ¹H NMR (300 MHz, DMSO-*d*₆): δ 5.52* and 6.29 (two s, 2H, NH₂), 7.47 (dd, 1H, H-5', *J* = 7.8, 4.8 Hz), 8.25 (dt, 1H, H-4', *J* = 7.9, 1.9 Hz), 8.59 (d, 1H, H-6', *J* = 3.5 Hz), 9.13 (d, 1H, H-2', *J* = 1.4 Hz), 12.34 and 13.51* (two s, 1H, NH).

3-(Pyridin-4-yl)-1H-1,2,4-triazole-5-amine (87zc)

Yield 98 % (method A); mp 272-274 °C (water-ethanol); ¹H NMR (300 MHz, DMSO-*d*₆): δ 5.53* and 6.28 (two s, 2H, NH₂), 7.81-7.83 (m, 2H, H- 3' and H-5'), 8.62-8.63 (m, 2H, H-2' and H-6'), 12.42 and 13.65* (two s, 1H, NH).

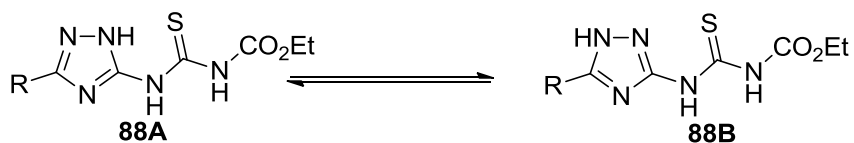
3-Benzhydryl-1*H*-1,2,4-triazole-5-amine (87zd)

Yield 78 % (method B); mp 211-212 °C (water-ethanol); ¹H NMR (300 MHz, DMSO-*d*₆): δ 5.28 (s, 1H, CH), 5.42* and 5.92 (two s, 2H, NH₂), 7.12-7.39 (m, 10H, Ph), 11.75 and 12.62* (two s, 1H, NH).

- General procedure for the synthesis of N-(1,2,4-triazole-3(5)-yl)-N'-carbethoxythiourea (**88**)^{26, 27, 238}

3(5)-amino-5(3)-(het)aryl-1,2,4-triazoles (3 mmol) was suspended in anhydrous dimethylformamide (DMF, 4 ml) and ethoxycarbonyl isothiocyanete (3.3 mmol) was then added . By stirring the mixture for 4.5-5 hours at room temperature, 50-60 ml water was added to it to get more precipitated product. The product was filtered and washed with cold water. The products obtained were recrystallized from ethanol or aqueous-ethanol system.

Table 21. Synthesis of N-(3(5)-aryl-1,2,4-triazol-5(3)-yl)-N'-carbethoxythioureas and their ¹H NMR spectral data



Cpd	R	¹ H NMR (300 MHz, DMSO- <i>d</i> ₆)						
		CO ₂ Et	Ar	tautomer A			tautomer B	
				NH	NH	N(1)H	2NH	N(1)H
88a	CH ₃ S- % yield: 73, mp: 169-170 °C (Ethanol)	1.26, t, 3H, <i>J</i> = 7.1 Hz; 4.22, q, 2H, <i>J</i> = 7.1 Hz	2.51, s, SMe	11.82	12.00	13.79	11.41; 11.52	13.93
88b	C ₆ H ₅ - % yield: 85 mp: 180-181 °C (Ethanol)	1.27, t, 3H, <i>J</i> = 7.1 Hz; 4.24, q, 2H, <i>J</i> = 7.1 Hz	7.51-7.52, m, 3H; 7.97- 7.99, m, 2H	11.87	12.07	13.88	11.67	14.47
88c	3-NO ₂ -C ₆ H ₄ - % yield: 73, mp: 211-212 °C, (Ethanol)	1.29, t, 3H, <i>J</i> = 7.2 Hz; 4.25 q, 2H, <i>J</i> = 7.2 Hz	7.81, br.t, 1H, <i>J</i> = 7.9 Hz; 8.31, br.d, 1H, <i>J</i> = 7.9 Hz; 8.39, d, 1H, <i>J</i> = 7.9 Hz; 8.72, br.s, 1H	11.89	12.13	14.18	11.61	14.81
88d	3-CF ₃ -C ₆ H ₄ - % yield: 78, mp: 239-241 °C, (Ethanol)	1.28, t, 3H, <i>J</i> = 7.0 Hz; 4.25, q, 2H, <i>J</i> = 7.0 Hz	7.67-7.96, m, 2H; 8.16-8.37, m, 2H	11.89	12.13	14.11	11.56	14.69

Table 21. Synthesis of *N*-(3(5)-aryl-1,2,4-triazol-5(3)-yl)-*N'*-carbethoxythioureas and their ¹H NMR spectral data (Contd.)

Cpd	R	¹ H NMR (300 MHz, DMSO- <i>d</i> ₆)						
		CO ₂ Et	Ar	tautomer A			tautomer B	
				NH	NH	N(1)H	2NH	N(1)H
88e	3-Cl-C ₆ H ₄ - % yield: 98, mp: 195-196 °C (Ethanol)	1.30, t, 3H, <i>J</i> = 7.1 Hz; 4.26, q, 2H, <i>J</i> = 7.1 Hz	7.43-7.69, m, 2H; 7.89-8.09, m, 2H	11.91	12.16	14.06	11.58	14.59
88f	3-Br-C ₆ H ₄ - % yield: 89, mp: 196-197 °C (Ethanol)	1.29, t, 3H, <i>J</i> = 7.2 Hz; 4.25, q, 2H, <i>J</i> = 7.2 Hz	7.39-7.58m, 1H; 7.59-7.80, m, 1H; 7.99, d, 1H, <i>J</i> = 7.9 Hz; 8.13, br.s, 1H	11.89	12.14	14.05	11.57	14.57
88g	3-F-C ₆ H ₄ - % yield: 80 mp: 192-193 °C (Ethanol)	1.29, t, 3H, <i>J</i> = 7.0 Hz; 4.26, q, 2H, <i>J</i> = 7.0 Hz	7.21-7.44, m, 1H; 7.48-7.67, m, 1H; 7.73, d, 1H, ³ <i>J</i> _{HF} = 9.8 Hz; 7.85, d, 1H, <i>J</i> = 7.9 Hz	11.89	12.15	14.04	11.58	14.59
88h	3-Me-C ₆ H ₄ - % yield: 87 mp: 175-176 °C (Ethanol)	1.28, t, 3H, <i>J</i> = 7.0 Hz; 4.25, q, 2H, <i>J</i> = 7.0 Hz	2.40, s, 3H, Me; 7.18-7.52, m, 2H; 7.80, d, 1H, <i>J</i> = 7.9 Hz; 7.83, s, 1H	11.88	12.18	13.90	11.57	14.42
88i	3-MeO-C ₆ H ₄ - % yield: 76 mp: 188-189 °C (Ethanol)	1.29, t, 3H, <i>J</i> = 7.2 Hz; 4.25, q, 2H, <i>J</i> = 7.2 Hz	3.85, s, 3H, OMe; 6.94-7.17, m, 1H; 7.33-7.51, m, 1H; 7.51, s, 1H; 7.59, d, 2H, <i>J</i> = 7.5 Hz	11.88	12.16	13.93	11.56	14.48

Table 21. Synthesis of *N*-(3(5)-aryl-1,2,4-triazol-5(3)-yl)-*N'*-carbethoxythioureas and their ¹H NMR spectral data (Contd.)

Cpd	R	1H NMR (300 MHz, DMSO- <i>d</i> ₆)						
		CO ₂ Et	Ar	tautomer A			tautomer B	
				NH	NH	N(1)H	2NH	N(1)H
88j	3-CN-C ₆ H ₄ - % yield: 75, mp: 182-184 °C, (Ethanol)	1.27, t, 3H, <i>J</i> = 7.0 Hz; 4.24 q, 2H, <i>J</i> = 7.0 Hz	7.49-8.71, m, 4H	11.87	12.11	14.12	11.56	14.62
88k	4-NO ₂ -C ₆ H ₄ - % yield: 97, mp: 200-201°C, (Ethanol)	1.28, t, 3H, <i>J</i> = 7.0 Hz; 4.26 q, 2H, <i>J</i> = 7.0 Hz	8.23, d, 2H, <i>J</i> = 8.7 Hz; 8.29-8.48, m, 2H	11.89	12.13	14.25	11.58	14.86
88l	4-CF ₃ -C ₆ H ₄ - % yield: 79, mp: 194-195 °C , (Ethanol-water)	1.28, t, 3H, <i>J</i> = 7.0 Hz; 4.25, q, 2H, <i>J</i> = 7.0 Hz	7.76-8.04, m, 2H; 8.19, d, 2H, <i>J</i> = 8.3 Hz	11.88	12.12	14.13	11.57	14.74
88m	4-Cl-C ₆ H ₄ - % yield: 94 mp: 192-193 °C , (Ethanol)	1.29, t, 3H, <i>J</i> = 7.2 Hz; 4.26, q, 2H, <i>J</i> = 7.2 Hz	7.43-7.77, m, 2H; 8.01, d, 2H, <i>J</i> = 8.3 Hz	11.87	12.16	14.00	11.62	14.55
88n	4-Br-C ₆ H ₄ - % yield: 88, mp: 220-221 °C , (Ethanol)	1.28, t, 3H, <i>J</i> = 7.0 Hz; 4.25, q, 2H, <i>J</i> = 7.0 Hz	7.61-7.85, m, 2H; 7.92, d, 2H, <i>J</i> = 8.3 Hz	11.86	12.13	14.00	11.59	14.55

Table 21. Synthesis of *N*-(3(5)-aryl-1,2,4-triazol-5(3)-yl)-*N'*-carbethoxythioureas and their ¹H NMR spectral data (Contd.)

Cpd	R	1H NMR (300 MHz, DMSO- <i>d</i> ₆)						
		CO ₂ Et	Ar	tautomer A			tautomer B	
				NH	NH	N(1)H	2NH	N(1)H
88m	4-Cl-C ₆ H ₄ - % yield: 94 mp: 192-193 °C , (Ethanol)	1.29, t, 3H, <i>J</i> = 7.2 Hz; 4.26, q, 2H, <i>J</i> = 7.2 Hz	7.43-7.77, m, 2H; 8.01, d, 2H, <i>J</i> = 8.3 Hz	11.87	12.16	14.00	11.62	14.55
88n	4-Br-C ₆ H ₄ - % yield: 88, mp:220-221 °C , (Ethanol)	1.28, t, 3H, <i>J</i> = 7.0 Hz; 4.25, q, 2H, <i>J</i> = 7.0 Hz	7.61-7.85, m, 2H; 7.92, d, 2H, <i>J</i> = 8.3 Hz	11.86	12.13	14.00	11.59	14.55
88o	4-F-C ₆ H ₄ - % yield: 86 mp: 209-210 °C , (Ethanol-water)	1.27, t, 3H, <i>J</i> = 7.0 Hz; 4.24, q, 2H, <i>J</i> = 7.0 Hz	7.22-7.50, m, 2H; 8.01, dd, 2H, <i>J</i> = 8.7 Hz, ³ <i>J</i> _{HF} = 5.3 Hz	11.85	12.10	13.92	11.52	14.44
88p	4-Me-C ₆ H ₄ - % yield: 80 mp: 215-216 °C , (Ethanol)	1.27, t, 3H, <i>J</i> = 7.0 Hz; 4.24, q, 2H, <i>J</i> = 7.0 Hz	7.21-7.46, m, 2H; 7.87, d, 2H, <i>J</i> = 7.9 Hz	11.86	12.13	13.85	11.53	14.24
88q	4-MeO-C ₆ H ₄ - % yield: 84 mp: 212 °C , (Ethanol)	1.27, t, 3H, <i>J</i> = 7.0 Hz; 4.23, q, 2H, <i>J</i> = 7.0 Hz	6.98-7.20, m, 2H; 7.91, d, 2H, <i>J</i> = 8.7 Hz	11.82	12.05	13.77	11.54	14.24

Table 21. Synthesis of *N*-(3(5)-aryl-1,2,4-triazol-5(3)-yl)-*N'*-carbethoxythioureas and their ¹H NMR spectral data (Contd.)

Cpd	R	1H NMR (300 MHz, DMSO- <i>d</i> ₆)						
		CO ₂ Et	Ar	tautomer A			tautomer B	
				NH	NH	N(1)H	2NH	N(1)H
88r	4-CN-C ₆ H ₄ - % yield: 85, mp: 198-200 °C, (Ethanol)	1.27, t, 3H, <i>J</i> = 7.0 Hz; 4.24 q, 2H, <i>J</i> = 7.0 Hz	7.95-8.14, m, 4H	11.87	12.10	14.18	11.56	14.77
88s	3,4 Di Cl- C ₆ H ₃ % yield: 79, mp: 190-191 °C, (Ethanol)	1.28, t, 3H, <i>J</i> = 7.0 Hz; 4.25, q, 2H, <i>J</i> = 7.0 Hz	7.69-7.89, m, 1H; 7.94, dd, 1H, <i>J</i> = 8.3, 1.5 Hz; 8.04- 8.24, m, 1H	11.89	12.12	14.11	11.56	14.62
88t	3,4 Di F- C ₆ H ₃ % yield: 83, mp: 196-198 °C, (Ethanol)	1.29, t, 3H, <i>J</i> = 7.0 Hz; 4.26, q, 2H, <i>J</i> = 7.0 Hz	7.47-7.71, m, 1H; 7.76-8.03, m, 2H	11.87	12.13	14.04	11.60	14.54
88u	3 Me, 4Br C ₆ H ₃ % yield: 88, mp:189-190 °C (Ethanol)	1.28, t, 3H, <i>J</i> = 7.0 Hz; 4.24, q, 2H, <i>J</i> = 7.0 Hz	2.42, s, Me;7.60- 7.83, m, 2H; 7.95, s, 1H	11.87	12.13	13.97	11.55	14.49
88v	C ₆ H ₅ CH ₂ S- %yield:76, mp: 141-142 °C, (Ethanol-water)	1.26, t, 3H, <i>J</i> = 7.0 Hz; 4.22, q, 2H, <i>J</i> = 7.0 Hz	4.35, s, 2H, CH ₂ ;7.23-7.45, m, 5H, Ph	11.79	11.98	13.85	11.55	14.02

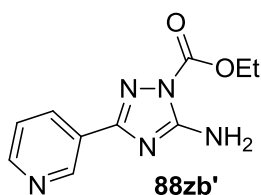
Table 21. Synthesis of *N*-(3(5)-aryl-1,2,4-triazol-5(3)-yl)-*N'*-carbethoxythioureas and their ¹H NMR spectral data (Contd.)

Cpd	R	1H NMR (300 MHz, DMSO- <i>d</i> ₆)						
		CO ₂ Et	Ar	tautomer A			tautomer B	
				NH	NH	N(1)H	2NH	N(1)H
88w	C ₆ H ₅ (CH ₂) ₂ S- % yield: 87, mp: 130-133 °C, (Ethanol)	1.25, t, 3H, <i>J</i> = 7.0 Hz; 4.22, q, 2H, <i>J</i> = 7.0 Hz	2.97, t, 2H, CH ₂ Ph, <i>J</i> = 7.3 Hz; 3.34, m, 2H, SCH ₂ ; 7.19-7.33, m, 5H, Ph	11.81	12.01	13.83	11.56	14.01
88x	C ₆ H ₅ (CH ₂) ₃ S- % yield: 71, mp: 118-120 °C, (Ethanol- water)	1.25, t, 3H, <i>J</i> = 7.0 Hz; 4.22, q, 2H, <i>J</i> = 7.0 Hz	1.95, q, 2H, CH ₂ CH ₂ CH ₂ , <i>J</i> = 7.3 Hz; 2.70, t, 2H, CH ₂ Ph, <i>J</i> = 7.5; 3.08, m, 2H, SCH ₂ ; 7.18, t, 2H, Ph, <i>J</i> = 7.5 Hz; 7.20, d, 1H, Ph, <i>J</i> = 7.2 Hz; 7.28, t, 2H, Ph, <i>J</i> = 7.3 Hz	11.81	11.99	13.80	11.41; 11.53	14.03
88y	2-furyl- % yield: 80, mp: 173 °C, (Ethanol)	1.27, t, 3H, <i>J</i> = 7.0 Hz; 4.24, q, 2H, <i>J</i> = 7.0 Hz	6.59-6.76, m, 1H; 6.91-7.11, m, 1H; 7.77- 7.98, m, 1H	11.78	12.01	14.00	11.70	14.50
88z	2-thiophenyl- % yield: 85, mp: 182-183 °C, (Ethanol)	1.27, t, 3H, <i>J</i> = 7.0 Hz; 4.24 q, 2H, <i>J</i> = 7.0 Hz	7.07-7.33, m, 1H; 7.47-7.88, m, 2H	11.85	12.07	13.90	11.47- 11.55	14.45
88za	2-pyridyl- % yield: 84, mp: 168-170 °C, (Ethanol)	1.26, t, 3H, <i>J</i> = 7.0 Hz; 4.22 q, 2H, <i>J</i> = 7.0 Hz	7.48-7.60, m, 1H; 7.95-8.07, m, 2H; 8.71, d, <i>J</i> = 3.7	11.81	12.09	14.06	11.52	14.76

Table 21. Synthesis of *N*-(3(5)-aryl-1,2,4-triazol-5(3)-yl)-*N'*-carbethoxythioureas and their ¹H NMR spectral data (Contd.)

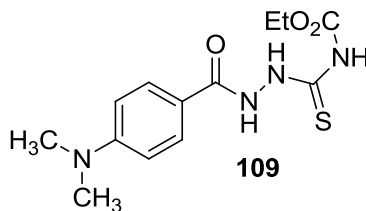
Cpd	R	1H NMR (300 MHz, DMSO- <i>d</i> ₆)						
		CO ₂ Et	Ar	tautomer A			tautomer B	
				NH	NH	N(1)H	2NH	N(1)H
88zb	3-pyridyl- % yield: 50, mp: 262-264 °C, (Ethanol)	1.27, t, 3H, <i>J</i> = 7.0 Hz; 4.24 q, 2H, <i>J</i> = 7.0 Hz	7.45-7.65, m, 1H; 8.30, d, 1H, <i>J</i> = 7.9; 8.59-8.74, m, 1H; 9.14, d, 1H, <i>J</i> = 1.5	11.87	12.11	14.10	11.56	14.66
88zd	(Ph) ₂ CH- % Yield:77, mp:169-170°C, (Water-Ethanol)	1.24, t, 3H, <i>J</i> = 7.0 Hz; 4.20, q, 2H, <i>J</i> = 6.8 Hz	5.65, s, CH, 7.13-7.49, m, 10H	11.80	12.11	13.65	11.47	13.90
88ze	H yield: 91, mp : 178-180 °C, (Ethanol-water)	1.25, t, 3H, <i>J</i> = 7.1 Hz; 4.21, q, 2H, <i>J</i> = 7.1 Hz	7.90 & 8.54, s, 1H	11.79	12.01	13.81	11.47	14.01

Ethyl 5-amino-3-(pyridine-3-yl)-1*H*-1,2,4-triazole-1-carboxylate (88zb')



Yield 40 %; mp 157-159 °C (ethanol); ¹H NMR (300 MHz, DMSO-*d*₆), δ 1.38 (t, 3H, CH₃, *J* = 7.0 Hz), 4.46 (q, 2H, CH₂, *J* = 7.0 Hz), 7.50-7.57 (m, 3H, Ar-H), 8.27 (d, 1H, Ar-H, *J* = 7.9 Hz), 8.67 (d, 1H, NH, *J* = 4.1 Hz), 9.11 (s, 1H, HN).

4-Carbethoxy-1-[4-(*N,N*-dimethylamino)benzoyl]thiosemicarbazide (**109**)²²⁵



Yield 89 %; mp 201°C (PhMe); ¹H NMR (300 MHz, DMSO-*d*₆): δ 1.26 (t, 3H, *J* = 7.1 Hz, CH₃), 2.99 (s, 6H, N(CH₃)₂), 4.21 (q, 2H, *J* = 7.1 Hz, CH₂), 6.73 (d, 2H, *J* = 9.0 Hz, H-3' & H-5'), 7.76 (d, 2H, *J* = 9.0 Hz, H-2' & H-6'), 10.55 (s, 1H, NH), 11.34 (s, 1H, NH), 11.39 (s, 1H, NH)

- General procedure for the synthesis of 2-substituted-5-thioxo-5,6-dihydro-4*H*-[1,2,4]triazolo[1,5-*a*][1,3,5]triazin-7-one (**H5a-H5g**)²⁶

To a stirred solution of NaOH (9 mmol) in ethanol (80%, 20 ml), *N*-(1,2,4-triazole-3(5)-yl)-*N*'-carbethoxythiourea was added and heated on water bath for 20 minutes with continuous stirring. After cooling, the solvent was evaporated under vacuum, and the residue was suspended in water (25 ml). The resulting suspension was acidified up to pH 1-3 using 2.5 M HCl. The precipitated product was filtered off, recrystallized with suitable solvent and dried under vacuum.

2-(Methylthio)-5-thioxo-5,6-dihydro-[1,2,4]triazolo[1,5-*a*][1,3,5]triazin-7(4*H*)-one (**H5a**)

Yield 64%; mp 263 °C (Ethanol-water); ESI-MS *m/z* 214.0 (M-1)⁺; purity > 95%; *t*_R 2.11 min (B); ¹H NMR (300 MHz, DMSO-*d*₆): δ 2.56 (s, 3H, SMe), 13.03 (s, 1H, NH), 14.10 (br. s, 1H, NH); ¹³C NMR (75 MHz, DMSO-*d*₆): δ 13.9 (SMe), 141.0 (C-2), 151.9 (C-9), 165.1 (C-7), 175.7 (C-5).

2-(Benzylthio)-5-thioxo-5,6-dihydro-[1,2,4]triazolo[1,5-*a*][1,3,5]triazin-7(4*H*)-one (H5ai)

Yield 89%; mp 249 °C (EtOH-water); ESI-MS *m/z* 290.1 (M-1)⁺; purity > 95%; *t_R* 14.77 min (C); ¹H NMR (300 MHz, DMSO-*d*₆): δ 4.40 (s, 2H, SCH₂Ph), 7.25-7.35 (m, 3H, H-3', H-4' and H-5'), 7.44 (d, 2H, H-2' and H-6', *J* = 6.8 Hz) 13.03 (s, 1H, NH), 14.30 (br. s, 1H, NH); ¹³C NMR (75 MHz, DMSO-*d*₆): δ 35.0 (CH₂), 127.9 (C-4'), 129.0 (C-2' and C-6'), 129.4 (C-3' and C-5'), 137.5 (C-1'), 141.0 (C-2), 151.9 (C-9), 164.0 (C-7), 175.7 (C-5).

2-(Phenethylthio)-5-thioxo-5,6-dihydro-[1,2,4]triazolo[1,5-*a*][1,3,5]triazin-7(4*H*)-one (H5aii)

Yield 94%; mp 232-234°C (EtOH-water); ESI-MS *m/z* 304.1 (M-1)⁺; purity > 95%; *t_R* 2.18 min (B); ¹H NMR (300 MHz, DMSO-*d*₆): δ 3.01 (t, 2H, CH₂Ph, *J* = 7.3 Hz), 3.37 (t, 2H, SCH₂, *J* = 7.3 Hz), 7.21-7.34 (m, 5H, Ph), 13.03 (s, 1H, NH), 14.21 (br. s, 1H, NH); ¹³C NMR (75 MHz, DMSO-*d*₆): δ 32.5 (SCH₂), 35.3 (PhCH₂), 126.9 (C-4'), 128.9 (C-2' and C-6'), 129.1 (C-3' and C-5'), 140.3 (C-1'), 141.0 (C-2), 151.8 (C-9), 164.2 (C-7), 175.6 (C-5).

2-((3-Phenylpropyl)thio)-5-thioxo-5,6-dihydro-[1,2,4]triazolo[1,5-*a*][1,3,5]triazin-7(4*H*)-one (H5aiii)

Yield 69%; mp 220-221 °C (EtOH-water); ESI-MS *m/z* 318.2 (M-1)⁺; purity > 95%; *t_R* 18.57 min (C); ¹H NMR (300 MHz, DMSO-*d*₆): δ 2.01 (q, 2H, CH₂CH₂CH₂, *J* = 7.3 Hz), 2.72 (t, 2H, CH₂Ph, *J* = 7.7 Hz), 3.12 (t, 2H, SCH₂, *J* = 7.2 Hz), 13.01 (s, 1H, NH), 14.12 (br. s, 1H, NH); ¹³C NMR (75 MHz, DMSO-*d*₆): δ 30.7 (CH₂CH₂CH₂),

30.9 (SCH₂), 34.4 (PhCH₂), 126.4 (C-4'), 128.8 (C-2' and C-6'), 128.9 (C-3' and C-5'), 141.0 (C-1'), 141.5 (C-2), 151.8 (C-9), 164.2 (C-7), 175.6 (C-5).

2-Phenyl-5-thioxo-5,6-dihydro-[1,2,4]triazolo[1,5-*a*][1,3,5]triazin-7(4*H*)-one (H5b)

Yield 78%; mp 258-259 °C (EtOH); ESI-MS *m/z* 244.1 (M-1)⁺; purity > 95%; *t_R* 2.16 min (B); ¹H NMR (300 MHz, DMSO-*d*₆): δ 7.53-7.55 (m, 3H, H-3', H-4' and H-5'), 8.04-8.07 (m, 2H, H-2' and H-6'), 13.12 (s, 1H, NH), 14.31 (br. s, 1H, NH); ¹³C NMR (75 MHz, DMSO-*d*₆): δ 127.1 (C-2' and C-6'), 129.5 (C-3' and C-5'), 129.7 (C-4'), 131.3 (C-1'), 141.7 (C-2), 151.9 (C-9), 162.4 (C-7), 175.8 (C-5).

2-(3-Nitrophenyl)-5-thioxo-5,6-dihydro-[1,2,4]triazolo[1,5-*a*][1,3,5]triazin-7(4*H*)-one (H5bi)

Yield 80%; mp 246-248 °C (acetic acid), ESI-MS *m/z* 289.1 (M-1)⁺; purity > 95%; *t_R* 13.15 min (C); ¹H NMR (300 MHz, DMSO-*d*₆): δ 7.86 (t, 1H, H-5', *J* = 8.1 Hz), 8.39 (dd, 1H, H-4', *J* = 8.1, 1.3 Hz), 8.47 (d, 1H, H-6', *J* = 7.5 Hz), 8.74 (s, 1H, H-2'), 13.19 (s, 1H, NH), 14.51 (br. s, 1H, NH); ¹³C NMR (75 MHz, DMSO-*d*₆): δ 120.9 (C-2'), 125.2 (C-4'), 130.6 (C-5'), 130.9 (C-6'), 132.4 (C-1'), 141.0 (C-3'), 148.1 (C-2), 151.7 (C-9), 160.0 (C-7), 175.3 (C-5).

5-Thioxo-2-(3-(trifluoromethyl)phenyl)-5,6-dihydro-[1,2,4]triazolo[1,5-*a*][1,3,5]triazin-7(4*H*)-one (H5bii)

Yield 81%; mp 268-270 °C (EtOH-water); ESI-MS *m/z* 312.1 (M-1)⁺; purity > 95%; *t_R* 2.15 min (B); ¹H NMR (300 MHz, DMSO-*d*₆): δ 7.81 (t, 1H, H-5', *J* = 7.7 Hz), 7.93 (d, 1H, H-4', *J* = 7.9 Hz), 8.27 (s, 1H, H-2'), 8.35 (d, 1H, H-6', *J* = 7.5 Hz), 13.18 (s, 1H, NH), 14.40 (br. s, 1H, NH); ¹³C NMR (75 MHz, DMSO-*d*₆): δ 122.6 (q,

CF₃, $J = 4.1$ Hz), 123.8 (q, C-2', $J = 272.5$ Hz), 127.2 (q, C-4', $J = 3.4$ Hz), 129.7 (q, C-5', $J = 32.0$ Hz), 130.2 (C-6'), 130.3 (C-3'), 130.5 (C-1'), 141.1 (C-2), 151.6 (C-9), 160.5 (C-7), 175.3 (C-5).

2-(3-Chlorophenyl)-5-thioxo-5,6-dihydro-[1,2,4]triazolo[1,5-*a*][1,3,5]triazin-7(4*H*)-one (H5biii)

Yield 65%; mp 266-267°C (acetic acid); ESI-MS m/z 278.0 (M-1)⁺; purity > 95%; t_R 14.63 min (C); ¹H NMR (300 MHz, DMSO-*d*₆): δ 7.55-7.63 (m, 2H, H-4' and H-5'), 8.00-8.02 (m, 2H, H-2' and H-6'), 13.16 (s, 1H, NH), 14.26 (br. s, 1H, NH); ¹³C NMR (75 MHz, DMSO-*d*₆): δ 125.7 (C-6'), 126.6 (C-2'), 131.1 (C-5') 131.6 (C-4'), 134.2 (C-3'), 141.6 (C-1'), 141.6 (C-2), 152.0 (C-9), 161.2 (C-7), 175.8 (C-5).

2-(3-Bromophenyl)-5-thioxo-5,6-dihydro-[1,2,4]triazolo[1,5-*a*][1,3,5]triazin-7(4*H*)-one (H5biv)

Yield 75%; mp 262-264 °C (acetic acid), ESI-MS m/z 324.0 (M-1)⁺; purity > 95%; t_R 2.19 min (B); ¹H NMR (300 MHz, DMSO-*d*₆): δ 7.52 (t, 1H, H-5', $J = 7.9$ Hz), 7.74 (d, 1H, H-4', $J = 7.9$ Hz), 8.05 (d, 1H, H-6', $J = 7.9$ Hz), 8.14 (s, 1H, H-2'), 13.18 (s, 1H, NH), 14.22 (br.s, 1H, NH); ¹³C NMR (75 MHz, DMSO-*d*₆): δ 122.6 (C-3'), 126.0 (C-6'), 129.4 (C-2') 131.9 (C-5'), 131.9 (C-4'), 133.9 (C-1'), 141.6 (C-2), 152.0 (C-9), 161.0 (C-7), 175.8 (C-5).

2-(3-Fluorophenyl)-5-thioxo-5,6-dihydro-[1,2,4]triazolo[1,5-*a*][1,3,5]triazin-7(4*H*)-one (H5bv)

Yield 72%; mp 283-285 °C (acetic acid); ESI-MS m/z 262.3 (M-1)⁺; purity > 95%; t_R 2.15 min (B); ¹H NMR (300 MHz, DMSO-*d*₆): δ 7.39 (td, 1H, H-5', $J = 8.5, 2.3$ Hz), 7.60 (dd, 1H, H-4', $J = 7.9, 13.9$ Hz), 7.75 (d, 1H, H-2', $J = 9.8$ Hz), 7.90 (d, 1H, H-

6', $J = 7.9$ Hz), 13.13 (s, 1H, NH), 14.33 (br. s, 1H, NH); ^{13}C NMR (75 MHz, DMSO-*d*₆): δ 13C NMR (75 MHz, DMSO-*d*₆): δ 114.1 (d, C-2', $J = 23.3$ Hz), 118.7 (d, C-4', $J = 21.1$ Hz), 122.7 (d, C-6', $J = 1.5$ Hz), 131.3 (d, C-5', $J = 8.0$ Hz), 131.5 (d, C-1', $J = 8.0$ Hz), 141.1 (C-9), 151.5 (C-7), 160.7 (d, C-2, $J = 2.9$ Hz), 162.2 (d, C-3', $J = 244.1$ Hz), 175.3 (C-5).

2-(3-Methylphenyl)-5-thioxo-5,6-dihydro-[1,2,4]triazolo[1,5-*a*][1,3,5]triazin-7(4*H*)-one (H5bvi)

Yield 80%; mp 259-261°C (EtOH-water); ESI-MS m/z 258.1 (M-1)⁺; purity > 95%; t_R 2.17 min (B); ^1H NMR (300 MHz, DMSO-*d*₆): δ 2.40 (s, 3H, Me), 7.34 (d, 1H, H-4', $J = 7.5$ Hz), 7.42 (t, 1H, H-5', $J = 7.5$ Hz), 7.84 (d, 1H, H-6', $J = 7.9$ Hz), 7.88 (s, 1H, H-2'), 13.09 (s, 1H, NH), 14.24 (br. s, 1H, NH); ^{13}C NMR (75 MHz, DMSO-*d*₆): δ 20.9 (Me), 123.7 (C-6'), 127.0 (C-2'), 128.8 (C-5'), 129.0 (C-4'), 131.3 (C-1'), 138.2 (C-3'), 141.2 (C-2), 151.3 (C-9), 161.9 (C-7), 175.2 (C-5).

2-(3-Methoxyphenyl)-5-thioxo-5,6-dihydro-[1,2,4]triazolo[1,5-*a*][1,3,5]triazin-7(4*H*)-one (H5bvii)

Yield 90%; mp 260 °C (acetic acid), ESI-MS m/z 274.1 (M-1)⁺; purity > 95%; t_R 2.15 min (B); ^1H NMR (300 MHz, DMSO-*d*₆): δ 3.84 (s, 3H, OMe), 7.11 (dd, 1H, H-4', $J = 8.1, 2.1$ Hz), 7.45 (t, 1H, H-5', $J = 7.9$ Hz), 7.54 (s, 1H, H-2'), 7.64 (d, 1H, H-6', $J = 7.5$ Hz), 13.10 (s, 1H, NH), 14.32 (br. s, 1H, NH); ^{13}C NMR (75 MHz, DMSO-*d*₆): δ 55.1 (OMe), 111.2 (C-2'), 116.6 (C-4'), 118.9 (C-6'), 130.1 (C-5'), 130.4 (C-1'), 141.1 (C-3'), 151.3 (C-2), 159.4 (C-9), 161.7 (C-7), 175.2 (C-5).

3-(7-Oxo-5-thioxo-4,5,6,7-tetrahydro-[1,2,4]triazolo[1,5-*a*][1,3,5]triazin-2-yl)benzotrile (H5bviii)

Yield 67 %; mp >300 °C (acetic acid); ESI-MS *m/z* 287.0 (M-1)⁺; purity > 94%; *t_R* 3.84 min (D); ¹H NMR (300 MHz, DMSO-*d*₆): δ 7.48-8.57 (m, 4H, Ar-H), 13.10 (s, 1H, NH), 14.38 (br. s, 1H, NH). ¹³C NMR (75 MHz, DMSO-*d*₆): δ 126.5 (C-3'), 129.7 (CN), 129.8 (C-2'), 130.0 (C-5'), 130.1 (C-1'), 135.6 (C-6'), 141.9 (C-4'), 152.2 (C-2), 162.1 (C-9), 168.1 (C-7), 176.0 (C-5).

2-(4-Nitrophenyl)-5-thioxo-5,6-dihydro-[1,2,4]triazolo[1,5-*a*][1,3,5]triazin-7(4*H*)-one (H5bix)

Yield 65%; mp > 300 °C (basification followed by acidification); ESI-MS *m/z* 289.1 (M-1)⁺; purity > 95%; *t_R* 2.13 min (B); ¹H NMR (300 MHz, DMSO-*d*₆): δ 8.29 (d, 2H, H-3' and H-5' *J* = 8.7 Hz), 8.39 (d, 2H, H-2' and H-6' *J* = 9.0 Hz), 13.21 (s, 1H, NH), 14.28 (br. s, 1H, NH); ¹³C NMR (75 MHz, DMSO-*d*₆): δ 124.3 (C2' and C-6'), 127.7 (C-3' and C-5'), 135.0 (C-4'), 141.1 (C-1'), 148.5 (C-2), 151.7 (C-9), 160.1 (C-7), 175.3 (C-5).

5-Thioxo-2-(4-(trifluoromethyl)phenyl)-5,6-dihydro-[1,2,4]triazolo[1,5-*a*][1,3,5]triazin-7(4*H*)-one (H5bx)

Yield 69%; mp 280 °C (EtOH-water); ESI-MS *m/z* 312.0 (M-1)⁺; purity > 95%; *t_R* 2.15 min (B); ¹H NMR (300 MHz, DMSO-*d*₆): δ 7.91 (d, 2H, H-3' and H-5', *J* = 8.3), 8.26 (d, 2H, H-2' and H-6', *J* = 8.3), 13.18 (s, 1H, NH), 14.36 (br. s, 1H, NH); ¹³C NMR (75 MHz, DMSO-*d*₆): δ 123.9 (q, CF₃, *J* = 272.2 Hz), 125.9 (q, C-3' and C-5', *J* = 3.4 Hz), 127.3 (C-2' and C-6'), 130.5 (q, C-4', *J* = 32.0 Hz), 133.0 (C-1'), 141.1 (C-2), 151.7 (C-9), 160.6 (C-7), 175.3 (C-5).

2-(4-Chlorophenyl)-5-thioxo-5,6-dihydro-[1,2,4]triazolo[1,5-*a*][1,3,5]triazin-7(4*H*)-one (H5bxi)

Yield 66%; mp 281-282 °C (EtOH-water); ESI-MS *m/z* 278.0 (M-1)⁺; purity > 95%; *t_R* 2.18 min (B); ¹H NMR (300 MHz, DMSO-*d*₆): δ 7.61 (d, 2H, H-3' and H-5', *J* = 8.3), 8.05 (d, 2H, H-2' and H-6', *J* = 8.3), 13.14 (s, 1H, NH), 14.31 (br. s, 1H, NH); ¹³C NMR (75 MHz, DMSO-*d*₆): δ 128.01 (C-4') 128.26 (C2' and C-6'), 129.08 (C-3' and C-5'), 135.32 (C-1'), 141.08 (C-2), 151.46 (C-9), 160.89 (C-7), 175.22 (C-5).

2-(4-Bromophenyl)-5-thioxo-5,6-dihydro-[1,2,4]triazolo[1,5-*a*][1,3,5]triazin-7(4*H*)-one (H5bxii)

Yield 73%; mp 292-293 °C (acetic acid); ESI-MS *m/z* 324.0 (M-1)⁺; purity > 95%; *t_R* 2.21 min (B); ¹H NMR (300 MHz, DMSO-*d*₆): δ 7.75 (d, 2H, H-3' and H-5' *J* = 8.3), 7.98 (d, 2H, H-2' and H-6' *J* = 8.3), 13.13 (s, 1H, NH), 14.35 (br. s, 1H, NH). ¹³C NMR (75 MHz, DMSO-*d*₆): δ 124.8 (C-4'), 128.9 (C-1'), 129.1 (C2' and C-6'), 132.6 (C-3' and C-5'), 141.7 (C-2), 152.0 (C-9), 161.6 (C-7), 175.8 (C-5).

2-(4-Fluorophenyl)-5-thioxo-5,6-dihydro-[1,2,4]triazolo[1,5-*a*][1,3,5]triazin-7(4*H*)-one (H5bxiii)

Yield 67%; mp 262 °C (EtOH-water); ESI-MS *m/z* 262.3 (M-1)⁺; purity > 95%; *t_R* 2.13 min (B); ¹H NMR (300 MHz, DMSO-*d*₆): δ 7.37 (dd, 2H, H-3' and H-5' *J* = 8.9, 8.9 Hz), 8.09 (dd, 2H, H-2' and H-6' *J* = 8.7, 5.7 Hz), 13.12 (s, 1H, NH), 14.20 (br. s, 1H, NH); ¹³C NMR (75 MHz, DMSO-*d*₆): δ 116.0 (d, C-3' and C-5', *J* = 21.8 Hz), 125.7 (d, C-1', *J* = 2.9 Hz), 128.9 (d, C-2' and C-6', *J* = 8.7 Hz), 141.1 (C-2), 151.4 (C-9), 161.0 (C-7), 163.5 (d, C-4', *J* = 247.8 Hz), 175.2 (C-5).

2-(4-Methylphenyl)-5-thioxo-5,6-dihydro-[1,2,4]triazolo[1,5-*a*][1,3,5]triazin-7(4*H*)-one (H5bxiv)

Yield 78%; mp 296-297 °C (EtOH-water); ESI-MS *m/z* 258.1 (M-1)⁺; purity > 95%; *t_R* 2.19 min (B); ¹H NMR (300 MHz, DMSO-*d*₆): δ 2.38 (s, 3H, ArMe), 7.34 (d, 2H, H-3' and H-5' *J* = 7.9), 7.94 (d, 2H, H-2' and H-6' *J* = 7.9), 13.07 (s, 1H, NH), 14.26 (br. s, 1H, NH). ¹³C NMR (75 MHz, DMSO-*d*₆): δ 20.95 (Me), 126.38 (C-4'), 126.46 (C-2' and C-6'), 129.45 (C-3' and C-5'), 140.44 (C-1'), 141.11 (C-2), 151.22 (C-9), 161.86 (C-7), 175.14 (C-5).

2-(4-Methoxyphenyl)-5-thioxo-5,6-dihydro-[1,2,4]triazolo[1,5-*a*][1,3,5]triazin-7(4*H*)-one (H5bxv)

Yield 63%; mp 270-271 °C (acetic acid); ESI-MS *m/z* 288.1(M-1)⁺; purity > 95%; *t_R* 2.15 min (B); ¹H NMR (300 MHz, DMSO-*d*₆): δ 3.84 (s, 3H, OMe), 7.08 (d, 2H, H-3' and H-5' *J* = 8.7 Hz), 7.99 (d, 2H, H-2' and H-6' *J* = 9.0 Hz), 13.07 (s, 1H, NH), 14.11 (br. s, 1H, NH); ¹³C NMR (75 MHz, DMSO-*d*₆): δ 55.25 (MeO), 114.29 (C-2' and C-6'), 121.52 (C-4'), 128.17 (C-3' and C-5'), 141.13 (C-1'), 151.20 (C-2), 161.12 (C-9), 161.75 (C-7), 175.12 (C-5).

4-(7-Oxo-5-thioxo-4,5,6,7-tetrahydro-[1,2,4]triazolo[1,5-*a*][1,3,5]triazin-2-yl)benzotrile (H5bxvi)

Yield 69%; mp > 300 °C (EtOH-water); ESI-MS *m/z* 287.0 (M-1)⁺; purity > 88%; *t_R* 3.73 min (D); ¹H NMR (300 MHz, DMSO-*d*₆): δ 8.02 (d, 2H, H-3' and H-5', *J* = 8.4 Hz), 8.12 (d, 2H, H-2' and H-6', *J* = 8.4 Hz), 13.11 (s, 1H, NH), 14.44 (br. s, 1H, NH); ¹³C NMR (75 MHz, DMSO-*d*₆): δ 126.3 (C-3' and C-5'), 128.1 (C-2' and C-6'),

131.6 (CN), 136.0 (C-4'), 141.2 (C-1'), 151.7 (C-2), 161.2 (C-9), 167.2 (C-5), 175.4 (C-7).

2-(3,4-Dichlorophenyl)-5-thioxo-5,6-dihydro-[1,2,4]triazolo[1,5-*a*][1,3,5]triazin-7(4*H*)-one (H5bxvii)

Yield 74%; mp 271-273 °C (acetic acid); ESI-MS *m/z* 314.0 (M-1)⁺; purity > 95%; *t_R* 2.23 min (B); ¹H NMR (300 MHz, DMSO-*d*₆): δ 7.82 (d, 1H, H-6', *J* = 8.3 Hz), 8.01 (dd, 1H, H-5', *J* = 8.3 Hz, *J* = 1.9 Hz), 8.16 (d, 1H, H-2', *J* = 1.9 Hz), 13.17 (s, 1H, NH), 14.35 (br. s, 1H, NH); ¹³C NMR (75 MHz, DMSO-*d*₆): δ 127.1 (C-6'), 128.5 (C-2'), 130.3 (C-5') 132.0 (C-4'), 132.4 (C-3'), 133.9 (C-1'), 141.6 (C-2), 152.2 (C-9), 160.4 (C-7), 175.9 (C-5).

2-(3,4-Difluorophenyl)-5-thioxo-5,6-dihydro-[1,2,4]triazolo[1,5-*a*][1,3,5]triazin-7(4*H*)-one (H5bxviii)

Yield 68%; mp 267-269 °C (acetic acid); ESI-MS *m/z* 280.3 (M-1)⁺; purity > 95%; *t_R* 2.16 min (B); ¹H NMR (300 MHz, DMSO-*d*₆): δ 7.57-7.66 (m, 1H, H-5'), 7.89-8.00 (m, 1H, H-2' and H-6'), 13.17 (s, 1H, NH), 14.40(br. s, 1H, NH); ¹³C NMR (75 MHz, DMSO-*d*₆): δ 115.5 (d, C-3', *J* = 18.9 Hz), 118.4 (d, C-5', *J* = 17.4 Hz), 123.8 (dd, C-6', *J* = 6.9, 3.3 Hz), 126.7 (dd, C-1', *J* = 6.5, 3.6 Hz), 141.1 (C-2), 149.6 (dd, C-4', *J* = 246.7, 12.7 Hz), 150.9 (dd, C-3', *J* = 250.0, 12.4 Hz), 151.6 (C-9), 160.1 (C-7), 175.3 (C-5).

2-(4-Bromo-3-methylphenyl)-5-thioxo-5,6-dihydro-[1,2,4]triazolo[1,5-*a*][1,3,5]triazin-7(4*H*)-one (H5bxix)

Yield 77%; mp 278-280 °C (acetic acid); ESI-MS *m/z* 338.0 (M-1)⁺; purity > 95%; *t_R* 6.1 min (D); ¹H NMR (300 MHz, DMSO-*d*₆): δ 2.44 (s, 3H, Me), 7.72-7.79 (m, 2H,

H-5' and H-6'), 8.00 (s, 1H, H-2'), 13.13 (s, 1H, NH), 14.30 (br. s, 1H, NH); ¹³C NMR (75 MHz, DMSO-*d*6): δ 22.9 (Me), 126.4 (C-4'), 127.2 (C-6'), 129.2 (C-2') 129.3 (C-5'), 133.4 (C-1'), 138.7 (C-3'), 141.7 (C-2'), 152.0 (C-9), 161.6 (C-7), 175.8 (C-5).

2-(Furan-2-yl)-5-thioxo-5,6-dihydro-[1,2,4]triazolo[1,5-*a*][1,3,5]triazin-7(4*H*)-one (H5c)

Yield 62%; mp 292-294 °C (EtOH-water); ESI-MS *m/z* 234.1 (M-1)⁺; purity > 95%; *t*_R 3.95 min (D); ¹H NMR (300 MHz, DMSO-*d*6): δ 6.62-6.74 (m, 1H, H-4'), 7.12 (d, 1H, *J* = 3.0, H-3'), 7.83-7.96 (m, 1H, H-5'), 13.13 (s, 1H, NH), 14.17 (br. s, 1H, NH); ¹³C NMR (75 MHz, DMSO-*d*6): δ 112.7 (C-4'), 113.2 (C-3'), 141.7 (C-5'), 145.1 (C-2'), 146.1 (C-2), 151.8 (C-9), 155.5 (C-7), 175.9 (C-5).

2-(Thiophen-2-yl)-5-thioxo-5,6-dihydro-[1,2,4]triazolo[1,5-*a*][1,3,5]triazin-7(4*H*)-one (H5d)

Yield 64%; mp 273°C (EtOH-water); ESI-MS *m/z* 250.0 (M-1)⁺; purity > 95%; *t*_R 2.13 min (B); ¹H NMR (300 MHz, DMSO-*d*6): δ 7.22 (dd, 1H, H-4', *J* = 4.1, 4.1 Hz), 7.74 (d, 1H, H-3' *J* = 3.4), 7.78 (d, 1H, H-5' *J* = 4.9 Hz), 13.11 (s, 1H, NH), 14.22 (br. s, 1H, NH); ¹³C NMR (75 MHz, DMSO-*d*6): δ 128.3 (C-4'), 128.4 (C-5'), 129.5 (C-3'), 131.7 (C-2'), 141.0 (C-2), 151.2 (C-9), 158.1 (C-7), 175.2 (C-5).

2-(Pyridin-2-yl)-5-thioxo-5,6-dihydro-[1,2,4]triazolo[1,5-*a*][1,3,5]triazin-7(4*H*)-one (H5e)

Yield 63%; mp 280-282 °C (EtOH-water); ESI-MS *m/z* 245.4 (M-1)⁺; purity > 95%; *t*_R 2.16 min (B); ¹H NMR (300 MHz, DMSO-*d*6): δ 7.54-7.57 (m, 1H, H-5'), 7.98-8.02 (m, 1H, H-3'), 8.11-8.13 (m, 1H, H-4'), 8.74- 8.75 (m, 1H, H-6'), 13.17 (s, 1H,

NH), 14.93 (br. s, 1H, NH); ¹³C NMR (75 MHz, DMSO-*d*₆), δ, 123.2 (C-4'), 125.8 (C-6'), 138.0 (C-5'), 141.8 (C-3'), 148.4 (C-1'), 150.4 (C-2), 152.0 (C-9), 162.1 (C-7), 176.0 (C-5).

5-Thioxo-5,6-dihydro-[1,2,4]triazolo[1,5-*a*][1,3,5]triazin-7(4*H*)-one (H5f)

Yield 54%; mp > 300°C (EtOH); ESI-MS *m/z* 168.1 (M-1)⁺; purity > 95%; *t_R* 2.11 min (B); ¹H NMR (300 MHz, DMSO-*d*₆): δ 8.17 (s, 1H, CH), 13.05 (s, 1H, NH), 14.05 (br. s, 1H, NH); ¹³C NMR (75 MHz, DMSO-*d*₆): δ 141.9 (C-2), 151.5 (C-9), 153.6 (C-7), 176.0 (C-5).

2-([1,1'-Diphenyl]-4-ylmethyl)-5-thioxo-5,6-dihydro-[1,2,4]triazolo[1,5-*a*][1,3,5]triazin-7(4*H*)-one (H5f)

Yield 63 %; mp 210-212 °C (EtOH-water); ESI-MS *m/z* 334.1 (M-1)⁺; purity > 95%; *t_R* 1.69 min (A); ¹H NMR (300 MHz, DMSO-*d*₆): δ 5.62 (s, 2H, PhCH₂), 7.21-7.41 (m, 9H, Ar-H), 12.96 (s, 1H, NH), 13.78 (br. s, 1H, NH); ¹³C NMR (75 MHz, DMSO-*d*₆): δ 50.5 (CH₂), 127.2 (C-3' and C-5'), 128.8 (C-2'', C-4'' and C-6''), 128.9 (C-3'' and C-5''), 129.3 (C-1', C-4' and C-1''), 141.5 (C-2' and C-6'), 141.7 (C-2), 151.6 (C-9), 166.8 (C-7), 175.8 (C-5).

- General procedure for the synthesis of 5-(methylthio)-2-substituted-[1,2,4]triazolo[1,5-*a*][1,3,5]triazin-7(6*H*)-one (**H6a-H6b**)²⁶

To a stirred solution of 2-substituted-5-thioxo-5,6-dihydro-4*H*-[1,2,4]triazolo[1,5-*a*][1,3,5]triazin-7-one (5 mmol) in 4 ml of 2.5 M NaOH, iodomethane (933 μl, 7.5 mmol) was added, the stirring was continued for 30 minutes. A solid precipitate was observed which upon acidification (pH 1-3) with 2.5 M HCl afforded another solid.

The precipitated solid was filtered, washed with ice cold water and recrystallized from water-ethanol system.

2,5-Bis(methylthio)-[1,2,4]triazolo[1,5-*a*][1,3,5]triazin-7(6*H*)-one (H6a)

Yield 54%; mp 241-243°C (Ethanol-water); ESI-MS *m/z* 228.0 (M-1)⁺; purity > 95%; *t_R* 4.28 min (B); ¹H NMR (300 MHz, DMSO-*d*₆): δ 2.57 (s, 3H, SMe), 2.58 (s, 3H, SMe), 13.41 (br. s, 1H, NH); ¹³C NMR (75 MHz, DMSO-*d*₆): δ 13.2 (SMe), 13.2 (SMe), 142.4 (C-2), 157.3 (C-9), 165.0 (C-5), 165.1 (C-7).

5-(Methylthio)-2-phenyl-[1,2,4]triazolo[1,5-*a*][1,3,5]triazin-7(6*H*)-one (H6b)

Yield 58%; mp 292-294°C (Ethanol-water); ESI-MS *m/z* 258.0 (M-1)⁺; purity > 95%; *t_R* 4.67 min (D); ¹H NMR (300 MHz, DMSO-*d*₆): δ 2.62 (s, 3H, SMe), 7.54-7.55 (m, 3H, H-3', H-4' and H-5'), 13.15 (br. s, 1H, NH); ¹³C NMR (75 MHz, DMSO-*d*₆): δ 13.9 (SMe), 127.1 (C-2' and C-6'), 129.4 (C-3' and C-5'), 130.4 (C-4'), 131.0 (C-1'), 143.8 (C-2), 157.9 (C-9), 163.1 (C-5), 165.3 (C-7).

- General procedure for the synthesis of 2-substituted-7-thioxo-6,7-dihydro-[1,2,4]triazolo[1,5-*a*][1,3,5]triazin-5(4*H*)-one (H3a-H3b)

In a suspension of 3(5)-amino-5(3)-(het)aryl-1,2,4-triazoles (3 mmol) in dry acetone (15 ml), ethoxycarbonyl isothiocyanate (3.3 mmol) was then added. The reaction mixture was allowed to stir at room temperature for 20 minutes and after that, the precipitated product was filtered off, washed with acetone and dried under vacuum. The obtained 3-substituted-5-amino-1-carbethoxylthiocarbamoyl-1,2,4-triazole was heated on water bath for 20 minutes after dissolving it in alkaline solution of ethanol (80%). After cooling, the solvent was evaporated under vacuum, and the residue was dissolved in water (25 ml). The resulting suspension was acidified up to pH 1-3 using

2.5 M HCl. The precipitated product was filtered off, recrystallized with suitable solvent and dried under vacuum.

2-(Methylthio)-7-thioxo-6,7-dihydro-[1,2,4]triazolo[1,5-*a*][1,3,5]triazin-5(4*H*)-one (H3a)

Yield 72%; mp 254-256 °C (EtOH-water); ESI-MS *m/z* 214.1 (M-1)⁺; purity > 95%; *t_R* 2.14 min (B); ¹H NMR (300 MHz, DMSO-*d*6): δ 2.57 (s, 3H, SMe), 13.03 (s, 1H, NH); ¹³C NMR (75 MHz, DMSO-*d*6): δ 13.9 (SMe), 146.6 (C-2), 149.9 (C-9), 165.9(C-5), 169.6 (C-7).

2-Phenyl-7-thioxo-6,7-dihydro-[1,2,4]triazolo[1,5-*a*][1,3,5]triazin-5(4*H*)-one (H3b)

Yield 59 %, mp 285-287 °C (EtOH-water), ESI-MS *m/z* 244.4 (M-1)⁺; purity > 95%; *t_R* 12.11 min (C); ¹H NMR (300 MHz, DMSO-*d*6): δ 7.53-7.55 (m, 3H, H-3', H-4' and H-5'), 8.04-8.06 (m, 2H, H-2' and H-6'), 13.12 (s, 1H, NH); ¹³C NMR (75 MHz, DMSO-*d*6): δ 127.2 (C-2' and C-6'), 129.5 (C-3'and C-5'), 129.7 (C-4'), 131.3 (C-1'), 146.7 (C-2), 150.1 (C-9), 162.9 (C-5), 170.8 (C-7).

- General procedure for the synthesis of 7-(methylthio)-2-substituted-[1,2,4]triazolo[1,5-*a*][1,3,5]triazin-5(4*H*)-one (H4a-H4b)

To a stirred solution of 2-substituted-5-thioxo-5,6-dihydro-4*H*- [1,2,4]triazole[1,5-*a*][1,3,5]triazin-7-one (5 mmol) in 4 ml of 2.5 M NaOH, iodomethane (933 μl, 7.5 mmol) was added, the stirring was continued for 30 min. A solid precipitate was observed which upon acidification (pH 1-3) with 2.5 M HCl afforded another solid. The precipitated solid was filtered, washed with ice cold water and recrystallized from water-ethanol system.

2,7-Bis(methylthio)-[1,2,4]triazolo[1,5-*a*][1,3,5]triazin-5(4*H*)-one (H4a)

Yield 67 %; mp 274-276 °C (EtOH-water); ESI-MS *m/z* 228.3 (M-1)⁺; purity > 95%; *t_R* 2.38 min; ¹H NMR (300 MHz, DMSO-*d*₆): δ 2.57 (two s, 6H, 2SMe), 12.98 (s, 1H, NH); ¹³C NMR (75 MHz, DMSO-*d*₆): δ 12.7 (SMe), 13.3 (SMe), 151.1 (C-2), 152.1 (C-9), 161.6(C-5), 165.5 (C-7).

7-(Methylthio)-2-phenyl-[1,2,4]triazolo[1,5-*a*][1,3,5]triazin-5(4*H*)-one (H4b)

Yield 61 %; mp 300-301 °C (EtOH-water); ESI-MS *m/z* 258.3(M-1)⁺; purity > 95%; *t_R* 14.40 min (C); ¹H NMR (300 MHz, DMSO-*d*₆): δ 2.61 (s, 3H, SMe), 7.53-7.55 (m, 3H, H-3', H-4' and H-5'), 8.04-8.06 (m, 2H, H-2' and H-6'), 13.06 (s, 1H, NH); ¹³C NMR (75 MHz, DMSO-*d*₆): δ 11.8 (SMe), 125.6 (C-2' and C-6'), 127.9 (C-3'and C-5'), 127.9 (C-4'), 129.82 (C-1'), 150.2 (C-2), 151.1 (C-9), 161.2 (C-5), 161.6 (C-7).

- General procedure for the synthesis of 2-substituted-[1,2,4]triazolo[1,5-*a*][1,3,5]triazin-5,7(4*H*,6*H*)-dione (**H2a-H2b**)

7-Methylsulfanyl- 2-substituted-4*H*-[1,2,4]triazolo[1,5-*a*][1,3,5]triazin-5-one (5 mmol) was suspended in aqueous NaOH (15 mmol) solution. To it, hydrogen peroxide (10 mmol) was added and allowed the reaction mixture to stir at 60-70 °C for 4 hours. The reaction mixture was acidified (pH 1-3) using 2.5 M HCl. The solid afforded was collected by filtration, washed well with cold water, and recrystallized by aqueous ethanol.

2-(Methylthio)-[1,2,4]triazolo[1,5-*a*][1,3,5]triazin-5,7(4*H*,6*H*)-dione (H2a)

Yield 68 %; mp 284-286 °C (EtOH-water); ESI-MS *m/z* 198.1 (M-1)⁺; purity > 95%; *t_R* 2.20 min; ¹H NMR (300 MHz, DMSO-*d*₆): δ 2.54 (s, 3H, SMe), 11.82 (s, 1H, NH),

12.82 (s, 1H, NH); ¹³C NMR (75 MHz, DMSO-*d*₆): δ 13.3 (SMe), 142.6 (C-2), 148.6 (C-9), 151.9 (C-5), 163.9 (C-7).

2-Phenyl-[1,2,4]triazolo[1,5-*a*][1,3,5]triazin-5,7(4*H*,6*H*)-dione (H2b)

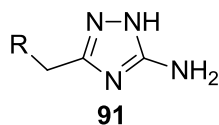
Yield 54%; mp 318-319 °C (EtOH-water), ESI-MS *m/z* 228.2 (M-1)⁺; purity > 95%; *t*_R 2.31 min; ¹H NMR (300 MHz, DMSO-*d*₆): δ 7.52-7.54 (m, 3H, H-3', H-4' and H-5'), 8.03-8.05 (m, 2H, H-2' and H-6'), 11.94 (s, 1H, NH), 12.90 (s, 1H, NH); ¹³C NMR (75 MHz, DMSO-*d*₆): δ 127.0 (C-2' and C-6'), 129.4 (C-3' and C-5'), 130.0 (C-4'), 131.0 (C-1'), 143.9 (C-2), 149.3 (C-9), 152.5 (C-5), 162.2 (C-7).

9.1.4 General procedure for the synthesis 2-benzyl-5-thioxo-5,6-dihydro[1,2,4]triazolo[1,5-*a*][1,3,5]triazin-7(4*H*)-one and its derivatives (H7, H8 and H9)

- General procedure for synthesis of benzyl-1*H*-1,2,4-triazol-5-amine and its derivatives (**91**)

A mixture of aryl acetic acid or aryl acetyl chloride (10 mmol) and aminoguanidine HCl (20 mmol) were heated in an oil bath for 20 minutes at 180-185 °C. After cooling, water (25 ml) was added with continuous stirring to make a homogeneous suspension. To it, 2 ml 5M NaOH was added to basify the suspension. The precipitated products ((het)arylamidoguanidines) was filtered, washed with water and dried. The (het)arylamidoguanidines (5 mmol) were treated with microwave irradiation power (100W) for 5 to 8 minutes in water. After cooling, the precipitated products were filtered off, washed with ice-cold water and recrystallized by ethanol or aqueous-ethanol.

- Synthesis of benzyl triazole and their ^1H NMR spectral data (* signals of the minor tautomeric form 3-amino-1,2,4-triazoles).



3-Benzyl-1*H*-1,2,4-triazole-5-amine (91a)

Yield 65 %; mp 155-156 °C (water); ^1H NMR (300 MHz, DMSO-*d*₆): δ 3.72 (s, 2H, CH₂), 5.08* and 5.85 (two s, 2H, NH₂), 7.17-7.26 (m, 5H, Ph), 11.68 and 12.52* (two s, 1H, NH).

3-(4-(Trifluoromethyl)benzyl)-1*H*-1,2,4-triazole-5-amine (91b)

Yield 72 %; mp 168-170 °C (water-ethanol); ^1H NMR (300 MHz, DMSO-*d*₆): δ 3.86 (s, 2H, CH₂), 5.16* and 5.88 (two s, 2H, NH₂), 7.48 (d, 2H, H-3' and H-5', $J = 8.0$ Hz), 7.63 (d, 2H, H-2' and H-6', $J = 8.0$ Hz), 11.74 and 12.55* (two s, 1H, NH).

3-(4-Chlorobenzyl)-1*H*-1,2,4-triazole-5-amine (91c)

Yield 78 %; mp 170 °C (water-ethanol); ^1H NMR (300 MHz, DMSO-*d*₆): δ 3.73 (s, 2H, CH₂), 5.09* and 5.84 (two s, 2H, NH₂), 7.27 (d, 2H, H-3' and H-5', $J = 8.4$ Hz), 7.32 (d, 2H, H-2' and H-6', $J = 8.1$ Hz), 11.68 and 12.48* (two s, 1H, NH).

3-(4-Bromobenzyl)-1*H*-1,2,4-triazole-5-amine (91d)

Yield 72 %; mp 176-177 °C (water-ethanol); ^1H NMR (300 MHz, DMSO-*d*₆): δ 3.72 (s, 2H, CH₂), 5.11* and 5.83 (two s, 2H, NH₂), 7.21 (d, 2H, H-3' and H-5', $J = 8.0$ Hz), 7.46 (d, 2H, H-2' and H-6', $J = 8.0$ Hz), 11.67 and 12.47* (two s, 1H, NH).

3-(4-Fluorobenzyl)-1*H*-1,2,4-triazole-5-amine (91e)

Yield 68 %; mp 157-159 °C (water-ethanol); ¹H NMR (300 MHz, DMSO-*d*₆): δ 3.72 (s, 2H, CH₂), 5.10* and 5.87 (two s, 2H, NH₂), 7.03-7.16 (m, 2H, H-3' and H-5'), 7.23-7.33 (m, 2H, H-2' and H-6'), 11.70 and 12.51* (two s, 1H, NH).

3-(4-Methylbenzyl)-1*H*-1,2,4-triazole-5-amine (91f)

Yield 81 %; mp 181-183 °C (water-ethanol); ¹H NMR (300 MHz, DMSO-*d*₆): δ 2.24 (s, 3H, Me), 3.66 (s, 2H, CH₂), 5.05* and 5.82 (two s, 2H, NH₂), 7.06 (d, 2H, H-3' and H-5', *J* = 7.2 Hz), 7.13 (d, 2H, H-2' and H-6', *J* = 8.0 Hz), 11.64 and 12.46* (two s, 1H, NH).

3-(4-Methoxybenzyl)-1*H*-1,2,4-triazole-5-amine (91g)

Yield 83 %; mp 170-172 °C (water-ethanol); ¹H NMR (300 MHz, DMSO-*d*₆): δ 3.68 (s, 2H, CH₂), 3.70 (s, 3H, MeO), 5.11* and 5.81 (two s, 2H, NH₂), 6.83 (d, 2H, H-3' and H-5', *J* = 8.5 Hz), 7.15 (d, 2H, H-2' and H-6', *J* = 8.8 Hz), 11.64 and 12.43* (two s, 1H, NH).

3-(4-Hydroxybenzyl)-1*H*-1,2,4-triazole-5-amine (91h)

Yield 68 %; mp 205-207 °C (water-ethanol); ¹H NMR (300 MHz, DMSO-*d*₆): δ 3.57 (s, 2H, CH₂), 5.10* and 5.76 (two s, 2H, NH₂), 6.64 (d, 2H, H-3' and H-5', *J* = 7.8 Hz), 7.02 (d, 2H, H-2' and H-6', *J* = 8.4 Hz), 9.13 (s, 1H, OH) 11.57 and 12.53* (two s, 1H, NH).

3-(4-Cyanobenzyl)-1*H*-1,2,4-triazole-5-amine (91i)

Yield 66 %; mp 212-213 °C (water-ethanol); ¹H NMR (300 MHz, DMSO-*d*₆): δ 3.86 (s, 2H, CH₂), 5.25* and 5.89 (two s, 2H, NH₂), 7.46 (d, 2H, H-3' and H-5', *J* = 8.5 Hz), 7.74 (d, 2H, H-2' and H-6', *J* = 8.3 Hz), 11.76 and 12.54* (two s, 1H, NH).

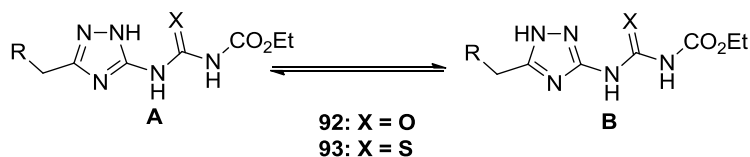
3-(3,4-Dichlorobenzyl)-1*H*-1,2,4-triazole-5-amine (91j)

Yield 67 %; mp 212-214 °C (water-ethanol); ¹H NMR (300 MHz, DMSO-*d*₆): δ 3.77 (s, 2H, CH₂), 5.14* and 5.90 (two s, 2H, NH₂), 7.24-7.27 (m, 1H, H-6'), 7.52-7.54 (m, 2H, H-2' and H-5'), 11.74 and 12.51* (two s, 1H, NH).

- General procedure for synthesis of N-(3(5)-substituted-benzyl-1,2,4-triazol-5(3)-yl)-N'-carbethoxythioureas/carbethoxyurea (**93**, **92**)

In a well stirred suspension of 3-benzyl-1*H*-1,2,4-triazole-5-amine and its derivatives (3 mmole) in anhydrous dimethylformamide (DMF, 4 ml), ethoxycarbonyl isothiocyanate (3.3 mmole) or ethoxycarbonyl isocyanate (3.3 mmole) was added and stirred the reaction mixture for 4.5-5 hours at room temperature. Following this step, 50-60 ml water was added to get more precipitated product. The product was filtered and washed with cold water. The products obtained were recrystallized from ethanol or aqueous-ethanol system.

Table 22. Synthesis of N-(3(5)-substituted-benzyl-1,2,4-triazol-5(3)-yl)-N'-carbethoxythioureas/carbetoxyurea and their ¹H NMR spectral data



Cpd	R	¹ H NMR (400 MHz, DMSO- <i>d</i> ₆)							
		CO ₂ Et	CH ₂	Ar	tautomer A			tautomer B	
					NH	NH	N(1)H	2NH	N(1)H
93a	C ₆ H ₅ - % Yield: 74, mp:160-163 °C (Ethanol)	1.24, t, 3H, <i>J</i> = 7.0 Hz; 4.20, q, 2H, <i>J</i> = 7.0 Hz	4.07	7.16-7.39, m, 5H	11.76	12.06	13.54	11.46	13.80
93b	4-CF ₃ C ₆ H ₄ % Yield: 82, mp:154-158 °C, (Water-Ethanol)	1.25, t, 3H, <i>J</i> = 7.0 Hz; 4.21, q, 2H, <i>J</i> = 6.7 Hz	4.09	7.52-7.54, m, 2H; 7.69-7.71, m, 2H	11.80	12.08	13.61	11.47	13.86
93d	4-ClC ₆ H ₄ % Yield: 83, mp:132-135 °C, (Water-Ethanol)	1.25, t, 3H, <i>J</i> = 6.9 Hz; 4.20, q, 2H, <i>J</i> = 6.9 Hz	4.08	7.31, d, <i>J</i> = 8.4 Hz, 2H; 7.39, d, <i>J</i> = 7.7 Hz, 2H	11.79	12.04	13.55	11.42	13.78
93e	4-BrC ₆ H ₄ % Yield: 80, mp:148-150 °C, (Water-Ethanol)	1.25, t, 3H, <i>J</i> = 7.0 Hz; 4.20, q, 2H, <i>J</i> = 7.0 Hz	4.06	7.25, d, <i>J</i> = 8.3 Hz, 2H; 7.51, d, <i>J</i> = 7.9 Hz, 2H	11.75	12.08	13.57	11.43	13.78
93f	4-FC ₆ H ₄ % Yield: 47, mp:133-135 °C, (Water-Ethanol)	1.25, t, 3H, <i>J</i> = 7.0 Hz; 4.20, q, 2H, <i>J</i> = 6.8 Hz	4.08	7.06-7.39, m, 4H	11.78	12.05	13.54	11.44	13.78
93g	4-MeC ₆ H ₄ % Yield: 75, mp:178-181 °C, (Water-Ethanol)	1.24, t, 3H, <i>J</i> = 7.0 Hz; 4.19, q, 2H, <i>J</i> = 6.8 Hz	4.01	2.26, s, 3H, Me; 7.11-7.17, m, 4H	11.78	12.04	13.49	11.42	13.75

Table 22. Synthesis of N-(3(5)-substituted-benzyl-1,2,4-triazol-5(3)-yl)-N'-carbethoxythioureas/carbetoxyurea and their ¹H NMR spectral data (Contd.)

Cpd	R	1H NMR (400 MHz, DMSO- <i>d</i> ₆)							
		CO ₂ Et	CH ₂	Ar	tautomer A			tautomer B	
					NH	NH	N(1)H	2NH	N(1)H
93h	4-MeOC ₆ H ₄ %Yield: 74, mp:164-166 °C, (Water-Ethanol)	1.25, t, 3H, <i>J</i> = 7.0 Hz; 4.20, q, 2H, <i>J</i> = 6.9 Hz	4.01	3.72, s, 3H, MeO; 6.88, d, 2H, <i>J</i> = 8.4 Hz; 7.20, d, 2H, <i>J</i> = 8.6 Hz	11.77	12.06	13.49	11.43	13.73
93i	4-OHC ₆ H ₄ %Yield: 76, mp: 198-200 °C, (Water-Ethanol)	1.25, t, 3H, <i>J</i> = 7.0 Hz; 4.20, q, 2H, <i>J</i> = 6.9 Hz	3.93	9.30, s, 1H, OH; 6.70, d, 2H, <i>J</i> = 8.3 Hz; 7.06, d, 2H, <i>J</i> = 8.4 Hz	11.77	12.03	13.46	11.41	13.69
93j	4-CNC ₆ H ₄ %Yield: 72, mp: 160-162 °C, (Water-Ethanol)	1.25, t, 3H, <i>J</i> = 7.0 Hz; 4.20, q, 2H, <i>J</i> = 7.0 Hz	4.15	7.50, d, 2H, <i>J</i> = 8.3 Hz; 7.80, d, 2H, <i>J</i> = 7.9 Hz	11.76	12.04	13.62	11.46	13.85
93k	3,4 Cl ₂ C ₆ H ₃ %Yield: 84, mp: 164-166 °C, (Water-Ethanol)	1.25, t, 3H, <i>J</i> = 7.0 Hz; 4.20, q, 2H, <i>J</i> = 6.9 Hz	4.12	7.28-7.30, m, 1H; 7.58-7.60, m, 2H	11.77	12.03	13.60	11.43	13.80
92	Ph-ethoxy urea %Yield: 68, mp:187-189 °C, (Water-Ethanol)	1.23, t, 3H, <i>J</i> = 7.0 Hz; 4.17, q, 2H, <i>J</i> = 7.0 Hz	3.88	7.20-7.44, m, 5H	10.41-10.51	10.59-10.68	13.13	9.95	13.55

- General procedure for synthesis of 2-benzyl-7-thioxo-6,7-dihydro-[1,2,4]triazolo[1,5-*a*][1,3,5]triazin-7(4*H*)-one and its derivatives (**H8-H8i**) and 2-benzyl-[1,2,4]triazolo[1,5-*a*][1,3,5]triazin-5,7(4*H*,6*H*)-dione (**H7**)

To a stirred solution of NaOH (9 mmol) in ethanol (80%, 20 ml), corresponding carbethoxyurea or carbethoxythiourea (3 mmol) was added and heated on water bath for 20 minutes with continuous stirring. After cooling, the solvent was evaporated under vacuum, and the residue was suspended in water (25 ml). The resulting suspension was acidified up to pH 1-3 using 2.5 M HCl. The precipitated product was filtered off, recrystallized with suitable solvent and dried under vacuum.

2-Benzyl-5-thioxo-5,6-dihydro-[1,2,4]triazolo[1,5-*a*][1,3,5]triazin-7(4*H*)-one (H8)

Yield 55 %; mp 246 °C (EtOH-water); ESI-MS *m/z* 242.3(M-1)⁺; purity > 95%; *t_R* 1.68 min (A); ¹H NMR (300 MHz, DMSO-*d*₆): δ 4.01(s, 2H, PhCH₂), 7.23-7.29 (m, 5H, Ph), 12.99 (s, 1H, NH), 14.10 (br. s, 1H, NH); ¹³C NMR (75 MHz, DMSO-*d*₆): δ 34.7 (CH₂), 127.1 (C-4'), 128.9 (C-2' and C-6'), 129.5 (C-3' and C-5'), 137.4 (C-1'), 141.6 (C-2), 151.5 (C-9), 165.0 (C-7), 175.8 (C-5).

5-Thioxo-2-(4-(trifluoromethyl)benzyl)-5,6-dihydro-[1,2,4]triazolo[1,5-*a*][1,3,5]triazin-7(4*H*)-one (H8a)

Yield 67 %; mp 280-281 °C (EtOH-water); ESI-MS *m/z* 326.1 (M-1)⁺; purity > 95%; *t_R* 4.53 min (A); ¹H NMR (300 MHz, DMSO-*d*₆): δ 4.15 (s, 2H, PhCH₂), 7.54 (d, 2H, H-3' and H-5', *J* = 7.9 Hz), 7.69 (d, 2H, H-2' and H-6', *J* = 7.9 Hz) 13.03 (s, 1H, NH), 14.12 (br. s, 1H, NH); ¹³C NMR (75 MHz, DMSO-*d*₆): δ 33.8 (CH₂), 124.3 (q, CF₃, *J* = 271.9 Hz), 125.1 (q, C-3' and C-5', *J* = 3.7 Hz), 127.4 (q, C-4', *J* = 31.8 Hz),

129.8 (C-2' and C-6'), 141.0 (C-1'), 141.7 (C-2), 151.1 (C-9), 163.8 (C-7), 175.2 (C-5).

2-(4-Chlorobenzyl)-5-thioxo-5,6-dihydro-[1,2,4]triazolo[1,5-*a*][1,3,5]triazin-7(4*H*)-one (H8b)

Yield 64 %; mp 241-243 °C (EtOH-water); ESI-MS *m/z* 292.2 (M-1)⁺; purity > 95%; *t_R* 5.44 min (D); ¹H NMR (300 MHz, DMSO-*d*₆): δ 4.02 (s, 2H, PhCH₂), 7.32 (d, 2H, H-3' and H-5', *J* = 8.6 Hz), 7.38 (d, 2H, H-2' and H-6', *J* = 8.5 Hz), 13.00 (s, 1H, NH), 14.14 (br. s, 1H, NH); ¹³C NMR (75 MHz, DMSO-*d*₆): δ 33.9 (CH₂), 128.7 (C-2' and C-6'), 131.3 (C-3' and C-5'), 131.8 (C-4'), 136.4 (C-1'), 141.6 (C-2), 151.6 (C-9), 164.6 (C-7), 175.8 (C-5).

2-(4-Bromobenzyl)-5-thioxo-5,6-dihydro-[1,2,4]triazolo[1,5-*a*][1,3,5]triazin-7(4*H*)-one (H8c)

Yield 65 %; mp 238-240 °C (EtOH-water); ESI-MS *m/z* 338.0 (M-1)⁺; purity > 95%; *t_R* 1.69 min (A); ¹H NMR (300 MHz, DMSO-*d*₆): δ 4.00 (s, 2H, PhCH₂), 7.26 (d, 2H, H-3' and H-5', *J* = 8.0 Hz), 7.51 (d, 2H, H-2' and H-6', *J* = 8.1 Hz) 12.98 (s, 1H, NH), 13.88 (br. s, 1H, NH); ¹³C NMR (75 MHz, DMSO-*d*₆): δ 33.40 (CH₂), 119.7 (C-4'), 131.1 (C-2' and C-6'), 131.2 (C-3' and C-5'), 136.2 (C-1'), 141.0 (C-2), 151.1 (C-9), 164.0 (C-7), 175.2 (C-5).

2-(4-Fluorobenzyl)-5-thioxo-5,6-dihydro-[1,2,4]triazolo[1,5-*a*][1,3,5]triazin-7(4*H*)-one (H8d)

Yield 72 %; mp 260-262 °C (EtOH-water); ESI-MS *m/z* 276.1 (M-1)⁺; purity > 95%; *t_R* 1.68 min (A); ¹H NMR (300 MHz, DMSO-*d*₆): δ 4.01 (s, 2H, PhCH₂), 7.11-7.16 (m, 2H, H-3' and H-5'), 7.32-7.35 (m, 2H, H-2' and H-6'), 13.00 (s, 1H, NH), 14.09

(br. s, 1H, NH); ^{13}C NMR (75 MHz, DMSO-*d*6): δ 33.8 (CH₂), 115.6 (d, C-3' and C-5', $J = 21.3$ Hz), 131.3 (d, C-2' and C-6', $J = 8.1$ Hz), 133.5 (d, C-1', $J = 3.7$ Hz), 141.6 (C-2), 151.5 (C-9), 161.6 (d, C-4', $J = 242.1$ Hz), 164.9 (C-7), 175.8 (C-5).

2-(4-Methylbenzyl)-5-thioxo-5,6-dihydro-[1,2,4]triazolo[1,5-*a*][1,3,5]triazin-7(4*H*)-one (H8e)

Yield 72 %; mp 244-246 °C (EtOH-water); ESI-MS m/z 272.1 (M-1)⁺; purity > 95%; t_{R} 1.68 min (A); ^1H NMR (300 MHz, DMSO-*d*6): δ 2.26 (s, 3H, Me), 3.96 (s, 2H, PhCH₂), 7.10 (d, 2H, H-3' and H-5', $J = 7.8$ Hz), 7.17 (d, 2H, H-2' and H-6', $J = 8.0$ Hz) 13.00 (s, 1H, NH), 14.03 (br. s, 1H, NH); ^{13}C NMR (75 MHz, DMSO-*d*6): δ 21.1 (Me), 34.3 (CH₂), 129.3 (C-2' and C-6'), 129.4 (C-3' and C-5'), 134.2 (C-4'), 136.1 (C-1'), 141.6 (C-2), 151.5 (C-9), 165.2 (C-7), 175.8 (C-5).

2-(4-Methoxybenzyl)-5-thioxo-5,6-dihydro-[1,2,4]triazolo[1,5-*a*][1,3,5]triazin-7(4*H*)-one (H8f)

Yield 78 %; mp 243-244 °C (EtOH-water); ESI-MS m/z 288.1 (M-1)⁺; purity > 95%; t_{R} 1.68 min (A); ^1H NMR (300 MHz, DMSO-*d*6): δ 3.72 (s, 3H, MeO), 3.93 (s, 2H, PhCH₂), 6.86 (d, 2H, H-3' and H-5', $J = 8.7$ Hz), 7.21 (d, 2H, H-2' and H-6', $J = 8.7$ Hz) 12.98 (s, 1H, NH), 14.09 (br. s, 1H, NH); ^{13}C NMR (75 MHz, DMSO-*d*6): δ 33.8 (CH₂), 55.5 (MeO), 114.2 (C-2' and C-6'), 129.2 (C-4'), 130.5 (C-3' and C-5'), 141.6 (C-1'), 151.4 (C-2), 158.5 (C-9), 165.3 (C-7), 175.8 (C-5).

2-(4-Hydroxybenzyl)-5-thioxo-5,6-dihydro-[1,2,4]triazolo[1,5-*a*][1,3,5]triazin-7(4*H*)-one (H8g)

Yield 65 %; mp 268-270 °C (EtOH-water); ESI-MS m/z 274.0 (M-1)⁺; purity > 95%; t_{R} 1.75 min (A); ^1H NMR (300 MHz, DMSO-*d*6): δ 3.87 (s, 2H, PhCH₂), 6.69 (d, 2H,

H-3' and H-5', $J = 8.2$ Hz), 7.08 (d, 2H, H-2' and H-6', $J = 8.2$ Hz), 9.26 (s, 1H, OH), 12.98 (s, 1H, NH), 14.05 (br. s, 1H, NH); ^{13}C NMR (75 MHz, DMSO- d_6): δ 33.9 (CH_2), 115.6 (C-2' and C-6'), 127.4 (C-4'), 130.4 (C-3' and C-5'), 141.6 (C-1'), 151.4 (C-2), 156.5 (C-9), 165.5 (C-7), 175.8 (C-5).

4-((7-Oxo-5-thioxo-4,5,6,7-tetrahydro-[1,2,4]triazolo[1,5-*a*][1,3,5]triazin-2-yl)methyl)benzotrile (H8h)

Yield 60 %; mp > 300 °C (EtOH-water); ESI-MS m/z 302.1 ($\text{M}-1$) $^+$; purity > 95%; t_R 1.64 min (A); ^1H NMR (300 MHz, DMSO- d_6): δ 4.10 (s, 2H, PhCH_2), 7.42 (d, 2H, H-3' and H-5', $J = 8.2$ Hz), 7.69 (d, 2H, H-2' and H-6', $J = 8.2$ Hz) 12.95 (s, 1H, NH), 13.71 (br. s, 1H, NH); ^{13}C NMR (75 MHz, DMSO- d_6): δ 34.0 (CH_2), 127.5 (C-4'), 129.1 (C-2' and C-6'), 129.3 (C-3' and C-5'), 141.1 (C-1'), 142.0 (C-2), 163.9 (C-9), 167.0 (C-7), 175.4 (C-5).

2-(3,4-Dichlorobenzyl)-5-thioxo-5,6-dihydro-[1,2,4]triazolo[1,5-*a*][1,3,5]triazin-7(4*H*)-one (H8i)

Yield 57 %; mp 265-267 °C (EtOH-water); ESI-MS m/z 326.1 ($\text{M}-1$) $^+$; purity > 95%; t_R 1.75 min (A); ^1H NMR (300 MHz, DMSO- d_6): δ 4.07 (s, 2H, PhCH_2), 7.30-7.33 (m, 1H, H-2'), 7.56-7.59 (m, 3H, H-5' and H-6'), 13.04 (s, 1H, NH), 14.15 (br. s, 1H, NH); ^{13}C NMR (75 MHz, DMSO- d_6): δ 33.5 (CH_2), 129.8 (C-6'), 130.0 (C-2'), 130.9 (5'), 131.3 (C-4'), 138.5 (C-1'), 141.6 (C-2), 151.6 (C-9), 164.1 (C-7), 175.8 (C-5).

2-Benzyl-[1,2,4]triazolo[1,5-*a*][1,3,5]triazine-5,7(4*H*,6*H*)-dione (H7)

Yield 47 %; mp > 300 °C (EtOH-water); ESI-MS m/z 242.3 ($\text{M}-1$) $^+$; purity > 95%; t_R 4.41 min (D); ^1H NMR (300 MHz, DMSO- d_6): δ 4.00 (s, 2H, PhCH_2), 7.04-7.61 (m, 5H, Ar-H), 11.81 (s, 1H, NH), 12.69 (br. s, 1H, NH); ^{13}C NMR (75 MHz, DMSO- d_6):

δ 34.8 (CH₂), 127.04 (C-4'), 128.8 (C-2' and C-6'), 129.5 (C-3' and C-5'), 137.5 (C-1'), 143.9 (C-2), 149.4 (C-9), 152.1 (C-7), 164.8 (C-5).

- General procedure for synthesis of 2-benzyl-5-(methylthio)-[1,2,4]triazolo[1,5-*a*][1,3,5]triazin-7(6*H*)-thione (**H9**)

To a stirred solution of 7-Phenyl-2-thioxo-2,3-dihydro-1*H*-pyrazolo[1,5-*a*][1,3,5]triazin-4-one in 4 ml of 2.5 M NaOH, iodomethane (933 μ l, 7.5 mmol) was added, the stirring was continued for 30 min. A solid precipitate was observed which upon acidification (pH 1-3) with 2.5 M HCl afforded another solid. The precipitated solid was filtered, washed with ice cold water and recrystallized from water-ethanol system.

2-Benzyl-5-(methylthio)-[1,2,4]triazolo[1,5-*a*][1,3,5]triazin-7(6*H*)-thione (H9)

Yield 54 %; mp 96-98°C (EtOH-water); ESI-MS m/z 272.3 (M-1)⁺; purity > 95%; t_R 2.08 min (A); ¹H NMR (300 MHz, DMSO-*d*₆): δ 2.54 (s, 3H, SMe), 4.04 (s, 2H, PhCH₂), 7.20-7.37 (m, 5H, Ar-H), 13.11 (br. s, 1H, NH); ¹³C NMR (75 MHz, DMSO-*d*₆): δ 13.2 (SMe), 34.4 (CH₂), 126.4 (C-4'), 128.2 (C-2' and C-6'), 128.8 (C-3' and C-5'), 137.1 (C-1'), 143.6 (C-2), 157.1 (C-9), 164.6 (C-7), 165.3 (C-5).

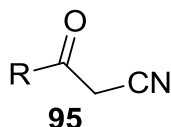
9.1.5 General procedure for the synthesis pyrazolo[1,5-*a*][1,3,5]triazin (H10, H11, H12 and H14)

- General procedure for synthesis of cyanoacetophenone (**95**)^{209, 210}

The bromoacetophenone (10 mmol) was dissolved in 20 ml ethanol and stirred together with a solution of 20 mmol NaCN in 10 ml water at room temperature for 1 hour. The brownish solution was filtered and the solvent evaporated to dryness in

vacuum. The residue was suspended in 50 ml water and stirred for additional 3 hours at room temperature. The mixture was filtered and the filtrate was acidified with concentrated hydrochloric acid to afford cyanoacetophenone.

- Synthesis of cyanoacetophenone and their ^1H NMR spectral data



3-Oxo-3-phenylpropanenitrile (95a)

Yield 79 %; mp 68-69 °C; ^1H NMR (300 MHz, DMSO-*d*6): δ 4.76 (s, 2H, CH₂), 7.54-7.99 (m, 5H, Ar-H).

3-Oxo-3-(4-chlorophenyl)-propanenitrile (95b)

Yield 82 %; mp 115-117 °C; ^1H NMR (300 MHz, DMSO-*d*6): δ 4.75 (s, 2H, CH₂), 7.65 (d, 2H, H-3' and -5', $J = 8.5$ Hz), 7.94 (d, 2H, H-2' and -6', $J = 8.6$ Hz).

3-Oxo-3-(4-bromophenyl)-propanenitrile (95c)

Yield 84 %; mp 146-148 °C; ^1H NMR (300 MHz, DMSO-*d*6): δ 4.74 (s, 2H, CH₂), 7.79 (d, 2H, H-3' and -5', $J = 8.6$ Hz), 7.86 (d, 2H, H-2' and -6', $J = 8.7$ Hz).

3-Oxo-3-(4-fluorophenyl)-propanenitrile (95d)

Yield 73 %; mp 50-52 °C; ^1H NMR (300 MHz, DMSO-*d*6): δ 4.76 (s, 2H, CH₂), 7.38-7.45 (m, 2H, H-3' and -5'), 8.00-8.05 (m, 2H, H-2' and -6')

3-Oxo-3-(4-methylphenyl)-propanenitrile (95e)

Yield 64 %; mp 90-92 °C; ^1H NMR (300 MHz, DMSO-*d*6): δ 2.39 (s, 3H, Me), 4.71 (s, 2H, CH₂), 7.37 (d, 2H, H-3' and -5', $J = 7.9$ Hz), 7.84 (d, 2H, H-2' and -6', $J = 8.3$ Hz).

3-Oxo-3-(4-methoxyphenyl)-propanenitrile (95f)

Yield 71 %; mp 100-102 °C; ¹HNMR (300 MHz, DMSO-*d*6): δ 3.86 (s, 3H, MeO), 4.67 (s, 2H, CH₂), 7.08 (d, 2H, H-3' and -5', *J* = 8.9 Hz), 7.91 (d, 2H, H-2' and -6', *J* = 8.8 Hz).

3-Oxo-3-(4-cyanophenyl)-propanenitrile (95g)

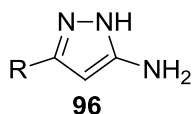
Yield 57 %; mp 102-104 °C; ¹HNMR (300 MHz, DMSO-*d*6): δ 4.80 (s, 2H, CH₂), 7.78-8.19 (m, 4H, Ar-H).

3-Oxo-3-(3,4-dichlorophenyl)-propanenitrile (95h)

Yield 72 %; mp 94-95 °C; ¹HNMR (300 MHz, DMSO-*d*6): δ 4.77 (s, 2H, CH₂), 7.38-8.31 (m, 3H, Ar-H).

- General procedure for synthesis of pyrazol-3-ylamine derivatives (**96**)²¹¹
Cyanoacetophenone (5 mmol) prepared by above mentioned procedure were subjected to microwave irradiation at 150 °C for one hour in ethanol in presence of hydrazine hydrate (10 mmol). After cooling, the ethanol was evaporated and the residue was triturated with diethyl ether (DEE) and precipitated products were filtered off, washed with DEE and recrystallized by DEE and methanol.

- Synthesis of pyrazol-3-ylamine derivatives and their ¹H NMR spectral data



3-Phenyl-1H-pyrazol-5-amine (96a)

Yield 75 %; mp 115-117 °C (DEE-methanol); ¹H NMR (300 MHz, DMSO-*d*6): δ 4.75 (br.s, 2H, NH₂), 5.75 (s, 1H, CH), 7.24-7.27 (m, 1H, H-4'), 7.35-7.39 (m, 2H, H-3' and -5'), 7.63-7.65 (m, 2H, H-2' and -6'), 11.89 (br.s, 1H, NH).

3-(4-Chlorophenyl)-1*H*-pyrazol-5-amine (96b)

Yield 88 %; mp 165-166 °C (DEE-methanol); ¹H NMR (300 MHz, DMSO-*d*₆): δ 5.28(br.s, 2H, NH₂), 5.76 (s, 1H, CH), 7.42 (d, 2H, H-3' and -5', *J* = 8.7 Hz), 7.67 (d, 2H, H-2' and -6', *J* = 8.7 Hz), 10.73 (br.s, 1H, NH).

3-(4-Bromophenyl)-1*H*-pyrazol-5-amine (96c)

Yield 81 %; mp 164-166 °C (DEE-methanol); ¹H NMR (300 MHz, DMSO-*d*₆): δ 4.91 (br.s, 2H, NH₂), 5.75 (s, 1H, CH), 7.55 (d, 2H, H-3' and -5', *J* = 8.5 Hz), 7.61 (d, 2H, H-2' and -6', *J* = 8.6 Hz), 11.80 (br.s, 1H, NH).

3-(4-Fluorophenyl)-1*H*-pyrazol-5-amine (96d)

Yield 61 %; mp 84-86 °C (DEE-methanol); ¹H NMR (300 MHz, DMSO-*d*₆): δ 4.83 (br.s, 2H, NH₂), 5.73 (s, 1H, CH), 7.20 (dd, 2H, H-3' and -5', *J* = 8.7, 8.7 Hz), 7.68 (dd, 2H, H-2' and -6', *J* = 8.8, 5.6 Hz), 11.69 (br.s, 1H, NH).

3-(4-Methylphenyl)-1*H*-pyrazol-5-amine (96e)

Yield 72 %; mp 148-150 °C (DEE-methanol); ¹H NMR (300 MHz, DMSO-*d*₆): δ 2.30 (s, 3H, Me), 4.75 (br.s, 2H, NH₂), 5.72 (s, 1H, CH), 7.17 (d, 2H, H-3' and -5', *J* = 7.9 Hz), 7.53 (d, 2H, H-2' and -6', *J* = 7.9 Hz), 11.80 (br.s, 1H, NH)

3-(4-Methoxyphenyl)-1*H*-pyrazol-5-amine (96f)

Yield 68 %; mp 129-131 °C (DEE-methanol); ¹H NMR (300 MHz, DMSO-*d*₆): δ 3.33 (s, 3H, MeO), 4.75 (br.s, 2H, NH₂), 5.68 (s, 1H, CH), 6.94 (d, 2H, H-3' and -5', *J* = 8.7 Hz), 7.57 (d, 2H, H-2' and -6', *J* = 8.7 Hz), 11.63 (br.s, 1H, NH).

3-(4-Cyanophenyl)-1H-pyrazol-5-amine (96g)

Yield 69 %; mp 176-178 °C (DEE-methanol); ¹H NMR (300 MHz, DMSO-*d*6): δ 5.02 (br.s, 2H, NH₂), 5.85 (s, 1H, CH), 7.79-7.86 (m, 4H, Ar-H), 11.94 (br.s, 1H, NH).

3-(3,4-Dichlorophenyl)-1H-pyrazol-5-amine (96h)

Yield 79 %; mp 138-140 °C (DEE-methanol); ¹H NMR (300 MHz, DMSO-*d*6): δ 4.99 (br.s, 2H, NH₂), 5.73 (s, 1H, CH), 7.59-7.66 (m, 2H, H-5' and 6'), 7.89-7.90 (m, 1H, H-2'), 11.82 (br.s, 1H, NH).

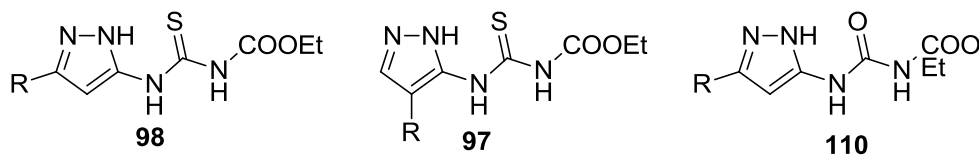
3-(*t*-Butyl)-1H-pyrazol-5-amine (96i)

Yield 76 %; oil; ¹H NMR (300 MHz, DMSO-*d*6): δ 1.18 (s, 9H, C(CH₃)₃), 4.38 (br.s, 2H, NH₂), 5.18 (s, 1H, CH), 10.80 (br.s, 1H, NH)

- General procedure for synthesis of N-carbethoxy-N'-(3-aryl-pyrazolyl)thiourea/urea derivatives (**97**, **98** and **110**)

In a well stirred suspension of aminopyrazol (3 mmol) in anhydrous dimethylformamide (DMF, 4 ml), ethoxycarbonyl isothiocyanate (3.3 mmol) or ethoxycarbonyl isocyanate (3.3 mmol) was added and stirred the reaction mixture for 4.5-5 hours at room temperature. Following this step, 50-60 ml water was added to this reaction mixture and the precipitate thus formed was filtered and washed with cold water and it was recrystallized from ethanol or aqueous-ethanol system.

Table 23. Synthesis of N-carbethoxy-N'-(3-aryl-pyrazolyl)thiourea/urea derivatives and their ¹H NMR spectral data



Cpd	R	¹ H NMR (300 MHz, DMSO- <i>d</i> ₆)					
		CO ₂ Et	CH	Ar	NH	NH	N(1)H
98a	Ph % yield: 89, mp: 275 °C , (Ethanol- water)	1.27, t, 3H, <i>J</i> = 7.1 Hz; 4.23, q, 2H, <i>J</i> = 7.1 Hz	7.39	7.37, t, 1H, <i>J</i> = 7.4 Hz; 7.47, t, 2H, <i>J</i> = 7.7 Hz; 7.74, d, 2H, <i>J</i> = 7.3 Hz	11.37	12.04	13.23
98b	4-ClC ₆ H ₄ % yield: 92, mp: 275-277 °C , (Ethanol-water)	1.27, t, 3H, <i>J</i> = 7.1 Hz; 4.23, q, 2H, <i>J</i> = 7.1 Hz	7.43	7.53, d, 2H, <i>J</i> = 8.2 Hz; 7.76, d, 2H, <i>J</i> = 8.5 Hz	11.38	12.04	13.29
98c	4-BrC ₆ H ₄ % yield: 89, mp: 279-281 °C , (Ethanol-water)	1.27, t, 3H, <i>J</i> = 7.0 Hz; 4.23, q, 2H, <i>J</i> = 7.0 Hz	7.44	7.66, d, 2H, <i>J</i> = 8.7 Hz; 7.70, d, 2H, <i>J</i> = 8.7 Hz	11.38	12.04	13.30
98d	4-FC ₆ H ₄ % yield: 80, mp: 255-257 °C , (Ethanol-water)	1.27, t, 3H, <i>J</i> = 7.0 Hz; 4.23, q, 2H, <i>J</i> = 7.0 Hz	7.38	7.31, t, 2H, <i>J</i> = 8.7 Hz; 7.78, dd, 2H, <i>J</i> = 8.7, 5.3 Hz	11.37	12.03	13.21
98e	4-MeC ₆ H ₄ % yield: 84, mp: 263-264 °C , (Ethanol-water)	1.27, t, 3H, <i>J</i> = 7.1 Hz; 4.23, q, 2H, <i>J</i> = 7.1 Hz	7.35	2.33, s, 3H, Ar- Me; 7.27, d, 2H, <i>J</i> = 8.0 Hz; 7.62, d, 2H, <i>J</i> = 8.2 Hz	11.35	12.03	13.13
98f	4-MeOC ₆ H ₄ % yield: 89, mp: 250 °C , (Ethanol- water)	1.27, t, 3H, <i>J</i> = 7.1 Hz; 4.23, q, 2H, <i>J</i> = 7.1 Hz	7.30	3.80, s, 3H, Ar- MeO; 7.03, d, 2H, <i>J</i> = 8.8 Hz; 7.66, d, 2H, <i>J</i> = 8.8 Hz	11.34	12.02	13.05
98g	4-CNC ₆ H ₄ % yield: 78, mp: 290-292 °C , (Ethanol-water)	1.26, t, 3H, <i>J</i> = 7.0 Hz; 4.22, q, 2H, <i>J</i> = 7.0 Hz	7.55	3.41, m, 4H	11.40	12.04	13.50
98h	(3,4) DiClC ₆ H ₃ % yield: 82, mp: 185 °C , (Ethanol- water)	1.27, t, 3H, <i>J</i> = 7.0 Hz; 4.22, q, 2H, <i>J</i> = 7.0 Hz	7.50	7.74, m, 2H; 8.05, m, 1H.	11.39	12.03	13.36

Table 23. Synthesis of N-carbethoxy-N'-(3-aryl-pyrazolyl)thiourea/urea derivatives and their ¹H NMR spectral data (Contd.)

Cpd	R	¹ H NMR (300 MHz, DMSO- <i>d</i> ₆)					
		CO ₂ Et	CH	Ar	NH	NH	N(1)H
98i	<i>t-butyl</i> % yield: 81, mp: 270 °C, (Ethanol-water)	1.24, t, 3H, <i>J</i> = 7.2 Hz; 4.21, q, 2H, <i>J</i> = 7.0 Hz	6.83	1.22-1.27, m, 12 H	11.25	11.97	12.43
97	Ph urea % yield: 89, mp: 250 °C, (Ethanol-water)	1.25, t, 3H, <i>J</i> = 7.0 Hz; 4.19, q, 2H, <i>J</i> = 7.0 Hz	6.79	7.31-7.39, m, 1H, 7.41-7.50, m, 2H, 7.69-7.79, m, 2H	10.06	1.43	12.90
110	8 ph thiourea % yield: 84, mp: 191-192 °C, (Ethanol-water)	1.26, t, 3H, <i>J</i> = 7.0 Hz; 4.21, q, 2H, <i>J</i> = 7.1 Hz	-	7.20, t, 1H, <i>J</i> = 7.5 Hz; 7.33, t, 2H, <i>J</i> = 7.6 Hz; 7.48, d, 2H, <i>J</i> = 7.8 Hz; 8.12, s, 1H	11.08	11.35	12.94

- General procedure for synthesis of 7-phenyl-2-thioxo-2,3-dihydro-1*H*-pyrazolo[1,5-*a*][1,3,5]triazin-4-one (**H11-H11h**), 8-phenyl-2-thioxo-2,3-dihydropyrazolo[1,5-*a*][1,3,5]triazin-4(1*H*)-one (**H14**), and 7-phenyl-1*H*-pyrazolo[1,5-*a*][1,3,5]triazin-2,4-dione (**H10**)^{41,44}

To a stirred solution of NaOH (9 mmol) in ethanol (80%, 20 ml), corresponding carbethoxyurea or carbethoxythiourea (3 mmol) was added and heated on water bath for 20 minutes with continuous stirring. After cooling, the solvent was evaporated under vacuum, and the residue was suspended in water (25 ml). The resulting suspension was acidified up to pH 1-3 using 2.5 M HCl. The precipitated product was filtered off, recrystallized with suitable solvent and dried under vacuum.

7-Phenyl-2-thioxo-2,3-dihydro-1H-pyrazolo[1,5-a][1,3,5]triazin-4-one (H11)

Yield 71%; mp 286-288 °C (Ethanol-water); ESI-MS m/z 243.0 (M-1)⁺; purity > 95%; t_R 5.32 min (B); ¹H NMR (300 MHz, DMSO-*d*6): δ 6.39 (s, 1H, CH), 7.38-7.54 (m, 3H, H-3', H-4' and H-5'), 7.88-8.00 (m, 2H, H-2' and H-6'), 12.75 (s, 1H, NH), 13.56 (s, 1H, NH); ¹³C NMR (75 MHz, DMSO-*d*6): δ 87.3 (C-8), 126.8 (C-3' and C-5'), 129.4 (C-2' and C-6'), 130.1 (C-4'), 131.7 (C-1'), 142.0 (C-7), 142.1 (C-9), 155.9 (C-4), 173.6 (C-2).

7-(4-Chloro-Phenyl)-2-thioxo-2,3-dihydro-1H-pyrazolo[1,5-a][1,3,5]triazin-4-one (H11a)

Yield 69%; mp 290-292 °C (Ethanol-water); ESI-MS m/z 277.2 (M-1)⁺; purity > 95%; t_R 6.37 min (B); ¹H NMR (300 MHz, DMSO-*d*6): δ 6.43 (s, 1H, CH), 7.54 (d, 2H, H-3' and H-5', $J = 8.3$), 7.98 (d, 2H, H-2' and H-6', $J = 8.3$), 12.79 (s, 1H, NH), 13.58 (s, 1H, NH). ¹³C NMR (75 MHz, DMSO-*d*6): δ 87.3 (C-8), 128.5 (C-2' and C-6'), 129.4 (C-3' and C-5'), 130.6 (C-4'), 134.7 (C-1'), 141.9 (C-7), 142.3 (C-9), 154.7 (C-4), 173.6 (C-2).

7-(4-Bromo-Phenyl)-2-thioxo-2,3-dihydro-1H-pyrazolo[1,5-a][1,3,5]triazin-4-one (H11b)

Yield 66%; mp > 300 °C (Ethanol-water); ESI-MS m/z 322.9 (M-1)⁺; purity > 95%; t_R 6.62 min (B); ¹H NMR (300 MHz, DMSO-*d*6): δ 6.42 (s, 1H, CH), 7.66 (d, 2H, H-3' and H-5', $J = 8.3$), 7.90 (d, 2H, H-2' and H-6', $J = 8.3$), 12.77 (s, 1H, NH), 13.58 (s, 1H, NH). ¹³C NMR (75 MHz, DMSO-*d*6): δ 87.3 (C-8), 123.4 (C-4'), 128.8 (C-2')

and C-6'), 131.0 (C-3' and C-5'), 132.3 (C-1'), 141.9 (C-7), 142.3 (C-9), 154.8 (C-4), 173.6 (C-2).

7-(4-Fluoro-Phenyl)-2-thioxo-2,3-dihydro-1H-pyrazolo[1,5-a][1,3,5]triazin-4-one (H11c)

Yield 74%; mp 270-272 °C (Ethanol-water); ESI-MS m/z 261.3 (M-1)⁺; purity > 95%; *t_R* 5.56 min (B); ¹H NMR (300 MHz, DMSO-*d*₆): δ 6.40 (s, 1H, CH), 7.30 (dd, 2H, H-3' and H-5' J = 8.9, 8.9 Hz), 8.00 (dd, 2H, H-2' and H-6' J = 8.7, 5.7 Hz), 12.75 (s, 1H, NH), 13.56 (s, 1H, NH). ¹³C NMR (75 MHz, DMSO-*d*₆): 86.6 (C-8), 115.7 (d, C-3' and C-5', J = 21.8 Hz), 127.7 (d, C-1', J = 2.9 Hz), 128.4 (d, C-2' and C-6', J = 8.7 Hz), 141.4 (C-7), 141.6 (C-9), 154.4 (C-4), 162.8 (d, C-4', J = 246.3 Hz), 173.0 (C-2).

7-(4-Methyl-Phenyl)-2-thioxo-2,3-dihydro-1H-pyrazolo[1,5-a][1,3,5]triazin-4-one (H11d)

Yield 65%; mp 286-288 °C (Ethanol-water); ESI-MS m/z 257.3 (M-1)⁺; purity > 95%; *t_R* 5.93 min (B); ¹H NMR (300 MHz, DMSO-*d*₆): δ 3.58 (s, 3H, ArMe), 6.49 (s, 1H, CH), 7.42 (d, 2H, H-3' and H-5' J = 7.9), 7.96 (d, 2H, H-2' and H-6' J = 8.3), 12.89 (s, 1H, NH), 13.69 (s, 1H, NH). ¹³C NMR (75 MHz, DMSO-*d*₆): δ 21.5 (ArMe), 87.1 (C-8), 126.7 (C-2' and C-6'), 129.0 (C-1'), 129.9 (C-3' and C-5'), 139.7(C-7), 142.0 (C-9), 156.0 (C-4), 173.5 (C-2).

7-(4-Methoxy-Phenyl)-2-thioxo-2,3-dihydro-1H-pyrazolo[1,5-a][1,3,5]triazin-4-one (H11e)

Yield 68%; mp 292-294°C (Ethanol-water); ESI-MS m/z 273.0 (M-1)⁺; purity > 95%; *t*_R 5.27 min (B); ¹H NMR (300 MHz, DMSO-*d*₆): δ 3.82 (s, 3H, ArMeO), 6.33 (s, 1H, CH), 7.03 (d, 2H, H-3' and H-5' J = 9.0), 7.88 (d, 2H, H-2' and H-6' J = 8.7), 12.72 (s, 1H, NH), 13.53 (s, 1H, NH). ¹³C NMR (75 MHz, DMSO-*d*₆): δ 55.8 (ArMeO), 86.9 (C-8), 114.8 (C-2' and C-6'), 124.2 (C-1'), 128.3 (C-3' and C-5'), 142.0 (C-7), 155.8 (C-9), 160.9 (C-4), 173.5 (C-2).

7-(4-Cyano-Phenyl)-2-thioxo-2,3-dihydro-1H-pyrazolo[1,5-a][1,3,5]triazin-4-one (H11f)

Yield 61%; mp > 300 °C (Ethanol-water); ESI-MS m/z 287.2 (M-1)⁺; purity > 95%; *t*_R 4.41 min (B); ¹H NMR (300 MHz, DMSO-*d*₆): δ 6.50 (s, 1H, CH), 7.97-8.16 (m, 4H, Ar-H), 12.82 (s, 1H, NH), 13.64 (s, 1H, NH). ¹³C NMR (75 MHz, DMSO-*d*₆): δ 87.6-87.7 (C-8), 126.6-126.8 (C-2' and C-6'), 128.6-130.4 (C-3' and C-5'), 131.9 (C-4'), 134.3 (CN), 135.5-135.8 (C-1'), 142.0-142.3 (C-7), 154.9-155.1 (C-9), 167.4-167.9 (C-4), 173.6 (C-2).

7-(3,4-Dichloro-Phenyl)-2-thioxo-2,3-dihydro-1H-pyrazolo[1,5-a][1,3,5]triazin-4-one (H11g)

Yield 63%; mp 287-289 °C (Ethanol-water); ESI-MS m/z 312.9 (M-1)⁺; purity > 95%; *t*_R 7.68 min (B); ¹H NMR (300 MHz, DMSO-*d*₆): δ 6.52 (s, 1H, CH), 7.71 (d, 1H, H-6', J = 8.3 Hz), 7.94 (dd, 1H, H-5', J = 8.5 Hz, J = 2.1 Hz), 8.18 (d, 1H, H-2', J = 1.9 Hz), 12.80 (s, 1H, NH), 13.63 (s, 1H, NH). ¹³C NMR (75 MHz, DMSO-*d*₆): δ

87.7 (C-8), 126.7 (C-6'), 128.4 (C-2'), 131.6 (C-5'), 132.3 (C-4'), 132.4 (C-3'), 132.5 (C-1'), 141.9 (C-7), 142.3 (C-9), 153.6 (C-4), 173.6 (C-2).

7-*t*-Butyl-2-thioxo-2,3-dihydro-1H-pyrazolo[1,5-*a*][1,3,5]triazin-4-one (H11h)

Yield 55%; mp 268-270 °C (Ethanol-water); ESI-MS m/z 223.1 (M-1)⁺; purity > 95%; t_R 4.71 min (D); ¹H NMR (300 MHz, DMSO-*d*6): δ 1.23 (s, 9H, *t*-but), 5.83 (s, 1H, CH), 12.59 (s, 1H, NH), 13.37 (s, 1H, NH). ¹³C NMR (75 MHz, DMSO-*d*6): δ 30.1 (3CH₃), 33.0 (*t*-but), 87.1 (C-8), 141.1 (C-7), 142.0 (C-9), 167.5 (C-4), 173.4 (C-2).

8-Phenyl-2-thioxo-2,3-dihydropyrazolo[1,5-*a*][1,3,5]triazin-4(1*H*)-one (H14)

Yield 60%; mp 222-224 °C (Ethanol-water); ESI-MS m/z 245.0 (M-1)⁺; purity > 95%; t_R 6.17 min (B); ¹H NMR (300 MHz, DMSO-*d*6): δ 7.02 (m, 5H, Ar-H), 8.17 (s, 1H, CH), 12.80 (s, NH, 1H). ¹³C NMR (75 MHz, DMSO-*d*6): δ 106.5 (C-8), 128.1 (C-4'), 129.2 (C-2' and C-6'), 129.5 (C-3' and C-5'), 130.2 (C-1'), 137.2 (C-7), 142.6 (C-9), 146.2 (C-4), 174.9 (C-2).

7-Phenyl-1*H*-pyrazolo[1,5-*a*][1,3,5]triazin-2,4-dione (H10)

Yield 55 %; mp 312-314 °C (Ethanol-water); ESI-MS m/z 227.1 (M-1)⁺; purity > 95%; t_R 4.42 min (D); ¹H NMR (300 MHz, DMSO-*d*6): δ 6.30 (s, 1H, CH), 7.40-7.49 (m, 3H, H-3', H-4' and H-5'), 7.92 (d, 2H, H-2' and H-6', $J = 8.7$ Hz), 11.61 (s, 1H, NH), 12.00 (s, 1H, NH). ¹³C NMR (75 MHz, DMSO-*d*6): δ 85.9 (C-8), 126.0 (C-3' and C-5'), 128.7 (C-2' and C-6'), 129.2 (C-4'), 131.5 (C-1'), 141.7 (C-7), 144.2 (C-9), 148.3 (C-4), 155.0 (C-2).

- General procedure for synthesis of 2-methylsulfanyl-7-phenyl-3*H*-pyrazolo[1,5-*a*][1,3,5]triazin-4-one (**H12**)

To a stirred solution of 7-phenyl-2-thioxo-2,3-dihydro-1*H*-pyrazolo[1,5-*a*][1,3,5]triazin-4-one (**H11**) in 4 ml of 2.5 M NaOH, iodomethane (933 μ l, 7.5mmol) was added, the stirring was continued for 30 minutes. A solid precipitate was observed which upon acidification (pH 1-3) with 2.5 M HCl afforded another solid. The precipitated solid was filtered, washed with ice cold water and recrystallized from water-ethanol system.

2-Methylsulfanyl-7-phenyl-3*H*-pyrazolo[1,5-*a*][1,3,5]triazin-4-one (H12)

Yield 46 %; mp 240-242°C (Ethanol-water); ESI-MS m/z 257.3(M-1)⁺; purity > 95%; t_R 6.27 min (B); ¹H NMR (300 MHz, DMSO-*d*6): δ 6.90 (s, 1H, CH), 7.41-7.54 (m, 3H, H-3', H-4' and H-5'), 7.96-8.01 (m, 2H, H-2' and H-6'), 12.92 (s, 1H, NH). ¹³C NMR (75 MHz, DMSO-*d*6): δ 13.6 (SMe), 94.9 (C-8), 126.6 (C-3' and C-5'), 129.3 (C-2' and C-6'), 129.8 (C-4'), 132.4 (C-1'), 143.8 (C-7), 150.0 (C-9), 156.0 (C-4), 157.7 (C-2).

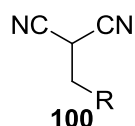
9.1.6 General procedure of synthesis of (8-benzyl-4-oxo-2-thioxo-1,2,3,4-tetrahydro pyrazolo[1,5-*a*][1,3,5]triazin-7-yl)-thiourea and their derivatives (13-13n)

- General procedure of synthesis of 2-benzyl-malononitrile and its derivatives (**100**)²¹²

In a 95% ethanolic (10 ml) solution of malononitrile (10 mmol) appropriate aromatic aldehyde (10 mmol) was added. The solution was stirred at room temperature until precipitation was complete or overnight. Following this step, additional ethanol (20

ml) was added and the mixture was cooled to 0 °C in an ice bath. NaBH₄ (5 mmol) was added to the vigorously stirred mixture and the reduction was completed in about 10 minutes. The reaction mixture was poured into a beaker containing cold water (40 ml) and 1.0 M HCl was added to quench all hydride. Additional cold water was introduced to afford more precipitation. The cold precipitate was collected by vacuum filtration and washed with cold water (Method A). If crystallization/precipitation did not occur, then the mixture was extracted using water and dichloromethane solvent system (Method B).

- Synthesis of 2-benzyl-malononitrile and its derivatives and their ¹H NMR spectral data



2-Benzyl-malononitrile (100a)

Yield 81 % (method A); mp 79 °C; ¹H NMR (300 MHz, DMSO-*d*₆): δ 3.33 (d, 2H, CH₂, *J* = 6.9 Hz), 5.11 (t, 1H, CH(CN)₂, *J* = 6.9 Hz), 7.33-7.41 (m, 5H, Ar-H).

2-(4-(Trifluoromethyl)benzyl)-malononitrile (100b)

Yield 76 % (method A); mp 68 °C; ¹H NMR (300 MHz, DMSO-*d*₆): δ 3.47 (d, 2H, CH₂, *J* = 6.6 Hz), 5.17 (t, 1H, CH(CN)₂, *J* = 6.9 Hz), 7.61 (d, 2H, H-3' and H-5', *J* = 8.1 Hz), 7.78 (d, 2H, H-2' and H-6', *J* = 8.1 Hz).

2-(4-Chlorobenzyl)-malononitrile (100c)

Yield 82 % (method A); mp 82 °C; ¹H NMR (300 MHz, DMSO-*d*₆): δ 3.34 (d, 2H, CH₂, *J* = 6.8 Hz), 5.10 (t, 1H, CH(CN)₂, *J* = 6.8 Hz), 7.40 (d, 2H, H-3' and H-5', *J* = 8.6 Hz), 7.47 (d, 2H, H-2' and H-6', *J* = 8.6 Hz).

2-(4-Bromobenzyl)-malononitrile (100d)

Yield 76 % (method A); mp 83-85 °C; ¹H NMR (300 MHz, DMSO-*d*₆): δ 3.33 (d, 2H, CH₂, *J* = 6.8 Hz), 5.10 (t, 1H, CH(CN)₂, *J* = 6.8 Hz), 7.34 (d, 2H, H-3' and H-5', *J* = 8.4 Hz), 7.60 (d, 2H, H-2' and H-6', *J* = 8.3 Hz).

2-(4-Fluorobenzyl)-malononitrile (100e)

Yield 69 % (method A); mp 113-115 °C; ¹H NMR (300 MHz, DMSO-*d*₆): δ 3.34 (d, 2H, CH₂, *J* = 6.9 Hz), 5.08 (t, 1H, CH(CN)₂, *J* = 6.9 Hz), 7.22 (dd, 2H, H-3' and H-5', *J* = 8.8, 8.8 Hz), 7.42 (d, 2H, H-2' and H-6', *J* = 8.6, 5.5 Hz).

2-(4-Phenylbenzyl)-malononitrile (100f)

Yield 78 % (method A); mp 114-116 °C; ¹H NMR (300 MHz, DMSO-*d*₆): δ 3.39 (m, 2H, CH₂), 5.15 (m, 1H, CH(CN)₂), 7.34-7.72 (m, 9H, Ar-H).

2-(4-Phenoxybenzyl)-malononitrile (100g)

Yield 74 % (method A); mp 98-100 °C; ¹H NMR (300 MHz, DMSO-*d*₆): δ 3.32 (d, 2H, CH₂, *J* = 6.8 Hz), 5.08 (t, 1H, CH(CN)₂, *J* = 6.9 Hz), 6.99-7.43 (m, 9H, Ar-H).

2-(4-Methylbenzyl)-malononitrile (100h)

Yield 73 % (method A); mp 72 °C; ¹H NMR (300 MHz, DMSO-*d*₆): δ 2.30 (s, 3H, Me), 3.29 (d, 2H, CH₂, *J* = 7.4 Hz), 5.06 (t, 1H, CH(CN)₂, *J* = 6.8 Hz), 7.19 (d, 2H, H-3' and H-5', *J* = 7.9 Hz), 7.25 (d, 2H, H-2' and H-6', *J* = 7.9 Hz).

2-(4-Ethylbenzyl)-malononitrile (100i)

Yield 82 % (method A); mp 52-54 °C; ¹H NMR (300 MHz, DMSO-*d*₆): δ 1.17 (t, 3H, CH₃, *J* = 7.6 Hz), 2.60 (d, 2H, CH₂, *J* = 7.6 Hz), 3.28 (d, 2H, CH₂, *J* = 5.5 Hz), 5.06 (t, 1H, CH(CN)₂, *J* = 6.5 Hz), 7.22 (d, 2H, H-3' and H-5', *J* = 7.6 Hz), 7.28 (d, 2H, H-2' and H-6', *J* = 7.9 Hz).

2-(4-Methoxybenzyl)-malononitrile (100j)

Yield 73 % (method A); mp 76-78 °C; ¹H NMR (300 MHz, DMSO-*d*₆): δ 3.26 (d, 2H, CH₂, *J* = 6.9 Hz), 3.75 (s, 3H, MeO), 5.03 (t, 1H, CH(CN)₂, *J* = 6.9 Hz), 6.94 (d, 2H, H-3' and H-5', *J* = 8.6 Hz), 7.29 (d, 2H, H-2' and H-6', *J* = 8.6 Hz).

2-(4-Hydroxybenzyl)-malononitrile (100k)

Yield 73 % (method A); mp 168-171 °C; ¹H NMR (300 MHz, DMSO-*d*₆): δ 3.19 (d, 2H, CH₂, *J* = 6.8 Hz), 4.98 (t, 1H, CH(CN)₂, *J* = 6.8 Hz), 6.75 (d, 2H, H-3' and H-5', *J* = 8.4 Hz), 7.16 (d, 2H, H-2' and H-6', *J* = 8.5 Hz), 9.49 (s, 1H, OH).

2-(4-Cyanobenzyl)-malononitrile (100l)

Yield 82 % (method A); mp 118-120 °C; ¹H NMR (300 MHz, DMSO-*d*₆): δ 3.47 (d, 2H, CH₂, *J* = 6.0 Hz), 5.17 (t, 1H, CH(CN)₂, *J* = 6.9 Hz), 7.59 (d, 2H, H-3' and H-5', *J* = 8.4 Hz), 7.89 (d, 2H, H-2' and H-6', *J* = 8.3 Hz).

2-(Furan-2-ylmethyl)malononitrile (100m)

Yield 85 % (method B); oil; ¹H NMR (300 MHz, DMSO-*d*₆): δ 3.45 (d, 2H, CH₂, *J* = 6.3 Hz), 5.13 (t, 1H, CH(CN)₂, *J* = 6.3 Hz), 6.39-6.42 (m, 1H, H-4'), 6.45-6.47 (m, 1H, H-3'), 7.67 (s, 1H, H-5').

2-(Thiophen-2-ylmethyl)malononitrile (100n)

Yield 56 % (method B); oil; ¹H NMR (300 MHz, DMSO-*d*₆): δ 3.60 (d, 2H, CH₂, *J* = 6.0 Hz), 5.11 (t, 1H, CH(CN)₂, *J* = 6.0 Hz), 7.05 (dd, 1H, H-4', *J* = 3.5 and 5.1 Hz), 7.12 (dd, 1H, H-3', *J* = 1.2 and 3.5 Hz), 7.50 (d, 1H, H-5', *J* = 1.3 and 5.1 Hz).

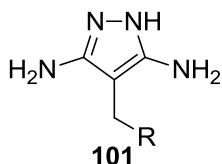
2-(Naphthalen-1-ylmethyl)malononitrile (100o)

Yield 55 % (method B); oil; ¹H NMR (300 MHz, DMSO-*d*₆): δ 3.89 (d, 2H, CH₂, *J* = 7.6 Hz), 5.89 (t, 1H, CH(CN)₂, *J* = 7.6 Hz), 7.48-8.30 (m, 8H, Ar-H).

- General procedure of synthesis of 4-benzyl-1*H*-pyrazol-3,5-diamine (**101**)

In an ethanolic suspension of 2-benzyl-malononitrile and its derivatives (3 mmol), hydrazine hydrate (6 mmol) was added and the resulting reaction mixture was refluxed for 3-10 hours. After refluxing, the ethanol was evaporated to dryness and the residue was recrystallized using suitable solvents or purified using column chromatography.

- Synthesis of 4-benzyl-1*H*-pyrazol-3,5-diamine and its derivatives and their ¹H NMR spectral data



4-Benzyl-1*H*-pyrazol-3,5-diamine (**101a**)

Yield 79 %; mp 144-146 °C (EA-hexane); ¹H NMR (300 MHz, DMSO-*d*₆): δ 3.49 (s, 2H, CH₂), 4.25 (br.s, 4H, (NH₂)₂), 7.07-7.24 (m, 5H, Ar-H), 9.69 (br.s, 1H, NH)

4-(4-(Trifluoromethyl)benzyl)-1*H*-pyrazol-3,5-diamine (**101b**)

Yield 67 %; mp 66-68 °C (EA-hexane); ¹H NMR (300 MHz, DMSO-*d*₆): δ 3.60 (s, 2H, CH₂), 4.37 (br.s, 4H, (NH₂)₂), 7.43 (d, 2H, H-3' and H-5', *J* = 8.0 Hz), 7.58 (d, 2H, H-2' and H-6', *J* = 8.0 Hz), 10.01 (br.s, 1H, NH).

4-(4-Chlorobenzyl)-1*H*-pyrazol-3,5-diamine (**101c**)

Yield 75 %; mp 152-154 °C (EA-hexane); ¹H NMR (300 MHz, DMSO-*d*₆): δ 3.48 (s, 2H, CH₂), 4.31 (br.s, 4H, (NH₂)₂), 7.22-7.28 (m, 4H, Ar-H), 9.85 (br.s, 1H, NH).

4-(4-Bromobenzyl)-1*H*-pyrazol-3,5-diamine (101d)

Yield 84 %; mp 166-168 °C (EA-hexane); ¹H NMR (300 MHz, DMSO-*d*₆): δ 3.47 (s, 2H, CH₂), 4.31 (br.s, 4H, (NH₂)₂), 7.17 (d, 2H, H-3' and H-5', *J* = 8.3 Hz), 7.40 (d, 2H, H-2' and H-6', *J* = 8.3 Hz), 9.97 (br.s, 1H, NH).

4-(4-Fluorobenzyl)-1*H*-pyrazol-3,5-diamine (101e)

Yield 59 %; mp 180-182 °C (EA-hexane); ¹H NMR (300 MHz, DMSO-*d*₆): δ 3.48 (s, 2H, CH₂), 4.30 (br.s, 4H, (NH₂)₂), 7.03 (dd, 2H, H-3' and H-5', *J* = 8.8, 8.8 Hz), 7.23 (dd, 2H, H-2' and H-6', *J* = 8.3, 5.8 Hz), 9.95 (br.s, 1H, NH).

4-(4-Phenylbenzyl)-1*H*-pyrazol-3,5-diamine (101f)

Yield 59 %; mp 180-182 °C (EA-hexane); ¹H NMR (300 MHz, DMSO-*d*₆): δ 3.55 (s, 2H, CH₂), 4.31 (br.s, 4H, (NH₂)₂), 7.25-7.72 (m, 9H, Ar-H), 10.01 (br.s, 1H, NH).

4-(4-Phenoxybenzyl)-1*H*-pyrazol-3,5-diamine (101g)

Yield 79 %; mp 128-130 °C (EA-hexane); ¹H NMR (300 MHz, DMSO-*d*₆): δ 3.49 (s, 2H, CH₂), 4.33 (br.s, 4H, (NH₂)₂), 6.81-7.47 (m, 9H, Ar-H), 10.63 (br.s, 1H, NH).

4-(4-Methylbenzyl)-1*H*-pyrazol-3,5-diamine (101h)

Yield 72 %; mp 168-170 °C (EA-hexane); ¹H NMR (300 MHz, DMSO-*d*₆): δ 2.23 (s, 3H, Me), 3.44 (s, 2H, CH₂), 4.21 (br.s, 4H, (NH₂)₂), 7.02 (d, 2H, H-3' and H-5', *J* = 7.9 Hz), 7.09 (d, 2H, H-2' and H-6', *J* = 7.9 Hz), 9.94 (br.s, 1H, NH).

4-(4-Ethylbenzyl)-1*H*-pyrazol-3,5-diamine (101i)

Yield 66 %; mp 138-140 °C (EA-hexane); ¹H NMR (300 MHz, DMSO-*d*₆): δ 1.13 (t, 3H, CH₃, *J* = 7.6 Hz), 2.53 (d, 2H, CH₂, *J* = 7.5 Hz), 3.40 (s, 2H, CH₂), 4.25 (br.s,

4H, (NH₂)₂), 7.04 (d, 2H, H-3' and H-5', *J* = 7.9 Hz), 7.12 (d, 2H, H-2' and H-6', *J* = 8.0 Hz), 9.63 (br.s, 1H, NH).

4-(4-Methoxybenzyl)-1*H*-pyrazol-3,5-diamine (101j)

Yield 65 %; mp 146-148 °C (EA-hexane); ¹H NMR (300 MHz, DMSO-*d*₆): δ 3.42 (s, 2H, CH₂), 3.69 (s, 3H, MeO), 4.22 (br.s, 4H, (NH₂)₂), 6.78 (d, 2H, H-3' and H-5', *J* = 8.5 Hz), 7.12 (d, 2H, H-2' and H-6', *J* = 8.4 Hz), 9.94 (br.s, 1H, NH).

4-(4-Hydroxybenzyl)-1*H*-pyrazol-3,5-diamine (101k)

Yield 76 %; mp 184-186 °C (EA-hexane); ¹H NMR (300 MHz, DMSO-*d*₆): δ 3.37 (s, 2H, CH₂), 4.20 (br.s, 4H, (NH₂)₂), 6.61 (d, 2H, H-3' and H-5', *J* = 8.4 Hz), 7.00 (d, 2H, H-2' and H-6', *J* = 8.4 Hz), 9.35 (br.s, 1H, NH and OH).

4-(4-Cyanobenzyl)-1*H*-pyrazol-3,5-diamine (101l)

Yield 74 %; mp 101-102 °C (EA-hexane); ¹H NMR (300 MHz, DMSO-*d*₆): δ 3.59 (s, 2H, CH₂), 4.39 (br.s, 4H, (NH₂)₂), 7.41 (d, 2H, H-3' and H-5', *J* = 8.4 Hz), 7.69 (d, 2H, H-2' and H-6', *J* = 8.3 Hz), 9.94 (br.s, 1H, NH).

4-(Furan-2-ylmethyl)-1*H*-pyrazol-3,5-diamine (101m)

Yield 59 %; mp 147-149 °C (EA-hexane); ¹H NMR (300 MHz, DMSO-*d*₆): δ 3.50 (s, 2H, CH₂), 4.27 (br.s, 4H, (NH₂)₂), 5.94-5.95 (m, 1H, H-4'), 6.28-6.30 (m, 1H, H-3'), 7.44-7.45 (m, 1H, H-5'), 9.85 (br.s, 1H, NH).

4-(Thiophen-2-ylmethyl)-1*H*-pyrazol-3,5-diamine (101n)

Yield 73 %; mp 118-120 °C (EA-hexane); ¹H NMR (300 MHz, DMSO-*d*₆): δ 3.69 (s, 2H, CH₂), 4.28 (br.s, 4H, (NH₂)₂), 6.80-6.83 (m, 1H, H-4'), 6.86-6.89 (m, 1H, H-3'), 7.19-7.23 (m, 1H, H-5'), 10.04 (br.s, 1H, NH).

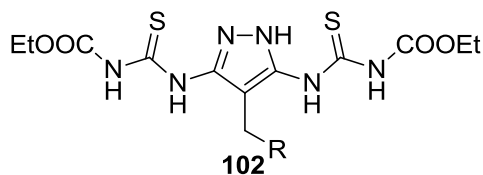
4-(Naphthalen-2-ylmethyl)-1*H*-pyrazol-3,5-diamine (101o)

Yield 55 %; oil; ¹H NMR (300 MHz, DMSO-*d*₆): δ 3.51 (s, 2H, CH₂), 4.01-4.08 (br.s, 4H, (NH₂)₂), 7.20-8.39 (m, 8H, Ar-H), 10.09 (br.s, 1H, NH).

- General procedure of synthesis of corresponding thiourea derivatives of pyrazol-3,5-diamine (**102**)

In a well stirred suspension of 4-benzyl-1*H*-pyrazol-3,5-diamine and its derivatives (3 mmol) in anhydrous dimethylformamide (DMF, 4 ml), ethoxycarbonyl isothiocyanete (6 mmol) was added and stirred the reaction mixture for 4.5-5 hours at room temperature. Following this step, 50-60 ml water was added to get more precipitated product. The product was filtered and washed with cold water. The products obtained were recrystallized from ethanol or aqueous-ethanol system.

Table 24. Synthesis of corresponding thiourea derivatives of pyrazol-3,5-diamine and their ^1H NMR spectral data



Cpd	R	% Yield & mp	^1H NMR (300 MHz, DMSO- d_6)					
			2CO ₂ Et	CH ₂	Ar	2NH	2NH	N(1)H
102a	Ph	% yield: 82, mp: 196-197 °C, (Ethanol-water)	1.23, t, 6H, $J = 7.0$ Hz; 4.16, q, 4H, $J = 7.0$ Hz	3.65	7.07-7.23, m, 5H	10.87	11.39	12.88
102b	4-CF ₃ C ₆ H ₄	% yield: 72, mp: 197-198 °C, (Ethanol-water)	1.21, t, 6H, $J = 7.1$ Hz; 4.14, q, 4H, $J = 7.1$ Hz	3.74	7.40, d, 2H, $J = 7.9$ Hz; 7.51, d, 2H, $J = 8.0$ Hz	10.72-10.97	11.21-11.62	12.93
102c	4-ClC ₆ H ₄	% yield: 80, mp: 196-198 °C, (Ethanol-water)	1.24, t, 6H, $J = 7.0$ Hz; 4.17, q, 4H, $J = 7.0$ Hz	3.63	7.12-7.33, m, 4H	10.70-10.99	11.20-11.60	12.90
102d	4-BrC ₆ H ₄	% yield: 88, mp: 200-201 °C, (Ethanol-water)	1.24, t, 6H, $J = 7.0$ Hz; 4.17, q, 4H, $J = 6.7$ Hz	3.61	7.13, d, 2H, $J = 8.4$ Hz; 7.34, d, 2H, $J = 8.4$ Hz	10.78-10.89	11.27-11.48	12.89
102e	4-FC ₆ H ₄	% yield: 76, mp: 204-206 °C, (Ethanol-water)	1.23, t, 6H, $J = 6.9$ Hz; 4.16, q, 4H, $J = 6.8$ Hz	3.62	6.95-6.99, m, 2H; 7.18-7.21, m, 2H	10.83	11.18-11.61	12.88
102f	4-PhC ₆ H ₄	% yield: 90, mp: 189-190 °C, (Ethanol)	1.14, t, 6H, $J = 7.0$ Hz; 4.07, q, 4H, $J = 6.8$ Hz	3.69	7.20-7.73, m, 9H	10.87	11.38	12.90
102g	4-PhOC ₆ H ₄	% yield: 86, mp: 184-186 °C, (Ethanol-water)	1.22, t, 6H, $J = 7.0$ Hz; 4.16, q, 4H, $J = 7.0$ Hz	3.63	6.67-7.43, m, 9H	10.80-10.93	11.32-11.51	12.88
102h	4-MeC ₆ H ₄	% yield: 89, mp: 184-186 °C, (Ethanol-water)	1.23, t, 6H, $J = 7.0$ Hz; 4.16, q, 4H, $J = 7.0$ Hz	3.59	2.21, s, 3H, Me; 6.96, d, 2H, $J = 7.9$ Hz; 7.04, d, 2H, $J = 7.9$ Hz	10.86	11.39	12.86
102i	4-EtC ₆ H ₄	% yield: 82, mp: 178-179 °C, (Ethanol-water)	1.23, t, 6H, $J = 7.0$ Hz; 4.16, q, 4H, $J = 6.4$ Hz	3.60	1.12, t, 3H, CH ₃ , $J = 7.6$ Hz; 4.16, q, CH ₂ , $J = 6.4$ Hz; 6.95-7.14, m, 4H	10.70-11.09	11.20-11.67	12.85

Table 24. Synthesis of corresponding thiourea derivatives of pyrazol-3,5-diamine and their ¹H NMR spectral data (Contd.)

Cpd	R	% Yield & mp	¹ H NMR (300 MHz, DMSO- <i>d</i> ₆)					
			2CO ₂ Et	CH ₂	Ar	2NH	2NH	N(1)H
102j	4-MeOC ₆ H ₄	% yield: 78, mp: 183-185 °C, (Ethanol-water)	1.23, t, 6H, <i>J</i> = 7.0 Hz; 4.16, q, 4H, <i>J</i> = 7.0 Hz	3.67	3.34, s, 3H, OMe; 6.72, d, 2H, <i>J</i> = 8.4 Hz; 7.07, d, 2H, <i>J</i> = 8.4 Hz	10.69-11.02	11.20-11.60	12.85
102k	4-OHC ₆ H ₄	% yield: 85, mp: 136-138 °C, (Ethanol-water)	1.24, t, 6H, <i>J</i> = 7.0 Hz; 4.17, q, 4H, <i>J</i> = 7.0 Hz	3.51	6.54, d, 2H, <i>J</i> = 8.4 Hz; 6.94, d, 2H, <i>J</i> = 8.4 Hz	10.87	11.38	12.82
102l	4-CNC ₆ H ₄	% yield: 86, mp: 232-234 °C, (Ethanol-water)	1.24, t, 6H, <i>J</i> = 7.0 Hz; 4.16, q, 4H, <i>J</i> = 7.0 Hz	3.73	7.38, d, 2H, <i>J</i> = 8.0 Hz; 7.63, d, 2H, <i>J</i> = 7.9 Hz	10.81	11.38	12.94
102m	2-Furyl-	% yield: 78, mp: 189-190 °C, (Ethanol-water)	1.25, t, 6H, <i>J</i> = 7.0 Hz; 4.20, q, 4H, <i>J</i> = 7.0 Hz	3.68	5.97-6.00, m, 1H; 6.24-6.29, m, 1H; 7.38-7.43, m, 1H	11.04	11.43	12.92
102n	2-thiophenyl-	% yield: 89, mp: 176 °C, (Ethanol-water)	1.24, t, 6H, <i>J</i> = 7.0 Hz; 4.18, q, 4H, <i>J</i> = 7.0 Hz	3.87	6.76-6.86, m, 2H; 7.22-7.26, m, 1H	10.99	11.45	12.91
102o	2-Naphthalinyl	% yield: 84, mp: 164-166 °C, (Ethanol-water)	1.22, t, 6H, <i>J</i> = 7.0 Hz; 4.12, q, 4H, <i>J</i> = 7.0 Hz	3.35	7.16-8.24, m, 9H	10.75-10.99	11.29	12.91

- General procedure of synthesis of (8-benzyl-4-oxo-2-thioxo-1,2,3,4-tetrahydropyrazolo[1,5-*a*][1,3,5]triazin-7-yl)-thiourea and its derivatives (**H13-H13n**)

To a stirred solution of NaOH (9 mmol) in ethanol (80%, 20 ml), corresponding carbethoxythiourea (3 mmol) was added and heated on water bath for 20 minutes with continuous stirring. After cooling, the solvent was evaporated under vacuum, and the residue was suspended in water (25 ml). The resulting suspension was acidified up to pH 1-3 using 2.5 M HCl. The precipitated product was filtered off, recrystallized with suitable solvent and dried under vacuum.

(8-Benzyl-4-oxo-2-thioxo-1,2,3,4-tetrahydro-pyrazolo[1,5-*a*][1,3,5]triazin-7-yl)-thiourea (H13)

Yield 73 %; mp 239-241 °C (EtOH-water); ESI-MS *m/z* 331.1 (M-1)⁺; purity > 95%; *t_R* 1.70 min (A); ¹H NMR (300 MHz, DMSO-*d*₆): δ 4.11(s, 2H, CH₂), 7.12-7.33 (m, 5H, Ph), 8.94 and 9.07 (two s, 2H, (C=S) NH₂), 10.06 (s, 1H, (C=S) NH), 12.70 (s, 1H, NH), 13.57 (br. s, 1H, NH); ¹³C NMR (75 MHz, DMSO-*d*₆): δ 24.2 (CH₂), 92.0 (C-8), 125.8 (C-4'), 127.8 (C-3' and C-5'), 128.2 (C-2' and C-6'), 138.5 (C-1'), 139.6 (C-7), 140.7 (C-9), 151.9 (C-4), 173.5 (C-2), 179.8 (NH(C=S)NH₂).

[8-(4-Trifluoromethyl-benzyl)-4-oxo-2-thioxo-1,2,3,4-tetrahydro-pyrazolo[1,5-*a*][1,3,5]triazin-7-yl]-thiourea (H13a)

Yield 71 %; mp 189-191 °C (EtOH-water); ESI-MS *m/z* 399. (M-1)⁺; purity > 95%; *t_R* 1.68 min (A); ¹H NMR (300 MHz, DMSO-*d*₆): δ 4.21 (s, 2H, CH₂), 7.39 (d, 2H, H-3' and H-5', *J* = 7.9 Hz), 7.65 (d, 2H, H-2' and H-6', *J* = 8.1 Hz), 8.95 and 9.10 (two s, 2H, (C=S) NH₂), 10.21 (s, 1H, (C=S) NH), 12.65 (s, 1H, NH), 13.53 (br. s, 1H, NH); ¹³C NMR (75 MHz, DMSO-*d*₆): δ 24.4 (CH₂), 91.0 (C-8), 124.4 (q, CF₃, *J* = 271.9 Hz), 124.9 (q, C-3' and C-5', *J* = 3.7 Hz), 126.7 (q, C-4', *J* = 31.5 Hz), 128.6 (C-2' and C-6'), 139.3 (C-1'), 140.9 (C-7), 144.8 (C-9), 151.9 (C-4), 173.6 (C-2), 179.9 (NH(C=S)NH₂).

[8-(4-Chloro-benzyl)-4-oxo-2-thioxo-1,2,3,4-tetrahydro-pyrazolo[1,5-*a*][1,3,5]triazin-7-yl]-thiourea (H13b)

Yield 78 %; mp 243-245 °C (EtOH-water); ESI-MS *m/z* 365.1 (M-1)⁺; purity > 95%; *t_R* 1.70 min (A); ¹H NMR (300 MHz, DMSO-*d*₆): δ 4.09 (s, 2H, CH₂), 7.18 (d, 2H, H-3' and H-5', *J* = 8.4 Hz), 7.33 (d, 2H, H-2' and H-6', *J* = 8.5 Hz), 8.94 and 9.05 (two

s, 2H, (C=S) NH₂), 10.11 (s, 1H, (C=S) NH), 12.69 (s, 1H, NH), 13.53 (br. s, 1H, NH); ¹³C NMR (75 MHz, DMSO-*d*₆): δ 23.7 (CH₂), 91.6 (C-8), 128.0 (C-3' and C-5'), 129.7 (C-2' and C-6'), 130.4 (C-4'), 138.7 (C-1'), 138.7 (C-7), 140.7 (C-9), 151.8 (C-4), 173.5 (C-2), 179.8 (NH(C=S)NH₂).

[8-(4-Bromo-benzyl)-4-oxo-2-thioxo-1,2,3,4-tetrahydro-pyrazolo[1,5-*a*][1,3,5]triazin-7-yl]-thiourea (H13c)

Yield 82 %; mp 222-224 °C (EtOH-water); ESI-MS *m/z* 411.1 (M-1)⁺; purity > 95%; *t*_R 1.73 min (A); ¹H NMR (300 MHz, DMSO-*d*₆): δ 4.07 (s, 2H, CH₂), 7.13 (d, 2H, H-3' and H-5', *J* = 8.4 Hz), 7.46 (d, 2H, H-2' and H-6', *J* = 8.4 Hz), 8.93 and 9.05 (two s, 2H, (C=S) NH₂), 10.09 (s, 1H, (C=S) NH), 12.67 (s, 1H, NH), 13.52 (br. s, 1H, NH); ¹³C NMR (75 MHz, DMSO-*d*₆): δ 23.8 (CH₂), 91.6 (C-8), 118.9 (C-4'), 130.2 (C-3' and C-5'), 131.0 (C-2' and C-6'), 138.8 (C-1'), 139.2 (C-7), 140.8 (C-9), 151.9 (C-4), 173.6 (C-2), 179.9 (NH(C=S)NH₂).

[8-(4-Fluoro-benzyl)-4-oxo-2-thioxo-1,2,3,4-tetrahydro-pyrazolo[1,5-*a*][1,3,5]triazin-7-yl]-thiourea (H13d)

Yield 65 %; mp 221-223 °C (EtOH-water); ESI-MS *m/z* 349.0 (M-1)⁺; purity > 95%; *t*_R 1.69 min (A); ¹H NMR (300 MHz, DMSO-*d*₆): δ 4.09 (s, 2H, CH₂), 7.10 (dd, 2H, H-3' and H-5', *J* = 8.9, 8.9 Hz), 7.20 (dd, 2H, H-2' and H-6', *J* = 8.7, 5.6 Hz), 8.94 and 9.05 (two s, 2H, (C=S) NH₂), 10.09 (s, 1H, (C=S) NH), 12.69 (s, 1H, NH), 13.55 (br. s, 1H, NH); ¹³C NMR (75 MHz, DMSO-*d*₆): δ 23.4 (CH₂), 92.7 (C-8), 114.8 (d, C-3' and C-5', *J* = 21.3 Hz), 129.6 (d, C-2' and C-6', *J* = 7.3 Hz), 135.7 (d, C-1', *J* = 2.9 Hz), 138.6 (C-7), 140.8 (C-9), 151.8 (C-4), 160.6 (d, C-4', *J* = 241.4 Hz), 173.5 (C-2), 179.8 (NH(C=S)NH₂).

(8-Biphenyl-4-ylmethyl-4-oxo-2-thioxo-1,2,3,4-tetrahydro-pyrazolo[1,5-*a*][1,3,5]triazin-7-yl)-thiourea (H13e)

Yield 70 %; mp 239-241 °C (EtOH-water); ESI-MS m/z 407.1 (M-1)⁺; purity > 95%; t_R 1.68 min (A); ¹H NMR (300 MHz, DMSO-*d*₆): δ 4.16 (s, 2H, CH₂), 7.27 (d, 2H, H-3'' and H-5'', $J = 8.2$ Hz), 7.33 (t, 1H, H-4'', $J = 7.3$ Hz), 7.44 (t, 2H, H-2'' and H-6'', $J = 7.7$ Hz), 7.58 (d, 2H, H-3' and H-5', $J = 8.2$ Hz), 7.63 (d, 2H, H-2' and H-6', $J = 7.5$ Hz), 8.98 and 9.12 (two s, 2H, (C=S) NH₂), 10.15 (s, 1H, (C=S) NH), 12.67 (s, 1H, NH), 13.52 (br. s, 1H, NH). ¹³C NMR (75 MHz, DMSO-*d*₆): δ 23.9 (CH₂), 92.0 (C-8), 126.4 (C-3' and C-5'), 126.5 (C-2' and C-6'), 127.1 (C-4'), 128.4 (C-3'' and C-5''), 128.8 (C-2'' and C-6''), 137.8 (C-1'), 138.8 (C-4''), 139.0 (C-1''), 139.9 (C-7), 140.8 (C-9), 151.9 (C-4), 173.6 (C-2), 179.8 (NH(C=S)NH₂).

[4-Oxo-8-(4-phenoxy-benzyl)-2-thioxo-1,2,3,4-tetrahydro-pyrazolo[1,5-*a*][1,3,5]triazin-7-yl]-thiourea (H13f)

Yield 81 %; mp 210-212 °C (EtOH-water); ESI-MS m/z 423.2 (M-1)⁺; purity > 95%; t_R 1.84 min (A); ¹H NMR (300 MHz, DMSO-*d*₆): δ 4.09 (s, 2H, CH₂), 6.81-7.45 (m, 9H, Ar-H), 8.96 and 9.07 (two s, 2H, (C=S) NH₂), 10.07 (s, 1H, (C=S) NH), 12.68 (s, 1H, NH), 13.53 (br. s, 1H, NH); ¹³C NMR (75 MHz, DMSO-*d*₆): δ 23.6 (CH₂), 92.1 (C-8), 118.1 (C-3' and C-5'), 118.6 (C-2' and C-6'), 123.0 (C-4'), 129.4 (C-3'' and C-5''), 129.9 (C-2'' and C-6''), 134.8 (C-1'), 138.6 (C-4''), 140.8 (C-1''), 151.9 (C-7), 154.6 (C-9), 156.9 (C-4), 173.5 (C-2), 179.8 (NH(C=S)NH₂).

[8-(4-Methyl-benzyl)-4-oxo-2-thioxo-1,2,3,4-tetrahydro-pyrazolo[1,5-*a*][1,3,5]triazin-7-yl]-thiourea (H13g)

Yield 76 %; mp 254-256 °C (EtOH-water); ESI-MS m/z 345.1 (M-1)⁺; purity > 95%; t_R 5.14 min (D); ¹H NMR (300 MHz, DMSO-*d*6): δ 2.25 (s, 3H, Me), 4.05 (s, 2H, CH₂), 7.04-7.09 (m, 5H, Ar-H), 8.93 and 9.03 (two s, 2H, (C=S) NH₂), 9.98 (s, 1H, (C=S) NH), 12.69 (s, 1H, NH), 13.55 (br. s, 1H, NH); ¹³C NMR (75 MHz, DMSO-*d*6): δ 20.5 (Me), 23.7 (CH₂), 92.4 (C-8), 112.7 (C-3' and C-5'), 128.7 (C-2' and C-6'), 134.8 (C-4'), 136.4 (C-1'), 138.3 (C-7), 140.7 (C-9), 151.9 (C-4), 173.5 (C-2), 179.7 (NH(C=S)NH₂).

[8-(4-Ethyl-benzyl)-4-oxo-2-thioxo-1,2,3,4-tetrahydro-pyrazolo[1,5-*a*][1,3,5]triazin-7-yl]-thiourea (H13h)

Yield 73 %; mp 228-230 °C (EtOH-water); ESI-MS m/z 359.1 (M-1)⁺; purity > 95%; t_R 1.71 min (A); ¹H NMR (300 MHz, DMSO-*d*6): δ 1.14 (t, 3H, CH₃, $J = 7.6$ Hz), 2.55 (q, 2H, CH₂, $J = 7.6$ Hz), 4.05 (s, 2H, CH₂), 7.07 (d, 2H, H-3' and H-5', $J = 8.3$ Hz), 7.11 (d, 2H, H-2' and H-6', $J = 8.5$ Hz), 8.94 and 9.07 (two s, 2H, (C=S) NH₂), 10.03 (s, 1H, (C=S) NH), 12.63 (s, 1H, NH), 13.54 (br. s, 1H, NH); ¹³C NMR (75 MHz, DMSO-*d*6): δ 15.7 (Me), 23.8 (CH₂), 27.7 (CH₂), 92.4 (C-8), 127.5 (C-3' and C-5'), 127.8 (C-2' and C-6'), 136.8 (C-4'), 138.6 (C-1'), 140.8 (C-7), 141.2 (C-9), 151.9 (C-4), 173.5 (C-2), 179.8 (NH(C=S)NH₂).

[8-(4-Methoxy-benzyl)-4-oxo-2-thioxo-1,2,3,4-tetrahydro-pyrazolo[1,5-*a*][1,3,5]triazin-7-yl]-thiourea (H13i)

Yield 69 %; mp 252-254 °C (EtOH-water); ESI-MS m/z 361.1 (M-1)⁺; purity > 95%; t_R 1.67 min (A); ¹H NMR (300 MHz, DMSO-*d*6): δ 3.71 (s, 3H, OMe), 4.03 (s, 2H,

CH₂), 6.84 (d, 2H, H-3' and H-5', *J* = 8.8 Hz), 7.10 (d, 2H, H-2' and H-6', *J* = 8.7 Hz), 8.95 and 9.04 (two s, 2H, (C=S) NH₂), 9.99 (s, 1H, (C=S) NH), 12.70 (s, 1H, NH), 13.56 (br. s, 1H, NH); ¹³C NMR (75 MHz, DMSO-*d*₆): δ 23.3 (CH₂), 54.9 (MeO), 92.7 (C-8), 113.6 (C-3' and C-5'), 128.8 (C-2' and C-6'), 131.4 (C-4'), 138.2 (C-1'), 140.7 (C-7), 151.9 (C-9), 157.5 (C-4), 173.5 (C-2), 179.7 (NH(C=S)NH₂).

[8-(4-Hydroxy-benzyl)-4-oxo-2-thioxo-1,2,3,4-tetrahydro-pyrazolo[1,5-*a*][1,3,5]triazin-7-yl]-thiourea (H13j)

Yield 80 %; mp 219-221 °C (EtOH-water); ESI-MS *m/z* 347.1 (M-1)⁺; purity > 95%; *t_R* 1.65 min (A); ¹H NMR (300 MHz, DMSO-*d*₆): δ 3.97 (s, 2H, CH₂), 6.66 (d, 2H, H-3' and H-5', *J* = 8.5 Hz), 6.96 (d, 2H, H-2' and H-6', *J* = 8.5 Hz), 8.94 and 9.03 (two s, 2H, (C=S) NH₂), 9.17 (s, 1H, OH), 9.90 (s, 1H, (C=S) NH), 12.68 (s, 1H, NH), 13.54 (br. s, 1H, NH); ¹³C NMR (75 MHz, DMSO-*d*₆): δ 23.3 (CH₂), 92.7 (C-8), 114.9 (C-3' and C-5'), 128.7 (C-2' and C-6'), 129.5 (C-4'), 138.2 (C-1'), 140.7 (C-7), 151.9 (C-9), 155.4 (C-4), 173.5 (C-2), 179.7 (NH(C=S)NH₂).

[8-(4-Cyano-benzyl)-4-oxo-2-thioxo-1,2,3,4-tetrahydro-pyrazolo[1,5-*a*][1,3,5]triazin-7-yl]-thiourea (H13k)

Yield 62 %; mp 259-262 °C (EtOH-water); ESI-MS *m/z* 356.1 (M-1)⁺; purity > 95%; *t_R* 1.65 min (A); ¹H NMR (300 MHz, DMSO-*d*₆): δ 4.20 (s, 2H, CH₂), 7.34 (d, 2H, H-3' and H-5', *J* = 8.3 Hz), 7.46 (d, 2H, H-2' and H-6', *J* = 8.3 Hz), 8.96 and 9.06 (two s, 2H, (C=S) NH₂), 10.22 (s, 1H, (C=S) NH), 12.74 (s, 1H, NH), 13.55 (br. s, 1H, NH); ¹³C NMR (75 MHz, DMSO-*d*₆): δ 24.7 (CH₂), 90.6 (C-8), 108.7 (CN), 118.9 (C-4'), 128.9 (C-3' and C-5'), 132.0 (C-2' and C-6'), 138.9 (C-1'), 140.8 (C-7), 145.8 (C-9), 151.8 (C-4), 173.6 (C-2), 179.7 (NH(C=S)NH₂).

(8-Furan-2-ylmethyl-4-oxo-2-thioxo-1,2,3,4-tetrahydro-pyrazolo[1,5-*a*][1,3,5]triazin-7-yl]-thiourea (H13l)

Yield 74 %; mp 227-229 °C (EtOH-water); ESI-MS *m/z* 321.0 (M-1)⁺; purity > 95%; *t_R* 1.67 min (A); ¹H NMR (300 MHz, DMSO-*d*₆): δ 4.13 (s, 2H, CH₂), 6.00 (d, 1H, H-3', *J* = 3.1 Hz), 6.34 (dd, 1H, H-4', *J* = 3.1, 1.9 Hz), 7.55 (d, 1H, H-5', *J* = 1.0 Hz), 8.98 and 9.09 (two s, 2H, (C=S) NH₂), 10.12 (s, 1H, (C=S) NH), 12.72 (s, 1H, NH), 13.54 (br. s, 1H, NH); ¹³C NMR (75 MHz, DMSO-*d*₆): δ 18.5 (CH₂), 89.2 (C-8), 105.5 (C-4'), 110.4 (C-3'), 138.5 (C-5'), 140.7 (C-2'), 141.6 (C-7), 151.8 (C-9), 152.9 (C-4), 173.5 (C-2), 179.8 (NH(C=S) NH₂).

(4-Oxo-8-thiophen-2-ylmethyl-2-thioxo-1,2,3,4-tetrahydro-pyrazolo[1,5-*a*][1,3,5]triazin-7-yl]-thiourea (H13m)

Yield 72 %; mp 242-244 °C (EtOH-water); ESI-MS *m/z* 337.0 (M-1)⁺; purity > 95%; *t_R* 1.68 min (A); ¹H NMR (300 MHz, DMSO-*d*₆): δ 4.30 (s, 2H, CH₂), 6.81 (d, 1H, H-3', *J* = 2.8 Hz), 6.92 (dd, 1H, H-4', *J* = 5.0, 3.5 Hz), 7.32 (d, 1H, H-5', *J* = 5.0 Hz), 8.97 and 9.06 (two s, 2H, (C=S) NH₂), 10.19 (s, 1H, (C=S) NH), 12.72 (s, 1H, NH), 13.61 (br. s, 1H, NH); ¹³C NMR (75 MHz, DMSO-*d*₆): δ 19.4 (CH₂), 92.1 (C-8), 124.0 (C-4'), 124.5 (C-5'), 126.7 (C-3'), 138.2 (C-2'), 140.7 (C-7), 142.6 (C-9), 151.6 (C-4), 173.5 (C-2), 179.8 (NH(C=S) NH₂).

(8-Naphthalen-2-ylmethyl-4-oxo-2-thioxo-1,2,3,4-tetrahydro-pyrazolo[1,5-*a*][1,3,5]triazin-7-yl]-thiourea (H13n)

Yield 63 %; mp 230-233 °C (EtOH-water); ESI-MS *m/z* 381.2 (M-1)⁺; purity > 95%; *t_R* 2.36 min (A); ¹H NMR (300 MHz, DMSO-*d*₆): δ 4.56 (s, 2H, CH₂), 6.85-6.26 (m, 11H, Ar-H), 9.00 and 9.26 (two s, 2H, (C=S) NH₂), 10.22 (s, 1H, (C=S) NH), 12.72

(s, 1H, NH), 13.48 (br. s, 1H, NH); ¹³C NMR (75 MHz, DMSO-*d*₆): δ 22.2 (CH₂), 90.0 (C-8), 123.1 (Ar-C), 123.8 (Ar-C), 125.5 (Ar-C), 125.6 (Ar-C), 125.7 (Ar-C), 126.2 (Ar-C), 128.2 (Ar-C), 131.5 (Ar-C), 133.1 (Ar-C), 135.4 (Ar-C), 139.1 (C-7), 140.8 (C-9), 152.6 (C-4), 173.5 (C-2), 179.9 (NH(C=S) NH₂).

9.2 Molecular modeling study

The CoMFA analysis was performed with the SYBYL-X 1.3 molecular modeling software. A total of 43 compounds (training set) and 13 compounds of series **H8** and its related structure (test set) comprised of 1,2,4-triazolo[1,5-*a*][1,3,5]triazine and pyrazolo[1,5-*a*][1,3,5]triazine scaffold was energy minimized using the SYBYL-X 1.3 standard Tripos force field with a distance dependent dielectric function until a root mean square (rms) deviation of 0.001 kcal/mol Å was achieved. The partial atomic charges required for the electrostatic interaction were computed using the Gasteiger-Huckel method. The most active compound (**H13**) was chosen as the template molecule and shared backbone or core structure was identified on which other molecules were aligned by database alignment method implemented in SYBYL-X 1.3. CoMFA steric and electrostatic interaction fields were calculated with the standard Tripos force field at each lattice intersection point of a regularly spaced grid of 2.0 Å. The values of the steric and electrostatic fields were truncated at 30 kcal/mol. To generate statistically significant 3D QSAR models, partial least squares (PLS) regression analysis was used. To aid visualization, the CoMFA results were graphically represented in contour maps.

9.3 Biological characterisation

9.3.1 *In vitro* thymidine phosphorylase enzyme assay

To evaluate *in-vitro* TP inhibitory activity of synthesized compounds, a spectrophotometric assay method was adopted, originally developed by Krenitsky (Krenitsky et al, 1979)²¹⁴. Briefly, recombinant thymidine phosphorylase, expressed in *E. coli* (T2807- Sigma Aldrich) and thymidine (substrate) were used in this assay. The absorbance at 290 nm was recorded on a Shimadzu UV Mini 1240 UV-Vis Spectrophotometer. 200mM and 10mM potassium phosphate buffers were prepared from anhydrous monobasic potassium phosphate and deionised water, and adjusted to pH 7.4 (A) and 7.0 (B) respectively using 1M NaOH solution. The enzyme was diluted just before use to a concentration of 1.5 units/ml with buffer B. For enzyme inhibition, 100µM stock solutions of test compounds in DMSO were serially diluted. 5 mM thymidine solution was prepared using buffer A.

Enzymatic reaction was initiated by addition of substrate (200 µl, 5mM) into a cuvette containing 780 µl of potassium phosphate buffer (pH 7.4), 10 µl of enzyme at concentration of 1.5 U, and 10 µl of test compounds dissolved in DMSO, which was mixed by rapid inversion, and decrease in absorbance due to conversion of thymidine to thymine was followed after 4, 8, 12, 16 and 20 min and from the slope of change in absorbance, the initial reaction rate was determined. Same experiments were performed using 10 µl of DMSO to calculate slope of uninhibited enzyme. For calculation of enzyme inhibition, the initial rates of change in absorbance at different concentrations of inhibitor were converted to % inhibition of enzyme, and plotted against inhibitor concentration using Graphpad Prism vs 4.0 to give the IC₅₀ at 50% inhibition.

The percentage activity of each inhibitor was calculated by the following formulae:

$$(i) \quad \text{Activity} = \frac{\text{Slope of inhibited enzyme}}{\text{Slope of uninhibited enzyme}} \times 100\%$$

$$(ii) \quad \text{Inhibition} = 100\% - \text{Activity}$$

All the experiments were carried out at least in duplicate.

9.3.2 Enzyme Inhibition kinetics Study

The inhibitory effect of enzyme was evaluated with varying concentration of thymidine (1000, 500, 300, 200, 100 μM) in the presence of different concentration of inhibitor. The saturating concentration of inorganic phosphate was fixed at 25 mM.

This experiment was also carried out with varying concentration of inorganic phosphate (20, 10, 5, 2 mM) in the presence of different concentration of inhibitor. The saturating concentration of thymidine was fixed at 1000 μM . The conversion of dThd to thymine was monitored for both substrates. All the experiments were conducted in triplicate.

9.3.3 MTT assay

MTT (3-(4,5-dimethylthiazol-2-yl)-2,5-diphenyl tetrazolium bromide) colorimetric assay²³⁹ was adopted to determine cytotoxicity of synthesized compounds on breast cancer cell line MDA-MB-231. In brief, cells grown to 80% confluence were diluted with suitable media and seeded at a density of 5000 cells/well in 96-well plates and were incubated for 24 hours. After that, the old media was aspirated out and 200 μl of the fresh media was added having inhibitor compounds that were dissolved in DMSO, and plates are incubated at 37 °C in a humidified atmosphere of 5% CO₂ for 72 hours.

DMSO (0.5 %) was used as vehicle control to ensure that solvent did not interfere with cell growth. After 72 hours, 50 µl of MTT was added to cells, and after 4 hours of incubation, the purple formazan precipitated formed was solubilized in DMSO. The absorbance was determined in a microtiter plate reader (Tecan Genios Spectrophotometer) at 570 nm. The % cell viability was determined by the following formula-

$$\% \text{ Cell viability} = \frac{(\text{Absorbance}_{\text{test}} - \text{Absorbance}_{\text{blank}})}{(\text{Absorbance}_{\text{veh ctrl}} - \text{Absorbance}_{\text{blank}})} \times 100\%$$

9.3.4 Gelatine zymography

Gelatine zymography was performed according to reported method with slight modifications (Liotta and Stetler-Stevenson 1990)²⁴⁰. MDA-MB-231 cells were seeded onto a six-well plates in RPMI with 10% FBS, and allowed to propagate to 80% confluence. The cells were then maintained in serum-free medium for at least 24 hours prior to designated treatments with compounds and PMA (80 nM). Following 24 hours incubation of cells with PMA, the conditioned medium was collected and centrifuged at 8000g for 8 minutes at 4 °C to remove cells and debris. Quantify the protein content of the conditioned medium using protein assay kit. The volume of each samples having equal amount of protein was adjusted by adding PBS to samples. The resulting sample was mixed with 3X loading buffer and subjected to electrophoresis on a 7.5% SDS-PAGE gel containing 0.1% (w/v) gelatine using 1X Tris-Glycin SDS running buffer at 100 V for 90-120 minutes. Following electrophoresis, the gels were washed in renaturing buffer (2.5% Triton X-100) for 30 minutes twice to remove SDS and then equilibrated for 30 minutes in 1X zymogram developing buffer (50mM tris, 10mM CaCl₂, 0.15M NaCl, pH-7.5). The gels were

subsequently incubated in fresh developing buffer at 37 °C for 24 hours to allow gelatine digestion. The gelatinolytic activity of MMPs was visualized by staining the gels with 1% coomassie blue R-250 in 50% methanol, 10% acetic acid, 40% water (v/v) and destained with 50% methanol, 10% acetic acid, 40% water (v/v) until clear bands suggestive of gelatine digestion were visualized.

9.3.5 Cell invasion assay

The cell invasion assay was conducted using BD BioCoat™ Matrigel™ Invasion Chambers according to the manufacturer's instructions. After treatment with different concentrations of compounds or DMSO, the MDA-MB-231 cells were harvested and 200 µl of cell suspension containing 1×10^6 cells/ml cells suspended in serum-free medium was seeded into the upper chamber of Matrigel-coated filter inserts. The culture media (600 µl) containing 10% FBS and/or chemoattractant was added to each well of the 24 well plate (lower compartment). The plate was incubated for 24 hours in a tissue culture incubator. After incubation, the non-invading cells as well as matrigel from the interior of the inserts were removed using cotton swabs. Cells that had invaded to the lower surface of the membrane were fixed with ethanol (70%) for 10 minutes, and stained with 0.2% crystal in 2% (v/v) ethanol/water for 15 minutes. The inserts were washed with water, allowed to be air-dried, and the invaded cells were detected and enumerated under a light microscope.

9.3.6 VEGF Assay

To quantify the VEGF expression in samples, a colorimetric enzyme-linked immunosorbent assay was performed according to the manufacturer's instructions.

After treatment of MDA-MB-231 cells with different concentrations of compounds or DMSO, the cell supernatant was collected and it was subjected to centrifugation (5000g for 5 minutes) to remove cells and debris. The samples were diluted with dilution buffer in desired proportion. Following this step, 0.1 ml of different VEGF standard solutions as well as properly diluted sample were placed into the precoated 96-well plate and incubate the plate at 37 °C for 90 minutes. Subsequently, the content of the plate were discarded and 0.1ml of biotinylated anti-human VEGF antibody working solution was added into each well and incubated for another 60 minutes. The plate was washed using 0.01 M TBS and 0.1ml of Avidin-Biotin-Peroxidase Complex working solution was added and incubated the plate for 30 minutes. After washing, 90 ul of prepared TMB colour developing agent was added into each well and incubated for 20-25 minutes. Thereafter, 0.1ml of prepared TMB stop solution was added into each well resulting in change of colour of content into yellow and the absorbance at 450 nm was measured.

9.3.7 IL-8 assay

The quantification of IL-8 in cell culture supernatant samples was performed according to manufacturer's instructions *via* a colorimetric enzyme-linked immunosorbent assay.

In this assay, 50 µl of reconstituted standard or sample were added to each well of human IL-8 coated 96-well plate and incubated for one hour at room temperature (20-25°C). The plates were washed using wash buffer and 50 µl of biotinylated anti-human IL-8 antibody was added into each well and incubated for another one hour at room temperature. After washing away the unbound biotinylated antibody, 100 µl of prepared Streptavidin-HRP Solution was pipetted to each well and incubated for 30

minutes. Thereafter, the wells were again washed, and 100 μ l of TMB substrate solution was added to the wells and placed the plates in the dark at room temperature for 30 minutes. The colour developed in each well was proportionate to the amount of IL-8 bound. The stop solution (100 μ l) was added that changed the colour from blue to yellow, and the intensity of the colour was measured at 450 nm.

Chapter 10

References

- 1) Dolzhenko, A. V.; Chui, W. K. Synthesis of 2-amino-*s*-triazino[1,2-*a*]benzimidazoles as potential antifolates from 2-guanidino- and 2-guanidino-5-methylbenzimidazoles. *Journal of Heterocyclic Chemistry* **2006**, 43, 95-100.
- 2) Dolzhenko, A. V.; Chui, W. K.; Chan, L. W. Synthesis and biological activity of fluorinated 2-amino-4-aryl-3,4-dihydro[1,3,5]triazino[1,2-*a*]benzimidazoles. *Journal of Fluorine Chemistry* **2005**, 126, 759-763.
- 3) Chauhan, D.; Chauhan, J. S.; Singh, J.; Bajpai, S. K.; Joshi, M. N. Synthesis and bioevaluation of some novel nucleosides as antiherptic agents. *Indian Journal of Chemistry - Section B Organic and Medicinal Chemistry* **2003**, 42, 215-218.
- 4) Muller, J. C.; Ramuz, H. Eur. Pat. Appl. EP 7643 19800206, 61 pp.
- 5) Flament, I. P. R.; Martin, R. H. Synthesis of 2,4-dihydroxy-1,3,5-triazine (allantoxaidine). *Helvetica Chimica Acta* **1959**, 42, 485-489.
- 6) Piskala, A.; Gut, J. Nucleic acids components and their analogs. XXXV. The reaction of ethyl orthoformate with urea. *Collection of Czechoslovak Chemical Communications* **1963**, 28, 2376-2380.
- 7) Sanemitsu Y; Nakayama, Y. A convenient one-step synthesis of 1,3-disubstituted 6-(methylthio)-2,4-dioxo-1,2,3,4-tetrahydro-1,3,5-triazines[6-(methylthio)-1,3,5-triazine 2,4(1*H*,3*H*)-diones. *Synthesis* **1984**, 9, 770-771.
- 8) Kantlehner, W.; Haug, E.; Speh, P.; Braeuner, H. J. Orthoamides, XLI. Preparation of 1,3-diaryl-6-methyl-5-(trimethylsilyl)-6-(trimethylsilyloxy)-1,3,5-triazinane-2,4-diones and formylation of 1,3-dialkyl- and 1,3-diaryl-6-methyl-1,3,5-triazine-2,4(1*H*,3*H*)-diones. *Liebigs Annalen der Chemie* **1985**, 1, 65-71.
- 9) Dolzhenko, A. V.; Chui, W. K. 1,2,4-triazolo[1,5-*a*][1,3,5]triazines (5-azapurines): synthesis and biological activity. *Heterocycles* **2006**, 68, 1723-1759.
- 10) Dolzhenko, A. V.; Dolzhenko, A. V.; Chui, W. K. Pyrazolo[1,5-*a*][1,3,5]triazines (5-aza-9-deazapurines). Synthesis and biological activity. *Heterocycles* **2008**, 75, 1575-1622.
- 11) Pellizzari, G.; Roncagliolo, C. Investigations over the Guanazol. *Gazzetta Chimica Italiana* **1901**, 31, 477-513.
- 12) Koppes, W.; Ammon, H. L.; Concha, M. C.; Gilardi, R.; Politzer, P.; Sitzmann M. E. Abstracts of papers, 220th ACS National Meeting, Washington, DC, US, August 20-24. *ORGN* **2000**, 493.
- 13) Carwright, D.; Urlwin-Smith, P. L. Pat. DE 2720792, **1977** (chem. Abstr., 88, 62423).

- 14) Ahmed, G. A. Studies on 3-amino-1,2,4-triazole. *Journal of the Indian Chemical Society* **1997**, 74, 624-625.
- 15) Akahoshi, F.; Takeda, S.; Okada, T.; Kajii, M.; Nishimura, H.; Sugiura, M.; Inoue, Y.; Fukaya, C.; Naito, Y.; Imagawa, T.; Nakamura, N. Synthesis and pharmacological activity of triazolo[1,5-*a*]triazine derivatives inhibiting eosinophilia. *Journal of Medicinal Chemistry* **1998**, 41, 2985-2993.
- 16) Bokaldere, R.; Grinsteins, V. 2-Substituted 7-amino-1,2,4-triazolo[1,5-*a*]-1,3,5-triazines. *Khimiya Geterotsiklicheskikh Soedinenii* **1970**, 563-564.
- 17) Ibrahim, M. K. A.; Elghandour, A. H. H.; Elshikh, S. M. M.; Mishaal, S. A. Utility of hydrazidoyl halides in heterocyclic chemistry: synthesis of pyrazol-5-yl-1,2,4-triazole, pyrazol-5-yl-thiadiazole and pyrazol-5-yl-triazolo[4,5-*b*]triazine derivatives. *Indian Journal of Chemistry, Section B: Organic Chemistry Including Medicinal Chemistry* **1997**, 36B, 91-95.
- 18) Dorokhov, V. A.; Amamchyan, A. R.; Bogdanov, V. S. Synthesis and NMR study of 7-aryl-1,2,4-triazolo[1,5-*a*]-1,3,5-triazines. *Izvestiya Akademii Nauk SSSR, Seriya Khimicheskaya* **1989**, 2386-2388.
- 19) Dorokhov, V. A.; Amamchyan, A. R.; Bogdanov, V. S.; Ugrak, B. I. Synthesis of 5-azaadenine derivatives from N-(1,2,4-triazol-5-yl)amidines. *Izvestiya Akademii Nauk SSSR, Seriya Khimicheskaya* **1991**, 241-243.
- 20) Reimlinger, H.; Lingier, W. R. F.; Vandewalle, J. J. M.; Merenyi, R. Condensed isoquinolines. V. Syntheses with 3-amino-s-triazolo[3,4-*a*]isoquinoline. *Chemische Berichte* **1971**, 104, 3947-3954.
- 21) Andotra, C. S.; Kumar, R.; Dham, S.; Langer, T. C. Bridgehead nitrogen heterocycles: Synthesis of some 2,6-substituted aryl-1,2,4-triazolo[1,5-*a*]-s-triazine-5,7(1*H*,6*H*)-dithiones as antibacterial and antifungal agents. *Indian Journal of Heterocyclic Chemistry* **1996**, 6, 139-140.
- 22) Andotra, C. S.; Dham, S.; Langer, T. C. Bridgehead nitrogen heterocycles: synthesis of 2,6-disubstituted aryl-1,2,4-triazolo[1,5-*a*]-s-triazine-5,7-diones. *Indian Journal of Heterocyclic Chemistry* **1995**, 4, 237-238.
- 23) Zohdi, H. F. Reactions with 5-(trifluoromethyl)-1*H*-1,2,4-triazol-3-amine: A convenient route to fluorinated triazolo[1,5-*c*]thiadiazine, triazolo[1,5-*a*]triazine, thiazoles and thiadiazoles. *Journal of Chemical Research, Synopses* **1998**, 536-537.
- 24) Andotra, C. S.; Kumar, R.; Dham, S.; Sharma, P. Bridgehead nitrogen heterocycles: synthesis and antibacterial and antifungal activities of 2-aryl-6-(*p*-chlorophenyl)-5-thioxo-1*H*-1,2,4-triazolo[1,5-*a*]-s-triazin-7-ones. *Indian Journal of Heterocyclic Chemistry* **1998**, 8, 139-142.

- 25) Hirata, T.; Wood Jr, H. B.; Driscoll, J. S. Rearrangement and elimination reactions in 1,2,4-triazole derivatives. *Journal of the Chemical Society, Perkin Transactions 1* **1973**, 1209-1212.
- 26) Bokaldere, R.; Liepina, A. s-Triazolo[1,5-a]-s-triazinonethiones. Synthesis and reactions. *Khimiya Geterotsiklicheskikh Soedinenii* **1973**, 2, 276-280.
- 27) Hirata, T.; Twanmoh, L.-M.; Wood Jr., H. B.; Goldin, A.; Driscoll, J. 5-Azapurines and the structures of sym-triazole intermediates. *Journal of Heterocyclic Chemistry* **1972**, 9, 99-106.
- 28) Capuano, L. S.; Juergen, H. Heterocyclizations. IX. Preparation of pyrazolo-, triazolo-, oxazolo-, and thiazolo-s-triazines with a bridgehead nitrogen and of an isopurine N-carboxylic ester. *Chemische Berichte* **1971**, 104, 3039-3047.
- 29) Checchi, S.; Ridi, M. Derivatives of 5-aminopyrazole. IV. Synthesis of heterocyclic derivatives. *Gazzetta Chimica Italiana* **1957** 87, 597-614.
- 30) Gupta, C. M.; Jones, G. H.; Moffatt, J. G. C-glycosyl nucleosides. 9. An approach to the synthesis of purine-related C-glycosides. *Journal of Organic Chemistry* **1976**, 41, 3000-3009.
- 31) Cartwright, D.; Urlwin-Smith, P.; Collins, D. J. Herbicidal pyrazolotriazinedione derivatives. Eur. Pat. Appl. EP 4171 A1 19790919 **1979**.
- 32) Fischer, E.; Kreutzmann, J.; Rembarz, G.; Rosenthal, S. Preparation and reactions of substituted pyrazolo[1,5-a][1,3,5]triazines. *Pharmazie* **1976**, 31, 546-548.
- 33) Fischer, E.; Rosenthal, S.; Kreutzmann, J. 4-Thioxo-3,4-dihydropyrazolo[2,3-a]-1,3,5-triazines. Pat. DD 123468 **1976**.
- 34) Vogel, A.; Troxler, F. 4-Aminopyrazolo[1,5-a]-s-triazines. Pat. DE 2424334 **1974**.
- 35) Kobe, J.; O'Brien, D. E.; Robins, R. K.; Novinson, T. Chemistry of 4-hydrazino-7-phenylpyrazolo[1,5-a]-1,3,5-triazines. *Journal of Heterocyclic Chemistry* **1974**, 11, 991-996.
- 36) Vogel, A.; Troxler, F. New synthesis of pyrazolo[1,5-a]-s-triazines. *Helvetica Chimica Acta* **1975**, 58, 761-771.
- 37) Vicentini, C. B.; Mares, D.; Tartari, A.; Manfrini, M.; Forlani, G. Synthesis of Pyrazole derivatives and their evaluation as photosynthetic electron transport inhibitors. *Journal of Agricultural and Food Chemistry* **2004**, 52, 1898-190.

- 38) Nie, Z.; Perretta, C.; Erickson, P.; Margosiak, S.; Almassy, R.; Lu, J.; Averill, A.; Yager, K. M.; Chu, S. Structure-based design, synthesis, and study of pyrazolo[1,5-*a*][1,3,5]triazine derivatives as potent inhibitors of protein kinase CK2. *Bioorganic & Medicinal Chemistry Letters* **2007**, 17, 4191-4195.
- 39) Tam, S. Y. K.; Hwang, J. S.; De las Heras, F. G.; Klein, R. S.; Fox, J. J. Nucleosides. CV. Synthesis of the 8-(β -D-ribofuranosyl)pyrazolo[1,5-*a*]-1,3,5-triazine isosteres of adenosine and inosine. *Journal of Heterocyclic Chemistry* **1976**, 13, 1305-1308.
- 40) Capuano, L.; Schrepfer, H. J. Heterocyclizations. IX. Preparation of pyrazolo-, triazolo-, oxazolo-, and thiazolo-s-triazines with a bridgehead nitrogen and of an isopurine N-carboxylic ester. *Chemische Berichte* **1971**, 104, 3039-3047.
- 41) Kobe, J.; Springer, R. H.; O'Brien, D. E. Pyrazolo[1,5-*a*][1,3,5]-triazines. Pat. US 3846423 **1974**.
- 42) Lubbers, T.; Angehrn, P.; Gmunder, H.; Herzig, S.; Kulhanek, J. Design, synthesis, and structure-activity relationship studies of ATP analogues as DNA gyrase inhibitors. *Bioorganic & Medicinal Chemistry Letters* **2000**, 10, 821-82.
- 43) Ullas, G. V.; Chu, C. K.; Ahn, M. K.; Kosugi, Y. Synthesis of C-nucleoside analog of (S)-9-(2,3-dihydroxypropyl)adenine and related acyclonucleosides. *Journal of Organic Chemistry* **1988**, 53, 2413-2418.
- 44) Koren, B.; Kovac, F.; Petric, A.; Stanovnik, B.; Tisler, M. Heterocycles. CXXXIII. Indazoles in organic synthesis. Formation of some fused heterocycles. *Tetrahedron* **1976**, 32, 493-497.
- 44a) Kristjan, S. G.; Brian, A. J.; Jason, W. Pyrazolopyrimidines and pyrazolotriazines with potent activity against herpesviruses. *Bioorganic & Medicinal chemistry lettres* **2009**, 19, 5689-5692.
- 45) Sarmah, A. K.; Close, M. E.; Mason, N. W. H. Dissipation and sorption of six commonly used pesticides in two contrasting soils of New Zealand. *Journal of Environmental Science and Health - Part B Pesticides, Food Contaminants, and Agricultural Wastes* **2009**, 44, 325-336.
- 46) Poucher, S. M.; Keddie, J. R.; Singh, P.; Caulkett, P. W. R.; Jones, G.; Collis, M. G. The in vitro pharmacology of ZM 241385, a potent, non-xanthine, A(2a) selective adenosine receptor antagonist. *British Journal of Pharmacology* **1995**, 115, 1096-1102.
- 47) Poucher, S. M.; Keddie, J. R.; Brooks, R.; Shaw, G. R.; McKillop, D. Pharmacodynamics of ZM 241385, a potent A(2a) adenosine receptor antagonist, after enteric administration in rat, cat and dog. *Journal of Pharmacy and Pharmacology* **1996**, 48, 601-606.

- 48) Ongini, E.; Dionisotti, S.; Gessi, S.; Irenius, E.; Fredholm, B. B. Comparison of CGS 15943, ZM 241385 and SCH 58261 as antagonists at human adenosine receptors. *Naunyn-Schmiedeberg's Archives of Pharmacology* **1999**, 359, 7-10.
- 49) Keddie, J. R.; Poucher, S. M.; Shaw, G. R.; Brooks, R.; Collis, M. G. In vivo characterisation of ZM 241385, a selective adenosine A2A receptor antagonist. *European Journal of Pharmacology* **1996**, 301, 107-113.
- 50) Robins, R. K.; Revankar, G. R.; O'Brien, D. E. Purine analog inhibitors of xanthine oxidase - Structure activity relationships and proposed binding of the molybdenum cofactor. *Journal of Heterocyclic Chemistry* **1985**, 22, 601-634.
- 51) Bekircan, O.; Kuxuk, M.; Kahveci, B.; Kolayli, S. Convenient synthesis of fused heterocyclic 1,3,5-triazines from some N-acyl imidates and heterocyclic amines as anticancer and antioxidant agents. *Archiv der Pharmazie* **2005**, 338, 365-372.
- 52) Andotra, C. S.; Dham, S.; Langer, T. C. Synthesis and biocidal activity of n-phenyl-2,6-substitute aryl-5-thione-1,2,4-triazolo[1,5-a]-s-triazine-7-ones. *Indian Journal of Heterocyclic Chemistry* **1996**, 5, 237-238.
- 53) Andotra, C. S.; Kumar, R.; Dham, S.; Sharma, P. Bridgehead nitrogen heterocycles : Synthesis and evaluation of antibacterial, antifungal activities of some 2-substituted aryl-6-p-chlorophenyl-5-thione(1H)-1,2,4-triazolo-[1,5-a]-s-triazine-7-ones. *Indian Journal of Heterocyclic Chemistry* **1998**, 8, 139-142.
- 54) Robins, R. K.; Revankar, G. R.; O'Brien, D. E.; Springer, R. H.; Novinson, T.; Albert, A.; Senga, K.; Miller, J. P.; Streeter, D. G. Purine analogue inhibitors of xanthine oxidase - structure activity relationships and proposed binding of the molybdenum cofactor. *Journal of Heterocyclic Chemistry* **1985**, 22, 601-34.
- 55) Raboisson, P.; Schultz, D.; Muller, C.; Reimund, J. M.; Pinna, G.; Mathieu, R.; Bernard, P.; Do, Q. T.; DesJarlais, R. L.; Justiano, H. Cyclic nucleotide phosphodiesterase type 4 inhibitors: Evaluation of pyrazolo[1,5-a]-1,3,5-triazine ring system as an adenine bioisostere. *European Journal of Medicinal Chemistry* **2008**, 43, 816-829.
- 56) De Zwart, M.; Vollinga, R. C.; Beukers, M. W.; Slegers, D. F.; Von Frijtag Drabbe Kunzel, J. K.; De Groote, M.; Ijzerman, A. P. Potent antagonists for the human adenosine A2B receptor. Derivatives of the triazolotriazine adenosine receptor antagonist ZM241385 with high affinity. *Drug Development Research* **1999**, 48, 95-103.
- 57) Raboisson, P.; Baurand, A.; Cazenave, J. P.; Gachet, C.; Schultz, D.; Spiess, B.; Bourguignon, J. J. A general approach toward the synthesis of C-

nucleoside pyrazolo[1,5-*a*]-1,3,5-triazines and their 3',5'-bisphosphate C-nucleotide analogues as the first reported in vivo stable P2Y1-receptor antagonists. *Journal of Organic Chemistry* **2002**, 67, 8063-8071.

- 58) Gilligan, P. J.; Folmer, B. K.; Hartz, R. A.; Koch, S.; Nanda, K. K.; Andreuski, S.; Fitzgerald, L.; Miller, K.; Marshall, W. J. Pyrazolo-[1,5-*a*]-1,3,5-triazine corticotropin-releasing factor (CRF) receptor ligands. *Bioorganic & Medicinal Chemistry* **2003**, 11, 4093-4102.
- 59) Darrow, J. W.; De Lombaert, S.; Blum, C.; Tran, J.; Giangiordano, M.; Griffith, D. A.; Carpino, P. A. Preparation of certain alkylene diamine-substituted pyrazolo[1,5-*a*]-1,5-pyrimidines and pyrazolo[1,5-*a*]-1,3,5-triazines as selective modulators of NPY1 receptors. Pat. WO 2001023387 **2001**.
- 60) Griffith, D. A. Pyrazolo[1,5-*a*][1,3,5]triazin-4-one derivatives as CB1 receptor antagonists. Pat. WO 2005049615 **2005**.
- 61) Friedkin, M.; Roberts, D. The enzymatic synthesis of nucleoside. *Journal of Biological Chemistry* **1954**, 207, 245-256.
- 62) Iltzsch, M. H.; El Kouni, M. H.; Cha, S. Kinetic studies of thymidine phosphorylase from mouse liver. *Biochemistry* **1985**, 24, 6799-6807.
- 63) Schwartz, M. Thymidine phosphorylase from *Escherichia coli*. Properties and kinetics. *European Journal of Biochemistry* **1971**, 21, 191-198.
- 64) El Kouni, M. H.; El Kouni, M. M.; Naguib, F. N. M. Differences in activities and substrate specificity of human and murine pyrimidine nucleoside phosphorylases: Implications for chemotherapy with 5- fluoropyrimidines. *Cancer Research* **1993**, 53, 3687-3693.
- 65) Peters, G. J.; Laurensse, E.; Leyva, A.; Pinedo, H. M. Purine nucleosides as cell-specific modulators of 5-fluorouracil metabolism and cytotoxicity. *European Journal of Cancer and Clinical Oncology* **1987**, 23, 1869-1881.
- 66) Desgranges, C.; Razaka, G.; Rabaud, M. Phosphorolysis of (E)-5-(2-bromovinyl)-2'-deoxyuridine (BVDU) and other 5-substituted-2'-deoxyuridines by purified human thymidine phosphorylase and intact blood platelets. *Biochemical Pharmacology* **1983**, 32, 3583-3590.
- 67) Heidelberger, C.; Anderson, S. W. Fluorinated pyrimidines. XXI. Tumor inhibitory activity of 5-trifluoromethyl-2'-deoxyuridine. *Cancer Research* **1964**, 24, 1979-1985.
- 68) Schwartz, E. L.; Baptiste, N.; Wadler, S.; Makower, D. Thymidine phosphorylase mediates the sensitivity of human colon carcinoma cells to 5-fluorouracil. *Journal of Biological Chemistry* **1995**, 270, 19073-19077.

- 69) Walko, C. M.; Lindley, C. Capecitabine: A review. *Clinical Therapeutics* **2005**, 27, 23-44.
- 70) Miyazono, K.; Okabe, T.; Urabe, A. Purification and properties of an endothelial cell growth factor from human platelets. *Journal of Biological Chemistry* **1987**, 262, 4098-4103.
- 71) Ishikawa, F.; Miyazono, K.; Hellman, U.; Drexler, H.; Wernstedt, C.; Hagiwara, K.; Usuki, K.; Takaku, F.; Risau, W.; Heldin, C. H. Identification of angiogenic activity and the cloning and expression of platelet-derived endothelial cell growth factor. *Nature* **1989**, 338, 557-562.
- 72) Furukawa, T.; Yoshimura, A.; Sumizawa, T.; Haraguchi, M.; Akiyama, S. I.; Fukui, K.; Ishizawa, M.; Yamada, Y. Angiogenic factor. *Nature* **1992**, 356, 668.
- 73) Asai, K.; Nakanishi, K.; Isobe, I.; Eksioglu, Y. Z.; Hirano, A.; Hama, K.; Miyamoto, T.; Kato, T. Neurotrophic action of gliostatin on cortical neurons. Identity of gliostatin and platelet-derived endothelial cell growth factor. *Journal of Biological Chemistry* **1992**, 267, 20311-20316.
- 74) Blank, J. G.; Hoffee, P. A. Purification and properties of thymidine phosphorylase from *Salmonella typhimurium*. *Archives of Biochemistry and Biophysics* **1975**, 168, 259-265.
- 75) Voytek, P. Purification of thymidine phosphorylase from *Escherichia coli* and its photoinactivation in the presence of thymine, thymidine, and some halogenated analogs. *Journal of Biological Chemistry* **1975**, 250, 3660-3665.
- 76) Kubilus, J.; Lee, L. D.; Baden, H. P. Purification of thymidine phosphorylase from human amniochorion. *Biochimica et Biophysica Acta* **1978**, 527, 221-228.
- 77) Barton, G. J.; Ponting, C. P.; Spraggon, G.; Finnis, C.; Sleep, D. Human platelet-derived endothelial cell growth factor is homologous to *Escherichia coli* thymidine phosphorylase. *Protein Science* **1992**, 1, 688-690.
- 78) Stenman, G.; Sahlin, P.; Dumanski, J. P.; Hagiwara, K.; Ishikawa, F.; Miyazono, K.; Collins, V. P.; Heldin, C. H. Regional localization of the human platelet-derived endothelial cell growth factor (ECGF1) gene to chromosome 22q13. *Cytogenetics and Cell Genetics* **1992**, 59, 22-23.
- 79) Hagiwara, K.; Stenman, G.; Honda, H.; Sahlin, P.; Andersson, A.; Miyazono, K.; Heldin, C. H.; Ishikawa, F.; Takaku, F. Organization and chromosomal localization of the human platelet-derived endothelial cell growth factor gene. *Molecular and Cellular Biology* **1991**, 11, 2125-2132.
- 80) Zhu, G. H.; Lenzi, M.; Schwartz, E. L. The Sp1 transcription factor contributes to the tumor necrosis factor-induced expression of the angiogenic

- factor thymidine phosphorylase in human colon carcinoma cells. *Oncogene* **2002**, 21, 8477-8485.
- 81) Finkenzeller, G.; Sparacio, A.; Technau, A.; Marmelstein, D.; Siemeister, G. Sp1 recognition sites in the proximal promoter of the human vascular endothelial growth factor gene are essential for platelet-derived growth factor-induced gene expression. *Oncogene* **1997**, 15, 669-676.
 - 82) Bronckaers, A.; Gago, F.; Balzarini, J.; Liekens, S. The dual role of thymidine phosphorylase in cancer development and chemotherapy. *Medicinal Research Reviews* **2009**, 29, 903-953.
 - 83) Schwartz, M. [59] Thymidine phosphorylase from Escherichia coli. *Methods in Enzymology* **1978**, 51, 442-445.
 - 84) Desgranges, C.; Razaka, G.; Raboud, M.; Bricaud, H. Catabolism of thymidine in human blood platelets. Purification and properties of thymidine phosphorylase. *Biochimica et Biophysica Acta* **1981**, 654, 211-218.
 - 85) Walter, M. R.; Cook, W. J.; Cole, L. B.; Short, S. A.; Koszalka, G. W.; Krenitsky, T. A.; Ealick, S. E. Three-dimensional structure of thymidine phosphorylase from Escherichia coli at 2.8 Å resolution. *Journal of Biological Chemistry* **1990**, 265, 14016-14022.
 - 86) Pugmire, M. J.; Cook, W. J.; Jasanoff, A.; Walter, M. R.; Ealick, S. E. Structural and theoretical studies suggest domain movement produces an active conformation of thymidine phosphorylase. *Journal of Molecular Biology* **1998**, 281, 285-299.
 - 87) Pugmire, M. J.; Ealick, S. E. The crystal structure of pyrimidine nucleoside phosphorylase in a closed conformation. *Structure* **1998**, 6, 1467-1479.
 - 88) Fox, S. B.; Moghaddam, A.; Westwood, M.; Turley, H.; Bicknell, R.; Gatter, K. C.; Harris, A. L. Platelet-derived endothelial cell growth factor/thymidine phosphorylase expression in normal tissues: An immunohistochemical study. *Journal of Pathology* **1995**, 176, 183-190.
 - 89) Shaw, T.; Smillie, R. H.; MacPhee, D. G. The role of blood platelets in nucleoside metabolism: Assay, cellular location and significance of thymidine phosphorylase in human blood. *Mutation Research* **1988**, 200, 99-116.
 - 90) Zhang, L.; Mackenzie, I. Z.; Rees, M. C. P.; Bicknell, R. Regulation of the expression of the angiogenic enzyme platelet-derived endothelial cell growth factor/thymidine phosphorylase in endometrial isolates by ovarian steroids and cytokines. *Endocrinology* **1997**, 138, 4921-4930.
 - 91) Fujimoto, J.; Ichigo, S.; Sakaguchi, H.; Hirose, R.; Tamaya, T. Expression of platelet-derived endothelial cell growth factor and its mRNA in uterine

- endometrium during the menstrual cycle. *Molecular Human Reproduction* **1998**, 4, 509-513.
- 92) Osuga, Y.; Toyoshima, H.; Mitsuhashi, N.; Taketani, Y. The presence of platelet-derived endothelial cell growth factor in human endometrium and its characteristic expression during the menstrual cycle and early gestational period. *Human Reproduction* **1995**, 10, 989-993.
- 93) Waguri, Y.; Otsuka, T.; Sugimura, I.; Matsui, N.; Asai, K.; Moriyama, A.; Kato, T. Gliostatin/platelet-derived endothelial cell growth factor as a clinical marker of rheumatoid arthritis and its regulation in fibroblast-like synoviocytes. *British Journal of Rheumatology* **1997**, 36, 315-321.
- 94) Boyle, J. J.; Wilson, B.; Bicknell, R.; Harrower, S.; Weissberg, P. L.; Fan, T. P. Expression of angiogenic factor thymidine phosphorylase and angiogenesis in human atherosclerosis. *Journal of Pathology* **2000**, 192, 234-242.
- 95) Creamer, D.; Jaggar, R.; Allen, M.; Bicknell, R.; Barker, J. Overexpression of the angiogenic factor platelet-derived endothelial cell growth factor/thymidine phosphorylase in psoriatic epidermis. *British Journal of Dermatology* **1997**, 137, 851-855.
- 96) Giatromanolaki, A.; Sivridis, E.; Maltezos, E.; Papazoglou, D.; Simopoulos, C.; Gatter, K. C.; Harris, A. L.; Koukourakis, M. I. Hypoxia inducible factor 1 α and 2 α overexpression in inflammatory bowel disease. *Journal of Clinical Pathology* **2003**, 56, 209-213.
- 97) Wang, E. H.; Yong, B. G.; In, S. M.; Cho, H. P.; Lee, K. H.; Sung, H. K.; Chang, S. K.; Choi, Y. J. Upregulation of thymidine phosphorylase in chronic glomerulonephritis and its role in tubulointerstitial injury. *Nephron - Clinical Practice* **2006**, 102, c133-c142.
- 98) Hirano, M.; Silvestri, G.; Blake, D. M.; Lombes, A.; Minetti, C.; Bonilla, E.; Hays, A. P.; Lovelace, R. E.; Butler, I.; Bertorini, T. E.; Threlkeld, A. B.; Mitsumoto, H.; Salberg, L. M.; Rowland, L. P.; DiMauro, S. Mitochondrial neurogastrointestinal encephalomyopathy (MNGIE): Clinical, biochemical, and genetic features of an autosomal recessive mitochondrial disorder. *Neurology* **1994**, 44, 721-727.
- 99) Haraguchi, M.; Tsujimoto, H.; Fukushima, M.; Higuchi, I.; Kuribayashi, H.; Utsumi, H.; Nakayama, A.; Hashizume, Y.; Hirato, J.; Yoshida, H.; Hara, H.; Hamano, S.; Kawaguchi, H.; Furukawa, T.; Miyazono, K.; Ishikawa, F.; Toyoshima, H.; Kaname, T.; Komatsu, M.; Chen, Z. S.; Gotanda, T.; Tachiwada, T.; Sumizawa, T.; Miyadera, K.; Osame, M.; Noda, T.; Yamada, Y.; Akiyama, S. I. Targeted deletion of both thymidine phosphorylase and uridine phosphorylase and consequent disorders in mice. *Molecular and Cellular Biology* **2002**, 22, 5212-5221.

- 100) Takebayashi, Y.; Yamada, K.; Miyadera, K.; Sumizawa, T.; Furukawa, T.; Kinoshita, F.; Aoki, D.; Okumura, H.; Yamada, Y.; Akiyama, S. I.; Aikou, T. The activity and expression of thymidine phosphorylase in human solid tumours. *European Journal of Cancer Part A* **1996**, 32, 1227-1232.
- 101) Peñerez-Peñerez, M. J.; Priego, E. M.; Hernaldiz, A. I.; Camarasa, M. J.; Balzarini, J.; Liekens, S. Thymidine phosphorylase inhibitors: Recent developments and potential therapeutic applications. *Mini-Reviews in Medicinal Chemistry* **2005**, 5, 1113-1123.
- 102) Pocher, F.; Spadari, S. Thymidine phosphorylase: A two-face janus in anticancer chemotherapy. *Current Cancer Drug Targets* **2001**, 1, 141-153.
- 103) Mainou-Fowler, T.; Angus, B.; Miller, S.; Proctor, S. J.; Taylor, P. R. A.; Wood, K. M. Micro-vessel density and the expression of vascular endothelial growth factor (VEGF) and platelet-derived endothelial cell growth factor (PdEGF) in classical Hodgkin lymphoma (HL). *Leukemia and Lymphoma* **2006**, 47, 223-230.
- 104) Reynolds, K.; Farzaneh, F.; Collins, W. P.; Campbell, S.; Bourne, T. H.; Lawton, F.; Moghaddam, A.; Harris, A. L.; Bicknell, R. Association of ovarian malignancy with expression of platelet-derived endothelial cell growth factor. *Journal of the National Cancer Institute* **1994**, 86, 1234-1238.
- 105) Takebayashi, Y.; Akiyama, S. I.; Akiba, S.; Yamada, K.; Miyadera, K.; Sumizawa, T.; Yamada, Y.; Murata, F.; Aikou, T. Clinicopathologic and prognostic significance of an angiogenic factor, thymidine phosphorylase, in human colorectal carcinoma. *Journal of the National Cancer Institute* **1996**, 88, 1110-1117.
- 106) Imazono, Y.; Takebayashi, Y.; Nishiyama, K.; Akiba, S.; Miyadera, K.; Yamada, Y.; Akiyama, S. I.; Ohi, Y. Correlation between thymidine phosphorylase expression and prognosis in human renal cell carcinoma. *Journal of Clinical Oncology* **1997**, 15, 2570-2578.
- 107) Takao, S.; Takebayashi, Y.; Che, X.; Shinchi, H.; Natsugoe, S.; Miyadera, K.; Yamada, Y.; Akiyama, S.; Aikou, T. Expression of thymidine phosphorylase is associated with a poor prognosis in patients with ductal adenocarcinoma of the pancreas. *Clinical Cancer Research* **1998**, 4, 1619-1624.
- 108) O'Byrne, K. J.; Koukourakis, M. I.; Giatromanolaki, A.; Cox, G.; Turley, H.; Steward, W. P.; Gatter, K.; Harris, A. L. Vascular endothelial growth factor, platelet-derived endothelial cell growth factor and angiogenesis in non-small-cell lung cancer. *British Journal of Cancer* **2000**, 82, 1427-1432.
- 109) Zhu, G. H.; Schwartz, E. L. Expression of the angiogenic factor thymidine phosphorylase in THP-1 monocytes: induction by autocrine tumor necrosis factor and inhibition by aspirin. *Molecular Pharmacology* **2003**, 64, 1251-1258.

- 110) Schwartz, E. L.; Wan, E.; Wang, F. S.; Baptiste, N. Regulation of expression of thymidine phosphorylase/platelet-derived endothelial cell growth factor in human colon carcinoma cells. *Cancer Research* **1998**, 58, 1551-1557.
- 111) Goto, H.; Kohno, K.; Sone, S.; Akiyama, S. I.; Kuwano, M.; Ono, M. Interferon \hat{I}^3 -dependent induction of thymidine phosphorylase/platelet-derived endothelial growth factor through \hat{I}^3 -activated sequence-like element in human macrophages. *Cancer Research* **2001**, 61, 469-473.
- 112) Sawada, N.; Ishikawa, T.; Fukase, Y.; Nishida, M.; Yoshikubo, T.; Ishitsuka, H. Induction of thymidine phosphorylase activity and enhancement of capecitabine efficacy by taxol/taxotere in human cancer xenografts. *Clinical Cancer Research* **1998**, 4, 1013-1019.
- 113) Blanquicett, C.; Gillespie, G. Y.; Nabors, L. B.; Miller, C. R.; Bharara, S.; Buchsbaum, D. J.; Diasio, R. B.; Johnson, M. R. Induction of thymidine phosphorylase in both irradiated and shielded, contralateral human U87MG glioma xenografts: implications for a dual modality treatment using capecitabine and irradiation. *Molecular cancer therapeutics* **2002**, 1, 1139-1145.
- 114) Griffiths, L.; Dachs, G. U.; Bicknell, R.; Harris, A. L.; Stratford, I. J. The influence of oxygen tension and pH on the expression of platelet-derived endothelial cell growth factor/thymidine phosphorylase in human breast tumor cells grown in vitro and in vivo. *Cancer Research* **1997**, 57, 570-572.
- 115) Guarcello, V.; Blanquicett, C.; Naguib, F. N. M.; El Kouni, M. H. Suppression of thymidine phosphorylase expression by promoter methylation in human cancer cells lacking enzyme activity. *Cancer Chemotherapy and Pharmacology* **2008**, 62, 85-96.
- 116) Moghaddam, A.; Zhang, H. T.; Fan, T. P. D.; Hu, D. E.; Lees, V. C.; Turley, H.; Fox, S. B.; Gatter, K. C.; Harris, A. L.; Bicknell, R. Thymidine phosphorylase is angiogenic and promotes tumor growth. *Proceedings of the National Academy of Sciences of the United States of America* **1995**, 92, 998-1002.
- 117) Haraguchi, M.; Miyadera, K.; Uemura, K.; Sumizawa, T.; Furukawa, T.; Yamada, K.; Akiyama, S. I.; Yamada, Y. Angiogenic activity of enzymes [7]. *Nature* **1994**, 368, 198.
- 118) Uchimiya, H.; Furukawa, T.; Okamoto, M.; Nakajima, Y.; Matsushita, S.; Ikeda, R.; Gotanda, T.; Haraguchi, M.; Sumizawa, T.; Ono, M.; Kuwano, M.; Kanzaki, T.; Akiyama, S. I. Suppression of thymidine phosphorylase-mediated angiogenesis and tumor growth by 2-deoxy-L-ribose. *Cancer Research* **2002**, 62, 2834-2839.
- 119) Miyadera, K.; Sumizawa, T.; Haraguchi, M.; Yoshida, H.; Konstanty, W.; Yamada, Y.; Akiyama, S. I. Role of thymidine phosphorylase activity in the

angiogenic effect of platelet-derived endothelial cell growth factor/thymidine phosphorylase. *Cancer Research* **1995**, 55, 1687-1690.

- 120) Asahara, T.; Masuda, H.; Takahashi, T.; Kalka, C.; Pastore, C.; Silver, M.; Kearne, M.; Magner, M.; Isner, J. M. Bone marrow origin of endothelial progenitor cells responsible for postnatal vasculogenesis in physiological and pathological neovascularization. *Circulation Research* **1999**, 85, 221-228.
- 121) Stevenson, D. P.; Milligan, S. R.; Collins, W. P. Effects of platelet-derived endothelial cell growth factor/thymidine phosphorylase, substrate, and products in a three-dimensional model of angiogenesis. *American Journal of Pathology* **1998**, 152, 1641-1646.
- 122) Hotchkiss, K. A.; Ashton, A. W.; Schwartz, E. L. Thymidine phosphorylase and 2-deoxyribose stimulate human endothelial cell migration by specific activation of the integrins $\alpha 5\beta 1$ and $\alpha v\beta 3$. *Journal of Biological Chemistry* **2003**, 278, 19272-19279.
- 123) Tenhunen, R.; Marver, H. S.; Schmid, R. Microsomal heme oxygenase. Characterization of the enzyme. *Journal of Biological Chemistry* **1969**, 244, 6388-6394.
- 124) Brown, N. S.; Jones, A.; Fujiyama, C.; Harris, A. L.; Bicknell, R. Thymidine phosphorylase induces carcinoma cell oxidative stress and promotes secretion of angiogenic factors. *Cancer Research* **2000**, 60, 6298-6302.
- 125) Takao, S.; Akiyama, S. I.; Yamada, Y.; Aikou, T. Suppression of angiogenesis and metastasis by a thymidine phosphorylase inhibitor. *Biotherapy* **2000**, 14, 419-422.
- 126) Nakajima, Y.; Gotanda, T.; Uchimiya, H.; Furukawa, T.; Haraguchi, M.; Ikeda, R.; Sumizawa, T.; Yoshida, H.; Akiyama, S. I. Inhibition of metastasis of tumor cells overexpressing thymidine phosphorylase by 2-deoxy-L-ribose. *Cancer Research* **2004**, 64, 1794-1801.
- 127) Rofstad, E. K.; Halsor, E. F. Vascular endothelial growth factor, interleukin 8, platelet-derived endothelial cell growth factor, and basic fibroblast growth factor promote angiogenesis and metastasis in human melanoma xenografts. *Cancer Research* **2000**, 60, 4932-4938.
- 128) Matsuura, T.; Kuratate, I.; Teramachi, K.; Osaki, M.; Fukuda, Y.; Ito, H. Thymidine phosphorylase expression is associated with both increase of intratumoral microvessels and decrease of apoptosis in human colorectal carcinomas. *Cancer Research* **1999**, 59, 5037-5040.
- 129) Ikeguchi, M.; Cai, J.; Fukuda, K.; Oka, S.; Katano, K.; Tsujitani, S.; Maeta, M.; Kaibara, N. Correlation between spontaneous apoptosis and the expression of angiogenic factors in advanced gastric adenocarcinoma. *Journal of Experimental and Clinical Cancer Research* **2001**, 20, 257-263.

- 130) Ikeda, N.; Adachi, M.; Taki, T.; Huang, C.; Hashida, H.; Takabayashi, A.; Sho, M.; Nakajima, Y.; Kanehiro, H.; Hisanaga, M.; Nakano, H.; Miyake, M. Prognostic significance of angiogenesis in human pancreatic cancer. *British Journal of Cancer* **1999**, *79*, 1553-1563.
- 131) Hata, K.; Fujiwaki, R.; Maede, Y.; Nakayama, K.; Fukumoto, M.; Miyazaki, K. Expression of thymidine phosphorylase in epithelial ovarian cancer: Correlation with angiogenesis, apoptosis, and ultrasound-derived peak systolic velocity. *Gynecologic Oncology* **2000**, *77*, 26-34.
- 132) Yao, L.; Itoh, S.; Furuta, I. Thymidine phosphorylase expression in oral squamous cell carcinoma. *Oral Oncology* **2002**, *38*, 584-590.
- 133) Ikeda, R.; Furukawa, T.; Kitazono, M.; Ishitsuka, K.; Okumura, H.; Tani, A.; Sumizawa, T.; Haraguchi, M.; Komatsu, M.; Uchimiya, H.; Ren, X. Q.; Motoya, T.; Yamada, K.; Akiyama, S. I. Molecular basis for the inhibition of hypoxia-induced apoptosis by 2-deoxy-D-ribose. *Biochemical and Biophysical Research Communications* **2002**, *291*, 806-812.
- 134) Ikeda, R.; Che, X. F.; Ushiyama, M.; Yamaguchi, T.; Okumura, H.; Nakajima, Y.; Takeda, Y.; Shibayama, Y.; Furukawa, T.; Yamamoto, M.; Haraguchi, M.; Sumizawa, T.; Yamada, K.; Akiyama, S. I. 2-Deoxy-D-ribose inhibits hypoxia-induced apoptosis by suppressing the phosphorylation of p38 MAPK. *Biochemical and Biophysical Research Communications* **2006**, *342*, 280-285.
- 135) Ikeda, R.; Furukawa, T.; Mitsuo, R.; Noguchi, T.; Kitazono, M.; Okumura, H.; Sumizawa, T.; Haraguchi, M.; Che, X. F.; Uchimiya, H.; Nakajima, Y.; Ren, X. Q.; Oiso, S.; Inoue, I.; Yamada, K.; Akiyama, S. I. Thymidine phosphorylase inhibits apoptosis induced by cisplatin. *Biochemical and Biophysical Research Communications* **2003**, *301*, 358-363.
- 136) Jeung, H. C.; Che, X. F.; Haraguchi, M.; Furukawa, T.; Zheng, C. L.; Sumizawa, T.; Rha, S. Y.; Jae, K. R.; Akiyama, S. I. Thymidine phosphorylase suppresses apoptosis induced by microtubule-interfering agents. *Biochemical Pharmacology* **2005**, *70*, 13-21.
- 137) Jeung, H. C.; Che, X. F.; Haraguchi, M.; Zhao, H. Y.; Furukawa, T.; Gotanda, T.; Zheng, C. L.; Tsuneyoshi, K.; Sumizawa, T.; Roh, J. K.; Akiyama, S. I. Protection against DNA damage-induced apoptosis by the angiogenic factor thymidine phosphorylase. *FEBS Letters* **2006**, *580*, 1294-1302.
- 138) Mori, S.; Takao, S.; Ikeda, R.; Noma, H.; Mataka, Y.; Wang, X.; Akiyama, S.; Aiko, T. Role of thymidine phosphorylase in Fas-induced apoptosis. *Human cell : official journal of Human Cell Research Society* **2001**, *14*, 323-330.
- 139) Mori, S. I.; Takao, S.; Ikeda, R.; Noma, H.; Mataka, Y.; Wang, X.; Akiyama, S. I.; Aikou, T. Thymidine phosphorylase suppresses Fas-induced apoptotic

signal transduction independent of its enzymatic activity. *Biochemical and Biophysical Research Communications* **2002**, 295, 300-305.

- 140) Langen, P.; Etzold, G.; Baerwolff, D.; Preussel, B. Inhibition of thymidine phosphorylase by 6-amino-thymine and derivatives of 6-aminouracil. *Biochemical Pharmacology* **1967**, 16, 1833-7.
- 141) Klein, R. S.; Lenzi, M.; Lim, T. H.; Hotchkiss, K. A.; Wilson, P.; Schwartz, E. L. Novel 6-substituted uracil analogs as inhibitors of the angiogenic actions of thymidine phosphorylase. *Biochemical Pharmacology* **2001**, 62, 1257-1263
- 142) Balzarini, J.; Gamboa, A. E.; Esnouf, R.; Liekens, S.; Neyts, J.; De Clercq, E.; Camarasa, M. J.; Pérez-Pérez, M. J. 7-Deazaxanthine, a novel prototype inhibitor of thymidine phosphorylase. *FEBS Letters* **1998**, 438, 91-95
- 143) Focher, F.; Ubiali, D.; Pregnotato, M.; Zhi, C.; Gambino, J.; Wright, G. E.; Spadari, S. Novel nonsubstrate inhibitors of human thymidine phosphorylase, a potential target for tumor-dependent angiogenesis. *Journal of Medicinal Chemistry* **2000**, 43, 2601-2607.
- 144) Murray, P. E.; McNally, V. A.; Lockyer, S. D.; Williams, K. J.; Stratford, I. J.; Jaffar, M.; Freeman, S. Synthesis and enzymatic evaluation of pyridinium-substituted uracil derivatives as novel inhibitors of thymidine phosphorylase. *Bioorganic and Medicinal Chemistry* **2002**, 10, 525-530.
- 145) Fukushima, M.; Suzuki, N.; Emura, T.; Yano, S.; Kazuno, H.; Tada, Y.; Yamada, Y.; Asao, T. Structure and activity of specific inhibitors of thymidine phosphorylase to potentiate the function of antitumor 2'-deoxyribonucleosides. *Biochemical Pharmacology* **2000**, 59, 1227-1236.
- 146) Matsushita, S.; Nitanda, T.; Furukawa, T.; Sumizawa, T.; Tani, A.; Nishimoto, K.; Akiba, S.; Miyadera, K.; Fukushima, M.; Yamada, Y.; Yoshida, H.; Kanzaki, T.; Akiyama, S. I. The effect of a thymidine phosphorylase inhibitor on angiogenesis and apoptosis in tumors. *Cancer Research* **1999**, 59, 1911-1916.
- 147) Takao, S.; Akiyama, S. I.; Nakajo, A.; Yoh, H.; Kitazono, M.; Natsugoe, S.; Miyadera, K.; Fukushima, M.; Yamada, Y.; Aikou, T. Suppression of metastasis by thymidine phosphorylase inhibitor. *Cancer Research* **2000**, 60, 5345-5348.
- 148) Hong, D. S.; Abbruzzese, J. L.; Bogaard, K.; Lassere, Y.; Fukushima, M.; Mita, A.; Kuwata, K.; Hoff, P. M. Phase I study to determine the safety and pharmacokinetics of oral administration of TAS-102 in patients with solid tumors. *Cancer* **2006**, 107, 1383-1390.
- 149) Temmink, O. H.; Emura, T.; de Bruin, M.; Fukushima, M.; Peters, G. J. Therapeutic potential of the dual-targeted TAS-102 formulation in the

- treatment of gastrointestinal malignancies. *Cancer Science* **2007**, 98, 779-789.
- 150) Overman, M. J.; Varadhachary, G.; Kopetz, S.; Thomas, M. B.; Fukushima, M.; Kuwata, K.; Mita, A.; Wolff, R. A.; Hoff, P. M.; Xiong, H.; Abbruzzese, J. L. Phase 1 study of TAS-102 administered once daily on a 5-day-per-week schedule in patients with solid tumors. *Investigational New Drugs* **2008**, 26, 445-454.
- 151) Cole, C.; Reigan, P.; Gbaj, A.; Edwards, P. N.; Douglas, K. T.; Stratford, I. J.; Freeman, S.; Jaffar, M. Potential tumor-selective nitroimidazolylmethyluracil prodrug derivatives: Inhibitors of the angiogenic enzyme thymidine phosphorylase. *Journal of Medicinal Chemistry* **2003**, 46, 207-209.
- 152) Reigan, P.; Gbaj, A.; Chinje, E.; Stratford, I. J.; Douglas, K. T.; Freeman, S. Synthesis and enzymatic evaluation of xanthine oxidase-activated prodrugs based on inhibitors of thymidine phosphorylase. *Bioorganic and Medicinal Chemistry Letters* **2004**, 14, 5247-5250.
- 153) Esteban-Gamboa, A.; Balzarini, J.; Esnouf, R.; De Clercq, E.; Camarasa, M. J.; Pérez-Pérez, M. J. Design, synthesis, and enzymatic evaluation of multisubstrate analogue inhibitors of *Escherichia coli* thymidine phosphorylase. *Journal of Medicinal Chemistry* **2000**, 43, 971-983.
- 154) Balzarini, J.; Degève, B.; Esteban-Gamboa, A.; Esnouf, R.; De Clercq, E.; Engelborghs, Y.; Camarasa, M. J.; Pérez-Pérez, M. J. Kinetic analysis of novel multisubstrate analogue inhibitors of thymidine phosphorylase. *FEBS Letters* **2000**, 483, 181-185.
- 155) Liekens, S.; Bilsen, F.; De Clercq, E.; Priego, E. M.; Camarasa, M. J.; Pérez-Pérez, M. J.; Balzarini, J. Anti-angiogenic activity of a novel multi-substrate analogue inhibitor of thymidine phosphorylase. *FEBS Letters* **2002**, 510, 83-88.
- 156) Allan, A. L.; Gladstone, P. L.; Price, M. L. P.; Hopkins, S. A.; Juarez, J. C.; Doñate, F.; Ternansky, R. J.; Shaw, D. E.; Ganem, B.; Li, Y.; Wang, W.; Ealick, S. Synthesis and evaluation of multisubstrate bicyclic pyrimidine nucleoside inhibitors of human thymidine phosphorylase. *Journal of Medicinal Chemistry* **2006**, 49, 7807-7815.
- 157) Pomeisl, K.; Holý, A.; Pohl, R. Pd-catalyzed Suzuki-Miyaura coupling reactions in the synthesis of 5-aryl-1-[2-(phosphonomethoxy)ethyl]uracils as potential multisubstrate inhibitors of thymidine phosphorylase. *Tetrahedron Letters* **2007**, 48, 3065-3067.
- 158) Liekens, S.; Hernández, A. I.; Ribatti, D.; De Clercq, E.; Camarasa, M. J.; Pérez-Pérez, M. J.; Balzarini, J. The nucleoside derivative 5'-O-trityl-inosine (KIN59) suppresses thymidine phosphorylase-triggered angiogenesis via a

- noncompetitive mechanism of action. *Journal of Biological Chemistry* **2004**, 279, 29598-29605.
- 159) Liekens, S.; Bronckaers, A.; Hernández, A. I.; Priego, E. M.; Casanova, E.; Camarasa, M. J.; Pérez-Pérez, M. J.; Balzarini, J. 5'-O-tritylated nucleoside nucleoside derivatives: Inhibition of thymidine phosphorylase and angiogenesis. *Molecular Pharmacology* **2006**, 70, 501-509.
- 160) Casanova, E.; Hernández, A. I.; Priego, E. M.; Liekens, S.; Camarasa, M. J.; Balzarini, J.; Pérez-Pérez, M. J. 5'-O-tritylinosine and analogues as allosteric inhibitors of human thymidine phosphorylase. *Journal of Medicinal Chemistry* **2006**, 49, 5562-5570.
- 161) Nencka, R.; Votruba, I.; Hřebabeký, H.; Tloušť'ová, E.; Horská, K.; Masojídková, M.; Holý, A. Design and synthesis of novel 5,6-disubstituted uracil derivatives as potent inhibitors of thymidine phosphorylase. *Bioorganic and Medicinal Chemistry Letters* **2006**, 16, 1335-1337.
- 162) Pomeisl, K.; Votruba, I.; Holý, A.; Pohl, R. Syntheses of base and side-chain modified pyrimidine 1-[2-(phosphonmethoxy)propyl] derivatives as potent inhibitors of thymidine phosphorylase (PD-ECGF) from SD-lymphoma. *Collection of Czechoslovak Chemical Communications* **2006**, 71, 595-624.
- 163) Pomeisl, K.; Holý, A.; Votruba, I.; Pohl, R. Syntheses of N3-substituted thymine acyclic nucleoside phosphonates and a comparison of their inhibitory effect towards thymidine phosphorylase. *Bioorganic and Medicinal Chemistry Letters* **2008**, 18, 1364-1367.
- 164) Khan, K. M.; Ambreen, N.; Hussain, S.; Perveen, S.; Iqbal Choudhary, M. Schiff bases of 3-formylchromone as thymidine phosphorylase inhibitors. *Bioorganic and Medicinal Chemistry* **2009**, 17, 2983-2988.
- 165) Hussain, S.; Gaffney, J.; Ahmed, N.; Slevin, M.; Iqbal Choudhary, M.; Ahmad, V. U.; Qasmi, Z.; Abbasi, M. A. An investigation of the kinetic and anti-angiogenic properties of plant glycoside inhibitors of thymidine phosphorylase. *Journal of Asian Natural Products Research* **2009**, 11, 159-167.
- 166) Nakajima, Y.; Haraguchi, M.; Furukawa, T.; Yamamoto, M.; Nakanishi, H.; Tatematsu, M.; Akiyama, S. I. 2-Deoxy-L-ribose inhibits the invasion of thymidine phosphorylase- overexpressing tumors by suppressing matrix metalloproteinase-9. *International Journal of Cancer* **2006**, 119, 1710-1716.
- 167) Liekens, S.; Balzarini, J.; Hernández, A. I.; De Clercq, E.; Priego, E. M.; Camarasa, M. J.; Pérez-Pérez, M. J. Thymidine phosphorylase is noncompetitively inhibited by 5'-O-trityl-inosine (KIN59) and related compounds. *Nucleosides, Nucleotides and Nucleic Acids* **2006**, 25, 975-980.
- 168) Longley, D. B.; Harkin, D. P.; Johnston, P. G. 5-Fluorouracil: Mechanisms of action and clinical strategies. *Nature Reviews Cancer* **2003**, 3, 330-338.

- 169) Miwa, M.; Ura, M.; Nishida, M.; Sawada, N.; Ishikawa, T.; Mori, K.; Shimma, N.; Umeda, I.; Ishitsuka, H. Design of a novel oral fluoropyrimidine carbamate, capecitabine, which generates 5-fluorouracil selectively in tumours by enzymes concentrated in human liver and cancer tissue. *European Journal of Cancer* **1998**, 34, 1274-1281.
- 170) Ishikawa, T.; Utoh, M.; Sawada, N.; Nishida, M.; Fukase, Y.; Sekiguchi, F.; Ishitsuka, H. Tumor selective delivery of 5-fluorouracil by capecitabine, a new oral fluoropyrimidine carbamate, in human cancer xenografts. *Biochemical Pharmacology* **1998**, 55, 1091-1097.
- 171) Toi, M.; Atiqur Rahman, M.; Bando, H.; Chow, L. W. C. Thymidine phosphorylase (platelet-derived endothelial-cell growth factor) in cancer biology and treatment. *Lancet Oncology* **2005**, 6, 158-166.
- 172) Liekens, S.; Bronckaers, A.; Pérez-Pérez, M. J.; Balzarini, J. Targeting platelet-derived endothelial cell growth factor/thymidine phosphorylase for cancer therapy. *Biochemical Pharmacology* **2007**, 74, 1555-1567.
- 173) Norman, R. A.; Barry, S. T.; Bate, M.; Breed, J.; Colls, J. G.; Ernill, R. J.; Luke, R. W. A.; Minshull, C. A.; McAlister, M. S. B.; McCall, E. J.; McMiken, H. H. J.; Paterson, D. S.; Timms, D.; Tucker, J. A.; Pauptit, R. A. Crystal structure of human thymidine phosphorylase in complex with a small molecule inhibitor. *Structure* **2004**, 12, 75-84.
- 174) Spraggon, G.; Stuart, D.; Ponting, C.; Finnis, C.; Sleep, D.; Jones, Y. Crystallization and X-ray diffraction study of recombinant platelet-derived endothelial cell growth factor. *Journal of Molecular Biology* **1993**, 234, 879-880.
- 175) EL Omari, K.; Bronckaers, A.; Liekens, S.; Pérez-Pérez, M.; Balzarini, J.; K., S. D. Structural basis for non-competitive product inhibition in human thymidine phosphorylase: implications for drug design. *Biochemical journal* **2006**, 399, 199-204.
- 176) Mitsiki, E.; Papageorgiou, A. C.; Iyer, S.; Thiyagarajan, N.; Prior, S. H.; Sleep, D.; Finnis, C.; Acharya, K. R. Structures of native human thymidine phosphorylase and in complex with 5-iodouracil. *Biochemical and Biophysical Research Communications* **2009**, 386, 666-670.
- 177) Karelson, M.; Lobanov, V. S.; Katritzky, A. R. Quantum-chemical descriptors in QSAR/QSPR studies. *Chemical Reviews* **1996**, 96, 1027-1043.
- 178) Free Jr, S. M.; Wilson, J. W. A mathematical contribution to structure-activity studies. *Journal of Medicinal Chemistry* **1964**, 7, 395-399.
- 179) Kubinyi, H. QSAR and 3D-QSAR in drug design. Part 1: Methodology. *Drug Discovery Today* **1997**, 2, 457-467.

- 180) Cramer Iii, R. D.; Patterson, D. E.; Bunce, J. D. Comparative molecular field analysis (CoMFA). 1. Effect of shape on binding of steroids to carrier proteins. *Journal of the American Chemical Society* **1988**, 110, 5959-5967.
- 181) Folkman, J.; Merler, E.; Abernathy, C.; Williams, G. Isolation of a tumor factor responsible for angiogenesis. *Journal of Experimental Medicine* **1971**, 133, 275-288.
- 182) Hlatky, L.; Hahnfeldt, P.; Folkman, J. Clinical application of antiangiogenic therapy: Microvessel density, what it does and doesn't tell us. *Journal of the National Cancer Institute* **2002**, 94, 883-893.
- 183) Weidner, N.; Semple, J. P.; Welch, W. R.; Folkman, J. Tumor angiogenesis and metastasis - Correlation in invasive breast carcinoma. *New England Journal of Medicine* **1991**, 324, 1-8.
- 184) Folkman, J. Tumor angiogenesis: therapeutic implications. *New England Journal of Medicine* **1971**, 285, 1182-1186.
- 185) Ferrara, N.; Gerber, H. P.; LeCouter, J. The biology of VEGF and its receptors. *Nature Medicine* **2003**, 9, 669-676.
- 186) Leung, D. W.; Cachianes, G.; Kung, W. J.; Goeddel, D. V.; Ferrara, N. Vascular endothelial growth factor is a secreted angiogenic mitogen. *Science* **1989**, 246, 1306-1309.
- 187) Senger, D. R.; Galli, S. J.; Dvorak, A. M.; Perruzzi, C. A.; Harvey, V.; Dvorak, H. F. Tumor cells secrete a vascular permeability factor that promotes accumulation of ascites fluid. *Science* **1983**, 219, 983-985.
- 188) Jain, R. K. Normalization of tumor vasculature: An emerging concept in antiangiogenic therapy. *Science* **2005**, 307, 58-62.
- 189) Kerbel, R.; Folkman, J. Clinical translation of angiogenesis inhibitors. *Nature Reviews Cancer* **2002**, 2, 727-739.
- 190) Ferrara, N.; Kerbel, R. S. Angiogenesis as a therapeutic target. *Nature* **2005**, 438, 967-974.
- 191) Fernando, N. H.; Hurwitz, H. I. Targeted therapy of colorectal cancer: Clinical experience with bevacizumab. *Oncologist* **2004**, 9, 11-18.
- 192) Lewis, C.; Murdoch, C. Macrophage responses to hypoxia: Implications for tumor progression and anti-cancer therapies. *American Journal of Pathology* **2005**, 167, 627-635.
- 193) Gunningham, S. P.; Currie, M. J.; Morrin, H. R.; Tan, E. Y.; Turley, H.; Dachs, G. U.; Watson, A. I.; Frampton, C.; Robinson, B. A.; Fox, S. B. The angiogenic factor thymidine phosphorylase up-regulates the cell adhesion molecule P-selectin in human vascular endothelial cells and is associated

with P-selectin expression in breast cancers. *Journal of Pathology* **2007**, 212, 335-344.

- 194) Muro, H.; Waguri-Nagaya, Y.; Mukofujiwara, Y.; Iwahashi, T.; Otsuka, T.; Matsui, N.; Moriyama, A.; Asai, K.; Kato, T. Autocrine induction of gliostatin/platelet-derived endothelial cell growth factor (GLS/PD-ECGF) and GLS-induced expression of matrix metalloproteinases in rheumatoid arthritis synoviocytes. *Rheumatology* **1999**, 38, 1195-1202.
- 195) Pula, G.; Mayr, U.; Evans, C.; Prokopi, M.; Vara, D. S.; Yin, X.; Astroulakis, Z.; Xiao, Q.; Hill, J.; Xu, Q.; Mayr, M. Proteomics identifies thymidine phosphorylase as a key regulator of the angiogenic potential of colony-forming units and endothelial progenitor cell cultures. *Circulation Research* **2009**, 104, 32-40.
- 196) Kitazono, M.; Takebayashi, Y.; Ishitsuka, K.; Takao, S.; Tani, A.; Furukawa, T.; Miyadera, K.; Yamada, Y.; Aikou, T.; Akiyama, S. I. Prevention of hypoxia-induced apoptosis by the angiogenic factor thymidine phosphorylase. *Biochemical and Biophysical Research Communications* **1998**, 253, 797-803.
- 197) Yano, S.; Kazuno, H.; Suzuki, N.; Emura, T.; Wierzba, K.; Yamashita, J. I.; Tada, Y.; Yamada, Y.; Fukushima, M.; Asao, T. Synthesis and evaluation of 6-methylene-bridged uracil derivatives. Part 1: Discovery of novel orally active inhibitors of human thymidine phosphorylase. *Bioorganic and Medicinal Chemistry* **2004**, 12, 3431-3441.
- 198) Baker, B. R.; Kelley, J. L. Irreversible enzyme inhibitors. CLXXI. Inhibition of FUDR phosphorylase from Walker 256 rat tumor by 5-substituted uracils. *Journal of Medicinal Chemistry* **1970**, 13, 461-466.
- 199) Ma, X.; Poon, T. Y.; Wong, P. T. H.; Chui, W. K. Synthesis and in vitro evaluation of 2,4-diamino-1,3,5-triazine derivatives as neuronal voltage-gated sodium channel blockers. *Bioorganic and Medicinal Chemistry Letters* **2009**, 19, 5644-5647.
- 200) Ma, X.; Woon, R. S. P.; Ho, P. C. L.; Chui, W. K. Antiproliferative activity against MCF-7 breast cancer cells by diamino-triazaspirodiene antifolates. *Chemical Biology and Drug Design* **2009**, 74, 322-326.
- 201) Dolzhenko, A. V.; Tan, B. J.; Chiu, G. N. C.; Chui, W. K. Synthesis and biological activity of fluorinated 7-aryl-2-pyridyl-6,7-dihydro[1,2,4]triazolo[1,5-a][1,3,5]triazin-5-amines [1]. *Journal of Fluorine Chemistry* **2008**, 129, 429-434.
- 202) Strogovich, A. Benzoylbiuret and its transformation in phenyldihydroxy- γ -triazine. *Buletinul Societatii de Stiinta din Cluj* **1929**, 4, 521-527.
- 203) Birtwell, S.; Curd, F. H. S.; Hendry, J. A.; Rose, F. L. Synthetic antimalarials. XXX. Some N1-aryl-N4,N5-dialkylbiguanides and

- observations on the conversion of guanylthioureas into biguanides. *Journal of the Chemical Society* **1948**, 1645-1657.
- 204) Suyama, T.; Kanai, M.; Nakayama, M. The reaction of 4,6-diamino-2*H*-1,3,5-thiadiazine-2-thione with amines. *Nippon Kagaku Kaishi* **1993**, 8, 952-956.
- 205) Suyama, T.; Saito, H.; Koyama, T.; Ishimaru, H. The reaction of 4,6-diamino-2*H*-1,3,5-thiadiazine-2-thione with nucleophilic reagents. *Nippon Kagaku Kaishi* **1991**, 12, 1655-1660.
- 206) Dolzhenko, A. V.; Chui, W. K. Synthesis of 5,7-diamino-1,2,4-triazolo[1,2-*a*][1,3,5]-triazines via annulation of 1,3,5-triazine ring onto 3(5)-amino-1,2,4-triazoles. *Heterocycles* **2007**, 71, 429-436.
- 207) Dolzhenko, A. V.; Pastorin, G.; Dolzhenko, A. V.; Chui, W. K. An aqueous medium synthesis and tautomerism study of 3(5)-amino-1,2,4-triazoles. *Tetrahedron Letters* **2009**, 50, 2124-2128.
- 208) Heras, M.; Fonta, D.; Linden, A.; Villalgordo, J. M. Synthesis of triazolo[1,5-*a*]triazin-7-one derivatives and highly functionalized [1,2,4]triazoles. *Helvetica chimica acta* **2003**, 86, 3204-3214.
- 209) Kamila, S.; Koh, B.; Biehl, E. R. Microwave-assisted "green" synthesis of 2-alkyl/ arylbenzothiazoles in one pot: A facile approach to anti-tumor drugs. *Journal of Heterocyclic Chemistry* **2006**, 43, 1609-1612.
- 210) Eagon, S.; Ball-Jones, N.; Haddenham, D.; Saavedra, J.; Delieto, C.; Buckman, M.; Singaram, B. Enantioselective reduction of α -substituted ketones mediated by the boronate ester TarB-NO₂. *Tetrahedron Letters* **2010**, 51, 6418-6421.
- 211) Kim, I.; Song, J. H.; Park, C. M.; Jeong, J. W.; Kim, H. R.; Ha, J. R.; No, Z.; Hyun, Y. L.; Cho, Y. S.; Sook Kang, N.; Jeon, D. J. Design, synthesis, and evaluation of 2-aryl-7-(3',4'-dialkoxyphenyl)-pyrazolo[1,5-*a*]pyrimidines as novel PDE-4 inhibitors. *Bioorganic and Medicinal Chemistry Letters* **2010**, 20, 922-926.
- 212) Tayyari, F.; Wood, D. E.; Fanwick, P. E.; Sammelson, R. E. Monosubstituted malononitriles: Efficient one-pot reductive alkylations of malononitrile with aromatic aldehydes. *Synthesis* **2008**, 279-285.
- 213) Al-Mousawi, S. M.; Moustafa, M. S.; Elnagdi, M. H. Studies with malononitrile derivatives: Synthesis and reactivity of 4-benzylpyrazole-3,5-diamine, 4-benzylisoxazole-3,5-diamine and thiazolidin-3-phenylpropanenitrile. *Heterocycles* **2008**, 75, 1371-1383.
- 214) Krenitsky, T. A.; Bushby, S. R. M. U.S. Patent, 4, 178,212, 1-8, Burroughs Welcome Co., Research Triangle Park, NC, **1979**.

- 215) Craig, P. N. Interdependence between physical parameters and selection of substituent groups for correlation studies. *Journal of Medicinal Chemistry* **1971**, 14, 680-684.
- 216) Okide, G. B. The synthesis of condensed 1,3,5-triazinium perchlorates from diazainium intermediates. *Journal of Heterocyclic Chemistry* **1994**, 31, 535-536.
- 217) Al-Masoudi, I. A.; Al-Soud, Y. A.; Al-Salihi, N. J.; Al-Masoudi, N. A. 1,2,4-Triazoles: Synthetic approaches and pharmacological importance (Review). *Chemistry of Heterocyclic Compounds* **2006**, 42, 1377-1403.
- 218) Katritzky, A. R.; Lagowski, J. M. Prototropic tautomerism of heteroaromatic compounds. IV. Five-membered rings with two or more hetero atoms. *Advance Heterocyclic Chemistry* **1963**, 18, 27-81.
- 219) Minkin, V. I.; Garnovskii, A. D.; Elguero, J.; Katritzky, A. R.; Denisko, O. V. The tautomerism of heterocycles: Five-membered rings with two or more heteroatoms. *Advances in Heterocyclic Chemistry*, **2000**; Vol. 76, pp 157-323.
- 220) Hansch, C.; Leo, A.; Taft, R. W. A survey of hammett substituent constants and resonance and field parameters. *Chemical Reviews* **1991**, 91, 165-195.
- 221) Hurst, D. T.; Stacey, A. D.; Nethercleft, M.; Rahim, A.; Harnden, M. R. The synthesis of some pyrimidinyl and thiazolyl ureas and thioureas and some related compounds. *Australian Journal of Chemistry* **1988**, 41, 1221-1229.
- 222) Kurzer, F.; Secker, J. L. Addition-cyclizations of ethoxycarbonyl isothiocyanate with hydrazine derivatives as a source of thiadiazoles and triazoles. *Journal of Heterocyclic Chemistry* **1989** 26, 355-360.
- 223) Bossio, R.; Marcaccini, S.; Parrini, V.; Pepino, R. Synthesis of 5H-benzimidazo[1,2-*a*][1,3,4]thiadiazolo[2,3-*d*][1,3,5]triazin-5-one and 12H-benzimidazo[1,2-*a*]pyrimido[6,1-*d*][1,3,5]triazin-12-one, two new heterocyclic ring systems. *Journal of Heterocyclic Chemistry* **1986**, 23, 889-891.
- 224) Matsui, T.; Nagano, M.; Tobitsuka, J.; Oyamada, K. Studies on organic sulfur compounds. XVI. Nucleophilic reaction of heterocyclic bases with alkoxy carbonyl isothiocyanates. *Chemical and Pharmaceutical Bulletin* **1974**, 22, 2118-2122.
- 225) Bera, H.; Dolzhenko, A. V.; Tan, G. K.; Koh, L. L.; Chui, W. K. 4-Carboxy-1-[4-(N,N-dimethylamino)benzoyl]thiosemicarbazide. *Acta Crystallographica Section E: Structure Reports Online* **2010**, 66, o1241.
- 226) Pérez González, M.; Terán, C.; Saíaz-Urra, L.; Teijeira, M. Variables selection methods in QSAR: An overview. *Current Topics in Medicinal Chemistry* **2008**, 8, 1606-1627.

- 227) Kurizaki, T.; Toi, M.; Tominaga, T. Relationship between matrix metalloproteinase expression and tumor angiogenesis in human breast carcinoma. *Oncology Reports* **1998**, *5*, 673-677.
- 228) Nagaoka, H.; Iino, Y.; Takei, H.; Morishita, Y. Platelet-derived endothelial cell growth factor/thymidine phosphorylase expression in macrophages correlates with tumor angiogenesis and prognosis in invasive breast cancer. *International Journal of Oncology* **1998**, *13*, 449-454.
- 229) Toi, M.; Ueno, T.; Matsumoto, H.; Saji, H.; Funata, N.; Koike, M.; Tominaga, T. Significance of thymidine phosphorylase as a marker of protumor monocytes in breast cancer. *Clinical Cancer Research* **1999**, *5*, 1131-1137.
- 230) Sullu, Y.; Demirag, G. G.; Yildirim, A.; Karagoz, F.; Kandemir, B. Matrix metalloproteinase-2 (MMP-2) and MMP-9 expression in invasive ductal carcinoma of the breast. *Pathology Research and Practice* **2011**, *207*, 747-753.
- 231) Overall, C. M.; López-Otín, C. Strategies for MMP inhibition in cancer: Innovations for the post-trial era. *Nature Reviews Cancer* **2002**, *2*, 657-672.
- 232) Hoeben, A.; Landuyt, B.; Highley, M. S.; Wildiers, H.; Van Oosterom, A. T.; De Bruijn, E. A. Vascular endothelial growth factor and angiogenesis. *Pharmacological Reviews* **2004**, *56*, 549-580.
- 233) Toi, M.; Inada, K.; Hoshina, S.; Suzuki, H.; Kondo, S.; Tominaga, T. Vascular endothelial growth factor and platelet-derived endothelial cell growth factor are frequently coexpressed in highly vascularized human. *Clinical Cancer Research* **1995**, *1*, 961-964.
- 234) Gomez, D. E.; Alonso, D. F.; Yoshiji, H.; Thorgeirsson, U. P. Tissue inhibitors of metalloproteinases: Structure, regulation and biological functions. *European Journal of Cell Biology* **1997**, *74*, 111-122.
- 235) Lacraz, S.; Nicod, L.; Galve-de Rochemonteix, B.; Baumberger, C.; Dayer, J. M.; Welgus, H. G. Suppression of metalloproteinase biosynthesis in human alveolar macrophages by interleukin-4. *Journal of Clinical Investigation* **1992**, *90*, 382-388.
- 236) Simeone, A. M.; Rene, N. A.; McMurtry, V. C.; Colella, S.; Krahe, R.; Tari, A. M. Cyclooxygenase-2 uses the protein kinase C/interleukin-8/urokinase-type plasminogen activator pathway to increase the invasiveness of breast cancer cells. *International Journal of Oncology* **2007**, *30*, 785-792.
- 237) Sehgal, P. B. Interleukin-6 induces increased motility, cell-cell and cell-substrate dyshesion and epithelial-to-mesenchymal transformation in breast cancer cells. *Oncogene* **2010**, *29*, 2599-2600.

- 238) Capuano, L.; Schrepfer, H. J. Heterocyclizations. IX. Preparation of pyrazolo-, triazolo-, oxazolo-, and thiazolo-s-triazines with a bridgehead nitrogen and of an isopurine N-carboxylic ester. *Chemische Berichte* **1971**, 104, 3039-3047.
- 239) Alley, M. C.; Scudiero, D. A.; Monks, A.; Hursey Czerwinski, M. L. M. J.; Fine, D. L.; Abbott, B. J.; Mayo, J. G.; Shoemaker, R. H.; Boyd, M. R. Feasibility of drug screening with panels of human tumor cell lines using a microculture tetrazolium assay. *Cancer Research* **1988**, 48, 589-601.
- 240) Liotta, L. A.; Stetler-Stevenson, W. G. Metalloproteinases and cancer invasion. *Seminars in Cancer Biology* **1990**, 1, 99-106.

